

**SYNDECAN-4 REGULATES  
CELL-SURFACE TRAFFICKING  
AND BIOLOGICAL ACTIVITY OF  
TRANSGLUTAMINASE-2**

*Alessandra Scarpellini*

**A thesis submitted in partial fulfilment of the  
requirements of Nottingham Trent University for the  
degree of Doctor of Philosophy**

*October 2009*



## **Declaration**

This work is the intellectual property of the author, and may also be owned by the research sponsor(s) and/or Nottingham Trent University.

You may copy up to 5% of this work for private study, or personal, non-commercial research. Any re-use of the information contained within this document should be fully referenced, quoting the author, title, university, degree level and pagination.

Queries or requests for any other use, or if a more substantial copy is required, should be directed in the first instance to the author.

## Abstract

Transglutaminase-2 (TG2) is a  $\text{Ca}^{2+}$ -dependent crosslinking enzyme involved in the post-translational modification of proteins via the formation of  $\text{N}\epsilon(\gamma\text{-glutamyl})\text{lysine}$  isodipeptides. TG2 is externalised in the extracellular matrix (ECM) through an unconventional and not fully understood pathway. Under normal conditions, TG2 modulates cell adhesion, proliferation and tissue repair. Under continuous cell insult higher expression and elevated extracellular trafficking of TG2 contribute to the pathogenesis of tissue scarring. TG2 is known to have affinity for heparin, and in a previous study cell-surface heparan sulphate (HS) has been implicated in extracellular TG2 mediated RGD-independent cell adhesion, a non-enzymatic process independent from the  $\alpha 5\beta 1$  integrin-binding to the RGD domain on FN (Verderio et al., 2003). Hence HS proteoglycan (HSPG) could act as cell surface co-receptor for FN-bound TG2 or contribute to the regulation of extracellular TG2 activity in cell adhesion and tissue repair.

The aims of this study were: 1) to study the role of externalised TG2 in cell adhesion in primary fibroblasts. 2) to investigate the role of HSPG syndecan-4 (Sdc-4), a crucial component of focal adhesions in TG2-mediated cell-adhesion. 3) to characterise the interaction between TG2 and HSPG, in particular Sdc-4, and to investigate how this interaction can influence TG2 biological functions *in vitro*. 4) to examine the role of Sdc-4 as a regulator of pro-fibrotic TG2 activity in experimental model of kidney fibrosis (UUO).

The results obtained have shown that: 1) externalised TG2 plays an important role in mediating early events of cell adhesion in primary fibroblasts. 2) FN-bound TG2 relies on the presence of Sdc-4 for its role in RGD-independent cell adhesion. 3) TG2 has a high affinity for HS ( $K_d \sim 20 \text{ nM}$ ) and it is associated with Sdc-4 at the cell surface in primary fibroblasts. 4) TG2 crosslinking activity at the cell surface relies on the presence of the HS chains of Sdc-4 and other HS proteoglycans. HS-binding does not have a direct role in TG2 activity regulation, but the presence of intact Sdc-4 is essential for TG2 localisation at the cell surface. 5) Sdc-4 is protective against the development of UUO and it regulates the release and activity of the pro-fibrotic factor TG2 in UUO, suggesting a possible co-operative role of TG2 and Sdc-4 in the development of kidney fibrosis.

In conclusion, HSPG, and in particular Sdc-4 emerged to have a crucial role in the cell-surface trafficking and regulation of TG2 biological activities both *in vitro* and *in vivo*.

## **Acknowledgements**

I'd like to say a massive Thank You to my supervisor, Elisabetta Verderio, for welcoming me in her lab and guiding me through my research project.

Thanks Tim Johnson for his help with the in vivo work and to Ellen Billett for the comments and suggestions on my work and thesis.

I'd like to thank Hugues Lortat-Jacob for the collaborative SPR work.

Thank you to all the technicians in NTU, especially Iain and Emma from Area 2 and Emma from biochem prep room, they were always ready to help.

Thanks to everybody in lab 107: Renee, for her friendship and help in the experimental work, Laurice, Amar, Shakthi, Shiva, Joao and Izhar for their support and friendship through the years.

Many other people in NTU have been with me during these years, and I'd like to thank in particular Christoph, Juncal and Muriel for being always there for me, no matter how far or how busy they were. Thank you as well to Christian, Asli, Heidi, Cheryl, Lyndsey, Bego, Julia and Rick for their help with lab work and, mostly for the chats and laughs. A special thank you to Lesley and Liz at the reception for the nice chats and for being always nice to me.

I'd like to thank my family for constantly supporting me and believing in my choices.

A special thank you goes to Vale, for her encouragement and for being patient with me in the stressful times...and there has been a lot!! It has been and it is great to have you with me.

## **Publications**

### **Journal articles**

A. Scarpellini, R. Germack, J. Lortat-Jacob, T. Muramatsu, E. Billett, T. Johnson, E.A.M. Verderio (2009). Heparan sulphate proteoglycans are receptors for the cell-surface biological activity and trafficking of transglutaminase-2. *J. Biol. Chem.*, 284 (27): 18411-18423.

E.A. Verderio, A. Scarpellini, T.S. Johnson (2009). Novel interactions of TG2 with heparan sulfate proteoglycans: reflection on physiological implications. *Amino Acids* 36: 671-677.

R. Iorio, A. Di Sandro, A. Scarpellini, S. Del Duca, D. Serafini-Fracassini, E. Verderio (2008). Visualisation of Transglutaminase-mediated cross-linking activity in germinating pollen by laser confocal microscopy. *Plant Biosystems*, 142 (2): 360-365.

### **Articles in preparation**

E.A.M. Verderio, A. Scarpellini, X. Li, D. Telci, G. Melino, R.A. Jones, M. Griffin (2009). Targeted deletion of *tgm-2* uncovers a role for extracellular transglutaminase-2 in RhoA downregulation during initial fibroblast adhesion to fibronectin.

## Conference communications and published abstracts

A. Scarpellini, H. Lortat-Jacob, T. Johnson and E.A.M Verderio. Syndecan-4 regulates the cell-surface trafficking and activity of pro-fibrotic factor Transglutaminase-2. XX International Symposium on Glycoconjugates, San Juan, Puerto Rico, November 29–December 4, 2009. Glycoconjugate Journal, in press. Oral and poster presentation.

A. Scarpellini, H. Lortat-Jacob, T. Johnson and E. Verderio. Syndecan-4 is required for the cell-surface trafficking and pro-fibrotic action of Transglutaminase-2. 6<sup>th</sup> International Conference on Proteoglycan. Aix Les Bains, France. September 13-17, 2009. Poster presentation.

A. Scarpellini, R. Germack, T. Johnson, T. Muramatsu, M. Griffin and E. Verderio. Direct association of transglutaminase-2 with syndecan-4 in the formation of RGD-independent focal adhesions on fibronectin. Biochemical Society Annual Symposium - Structure and function in cell adhesion, Manchester, UK, December 3-5, 2007. Biochemical Society Transactions, Vol 36 (2) April 2008. Poster presentation.

E.A.M. Verderio, A. Scarpellini, X. Li, D. Telci, T. Muramatsu, G. Melino, R.A. Jones and M. Griffin. Targeted deletion of tgm-2 uncovers a role for extracellular transglutaminase-2 in RhoA downregulation during fibroblasts adhesion to fibronectin. Biochemical Society Annual Symposium - Structure and function in cell adhesion, Manchester, UK, December 3-5, 2007. Biochemical Society Transactions, 36 (2) April 2008. Oral presentation by E.A.M. Verderio.

A. Scarpellini, R. Germack, T. Johnson, T. Muramatsu and E. Verderio. Direct association of Transglutaminase-2 with Syndecan-4 in the formation of RGD-independent focal adhesions on fibronectin. 9th International Conference on Protein Crosslinking and Transglutaminases (PCL9), Marrakech, Morocco, Sept. 1-5, 2007. Poster presentation.

E.A.M. Verderio, A. Scarpellini, X. Li, D Telci, G. Melino, RA. Jones and M. Griffin. Heterotypic association of Transglutaminase to fibronectin is critical for downregulation of RhoA activity during cell adhesion. 9th International Conference on Protein Crosslinking and Transglutaminases (PCL9), Marrakech, Morocco, Sept. 1-5, 2007. Oral presentation by EAM Verderio.

A. Scarpellini, R. Germack, H. Lortat-Jacob, T. Muramatsu and E. Verderio. Tissue Transglutaminase is a heparan sulfate binding protein which co-operates with Syndecan 4 in the formation of focal adhesions on fibronectin. XIX International Symposium on Glycoconjugates, Cairns, Australia, July 15-20, 2007. Journal 24 (6/7) October 2007 (092). Oral presentation.

A. Scarpellini, J.L. Haylor, T Muramatsu, T.S. Johnson and E.A.M. Verderio. Syndecan-4 knockout is protective in the unilateral ureteral obstruction model of renal scarring. XIX International Symposium on Glycoconjugates, Cairns, Australia, July 15-20, 2007. Glycoconjugate Journal 24 (6/7) October 2007 (043). Oral presentation by E.A.M. Verderio.

## Abbreviations

AAMP	Angio-associated migratory cell protein
AD	Alzheimer's disease
Ala	Alanine
ALP	Alkaline phosphatase
Amp	Ampicillin
Apo	Apolipoprotein
Arg	Arginine
Asn	Asparagine
Asp	Aspartic acid
AT	Annealing temperature
ATIII	Antithrombin
ATP	Adenosine triphosphate
Bmax	Maximum binding
BMP	Bone morphogenetic protein
bp	Base pair
BSA	Bovine serum albumine
BTC	Byotinylated cadaverine
BTC	Biotin cadaverine
CAM	Cell adhesion molecule
CBD	Cellbinding domain
cDNA	Complementary deoxyribonucleic acid
CE	Cornified envelope
CHO	Chinese hamster ovary
CMV	Cytomegalovirus
CS	Chondroitin sulphate
Ct	Cycle threshold
Cys	Cysteine
DAPI	4',6-diamidino-2-phenylindole
DEPC	Diethyl pyrocarbonate
DMEM	Dulbecco's modified Eagle's medium
DMSO	Dimethyl sulfoxide
DNA	Deoxyribonucleic acid
dNTP	Deoxyribonucleotide triphosphate
DP1	Dorsal protein 1
DS	Dermatan sulphate
DTT	Dithiothreitol
ECL	Enhanced chemiluminescence
ECM	Extracellular matrix
EC-SOD	Extracellular superoxide dismutase
EDTA	Ethylenediaminetetraacetic acid

EGFP	Enhanced green fluorescent protein
ELISA	Enzyme-linked immunosorbent assay
ELSA	Enzyme-linked sorbent assay
FA	Focal adhesion
FAK	Focal adhesion kinase
FCS	Foetal calf serum
FGF	Fibroblast growth factor
FITC	Fluorescein isothiocyanate
FN	Fibronectin
FXIII	Factor XIII
GAG	Glycosaminoglycan
GAPDH	Glyceraldehyde-3-phosphate dehydrogenase
GDP	Guanosine diphosphate
Gln	Glutamine
Glu	Glutamate
Gly	Glycine
GPI	Glycosylphosphatidylinositol
gpTG2	Guinea pig liver TG2
GTP	Guanosine triphosphate
HB	Heparin binding
HB-EGF	Heparin-binding EGF-like growth factor
HBS-EP	Hepes containing 150mM Sodium Chloride, 2mM EDTA, 0.005% Polysorbate 20
His	Histidine
HOB	Human osteoblasts
HRP	Horseradish peroxidase
HS	Heparan sulphate
HSD	Highly sulphated domain
HSPG	Heparan sulphate proteoglycan
htt	Hungtingin
IGFBP	Insulin-like growth factor binding proteins
IL	Interleukin
Ileu	Isoleucine
Kan	Kanamycin
Kd	Dissociation constant
KS	Keratan sulphate
LB	Luria Bertani
Leu	Leucine
LPA	Lysophosphatidic acid
LPL	Lipoprotein lipase
Lys	Lysine
MEF	Mouse embryonic fibroblasts

Met	Methionine
MMP	Matrix metalloproteinases
Mr	Relative molecular mass
mRNA	Messenger RNA
NCAM	Neural cell-adhesion molecule
Neo	Neomycin
NF-kB	Nuclear factor kB
NLS	Nuclear localisation signal
NO	Nitric oxide
PAGE	Polyacrylamide gel electrophoresis
PBS	Phosphate buffer saline
PCR	Polymerase chain reaction
PD	Parkinson's disease
PDGF-A	Platelet-derived growth factor alpha polypeptide
PDI	Protein disulfide isomerase
PG	Proteoglycan
PIP2	Phosphatidylinositol (4,5) bisphosphate
PKC	Protein kinase C
PLC	Phospholipase C
PMSF	Phenylmethylsulphonyl fluoride
Pro	Proline
RAR	Retinoic acid receptor
Rb	Retinoblastoma protein
RE	Responsive element
RNA	Ribonucleic acid
rpm	Revolutions per minute
RT	Reverse transcriptase
RT-PCR	Reverse transcription PCR
RU	Resonance unit
RXR	Retinoid X receptor
SD	Standard deviation
Sdc	Syndecan
SDS	Sodium dodecyl sulfate
Ser	Serine
SF	Stress fibres
siRNA	Small interfering RNA
SLRP	Small Leu-rich proteoglycan
SPR	Surface Plasmon resonance
TAE	Tris/acetate/EDTA
TBS	Tris-buffered saline
TBST	Tris-buffered saline containing 0.5 % (v/v) Tween-20
TE	Tris/EDTA

TEMED	N,N,N',N'-Tetramethylethylenediamine
TET	Tetracycline
TFPI	Tissue factor pathway inhibitor
TG	Transglutaminase
TGF	Transforming growth factor
TMB	3,3,5,5-tetramethylbenzidine
TNF	Tumour necrosis factor
TRE	TGF $\beta$ responsive element
TRITC	Tetramethyl Rhodamine Iso-Thiocyanate
Tyr	Tyrosine
UMD	Unmodified domain
UNX	Unilateral nephrectomy
UUO	Unilateral ureteral obstruction
Val	Valine
Vg1	Vitellogenin1
vWF	Von Willebrand factor

## Contents

<b>CHAPTER 1: INTRODUCTION.....</b>	<b>1</b>
<b>1.1 The Transglutaminase family.....</b>	<b>1</b>
1.1.1 Post-translational modification of proteins.....	1
1.1.2 Regulation of TG activity.....	3
1.1.3 Substrates of transglutaminases.....	5
<b>1.2 Transglutaminases in mammalian tissues .....</b>	<b>5</b>
1.2.1 Factor XIII.....	7
1.2.2 Keratinocyte TG (Type 1 or TG <sub>K</sub> ) .....	9
1.2.3 Epidermal TG (Type 3 or TG <sub>E</sub> ).....	10
1.2.4 Prostate TG (Type 4 or TG <sub>P</sub> ).....	11
1.2.5 TG X (Type 5).....	11
1.2.6 TG Y (Type 6).....	12
1.2.7 TG Z (Type 7).....	12
1.2.8 Erythrocyte membrane protein band 4.2 .....	12
1.2.9 Tissue TG (Type 2 or TG <sub>T</sub> ).....	13
1.2.9.1 Organisation and regulation of TG2 gene.....	13
1.2.9.2 Structure of TG2.....	15
1.2.9.3 TG2 and cell adhesion .....	16
1.2.9.4 TG2-related diseases.....	18
1.2.9.4.1 Celiac disease.....	18
1.2.9.4.2 Diabetes .....	18
1.2.9.4.3 Neurodegenerative diseases .....	19
1.2.9.4.4 Cancer .....	20
1.2.9.5 TG2 in wound healing and fibrosis .....	21
1.2.9.6 Cellular localisation of TG2 .....	22
1.2.9.6.1 Cytosolic TG2.....	22
1.2.9.6.2 Nuclear TG2 .....	23
1.2.9.6.3 Extracellular TG2 .....	24
<b>1.3 Glycosaminoglycans.....</b>	<b>25</b>
1.3.1 Heparan sulphate.....	26
1.3.2 Heparin binding proteins.....	26
<b>1.4 Proteoglycans .....</b>	<b>27</b>

1.4.1	Extracellular matrix proteoglycans .....	29
1.4.2	Proteoglycans of secretory granules.....	29
1.4.3	Basement membrane proteoglycans.....	29
1.4.4	Membrane-bound proteoglycans.....	30
1.4.5	The syndecan family .....	31
1.4.5.1	Syndecan-1 .....	33
1.4.5.2	Syndecan-2.....	33
1.4.5.3	Syndecan-3 .....	34
1.4.5.4	Syndecan-4.....	34
1.4.6	Syndecan-4 in tissue injury and wound healing .....	36
 <b>CHAPTER 2: MATERIALS AND METHODS .....</b>		<b>37</b>
<b>2.1</b>	<b>Materials.....</b>	<b>37</b>
2.1.1	Cell culture.....	37
2.1.1.1	Reagents .....	37
2.1.1.2	Plastic ware.....	37
2.1.2	Laboratory reagents.....	37
2.1.2.1	Peptides .....	37
2.1.2.2	Enzymes .....	38
2.1.2.3	Antibodies.....	38
2.1.2.4	Molecular biology reagents .....	39
2.1.2.4.1	Antibiotics.....	39
2.1.2.4.2	Cloning and Expression vectors.....	39
2.1.2.4.3	PCR primers.....	39
2.1.2.5	Chemicals .....	41
2.1.3	Laboratory equipment .....	43
2.1.4	Companies.....	44
<b>2.2</b>	<b>Methods .....</b>	<b>46</b>
2.2.1	Cell culture.....	46
2.2.1.1	Cell lines .....	46
2.2.1.2	Cell culture conditions.....	46
2.2.1.3	Sub-culture of cells.....	47
2.2.1.4	Cell counting .....	47
2.2.1.5	Cryo-preservation of cells .....	47
2.2.1.6	Resuscitation of cryo-preserved cells .....	47
2.2.1.7	Isolation of primary dermal fibroblasts .....	47

2.2.1.8	Cell transfection.....	48
2.2.2	Preparation of matrices for cell adhesion.....	49
2.2.2.1	Fibronectin coating.....	49
2.2.2.2	Preparation of TG2-FN matrices.....	49
2.2.3	Immunocytochemistry.....	50
2.2.4	Detection of actin stress fibres.....	50
2.2.5	Preparation of protein extracts for Western blotting.....	51
2.2.5.1	Total protein extract.....	51
2.2.5.2	Cell fractionation.....	51
2.2.5.3	Determination of protein concentration.....	51
2.2.6	Denaturing sodium dodecyl sulfate polyacrylamide gel electrophoresis (SDS-PAGE).....	52
2.2.6.1	Preparation of polyacrylamide gels.....	52
2.2.6.2	Separation of samples via SDS-PAGE.....	53
2.2.7	Western blotting and immunoprobng of proteins.....	53
2.2.7.1	Western blotting.....	53
2.2.7.2	Membrane staining with red ponceau.....	54
2.2.7.3	Immunoprobng.....	54
2.2.7.4	Enhanced Chemiluminescence (ECL) development system.....	55
2.2.7.5	Stripping and reprobing membranes.....	55
2.2.7.6	Quantification of immunodetected proteins.....	56
2.2.8	Protein immunoprecipitation.....	56
2.2.9	Detection of TG activity.....	57
2.2.9.1	Preparation of cell extracts for TG activity assay.....	57
2.2.9.2	TG activity measurement.....	57
2.2.9.3	In situ TG activity assay.....	58
2.2.10	Molecular biology techniques.....	59
2.2.10.1	Transformation of bacteria with plasmid DNA.....	59
2.2.10.2	Storage of bacteria colonies.....	60
2.2.10.3	Amplification and extraction of plasmid DNA.....	60
2.2.10.4	Agarose gel electrophoresis of DNA.....	61
2.2.10.5	Restriction enzyme digestion of plasmid DNA.....	61
2.2.10.6	Dephosphorylation of plasmid DNA.....	61
2.2.10.7	Isolation of DNA from agarose gel.....	61
2.2.10.8	Ligation.....	62
2.2.10.9	RNA extraction.....	62
2.2.10.10	Quantification of nucleic acids.....	63
2.2.10.11	Reverse transcriptase polymerase chain reaction (RT-PCR).....	63

2.2.10.12	Polymerase chain reaction (PCR) .....	63
2.2.11	Subcloning of TG2 and Sdc-4 cDNA into mammalian expression vectors .....	64
2.2.11.1	Real time PCR .....	66
2.2.11.2	Mice genotyping .....	67
2.2.12	Transglutaminase-2 binding studies to heparin/HS .....	68
2.2.12.1	ELISA-based assay to measure TG2 binding to heparin and heparan sulfates .....	68
2.2.12.1.1	Immobilisation of heparin and fibronectin for solid binding assay .....	68
2.2.12.1.2	Solid binding assay .....	68
2.2.12.2	Surface Plasmon Resonance (SPR) .....	69
2.2.12.3	Cell adhesion to heparin/HS-coated plates .....	70
2.2.13	Statistical analysis .....	70

## **CHAPTER 3: OUTSIDE-IN ROLE OF TG2 IN CELL ADHESION: IMPLICATION OF SDC-4..... 71**

<b>3.1</b>	<b>Introduction.....</b>	<b>71</b>
<b>3.2</b>	<b>Results.....</b>	<b>74</b>
3.2.1	TG2 localisation in primary fibroblasts.....	74
3.2.2	Role of TG2 in the early stages of cell adhesion.....	78
3.2.3	Matrix-Transglutaminase-2 has an RGD-independent role in FAK activation.....	84
3.2.4	Importance of Sdc-4 in RGD-independent FAK phosphorylation induced by matrix TG2.....	87
<b>3.3</b>	<b>Discussion .....</b>	<b>94</b>

## **CHAPTER 4: INVESTIGATION ON TG2 BINDING TO SDC-4..... 98**

<b>4.1</b>	<b>Introduction.....</b>	<b>98</b>
4.1.1	Interactions of proteins with Heparin/HS.....	98
4.1.2	TG2 affinity for heparin .....	100
<b>4.2</b>	<b>Results.....</b>	<b>101</b>
4.2.1	Affinity of TG2 for heparin/HS .....	101
4.2.2	Cell-surface TG2 interacts with heparin and HS chains.....	108
4.2.3	Direct co-association of TG2 and HS chains of Sdc-4 at the cell surface.....	110
4.2.4	Binding of TG2 to Sdc-4 is not mediated by fibronectin .....	117
4.2.5	Visualisation of TG2-Sdc-4 association by fluorescence microscopy .....	121

4.3	Discussion .....	122
<b>CHAPTER 5: ROLE OF SDC-4 IN THE TRAFFICKING AND CELL-SURFACE LOCALIZATION OF TG2</b>		<b>126</b>
5.1	<b>Introduction.....</b>	<b>126</b>
5.1.1	Insight on TG2 cell-surface trafficking .....	126
5.1.2	Possible role of HS in mediating the cell-surface biological action of TG2 .....	127
5.2	<b>Results.....</b>	<b>128</b>
5.2.1	Role of Sdc-4 in the cell-surface localisation of TG2 in primary fibroblasts.....	128
5.2.2	Sdc-4 influences TG2 activity at the cell-surface.....	142
5.3	<b>Discussion .....</b>	<b>152</b>
<b>CHAPTER 6: PHYSIOLOGICAL SIGNIFICANCE OF TRANSGLUTAMINASE-2 BINDING TO SYNDECAN-4 IN KIDNEY FIBROSIS-----</b>		<b>154</b>
6.1	<b>Introduction-----</b>	<b>154</b>
6.1.1	TG2 and kidney fibrosis -----	154
6.1.2	Sdc-4 and renal diseases -----	155
6.1.3	TG2 and HSPG in kidney fibrosis -----	156
6.2	<b>Materials and Methods -----</b>	<b>158</b>
6.2.1	Experiment design -----	158
6.2.2	Induction of UUO-----	158
6.2.3	Preparation of kidney paraffin sections -----	159
6.2.4	Preparation of kidney cryosections -----	159
6.2.5	Masson's trichrome staining on kidney tissues-----	159
6.2.6	Multiphase image analysis-----	160
6.2.7	Measurement of Hydroxyproline by Amino Acid Analyser.-----	160
6.2.8	Detection of <i>in situ</i> TG activity in kidney tissues-----	161
6.3	<b>Results-----</b>	<b>162</b>
6.3.1	Lack of Sdc- is protective against the development of kidney fibrosis -----	162
6.3.2	Lack of Sdc-4 leads to lower in situ Transglutaminase activity -----	172
6.4	<b>Discussion-----</b>	<b>179</b>

**CHAPTER 7: GENERAL DISCUSSION .....182**  
**BIBLIOGRAPHY.....188**  
**APPENDIX.....213**

## Figures

<b>FIGURE 1-1</b> BIOCHEMICAL ACTIVITIES OF TRANSGLUTAMINASES .....	2
<b>FIGURE 1-2</b> STRUCTURE OF TG2 .....	3
<b>FIGURE 1-3</b> ALIGNMENT OF THE CATALYTIC SITE REGION OF THE HUMAN TG PROTEINS.....	7
<b>FIGURE 1-4</b> ACTIVATION OF FACTOR XIII.....	8
<b>FIGURE 1-5</b> CROSSLINKING REACTION CATALYSED BY FACTOR XIII A .....	8
<b>FIGURE 1-6</b> REPRESENTATION OF TG2 CORE PROMOTER AND REGULATORY FACTORS .....	14
<b>FIGURE 1-7</b> STRUCTURAL AND FUNCTIONAL ELEMENTS OF HUMAN TG2.....	16
<b>FIGURE 1-8</b> STRUCTURE OF GAG CHAINS .....	25
<b>FIGURE 1-9</b> PROTEOGLYCANS CLASSIFICATION .....	28
<b>FIGURE 1-10</b> STRUCTURE OF THE SDC FAMILY MEMBERS.....	32
<b>FIGURE 3-1</b> SIGNALLING EVENTS LEADING TO FA AND SF FORMATION UPON CELL ADHESION TO FN.....	72
<b>FIGURE 3-2</b> LOCALIZATION OF TG2 IN PRIMARY FIBROBLASTS ADHERING ON FN.....	74
<b>FIGURE 3-3</b> EXTRACELLULAR TG ACTIVITY IN PRIMARY FIBROBLASTS .....	75
<b>FIGURE 3-4</b> RT-PCR-BASED STUDY OF TG FAMILY MEMBERS IN MEF.....	76
<b>FIGURE 3-5</b> TG2 DISTRIBUTION IN MEF .....	77
<b>FIGURE 3-6</b> LACK OF TG2 IMPAIRS VINCULIN FA FORMATION.....	78
<b>FIGURE 3-7</b> LACK OF TG2 IMPAIRS ACTIN SF FORMATION .....	79
<b>FIGURE 3-8</b> BIOCHEMICAL CHARACTERISATION OF PEGFP-TG2 CONSTRUCT .....	81
<b>FIGURE 3-9</b> VINCULIN-CONTAINING FA FORMATION IS RESCUED BY RE-EXPRESSION OF TG2 CDNA .....	82
<b>FIGURE 3-10</b> FA FORMATION OF TG2 -/- MEF IS RESCUED BY EXTRACELLULAR TG2.....	83
<b>FIGURE 3-11</b> LACK OF TG2 IMPAIRS EARLY FAK PHOSPHORYLATION .....	84
<b>FIGURE 3-12</b> ADHESION TO FN-BOUND TG2 PROMOTES FAK PHOSPHORYLATION (Y397) IN TG2 -/- MEF IN A RGD-INDEPENDENT WAY .....	86
<b>FIGURE 3-13</b> ADHESION TO FN-BOUND BSA DOES NOT INDUCE RGD-INDEPENDENT FAK PHOSPHORYLATION (Y397).....	87
<b>FIGURE 3-14</b> CO-OPERATION OF SDC-4 AND TG2 IN RGD-INDEPENDENT FAK PHOSPHORYLATION .....	88
<b>FIGURE 3-15</b> CONTROLS ON THE EXPRESSION OF PCDNAHS4 VECTOR IN SDC-4 -/- CELLS .....	89
<b>FIGURE 3-16</b> ADD-BACK OF SDC-4 RESCUES TG2-MEDIATED RGD-INDEPENDENT FAK PHOSPHORYLATION IN SDC-4 -/- MDF.....	90
<b>FIGURE 3-17</b> CO-OPERATIVE ROLE OF SDC-4 AND TG2 IN SF FORMATION DURING RGD- INDEPENDENT CELL ADHESION.....	92
<b>FIGURE 3-18</b> RE-INTRODUCTION OF SDC-4 IN SDC-4 -/- MDF RESTORES TG2- MEDIATED RGD-INDEPENDENT SF FORMATION.....	93

<b>FIGURE 4-1</b> HEPARIN BINDING PROTEINS WITH PREDICTED SECONDARY STRUCTURE .....	100
<b>FIGURE 4-2</b> TG2 BINDING TO IMMOBILISED FN .....	102
<b>FIGURE 4-3</b> TG2 BINDING TO HEPARIN .....	103
<b>FIGURE 4-4</b> WESTERN BLOT ANALYSIS OF TG2-HEPARIN BINDING REACTION .....	104
<b>FIGURE 4-5</b> INTERFERENCE OF POSITIVELY CHARGED IONS ON TG2-BINDING TO IMMOBILISED HEPARIN.....	105
<b>FIGURE 4-6</b> BINDING OF TG2 TO HS .....	106
<b>FIGURE 4-7</b> SPR ANALYSIS OF TG2 AFFINITY FOR HEPARIN.....	107
<b>FIGURE 4-8</b> CELL ADHESION STUDIES ON HEPARIN/HS-COATED PLATES .....	109
<b>FIGURE 4-9</b> SDC-4 DETECTION IN TOTAL MEMBRANE EXTRACT FROM HOB.....	112
<b>FIGURE 4-10</b> TG2 DETECTION IN SDC-4 IMMUNOPRECIPITATES FROM HOB AND HOB-TG14.....	113
<b>FIGURE 4-11</b> SDC-4 DETECTION IN TG2 IMMUNOPRECIPITATES FROM HOB AND HOB-TG14.....	114
<b>FIGURE 4-12</b> TG2 DETECTION IN SDC-4 IMMUNOPRECIPITATES FROM SWISS 3T3 CELLS WITH INDUCIBLE EXPRESSION OF TG2 .....	115
<b>FIGURE 4-13</b> IMMUNOPRECIPITATION OF TG2 AND SDC-4 LARGELY RELIES ON SDC-4 HS CHAINS (1).....	116
<b>FIGURE 4-14</b> IMMUNOPRECIPITATION OF TG2 AND SDC-4 LARGELY RELIES ON SDC-4 HS CHAINS (2).....	117
<b>FIGURE 4-15</b> SCHEME OF TRIANGULAR ASSOCIATION OF TG2, SDC-4 AND FN .....	118
<b>FIGURE 4-16</b> INHIBITION OF TG2 BINDING TO FN USING P3 PEPTIDE .....	119
<b>FIGURE 4-17</b> IMMUNOPRECIPITATION OF TG2 AND SDC-4 IN THE PRESENCE OF COMPETITIVE CONCENTRATIONS OF P3 PEPTIDE.....	120
<b>FIGURE 4-18</b> CO-LOCALISATION OF TG2 AND SDC-4 IN HOB .....	121
<b>FIGURE 4-19</b> PUTATIVE HEPARIN-BINDING SITE CONSERVED IN TG2 FROM DIFFERENT SPECIES .....	124
<b>FIGURE 5-1</b> TG2 STAINING IN WILD TYPE AND SDC-4 NULL MDF.....	129
<b>FIGURE 5-2</b> VISUALISATION OF TG2 BY DUAL PHASE CONTRAST CONFOCAL MICROSCOPY .....	130
<b>FIGURE 5-3</b> CO-STAINING OF TG2 AND SF IN WILD TYPE AND SDC-4 NULL MDF.....	131
<b>FIGURE 5-4</b> TG2 LOCALISATION IN WILD TYPE AND SDC-4 NULL MDF ADHERING ON FN.....	133
<b>FIGURE 5-5</b> CO-STAINING OF TG2 AND SDC-4 IN MDF.....	134
<b>FIGURE 5-6</b> ANALYSIS OF TG2 DISTRIBUTION IN CELL COMPARTMENTS OF WILD TYPE AND SDC-4 NULL MDF.....	136
<b>FIGURE 5-7</b> CELLULAR DISTRIBUTION OF TG ACTIVITY IN WILD TYPE AND SDC-4 NULL MDF.....	137
<b>FIGURE 5-8</b> TOTAL TG ACTIVITY MEASUREMENT IN WILD TYPE AND TG2 NULL MEF.....	138

<b>FIGURE 5-9</b> MATRIX-TG2 DISTRIBUTION IN WILD TYPE AND SDC-4 NULL CELLS .....	140
<b>FIGURE 5-10</b> ANALYSIS OF TG2 EXPRESSION IN PRIMARY FIBROBLASTS .....	141
<b>FIGURE 5-11</b> CELL SURFACE HS AFFECT EXTRACELLULAR TG2 ACTIVITY OF MDF ADHERING ON FN. ....	143
<b>FIGURE 5-12</b> TITRATION OF TG2-ACTIVITY INHIBITION BY SURFEN.....	144
<b>FIGURE 5-13</b> DOSE-RESPONSE CURVES OF TG2 IN THE PRESENCE OF SURFEN .....	144
<b>FIGURE 5-14</b> SDC-4 RESCUES THE LEVEL OF EXTRACELLULAR TG2 ACTIVITY IN PRIMARY FIBROBLASTS .....	145
<b>FIGURE 5-15</b> ANALYSIS ON SURFEN EFFECT ON CELL-ADHESION ON FN .....	147
<b>FIGURE 5-16</b> <i>IN SITU</i> MEASUREMENT OF EXTRACELLULAR TG2 ACTIVITY. ....	149
<b>FIGURE 5-17</b> VALIDATION OF FITC-CADAVERINE INCORPORATION AS TG2 ACTIVITY ASSAY FOR PRIMARY FIBROBLASTS .....	150
<b>FIGURE 5-18</b> STUDY OF HEPARIN-BINDING EFFECT ON TG2 ACTIVITY .....	151
<b>FIGURE 6-1</b> EXTRACELLULAR MATRIX ACCUMULATION AFTER INDUCTION OF KIDNEY FIBROSIS-MASSON'S TRICHROME STAINING.....	164
<b>FIGURE 6-2</b> QUANTIFICATION OF SCARRING INDEX IN NORMAL AND FIBROTIC (UUO) KIDNEYS .....	165
<b>FIGURE 6-3</b> COLLAGEN ACCUMULATION IN THE PROXIMAL TUBULES AFTER UUO INDUCTION .....	166
<b>FIGURE 6-4</b> COLLAGEN ACCUMULATION IN THE GLOMERULI AFTER UUO INDUCTION.....	167
<b>FIGURE 6-5</b> QUANTIFICATION OF SCARRING INDEX IN THE UNTREATED KIDNEYS OF MICE WITH UUO INDUCTION.....	168
<b>FIGURE 6-6</b> EFFECT OF GENDER ON SCARRING INDEX OF NORMAL KIDNEYS.....	169
<b>FIGURE 6-7</b> EFFECT OF GENDER ON SCARRING INDEX ON KIDNEYS SUBJECTED TO UUO .....	170
<b>FIGURE 6-8</b> HYDROXY-PRO QUANTIFICATION IN NORMAL AND FIBROTIC KIDNEYS.....	171
<b>FIGURE 6-9</b> MEASUREMENT OF TG ACTIVITY IN SITU IN NORMAL AND FIBROTIC (UUO) KIDNEYS FROM WILD TYPE MICE.....	173
<b>FIGURE 6-10</b> MEASUREMENT OF TG ACTIVITY IN SITU IN NORMAL AND FIBROTIC (UUO) KIDNEYS FROM SDC-4 <sup>-/-</sup> MICE .....	174
<b>FIGURE 6-11</b> QUANTIFICATION OF TG IN SITU ACTIVITY IN NORMAL AND FIBROTIC (UUO) KIDNEYS .....	175

**FIGURE 6-12** CORRELATION BETWEEN TG ACTIVITY AND RENAL SCARRING INDEX AFTER THE INDUCTION OF UUO. ....176

**FIGURE 6-13** EFFECT OF SDC-4 ON THE CORRELATION BETWEEN TG IN SITU ACTIVITY AND SCARRING INDEX .....177

**FIGURE 6-14** TG2 LEVEL IN KIDNEY EXTRACTS FROM WILD TYPE AND SDC-4 NULL MICE.....178

**FIGURE 7-1** EVENTS MEDIATED BY TG2 ASSOCIATION WITH SDC-4 .....187

## Tables

<b>TABLE 1-1</b> HUMAN TRANSGLUTAMINASES: GENES AND PROTEINS .....	6
<b>TABLE 1-2</b> CLASSIFICATION OF PROTEOGLYCANS BASED ON CELLULAR LOCALISATION AND PREDOMINANT GAG CHAIN .....	28
<b>TABLE 2-1</b> PRIMERS USED FOR PCR REACTIONS ON GENOMIC DNA .....	40
<b>TABLE 2-2</b> PRIMERS USED FOR PCR REACTIONS ON CDNA .....	41
<b>TABLE 2-3</b> PARAMETERS FOR CELL TRANSFECTION USING NUCLEOFECTOR KIT, AMAXA. ....	48
<b>TABLE 2-4</b> COMPOSITION OF SDS-PAGE RESOLVING GELS CONTAINING DIFFERENT ACRYLAMIDE AMOUNTS .....	52
<b>TABLE 2-5</b> COMPOSITION OF SDS-PAGE STACKING GELS CONTAINING DIFFERENT ACRYLAMIDE AMOUNTS .....	53
<b>TABLE 2-6</b> DILUTION FACTORS FOR PRIMARY ANTIBODIES USED FOR PROTEIN IMMUNODETECTION VIA WESTERN BLOTTING.....	54
<b>TABLE 2-7</b> DILUTION FACTORS FOR SECONDARY ANTIBODIES USED FOR PROTEIN IMMUNODETECTION IN WESTERN BLOTTING.....	55
<b>TABLE 6-1</b> EXPERIMENTAL DESIGN FOR IN VIVO STUDY ON SDC-4 AND TG2 CONTRIBUTION TO KIDNEY FIBROSIS .....	158

## ***Chapter 1: Introduction***

### ***1.1 The Transglutaminase family***

The term transglutaminase (TG) was introduced in 1957 by Sarkar and colleagues (Sarkar et al., 1957) to describe the transamidating activity detected in brain and liver extracts from guinea pig. After this first discovery, transglutaminase activity has been described in microorganisms (Kanaji et al., 1993), plants (Del Duca et al., 1995), invertebrates (Mehta et al., 1992; Singh and Mehta, 1994) and higher animals, including fish (Oppen-Berntsen et al., 1990; Yasueda et al., 1994), amphibians (Zhang and Masui, 1997) and birds (Puszkin and Raghuraman, 1985).

#### **1.1.1 Post-translational modification of proteins**

The main role of transglutaminases is the post-translational modification of proteins (Figure 1-1), which mainly occurs through transamidation. The most studied reaction is protein crosslinking, consisting in the formation of a N<sup>ε</sup>(γ-glutamyl)lysine isodipeptide bond between a deprotonated Lys residue (donor) of one protein and a Gln residue (acceptor) of a second protein or of the same polypeptide chain (Lorand and Graham, 2003). The transamidation reaction is Ca<sup>2+</sup>-dependent and it occurs in two separate steps; firstly the acceptor binds to the enzyme forming a γ-glutamylthioester with the Cys residue of the active site. The complex formed is defined as an acylenzyme intermediate; ammonia (NH<sub>3</sub>) is released during this process and it is immediately protonated to the NH<sub>4</sub><sup>+</sup> form under physiological conditions. In the second step the donor binds to the acylenzyme intermediate and attacks the γ-glutamylthioester bond, re-establishing the original form of the Cys in the TG active centre. The covalent isodipeptide bond formed by TG is stable and resistant to proteolysis, thus increasing the resistance of crosslinked proteins (and therefore tissues where they are localised) to chemical, enzymatic and physical degradation (Folk and Finlayson, 1977).

Even though the crosslinking is considered as the main protein-modification, other TG-catalysed reactions (Figure 1-1) have important roles in cell/tissue homeostasis. For example, protein esterification, catalysed by TG1 has an essential role in the final differentiation of keratinocytes (Nemes et al., 1999). Deamidation, which replaces a

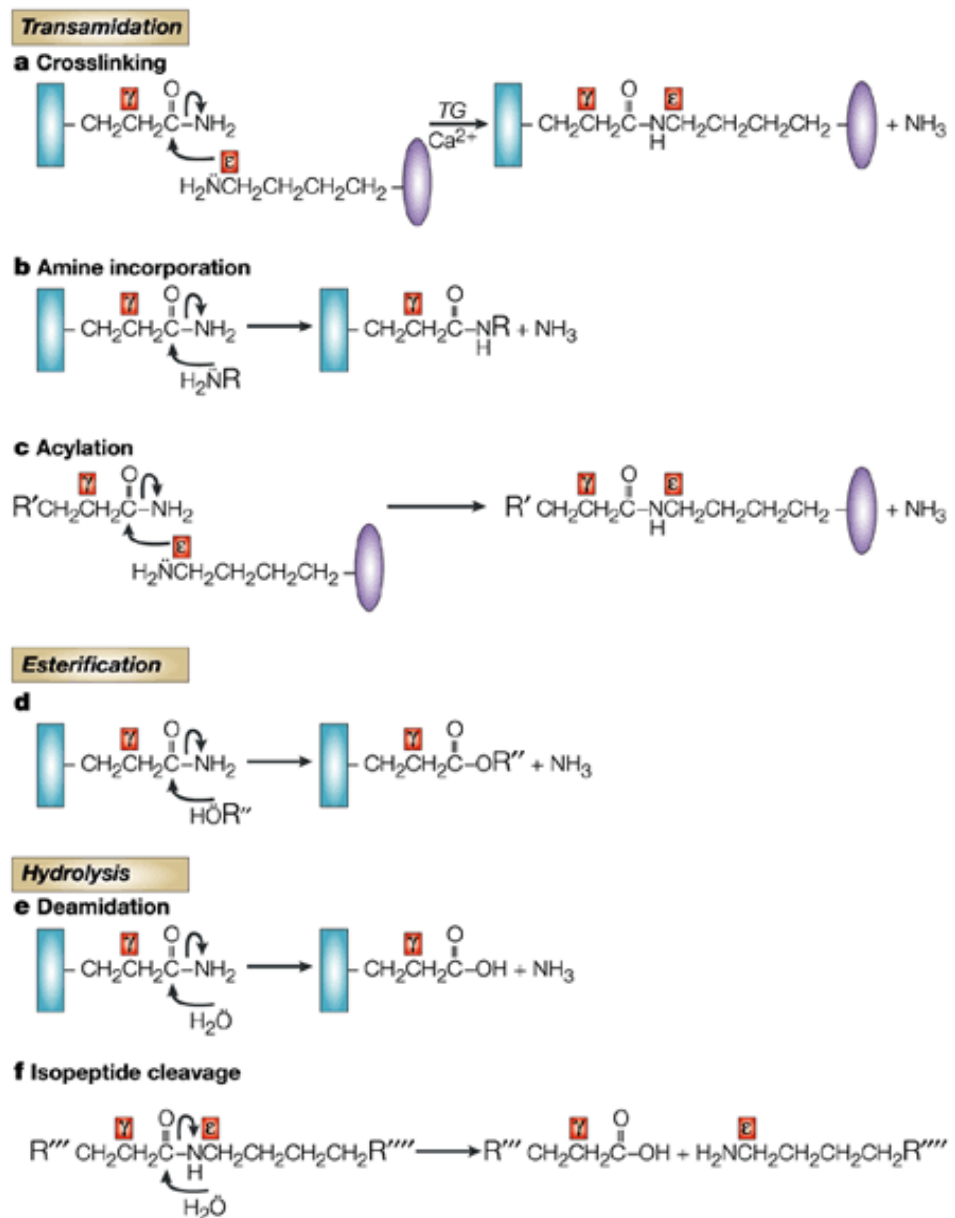


**Figure 1-1 Biochemical activities of transglutaminases.** Image taken from Lorand and Graham (2003).

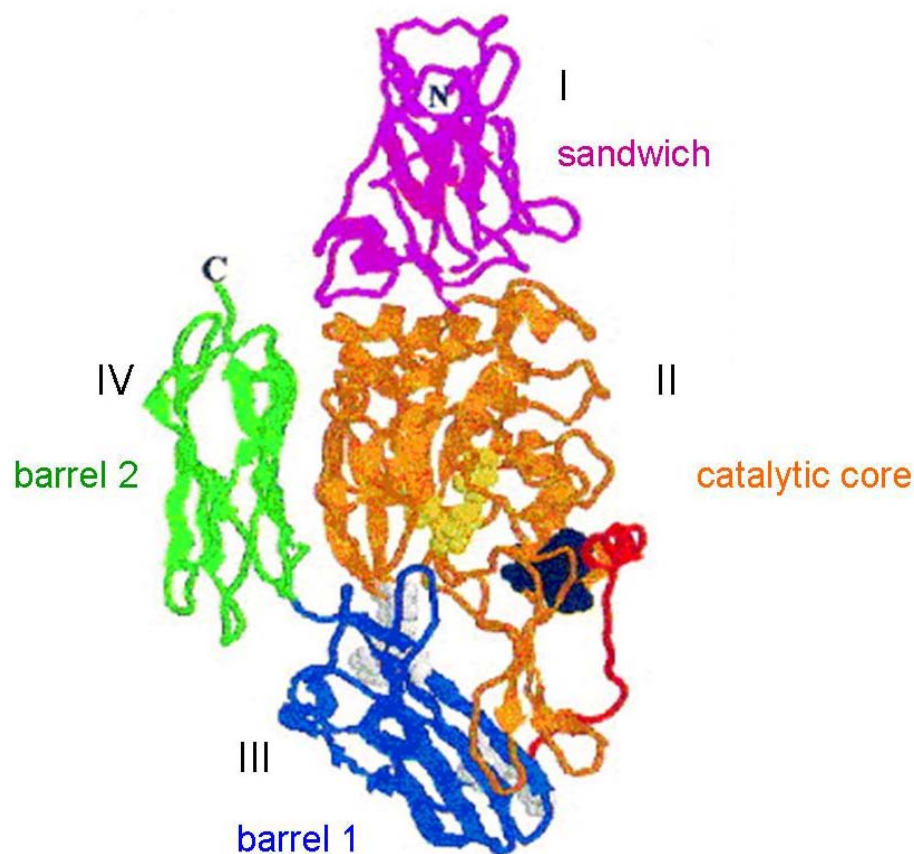


**Figure 1-2 Structure of TG2.** Adapted from (Griffin et al., 2002). The backbone structure of TG2 is represented; domains I-V are represented in magenta, orange, blue and green respectively. The regulatory loop between domain II and III is shown in red. Amino acids involved in the active site (Cys277, His335, Asp358),  $\text{Ca}^{2+}$ -binding (Ser449, Pro446, Glu451, Glu452) and GTP interaction (Ser171, Lys173, Arg478, Val479, Arg580) are coloured in yellow, dark blue and grey, in order.

### 1.1.2 Regulation of TG activity

Tissue transglutaminase (tTG or TG2) is used as a model to study the catalytic mechanism of all the TG family. In this process, the Cys of the active plays a central role, forming an acyl-enzyme thioester intermediate with a peptide-bound Gln; this intermediate can then react with a nucleophile (primary amine, peptide-bound Lys or water), resulting in amine incorporation, protein crosslinking or deamidation (Folk and Finlayson, 1977). Even though there is a certain level of substrate specificity in TG2-mediated transamidation, many proteins can be potential targets, given their abundance of exposed Gln and Lys residues (Esposito and Caputo, 2005); for this reason, cofactors and spatial localisation of

TG2 play important roles in preventing excessive protein crosslinking and potential autoimmune activation following protein deamidation.

The charge-relay catalytic triad of TG2 (Cys277, His335, Asp358) is analogous to the one of thiol proteinases like papain; Cys277 localisation makes it highly reactive in the presence of the activator  $\text{Ca}^{2+}$ , and determines the formation of thioesters with peptidylglutamine partners in the protein substrate. The activity is largely decreased in the absence of  $\text{Ca}^{2+}$ , when the enzyme assumes the basic latent conformation and the active site, located within domain 2 is “buried” by domains 3 and 4, thus preventing the contact with substrates. In these conditions, also, Cys277 reactivity is diminished by the formation of hydrogen bonds with either Cys336 or the phenolic hydroxyl group of Tyr525. The structure of TG2 is shown in Figure 1-2.

The first insight into TG2 GTPase activity came from the discovery that its transamidating activity was inhibited by GTP in an allosteric fashion (Achyuthan and Greenberg, 1987; Greenberg et al., 1991). Later on, a novel G protein ( $G_h$ ) isolated from rat liver plasma membrane came out to be TG2, thus indicating the binding/hydrolysis potential of TG2 (Nakaoka et al., 1994). TG2 has a high affinity for GTP/GDP and can hydrolyse GTP in a rate comparable to small Ras-type G-proteins and  $\alpha$  subunits of large heterotrimeric G proteins; the GTP/GDP-bound form does not have transamidating activity, that can however be restored in the presence of  $\text{Ca}^{2+}$  (Achyuthan and Greenberg, 1987). This represents an efficient mechanism of regulating the different functions of TG2 in separate cell compartments: in the cytosol, where the concentration of free  $\text{Ca}^{2+}$  is low (0.1  $\mu\text{M}$ ) and GTP is present at a concentration of 100-150  $\mu\text{M}$ , TG2 is mainly in GTP/GDP-bound form. If cells are treated with a calcium ionophore (i.e. calcimycin), which transport free calcium across membranes by diffusion, the intracellular level of  $\text{Ca}^{2+}$  becomes high enough to activate TG2 (Siefiring, Jr. et al., 1978; Zhang et al., 1998). An analogous situation is present when the cell loses calcium homeostasis following tissue damage, apoptosis or necrosis (Afford and Randhawa, 2000; Nicholas et al., 2003); in this case, TG2-mediated crosslinking can prevent the release of intracellular proteins and the consequent inflammatory response (Fesus et al., 1987). TG2 is also secreted to the cell surface and extracellular matrix, where the higher  $\text{Ca}^{2+}$ -concentration (0.5-1.5 mM) switches the enzyme into the catalytically active form, which is responsible for protein crosslinking (Achyuthan and Greenberg, 1987; Lansdown, 2002).

### **1.1.3 Substrates of transglutaminases**

TG substrates have been identified in the extracellular space and in the intracellular compartment, and their expression is a key regulator of the specific functions of TG family members. Many extracellular proteins are known substrates of the cross-linking reactions, for example fibronectin (Barsigian et al., 1991), collagen (Kleman et al., 1995), vitronectin (Sane et al., 1988) and osteonectin (Prince et al., 1991); these substrates point to a role for TG in the stabilisation of the extracellular matrix (Kleman et al., 1995). Several cytoskeletal proteins have also been characterised as TG substrates, such as actin, tubulin and cytokeratin (Robinson et al., 2007), thus suggesting a role for TG in the covalent stabilisation of the cytoskeleton in a similar way to its action in the ECM. Another class of TG substrates is represented by histones, which can be modified by TG2 *in vitro*, affecting chromatin condensation which occurs during apoptosis (Ballestar et al., 1996).

The study of specific crosslinking substrates of TG activity is not easy, since the products of transamidation are highly cross-linked insoluble polymers with a complicated structure, thus difficult to analyse. Furthermore, when the products of TG activity are investigated *in vitro*, the concentration of  $\text{Ca}^{2+}$  used to activate the enzymes can activate a variety of other enzymes, including proteases (i.e. calpain), introducing another source of protein modification independent from TG (Velasco et al., 1990). Moreover, the state of phosphorylation (Owen et al., 1988), the proteolytic cleavage or the loss of native compact structure of a protein can influence their transamidation (Griffin et al., 2002). Studies based on incorporation of labelled primary amines or Gln-rich peptides have shown that different TG are selective in the Gln residues used for the transamidation, even within the same substrate protein (Fesus et al., 1986); also, in different tissues, distinct proteins can act as either acyl donors or acceptors or both. A list of TG substrates is presented in Appendix 1.

## ***1.2 Transglutaminases in mammalian tissues***

Nine distinct genes for transglutaminases have been isolated in mammalian tissues, and they include factor XIII (zymogen that is activated into transglutaminase factor XIIIa), keratinocytes TG, ubiquitous type 2 TG, epidermal TG, prostatic TG, type 5-7 TG and the TG-like erythrocyte-band 4.2 (Table 1-1).

Protein	Gene	Gene locus	Gene size (kb)	Number of exons	Amino acid residues	Molecular weight (kDa)
TG1	TGM1	14q11.2-13	14	15	814	90
TG2	TGM2	20q11-12	37	13	686	78
TG3	TGM3	20q11-12	43	13	692	77
TG4	TGM4	3p21-p22	35	13	684	77
TG5	TGM5	15q15.2	35	13	720	81
TG6	TGM6	20q11	45	13	625	70
TG7	TGM7	15q15.2	26	12	710	80
F XIIIa	F13A1	6p24-25	160	15	732	83
Band 4.2	EPB4.2	15q15.2	20	13	690	72

**Table 1-1 Human transglutaminases: genes and proteins.** *Adapted from Mehta (2005).*

The mammalian TG isoforms have a high level of structural homology, belong to the superfamily of papain-like proteins and are codified by genes that arose from duplication/rearrangement of an ancestral gene. All the members of the TG family contain a catalytic triad of Cys-His-Asp or Cys-His-Asn, with the exception of erythrocyte band 4.2 which presents an Ala residue instead of the Cys of the active site, resulting in a loss of activity (Figure 1-3).

```

361 LSYLRTGYSV P YGQCWVFA G VTTTVLRCLG TG1
263 RWKNHGCQRV K YGQCWVFA A VACTVLRCLG TG2
259 NWKKS GFSPV R YGQCWVFA G TLNTALRSLG TG3
254 QQYYNTKQAV CF GQCWVFA G ILTTVLRALG TG4
269 QWHATGCQPV R YGQCWVFA A VMCTVMRCLG TG5
260 KWLKGRYPV K YGQCWVFA G VLCTVLRCLG TG6
265 QWSARGGQPV K YGQCWVFA S VMCTVMRCLG TG7
301 LEYRSSETPV R YGQCWVFA G VFNTFLRCLG FXIIIa
263 QMLTGRGRPV YD GQAWVLA A VACTVLRCLQ Bands 4.2

```

**Figure 1-3 Alignment of the catalytic site region of the human TG proteins.** *Alignment redrawn from Mehta (2005). The amino acids of the core fold containing the catalytic cysteine residue (C) are shown in bold red text.*

### 1.2.1 Factor XIII

Factor XIII (FXIII), or fibrin stabilising factor, is a well characterised plasma transglutaminase with a Mr of 83 kDa involved in blood coagulation. It circulates in the blood in form of a heterotetramer (A<sub>2</sub>B<sub>2</sub>) (Lorand et al., 1980) composed by two catalytic A subunits (XIIIa), consisting of 731 amino acids (Ichinose et al., 1986a), and two non-catalytic B subunits (XIIIb), consisting of 641 amino acids (Ichinose et al., 1986b). Sequence analysis showed that the B subunit is related to the family of proteins containing the small consensus repeats, or Sushi domains (involved in protein–protein and protein–ligand interactions) (Ichinose et al., 1990); B subunits are also highly sialylated, resulting in an elevated heterogeneity (Lorand et al., 1981). Analysis of the A subunit showed instead homology with Ca<sup>2+</sup>-dependent transglutaminases, with the papain-like catalytic domain made of Cys-His-Asp (Pedersen et al., 1994). In particular, the catalytic subunit presents four distinct domains: an N-terminal β-sandwich, the papain-like active site, a barrel 1 and a barrel 2 domain (Yee et al., 1994). FXIII is a zymogen and it is activated in the final stages of the coagulation process by the subsequent action of thrombin and Ca<sup>2+</sup>, as illustrated in Figure 1-4. In the first step, thrombin catalyses the cleavage of a 37 residue peptide (activation peptide) from the N-terminus of the two A subunits by hydrolysing the peptide bond between Arg37 and Gly38 (Schwartz et al., 1973; Takagi and Doolittle, 1975); the cleavage of activation peptides also weakens the interactions between A and B

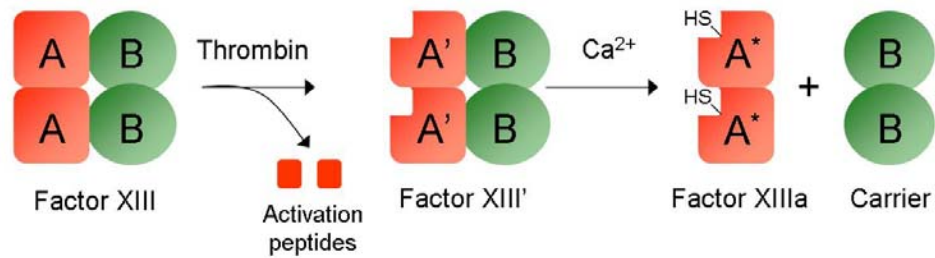


**Figure 1-4 Activation of Factor XIII.** In the first step the zymogen FXIII is converted by thrombin to FXIII' allozymogen, that does not have catalytic activity; in the second step the calcium-dependent dissociation of the B subunits determines the conformational changes necessary for the presentation of the catalytic site in the catalytic subunit.

Thrombin plays a central role in the homeostatic process by synchronising the conversion of fibrinogen into fibrin and the activation of FXIII; moreover, fibrin itself can accelerate the thrombin-mediated activation of FXIII (Janus et al., 1983; Lewis et al., 1985) and facilitate the dissociation of the inert modified zymogen FXIII' generating the active enzyme at a physiological plasma concentration of Ca<sup>2+</sup>. The dissociation step can also take place in the absence of Ca<sup>2+</sup>, but the presence of fibrin is essential, this is a regulatory mechanism that allows crosslinking activity of FXIIIa to take place only when the specific substrate is present (Curtis et al., 1974).

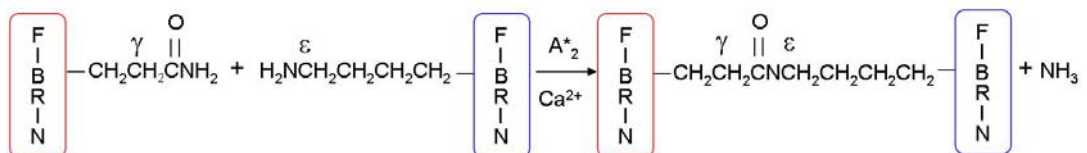


**Figure 1-5 Crosslinking reaction catalysed by factor XIIIa.**

The crosslinking reaction catalysed by the active FXIIIa (Figure 1-5) is a transamidation that occurs between specific Gln and Lys residues on adjacent proteins (fibrin fibres or molecules incorporated in the fibrin matrix). There are two different kinds of crosslinking taking place: the first one determines the end-to-end linear association of fibrin units, the second one involves  $\alpha$  chains of fibrin molecules located in separated filaments; together, the two processes contribute to the formation of strong urea-insoluble clots (Chen and Doolittle, 1971; McKee et al., 1970). The crosslinking action of FXIIIa has little effect on the morphology of the single fibrin fibres, but it changes dramatically the properties of the clot, providing it with stiffness that allows wound closure and with resistance against thrombolytic enzymes (Lorand, 2001). In particular, the resistance to thrombolytic agents is determined by FXIIIa-mediated covalent attachment of the  $\alpha_2$  plasmin inhibitor present in plasma to the  $\alpha$  chains of some fibrin fibres (Ichinose et al., 1983; Sakata and Aoki, 1982).

There are several pathological conditions related to the deficiency of FXIII, which is an autosomal recessive disorder often diagnosed after birth from bleeding of the umbilical cord (Seitz et al., 1989). Common symptoms are superficial bruises and hematomas in subcutaneous tissue and muscle, sometimes accompanied by bleeding, moreover, affected individuals can present abnormal wound healing and repetitive spontaneous miscarriage due to impaired haemostasis and angiogenesis; these symptoms can be reversed by FXIII supplementation (Muszbek et al., 2008). In 25% of the patients FXIII deficiency causes intracranial haemorrhage, which is the main cause of death (Ichinose, 2005).

### **1.2.2 Keratinocyte TG (Type 1 or TG<sub>K</sub>)**

TG1 is expressed in the granular, suprabasal and spinous layers of the epidermis (Iizuka et al., 2003; Thacher and Rice, 1985), where is involved in the formation of the cornified envelope (CE), the outermost protective layer of the epidermis. TG1 is present as a zymogen of approximately 106 kDa, with a low specific activity, in differentiating keratinocytes. When the cells reach the final stages of the differentiation, TG1 is converted by proteolysis into a 10, 33 and 67 kDa complex, where the different subunits are held together via non-covalent binding (Kim et al., 1995). This complex is characterised by high transamidating activity and is responsible for the enzymatic action of TG1. Calpain (intracellular, Ca<sup>2+</sup>-dependent) and cathepsin D (lysosomal) are the candidate proteases

involved in the formation of the 10/33/67 kDa complex by cleavage of the cleavage sites exposed at the N-terminus of each fragment (Egberts et al., 2004; Kim and Bae, 1998). Even though TG3 and TG5 are involved in CE formation together with TG1, it appears that the different enzymes are involved in separate processes, since mice lacking TG1 have an aberrant CE formation that can not be compensated by TG3 or TG5 (Hitomi, 2005; Matsuki et al., 1998). Mutations in TG1 are also the most common cause of autosomal recessive congenital ichthyosis (ARCI), presenting a structurally defective or attenuated cornified cell envelope (Mehta, 2005). Several of these mutations have been characterised and mostly consist of missense or nonsense mutations leading to changes in the binding site for transcription factors in the promoter region (Herman et al., 2009).

### **1.2.3 Epidermal TG (Type 3 or TG<sub>E</sub>)**

Type 3 transglutaminase is expressed in several tissues, but the main role is in the epidermis, where, together with TG1 (paragraph 1.2.2) it participates in the formation of the CE through the crosslinking of different components (Candi et al., 1999). The most abundant substrates of TG3 are loricrin, small Pro-rich proteins (SPRs) and involucrin; these proteins are rich in Gln and lys and their main function is the composition of the CE. TG3 has also a role in the hair follicle, where the crosslinking of trichohyalin and keratin intermediate filaments determines the morphogenesis of the hair fibre by hardening the inner root cover (Lee et al., 1996). Preliminary studies performed on TG3 *-/-* mice demonstrated the role of the enzyme in the ultrastructure of hair and whiskers related to altered crosslinking (Thiebach et al., 2007). The enzyme is expressed as a soluble pro-enzyme of 77 kDa, which is converted by cathepsin L-mediated proteolysis into two globular domains that remain held together, an N-terminal of 50 kDa, bearing the active site, and a C-terminal of 27 kDa (Cheng et al., 2006; Kim et al., 1990). The site for proteolytic digestion is located in a flexible loop which connects the two domains; this loop is specific for transglutaminase 3 in terms of length and sequence, and the cleavage of analogous sites in TG2 or FXIII determines loss of activity of the enzymes (Kim et al., 2001). There is biochemical and crystallographic evidence of TG3 active site binding to GTP/GDP with a structural motif conserved between TG3 and TG2; as shown for TG2, TG3 is also able to hydrolyse GTP (Ahvazi et al., 2004; Candi et al., 2004).

To date, there are not TG3 mutations linked to specific diseases, but the expression of TG3 has been shown to be down-regulated in certain cancers such as oesophageal, head and neck squamous cell carcinoma and in laryngeal carcinoma (Mehta, 2005)

#### **1.2.4 Prostate TG (Type 4 or TG<sub>p</sub>)**

Many of the information regarding prostate transglutaminase, or TG4, came from the rat isoforms of the enzyme, dorsal protein 1 (DP1) (Ho et al., 1992). In rat the enzyme is highly expressed in the dorsal prostate, coagulatory gland and lateral type 1 prostate (Hayashi et al., 1991), and the expression is regulated by androgens (Ho et al., 1992). The main function of DP1 is considered to be the cross-linking of proteins involved in the formation of the copulatory plug after mating (Wilson and French, 1980).

The human isoform of TG4 has a lower level of expression compared to DP1 and its function has not been fully determined yet. The enzyme may be involved in semen coagulation or in the process of semen transfer to the female by crosslinking seminal plasma components to the surface of the male gametes (Dubbink et al., 1998; Porta et al., 1986). Interestingly, there is only one transcript produced by the gene codifying for human TG4, that can then mature in two splicing isoforms, one of which is characterised by in frame insertions of an antisense Alu sequence of 135 bp. The Alu sequence does not interfere with the functionality of the enzyme, but may play a role in the localisation of the protein within the cell and possibly in the excretion of prostate transglutaminase (Makalowski et al., 1994).

#### **1.2.5 TG X (Type 5)**

TG5 cDNA was firstly isolated from human foreskin keratinocytes; further studies showed that TG5 is mainly expressed in the granular layer of the epidermis where it is involved in keratinocytes differentiation and, together with TG1 and TG3 it contributes to the formation of the CE (Candi et al., 2002). Recent studies have shown TG5 expression in other tissues, such as mammary and salivary glands, prostate and placenta, thus suggesting the involvement of the enzyme in other physiological functions (Candi et al., 2004). In an analogous way to TG1 and TG3, TG5 is synthesised as an 81 kDa protein that does require proteolytic degradation to become active (Pietroni et al., 2008). As shown for TG2 and TG3, TG5 is also able to bind and hydrolyse GTP (Candi et al., 2004); GTP/GDP binding

is a regulator of the  $\text{Ca}^{2+}$ -dependent crosslinking activity of the enzyme, even though the ability of GTP/GDP to inhibit TG5 activity is lower compared to the inhibition potential on TG2; TG5 also responds less to  $\text{Ca}^{2+}$ -mediated activation compared to TG2 (Candi et al., 2004).

Mutations which cause loss of function of TG5 are linked to acral peeling skin syndrome, an autosomal recessive genodermatosis characterized by the shedding of the outer epidermis (Cassidy et al., 2005).

### **1.2.6 TG Y (Type 6)**

TG6 is part of the TG expressed and active in the basal epidermal layers and it is the closest homologue of TG3 (Grenard et al., 2001); as TG3, TG6 appears to be involved in the formation of CE and in hair morphogenesis (Thiebach et al., 2007).

### **1.2.7 TG Z (Type 7)**

TG7 is codified by a gene localised on chromosome 15 in a cluster including the gene for TG5 and for the erythrocyte band 4.2 and it was initially identified in human prostate carcinoma tissue by Grenard and colleagues (Grenard et al., 2001). Studies on the expression of the enzyme have shown a widespread low expression level, with peaks in the female reproductive system (uterus, placenta, ovaries and mammary gland), fetal tissues, testis and lungs (Grenard et al., 2001). No specific functions have been ascribed to TG7 so far, but the putative protein is known to possess transamidating activity and it contains a conserved  $\text{Ca}^{2+}$ -binding site.

### **1.2.8 Erythrocyte membrane protein band 4.2**

Human erythrocyte band 4.2 is a highly expressed membrane-associated protein of 77 kDa (Korsgren and Cohen, 1986; Korsgren and Cohen, 1988) with an essential but still not fully defined function in erythrocytes (Ideguchi et al., 1990; Rybicki et al., 1988). Protein band 4.2 has high sequence homology with guinea pig liver transglutaminase and subunit A of factor XIII, including the region containing the active site for transamidation activity (Folk, 1980; Lorand and Conrad, 1984). Interestingly, however, the protein does not have demonstrable crosslinking activity when tested in vitro (Korsgren et al., 1990), therefore its

role in erythrocyte functionality could be purely structural. Studies on the expression pattern of protein band 4.2 have revealed high expression level in bone marrow, fetal spleen and fetal liver, in accordance with its role in hematopoietic cells; no expression was detected in the other tissues (Grenard et al., 2001).

### **1.2.9 Tissue TG (Type 2 or TG<sub>T</sub>)**

TG2 is a widespread member of the TG family, with distinct functions in different cellular locations. TG2 is a peculiar member of the TG family since it can act as a GTPase (Nakaoka et al., 1994), protein disulfide isomerase (Hasegawa et al., 2003) and protein kinase (Mishra et al., 2007) together with having transamidating activity.

#### **1.2.9.1 Organisation and regulation of TG2 gene**

The gene for TG2 measures 32.5 kb and is located in chromosome 20 of the human genome (in mouse the gene is localised in chromosome 2, in a region syntenic to human chromosome 20) (Nanda et al., 1999). The gene contains 13 exons and 12 introns, with intron size ranging from 921 bp to >5kb and a total codifying region of 4 kb, of which 50% is constituted by exon XIII, containing the coding region of the protein C-terminus (Gentile et al., 1994; Lu et al., 1995). There are several responsive elements and binding sites for regulating factors in a functional TG2 promoter, as indicated in Figure 1-6. In particular, CAAT and TATA boxes, together with 4 SP sites upstream to the ATG starting codon are sufficient to guarantee a high constitutive transcription level (Lu et al., 1995). SP1 and SP2 sites can be methylated, and this has an influence on the level of expression of TG2 in different cell types/tissues (Aeschlimann and Thomazy, 2000). Methylation has a function in negative regulation of TG2 expression, thus balancing the high basal level of transcription (Lu et al., 1995). On the other side, treatment of cell with DNA demethylating drug 5-azacytidine determines an increase in TG2 level (Lu and Davies, 1997). Retinoids have a strong effect in promoting TG2 transcription in several cell types and they are considered as the most generalised inducers of TG2 expression (Aeschlimann and Thomazy, 2000). It has been shown that treatment of rats with retinoic acid determines an augmented TG2 expression and activity (Driscoll et al., 1997), whereas lack of vitamin A can determine a decreased level of TG2 expression in some body tissues (Aeschlimann and Paulsson, 1994; Verma et al., 1992). There are experimental evidence of the action of different retinoids in TG2 activation; the specificity of expression of these molecules and

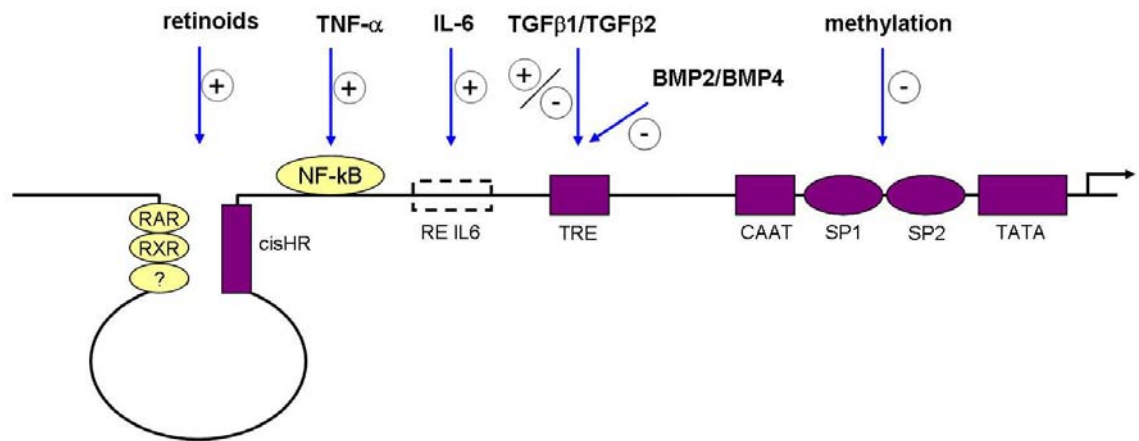


**Figure 1-6 Representation of TG2 core promoter and regulatory factors.** Redrawn from (Aeschlimann and Thomazy, 2000). RAR, retinoic acid receptor; RXR, retinoid X receptor; cisHR, cis regulatory element for retinoid activation; RE IL6, interleukin-6 responsive element; TRE, TGF- $\beta$  response element; SP1 and SP2, SP1 and SP2 binding sites; NF-kB, nuclear factor kB; TNF- $\alpha$ , tumour necrosis factor- $\alpha$ ; IL-6, interleukin-6; TGF $\beta$ 1 and TGF $\beta$ 2, transforming growth factor  $\beta$ 1 and  $\beta$ 2; BMP2 and BMP4, bone morphogenetic protein 2 and 4.

TG2 promoter also contains a responsive element (TRE) for members of the transforming growth factor- $\beta$  (TGF- $\beta$ ) family, in particular TGF- $\beta$ 1 and TGF- $\beta$ 2, which can induce or inhibit TG2 expression in a tissue-specific manner. In particular, there is a regulatory loop involving TG2 and TGF- $\beta$ 1, since the expression of the growth factor is positively regulated by TG2 (Kojima et al., 1993). TRE element also is involved in the transcriptional repression mediated by bone morphogenetic proteins (BMP) 2 and 4 (Ritter and Davies, 1998). Another class of molecules involved in the regulation of TG2 expression is pro-inflammatory cytokines, in particular interleukin-6 (IL-6) can positively affect TG2 transcription by binding its responsive element localised in TG2 promoter (RE IL-6) (Ikura et al., 1994; Lu et al., 1995). Tumour necrosis factor- $\alpha$  (TNF- $\alpha$ ) also induces TG2

expression through its binding to nuclear factor kB (NF-kB) site on the TG2 promoter (Kuncio et al., 1998; Lu et al., 1995).

### 1.2.9.2 Structure of TG2

All the information available on TG2 structure comes from the enzyme crystallised in the GDP-bound form; so far the Ca<sup>2+</sup>-bound form has not been resolved so the information about Ca<sup>2+</sup>-binding are only derived from studies of homology with factor XIII. TG2 has four separate domains: an N-terminal  $\beta$ -sandwich, a catalytic core, and two  $\beta$ -barrel domains at the C-terminal (Noguchi et al., 2001) (Figure 1-2 and Figure 1-7). The  $\beta$ -sandwich domain contains binding sites for FN and integrins, represented respectively by residues <sup>2</sup>AEELVLE<sup>7</sup> and by the 28 kDa N-terminal region of the protein (Fesus and Piacentini, 2002; Gaudry et al., 1999). The catalytic core contains the catalytic triad represented by Cys277, His335 and Asp358 together with residues involved in the stabilisation of the active site, in particular Trp241, essential for catalytic activity (Murthy et al., 2002). When the enzyme is bound to a guanine nucleotide, two loops block the access to the catalytic site and the Cys277 is hydrogen-bond to a Tyr residue (Liu et al., 2002). The first  $\beta$ -barrel domain includes a GTP/GDP binding site that is unique for TG2 and is codified by exon X, which presents low sequence homology with the same exon from other members of the TG family (Liu et al., 2002). As shown in Figure 1-7, some of the residues essential for GTP hydrolysis are situated in the catalytic core (Iismaa et al., 2000). The second of the two  $\beta$ -barrel domains contains a binding site for phospholipase C, important in the function of TG2 as signal transduction factor (Hwang et al., 1995). TG2 also presents two regions corresponding to nuclear localisation signals (NLS<sub>1</sub> and NLS<sub>2</sub>), predicted by comparison with non-structural proteins of influenza virus (Peng et al., 1999). Two different conformations have been proposed for TG2, an open and a closed one, with distinct features (Begg et al., 2006; Pinkas et al., 2007); the close conformation is analogous to the GTP/GDP form of TG2 and it is characterised by a compact structure.

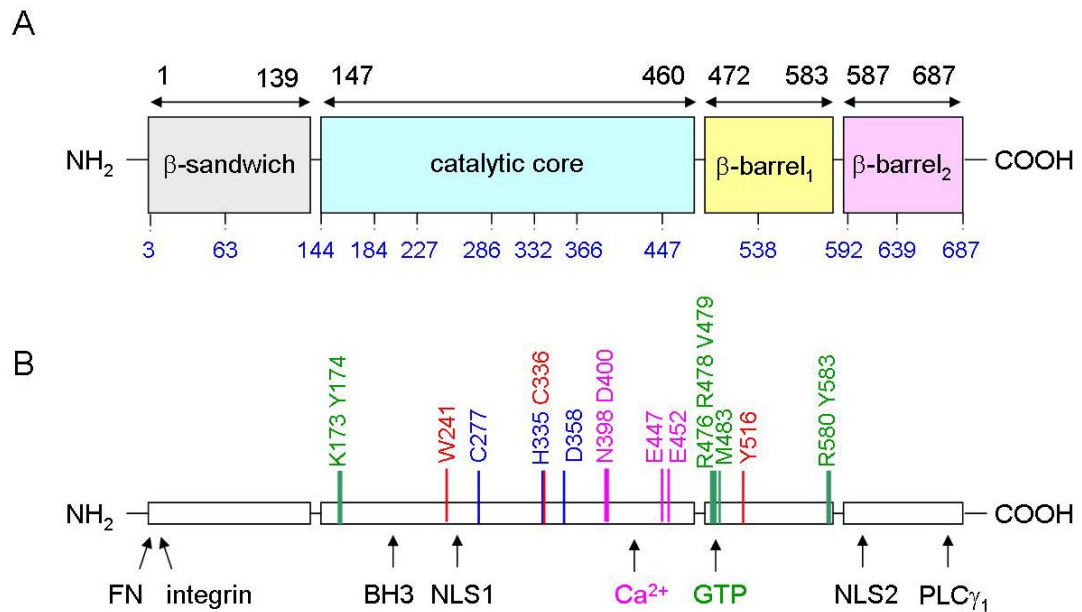


**Figure 1-7 Structural and functional elements of human TG2.** (A) Structural domains are shown, with first and last codifying residue. In blue the last amino acid codifying for each codon is shown. (B) Functional domains are pointed by the arrows; catalytic triad is indicated in blue, active residues for transamidating activity in red; residues involved in GTP/GDP binding are shown in green, putative residues involved in  $\text{Ca}^{2+}$ -binding in pink. FN, fibronectin; BH3, BH3 motif of the Bcl-2 protein family; NLS1 and 2, nuclear localization signals predicted on the basis of homology to the NLS of the NS1 non-structural protein of influenza virus;  $\text{PLC}\gamma$ , interaction site for phospholipase  $\text{C}\gamma$  (Fesus and Piacentini, 2002).

### 1.2.9.3 TG2 and cell adhesion

The localisation of TG2 at the cell surface and in the ECM has been demonstrated in several cell types, such as fibroblasts, macrophages, hepatocytes and endothelial cells (Fesus and Piacentini, 2002; Gaudry et al., 1999; Kojima et al., 1997; Lorand and Graham, 2003; Verderio et al., 1998). Several experimental findings suggest a role for extracellular TG2 in cell adhesion and migration through its interaction and enzymatic action with the cell surface and ECM components. Initial in vitro cell-adhesion assays showed that NIH 3T3 fibroblasts induced to over-express TG2 are more resistant to trypsin-induced detachment (Gentile et al., 1992). On the other side, reduced expression of TG2 or inactivation of the enzyme determines a reduced level of cell adhesion and spreading

(Jones et al., 1997). There are some controversies regarding the mechanism correlating TG2 to cell adhesion, since some studies demonstrate the importance of TG2-mediated cross-links of ECM components (Aeschlimann and Thomazy, 2000; Jones et al., 1997) and some others suggest that the involvement of TG2 is independent from its transamidation activity (Akimov et al., 2000; Balklava et al., 2002; Takahashi et al., 2000). The latter studies suggest a role for TG2 as co-receptor for  $\beta_1$  and  $\beta_3$  integrins in the cell-adhesion to the 42 kDa gelatin-binding domain of FN (Akimov et al., 2000) or, conversely, an independent adhesive role for TG2 correlated to the specific binding of integrins  $\alpha_4\beta_1$  and  $\alpha_9\beta_1$  (Takahashi et al., 2000). More recently, a novel role for TG2 in cell adhesion, independent from interactions of integrins  $\alpha_5\beta_1$  with the Arg-Gly-Asp (RGD) domain of FN has been discovered (Verderio et al., 2003). In this mechanism, TG2 action is independent from its cross linking potential and it is related to the formation of an extracellular complex of TG2 and FN. This system could have a critical importance in situations of cell stress, when the ordinary cell-adhesion, related to the interaction of integrins to FN can be compromised by FN fragmentation.

TG2 has been ascribed different roles in regulating cell-matrix interactions, based on its crosslinking activity or independent from the enzymatic reaction (Akimov et al., 2000; Balklava et al., 2002). It has been demonstrated that TG2 over-expression in fibroblasts has a marginal effect in enhancing cell attachment, but can significantly alter cell spreading modulating the interactions of the cells with the adhesion substrate (Stephens et al., 2004). Focal adhesions (FA) are the contact points between adhering cells and the substrate and they have a function in both cellular support and signal transmission between the cytoskeleton and the extracellular environment. FA are molecular complexes constituted by structural molecules (vinculin, talin, actin), transmembrane receptors, such as Sdc-4, and signalling molecules, in particular focal adhesion kinase (FAK). For the assembly of FA it is necessary for both  $\alpha_5\beta_1$  integrin clusters and Sdc-4 to bind the ECM component FN (RGD domain and heparin-binding domain) (Jeong et al., 2001). FAK is the main FA component involved in cell-spreading and migration and its action is mediated by the small GTPase RhoA, which influences actin reorganisation. Loss of FAK is correlated with decreased cell migration and an increased FA size (Ren et al., 2000), on the other side, FAK over-expression determines increased cell motility (Owen et al., 1999). The role of FAK in initial cell adhesion depends on its activation, which occurs by Sdc-4 mediated auto-phosphorylation of Tyr397 (Y397) (Wilcox-Adelman et al., 2002); this explains the

increased level of FAK phosphorylation at Y397 when, during initial cell adhesion events, Sdc-4 on the cell surface binds FN. It has been demonstrated that the role of Sdc-4 in cell spreading can be encompassed by stimulating directly RhoA with lysophosphatidic acid (LPA) (Wilcox-Adelman et al., 2002).

#### **1.2.9.4 TG2-related diseases**

TG2 is known to participate in the pathogenesis of several diseases, including celiac disease (Molberg et al., 2000), cancer (Mangala and Mehta, 2005) and neurodegenerative diseases (Hoffner and Djian, 2005). The role of TG2 in these diseases is mainly related to its enzymatic activity; therefore several inhibitors directed to the active site of TG2 are being studied as a therapeutic strategy to inhibit the establishment of the diseases (Huang et al., 2009; Siegel and Khosla, 2007).

##### **1.2.9.4.1 *Celiac disease***

Celiac disease is a T-cell mediated disorder of the small intestine which affects 1-2 % of the general population and 0.5 % of European population. The disease is caused by prolamins, a class of proteins present in wheat, barley and rye (Sollid, 2000); these proteins, being rich in Pro and Glu, are resistant to natural gastric, pancreatic and intestinal proteases, and peptidases. Therefore the digestive process leaves small peptides (longer than 9 amino acids) that can penetrate in the intestinal lamina, where they cause inflammation and destruction of intestinal architecture by activating a T-cell mediated immune response (Piper et al., 2004; Shan et al., 2002; Sollid, 2000). TG2 has a double role in the etiology of the disease, firstly it converts Gln of prolamine peptides to Glu through deamidation (see Figure 1-1); this increases the affinity of the peptides for HLA-DQ2/8 proteins, which mediate T-cell response (Quarsten et al., 1999; Xia et al., 2006). Secondly, TG2 is the target of an autoimmune response in celiac patients (Dieterich et al., 1997), that produces anti TG2 antibodies which co-localise with TG2 in the small intestine (Korponay-Szabo et al., 2004) and in the blood (Sardy et al., 1999). Anti TG2 antibodies in blood are used as a diagnostic tool for celiac disease.

##### **1.2.9.4.2 *Diabetes***

TG2 is the main member of the TG family expressed in pancreatic islets, where it modulates glucose-stimulated insulin secretion through its transamidating activity (Bungay et al., 1986).

Type 1 diabetes (insulin-dependent diabetes) is an autoimmune disease characterised by loss of insulin secretion as a consequence of pancreatic islet  $\beta$ -cells destruction mediated by T cells (Mallone and Van Endert, 2008). Experimental evidence indicated a role for the gut immune system in the development of type-1 diabetes, similarly to what happens in celiac disease, and suggested an association between the two pathologies (Maglio et al., 2009). This idea was confirmed by the finding that anti-TG2 antibodies, characteristic of celiac disease, can be found in the small intestine of most type-1 diabetes patients and that the production of anti-TG2 antibodies appears to be gluten-sensitive (Maglio et al., 2009).

TG2 is also involved in the pathogenesis of type-2 diabetes, characterised by high blood glucose level due to both insulin-deficiency and insulin-resistance. Several TG2 mutations, located in the area of the active site have been linked to type-2 diabetes, in accordance with the role of TG2 in the secretion of insulin (Porzio et al., 2007). Mutated TG2 also seems to interact with factors which regulate insulin-resistance, thus determining the high blood glucose status (Porzio et al., 2007).

#### 1.2.9.4.3 *Neurodegenerative diseases*

Several neurodegenerative diseases are characterised by the accumulation of protein aggregates in the brain, resulting from TG-mediated cross-linking. TG2 expression and activity are upregulated in many neurodegenerative diseases, and TG2 has been shown to account for at least two thirds of the total transamidase activity in mouse brain, where it is mainly localised in neurons (Krasnikov et al., 2005). TG2 is involved in the pathogenesis of Huntington's disease, an autosomal dominant disorder characterised by neuronal cell apoptosis leading to progressive motor dysfunction and dementia. Patients affected by Huntington's disease present insoluble aggregates of the cytosolic protein huntingtin (htt) in the striatum and cortex, and there is a positive correlation between the amount of aggregates and the severity of the disease, so the aggregates have been considered the cause of neurotoxicity (MacDonald et al., 1993). The cause of Huntington's disease is an expansion of CAG repeats (codifying for Gln) in the gene encoding htt protein; this modification determines the production of an htt protein with a poly-Gln N-terminus (MacDonald et al., 1993). Since Gln is a potential substrate of TG-mediated crosslinking, TG2 was initially implicated in the formation of the insoluble htt aggregates (Hoffner and Djian, 2005). It was demonstrated that the soluble mutant htt protein determines neurotoxicity, not the aggregates (Ruan and Johnson, 2007). It is still unclear whether TG2

plays a role in aggregate formation, since crossing R6/1 or R6/2 mice (animal model for Huntington's disease) with TG2 null mice determines an increased number of protein aggregates compared to the controls; these mice also show an increased life span, in accordance with the non-neurotoxicity of htt aggregates (Mastroberardino et al., 2002). In vitro studies have shown that TG2-mediated crosslinks can increase the solubility of htt aggregates, so TG2 could have an implication in the pathogenesis of Huntington's disease by promoting the neurotoxic action of soluble htt proteins (Iismaa et al., 2009; Lai et al., 2004).

Alzheimer's disease (AD), the most common cause of dementia in the elderly, is a progressive neurodegenerative disorder characterised by the presence of extracellular senile plaques composed of aggregated amyloid- $\beta$  protein and intracellular neurofibrillary tangles consisting of a highly phosphorylated form of the protein tau (Siegel and Khosla, 2007). These proteins are good substrates of TG *in vitro* (Junn et al., 2003), moreover TG activity and TG2 expression are higher in diseased regions of PD brains compared to normal regions (Ruan and Johnson, 2007). Despite these observations suggesting a role for TG2 in the formation of protein aggregates, to date there are no demonstrations of TG2 involvement in aggregate formation in vivo (Iismaa et al., 2009). Interestingly, a short-splice variant of TG2, encoding for a protein lacking the GTP-binding site, has been found in AD cerebral cortex (Citron et al., 2002); this variant, lacking the inhibition by GTP, could be involved in the aggregates formation or stabilisation.

Parkinson's disease (PD) is the second most common neurodegenerative disease, affecting 1% of the population over the age of 65 years. PD determines the degeneration of dopaminergic neurons accompanied by the formation of  $\alpha$ -synuclein protein aggregates (Lewy bodies) localised in cytoplasm of affected neurons (Hoffner and Djian, 2005). As for AD, TG2 mRNA and protein level is upregulated in PD brains compared to normal age-matched controls (Bailey et al., 2005). As for AD, even though  $\alpha$ -synuclein is a good TG2-substrate in vitro, there is no evidence for a direct role of TG2 in the formation of Lewy bodies in vivo and the function of TG2 in PD is not clear (Bailey et al., 2005; Iismaa et al., 2009).

#### 1.2.9.4.4 **Cancer**

There are several pieces of experimental evidence indicating TG2 involvement in the development of several types of cancer, in fact TG2 is upregulated in cancerous tissues

such as glioblastomas (Yuan et al., 2007), malignant melanomas (Fok et al., 2006) and pancreatic ductal adenocarcinomas (Verma et al., 2006). Moreover, there is a positive correlation between TG2 expression levels and metastatic potential and chemotherapeutic resistance of certain cancers (Mehta et al., 2004). Different mechanisms have been proposed for TG2-mediated oncogenesis, firstly TG2 can activate the transcription factor NF- $\kappa$ B by crosslinking its inhibitory subunit; this promotes the expression of Bcl-xL and BFL1, anti-apoptotic proteins (Lee et al., 2004; Mann et al., 2006). Another mechanism involves TG2-mediated activation of FAK, which, in turn, activates anti-apoptotic factors promoting uncontrolled cell growth (Verma et al., 2006). TG2 has also been shown to have anti-apoptotic effect in some cell types and, on the contrary, TG2 down-regulation via siRNA or inhibitors makes the cells more sensitive to apoptosis (Antonyak et al., 2004). In certain types of cancer, however, TG2 expression is down-regulated, and it seems to act as tumour suppressing protein (Jones et al., 2006; Xu et al., 2006), thus the role of TG2 in cancer appears to be correlated to the type, stage and location of the cancer and to the cancer cell type. Summarising, the expression of TG2 appears to be upregulated in primary tumours and during tumour progression, while the enzyme is downregulated in secondary metastatic tumours (in accordance with the role of TG2 in cell adhesion) and in case of resistance to chemotherapy (Hwang et al., 2008; Kotsakis and Griffin, 2007). It has been demonstrated that the interaction of externalised TG2 with the ECM is an important regulator of tumour growth, metastatic spread and angiogenesis, therefore, factors that control TG2 externalisation and localisation at the cell surface and matrix metalloproteases, which degrade TG2, could play a role in regulating TG2 involvement in cancer development.

#### **1.2.9.5 TG2 in wound healing and fibrosis**

Wound healing is a complex process occurring in any compartment of the body and it consists of three overlapping and inter-related events: inflammation, proliferation and remodelling (Singer and Clark, 1999). The process sees the participation of different cell types, cytokines and other factors, including transglutaminases, involved in tissue repair and stabilisation (Griffin et al., 2002; Lorand and Graham, 2003).

TG2 over-expression and increased transamidating activity have been monitored in wound healing models both *in vivo* (Haroon et al., 1999) and *in vitro* (Nicholas et al., 2003; Verderio et al., 2004). The role of TG2 seems to be the stabilisation of the wound area and

of the neo-formed tissue. When the repair process is completed, then TG2 level is reduced through proteolytic degradation and the enzyme is mainly present in its fragmented forms. The importance of TG2 in the repair process is related to the fact that the enzyme can be externalised, thus having access to ECM components; in fact, TG2 externalisation is significantly increased in situations of cell-stress and tissue damage (Haroon et al., 1999; Johnson et al., 1999; Li et al., 2002; Upchurch et al., 1991).

TG2 is also involved in abnormal wound repair mechanism, characterised by an excessive accumulation of ECM components and leading to the development of fibrotic diseases (Singer and Clark, 1999). During the normal wound healing process, new ECM is deposited and it plays an important role in supporting cell migration in the wounded area. After the migration is completed, the matrix is degraded and this contributes to the wound closure (Verderio et al., 2004); the degradation process is regulated by metalloproteinases (MMPs), plasminogen activators and inhibitors of proteases. TG2, being able to crosslink several ECM components, is involved in ECM stabilisation and protection by the action of MMP (Verderio et al., 2004). Furthermore, TG2 can influence matrix deposition by activating fibrogenic cytokine transforming growth factor  $\beta$ 1 (TGF  $\beta$ 1), which controls proliferation and ECM synthesis of fibroblasts (Nunes et al., 1997; Verderio et al., 1999); in turns, TGF  $\beta$ 1 can activate TG2 expression through the TGF- $\beta$ 1 responsive element on the TG2 promoter (Figure 1-6), thus generating a loop which determines the progression of the wound healing process into tissue fibrosis. TG2 has been shown to activate TGF- $\beta$ 1 through two separate ways, both dependent on its transamidating activity, the first way involves direct activation of latent TGF- $\beta$ 1 in the ECM, while the second involves TG2-mediated NF- $\kappa$ B activation (Telci et al., 2009).

#### **1.2.9.6 Cellular localisation of TG2**

TG2 is reported to be an ubiquitous enzyme, with considerable levels of the protein present in the cytosol, nucleus, plasma membrane and in the extracellular matrix (Fesus and Piacentini, 2002).

##### **1.2.9.6.1 Cytosolic TG2**

In the cytosol, given the insufficient  $\text{Ca}^{2+}$  concentration for TG2 activation and the presence of inactivating levels of GTP, TG2 transamidating activity is mainly latent and the enzyme mostly acts as a GTPase involved in signal transduction (Monsonego et al.,

1998). TG2 crosslinking activity seems to be activated intracellularly only during apoptosis, even though there is a debate on the pro- or anti-apoptotic role of TG2 transamidating activity in cell death (Gundemir and Johnson, 2009). In fact, according to the cell type analysed and the agent inducing apoptosis, TG2 activity appears to have opposite roles in determining cell fate (Fesus and Szondy, 2005), by either protecting cells from apoptosis (Yamaguchi and Wang, 2006) or facilitating the cell death process (Tucholski and Johnson, 2002). Despite the contradictory role ascribed to crosslinking activity, it is known that guanine nucleotide binding of TG2 is protective against apoptosis (Datta et al., 2007), even though it is not clear if this depends on the action of TG2 as a G-protein or on the inhibition of the crosslinking activity. Another event when cytosolic TG2 crosslinking is involved is cell differentiation; one example is chondrocyte hypertrophic differentiation, promoted by TG2 mediated oligomerisation of activating cytokines (Cecil and Terkeltaub, 2008).

TG2 can also act as Ser/Thr kinase in apoptosis signalling upon PKA-induced phosphorylation (Mishra et al., 2007b). In human breast cancer TG2 kinase activity was reported to activate insulin-like growth factor (IGF) binding protein-3 (IGFBP-3) thus determining an IGF-independent activation of signalling, leading to apoptosis (Mishra and Murphy, 2004).

Another function ascribed to TG2 in the endoplasmic reticulum is the one of protein disulfide isomerase (PDI), involved in the regulation of protein conformation (Hasegawa et al., 2003); an example of this activity is the TG2-mediated conversion of inactive/denatured RNaseA into the native active form. TG2 PDI function does not involve the active site for protein transamidation, nor does it require the presence of  $\text{Ca}^{2+}$ , and is not influenced by the presence of guanine nucleotides (Hasegawa et al., 2003).

#### 1.2.9.6.2 *Nuclear TG2*

TG2 is translocated from the cytosol to the nucleus through a mechanism involving nuclear transport protein importin- $\alpha$ 3 (Peng et al., 1999). In this cell compartment TG2 is involved in post-translational histone modification by crosslinking of core histone subunits; this modification regulates the chromatin structure, thus influencing mitosis, transcription, DNA replication and DNA repair (Mishra et al., 2007a; Peng et al., 1999). Recent studies have shown that TG2 also modifies histones through its Ser/Thr kinase activity, in particular in situations of cell stress and apoptosis (Mishra et al., 2007). TG2 nuclear

kinase activity has also an important function in the regulation of retinoblastoma protein (Rb) a primarily nuclear protein with a key role in the regulation of apoptosis (Mishra et al., 2007).

#### 1.2.9.6.3 *Extracellular TG2*

The mechanism of TG2 externalisation at the cell surface and in the ECM is still unknown, since the enzyme is a leaderless protein and does not have post-translational modifications linked to the targeting to the endoplasmic reticulum or to the Golgi (Thomazy and Fesus, 1989). It has been reported that TG2 needs to have an intact active site to be externalised, in fact, Swiss 3T3 fibroblasts induced to over-express a mutant TG2 where Cys 277 of the active site was substituted by Ser, showed a significantly lower level of externalised TG2 compared to the same cells induced to over-express normal TG2 (Balklava et al., 2002). Very recently, (Telci et al., 2009), using the same cell system of Swiss 3T3 fibroblasts with inducible TG2 expression have demonstrated that TG2 transamidating activity is not essential for enzyme externalisation, since the process was not affected by active site directed TG inhibitor R283. It is therefore possible that the presence of Cys at the active site is required to have a specific conformation necessary for the secretion process, independently from the catalytic state of the enzyme.

Once TG2 is externalised, it is mainly associated to cell surface and ECM FN (Akimov et al., 2000; Verderio et al., 1998), which is stabilised by the formation of  $\text{Ca}^{2+}$ -dependent cross-links (Jones et al., 1997). On the other side, the association with FN protects TG2 against proteolytic degradation (Belkin et al., 2001) and controls its enzymatic activity in order to prevent an excessive crosslinking in the  $\text{Ca}^{2+}$ -rich extracellular environment (LeMosy et al., 1992). Probably, after the externalisation and association with FN, TG2 gradually loses its activity and becomes a structural element of the ECM; this is supported by the finding that under physiological conditions extracellular TG2 is mostly inactive and only gets activated following tissue injury (Siegel et al., 2008). It has been shown that a matrix constituted by TG2 in complex with FN (TG2-FN matrix) can promote a novel cell adhesion pathway independent from the classical adhesion mediated by  $\alpha_5\beta_1$  integrins (Verderio et al., 2003). TG2-mediated RGD-independent adhesion has been shown to rely on the presence of cell surface heparan sulphate (HS), in fact it is inhibited by a treatment of the cells with heparitinase, which digests HS chains (Verderio et al., 2003); this suggests a possible implication of HS in the regulation of TG2 extracellular activity.

### 1.3 Glycosaminoglycans

Glycosaminoglycans (GAG) are linear polysaccharides of high molecular weight consisting of repeating disaccharide units formed by an amino sugar (N-acetylglucosamine, glucosamine with various N-substitutions, or N-acetylgalactosamine) and an uronic acid (glucuronic acid or iduronic acid) or galactose (Hacker et al., 2005). GAG chains are characterised by a high level of heterogeneity, due to the different hexosamine, hexose or hexuronic acid that they contain and to the geometry of the glycosidic linkage between these units ( $\alpha$  or  $\beta$ ) (Sasisekharan and Venkataraman, 2000). They are the most abundant heteropolysaccharides in vertebrates, involved in the binding and regulation of several proteins including chemokines, growth factors, cytokines morphogenic enzymes and adhesion molecules (Jackson et al., 1991). GAG can be separated in two main groups: unsulphated proteoglycans, including hyaluronic acid (HA) and sulphated ones, including chondroitin sulphate (CS), dermatan sulphate (DS), keratan sulphate (KS), heparin and heparan sulphate (HS). CS and DS are localised in the ECM, while heparin/HS proteoglycans are usually associated to the cell surface. The majority of GAG chains in vertebrates are present in the form of proteoglycans, linked to a core protein.

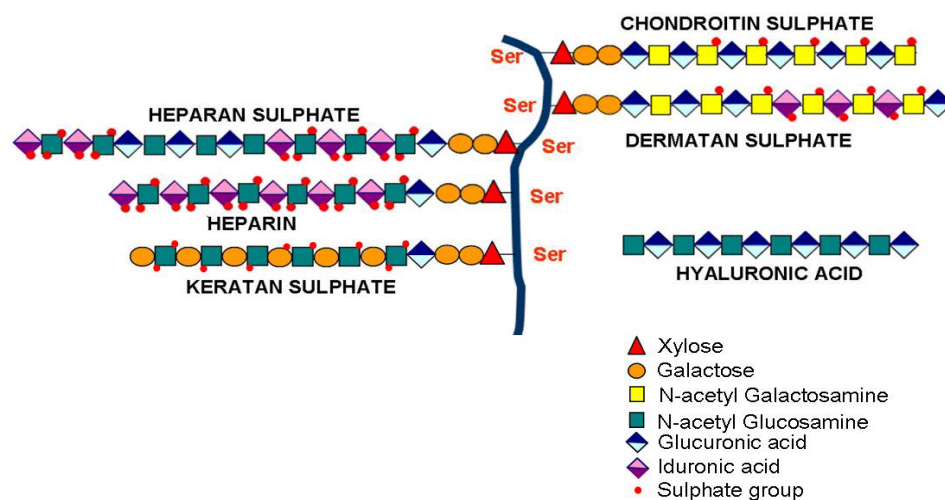


**Figure 1-8 Structure of GAG chains.** *The composition and sulphation level of the main GAG chains, attached to a core protein is shown; the core protein is represented in dark blue and the Ser residues adjacent to the GAG attachment site are indicated. The composition of hyaluronic acid, not attached to a core protein, is also represented.*

### 1.3.1 Heparan sulphate

Heparan sulphate is a linear polysaccharide present in all animal tissues in the form of proteoglycan; HS chains at the cell surface are mostly attached to syndecans and glypicans core proteins (Bernfield et al., 1999). In contrast with other complex carbohydrates, overall HS structure is conserved from flies to humans. HS synthesis starts with the formation of the region for protein linking, followed by elongation and modification of the chain. The length of HS chains can vary over 10-fold with cell type and core protein, but the chain termination mechanisms are mostly unknown (Bernfield et al., 1999). Generally HS chains consist of 50-150 disaccharides and are modified by enzymatic reactions in which the products of one are substrates for the following one. The specific expression of modifying enzymes and the availability of substrates/cofactors generate a huge diversity of HS chains. HS chains on the same core protein from different cell types can show consistent and reproducible structural differences: variations in domain number, spacing or size and O-sulfation pattern (Kato et al., 1994). In all HS chains it is possible to recognise highly sulphated domains (HSD), resembling heparin domains, alternated to unmodified domains (UMD) (Maccarana et al., 1996). HSD, often involved in HS interactions with binding partners, are rigid and highly anionic and can have access to basic residues on protein surfaces thanks to the adjacent, more flexible, UMD. HS chains are responsible for much of the biological activity of HS proteoglycans (HSPG); the core proteins, that dictate cellular location and metabolism of HS chains, have evolved to maximise the efficiency of HS chains in their roles (Bernfield et al., 1999; Varki et al., 2009).

### 1.3.2 Heparin binding proteins

Proteins bind HS chains via basic residues on their surfaces, mostly via distinct protein domains (Bernfield et al., 1999). Binding domains of recent evolution show sequence resemblance and are easy to identify, but domains that arose during ancient times may only be apparent after 3D structural analysis (Doolittle, 1995). Some HS binding proteins contain linear clusters of basic residues often in a distinct pattern, but most differ in their HS-binding sequences, indicating ancient origin (Hileman et al., 1998).

Cell surface HS can immobilise the ligand, increase its local concentration, change its conformation, present it to signalling receptors or modify the molecular encounters

between ligands and receptors. The general effect is generally to enhance receptor activation at low ligand concentrations (Carey et al., 1997).

## ***1.4 Proteoglycans***

Proteoglycans consist of one or more GAG chains covalently bound to a core protein at specific sites; these chains are attached to the core protein in the Golgi, before proteoglycan externalisation. For most of the proteoglycans, the GAG chains represent the predominant part of the molecule, conferring a molecular weight that varies from 100 to 10,000 kDa; given that, it comes natural that the GAG chains are the main determinant of proteoglycans chemical properties and interactions with binding partners (Gandhi and Mancera, 2008). These molecules are characterised by a huge structural variability that is due to the variety of core proteins and to their level of substitution (number, type and composition of GAG chains). The stoichiometry of GAG chains substitution, determining which GAG attachment sites are preferably used, is also involved in generating variability. Some proteoglycans can be “part time”, presenting or not bound GAG chains or binding truncated oligosaccharides. Finally, the same proteoglycans can present essential differences if expressed in different cell types, showing a different number, length and sulphation pattern of the GAG chains (Bernfield et al., 1999). It is possible to distinguish two main classes of proteoglycans: membrane proteoglycans (glypican and syndecans) and proteoglycans of the extracellular matrix (Aggrecan, Perlecan, Decorin and Biglycan), as illustrated in Figure 1-9 (Varki et al., 2009). The extracellular space, the ECM, consists of fibrous proteins (collagens and elastins), providing elasticity and tensile strength and adhesive glycoproteins (fibronectin, laminin and tenascin); the various proteoglycans interact with these components to form a hydrated gel resistant to compressive force, thus stabilising the ECM. In some cells, proteoglycans are stored in secretory granules, where they are involved in regulating the availability of positively charged components such as proteases and bioactive amines (Varki et al., 2009).

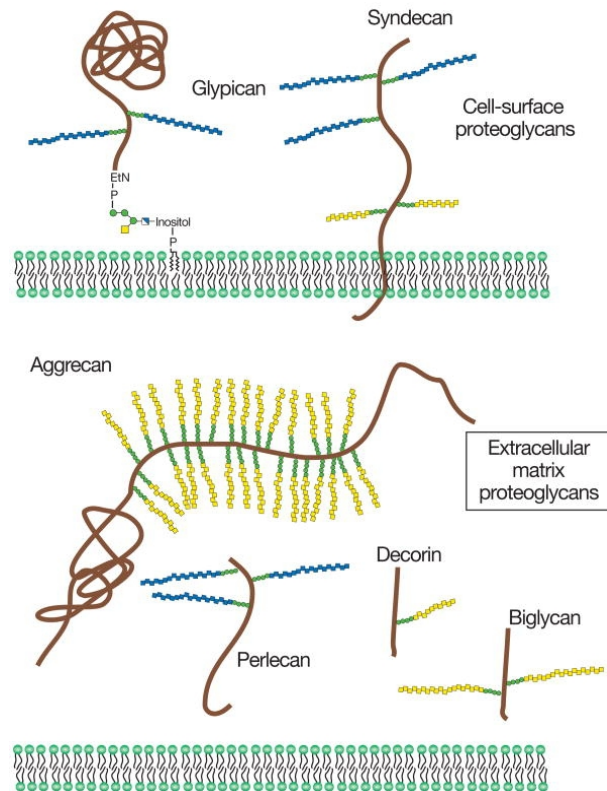


**Figure 1-9 Proteoglycans classification.** Image from (Varki et al., 2009). The structure of the main cell-surface and extracellular matrix proteoglycans is represented.

Localisation	GAG chain	Core protein size (kDa)	Principal members
ECM	HA, CS, KS	225-250	Aggrecan, versican
Collagen-associated	CS, DS, KS	40	Decorin, biglycan, fibromodulin
Basement membrane	HS	120	Perlecan
Cell-surface	HS, CS	33-60	Syndecans, glypicans
Intracellular granules	Heparin, CS	17-19	Serglycin

**Table 1-2 Classification of proteoglycans based on cellular localisation and predominant GAG chain.** ECM, extracellular matrix; CS, chondroitin sulfate; DS, dermatan sulfate; KS, keratan sulfate; HA, hyaluronic acid; HS, heparan sulfate.

### **1.4.1 Extracellular matrix proteoglycans**

Interstitial proteoglycans are only produced in vertebrates and their composition varies according to the tissue analysed. Two main classes of molecules can be identified: small Leu-rich proteoglycans (SLRP) and the aggrecan family of proteoglycans. The first group, characterised by Leu-rich repeats flanked by Cys in the central domain, carries CS, DS or KS chains and it is involved in the stabilisation of collagen fibres (Varki et al., 2009). The second group consists of aggrecan, versican, brevican and neurocan, characterised by the presence of an N-terminal domain which is able to bind hyaluronan, a central domain binding CS chains and a C-terminal domain containing a C-type lectin domain (Roughley, 2006). The larger part of information regarding this family is related to aggrecan, which is the major proteoglycan in the cartilage. Aggrecan can contain up to 100 CS or KS chains, reaching a molecular weight of 2500 kDa; these chains can be highly hydrated and form a filling gel that contributes to the physical strength of cartilaginous tissue and provides resistance to compressive loads (Roughley, 2006). Versican, mainly produced by cells of the connective tissue seems to be involved in neural crest and axonal migration. Neurocan and brevican are expressed in the late phases of development of the central nervous system and act inhibiting neurite growth.

### **1.4.2 Proteoglycans of secretory granules**

The main proteoglycan contained in cytoplasmic secretory granules is serglycin, which can be found in endothelial, endocrine and haematopoietic cells (Kolset and Gallagher, 1990). Serglycin can carry a variable number of CS or, most importantly, heparin chains; notably, heparin is only made on serglycin contained in secretory granules of secretory tissue type mast cells. Given the properties of their GAG chains, serglycin-expressing cells participate to a wide range of biological activities, such as regulation of blood coagulation, tumour cell killing and bacteria defence during wound repair (Kolset et al., 2004).

### **1.4.3 Basement membrane proteoglycans**

Depending on the tissue considered, four different proteoglycans can be isolated in the basement membrane (layer of the ECM that lies against epithelial cells): perlecan, agrin, collagen type XVIII and leprecan (Iozzo, 2005). The first three carry HS chains, with the

exception of perlecan, which can also carry CS chains in cartilage, while leprecan carries CS chains. Perlecan and agrin are the best characterised members of this group; the former is involved in embryogenesis and tissue morphogenesis, especially in cartilage, the latter acts in neuromuscular junctions and renal tubules, where it determines the filtrating properties of the glomerulus (Varki et al., 2009).

#### **1.4.4 Membrane-bound proteoglycans**

The two major families of membrane-bound proteoglycans consist of syndecans (Sdc) and glypicans (Bernfield et al., 1999). The Sdc family includes four members, as described in paragraph 1.4.5; all of them are characterised by a small cytoplasmic domain, a hydrophobic transmembrane domain and a large extracellular domain, carrying HS and, in smaller amount, CS chains (Kokenyesi and Bernfield, 1994). HS chains of syndecans can bind a large variety of extracellular molecules, concentrating them in specific areas of the cell surface and facilitating their binding to specific receptors (Bernfield et al., 1992). Given their structure, syndecans are also able to transmit signals from the extracellular environment to the cytosol and cytoskeleton, acting in signal transduction (Anderson, 1998). Sdc ectodomains, carrying the GAG chains, can be shed by action of metalloproteases and be released in the ECM, where they can be involved in the regulation of important biological functions by competing with membrane-bound Sdc for the binding of specific ligands; the shedding process also regulates the availability of proteoglycans at the cell surface (Bernfield et al., 1999).

The glypican family consists of six members, all attached to the cell surface by a C-terminal glycosylphosphatidylinositol (GPI) anchor. The core protein of glypicans is rich in cysteine residues and has a globular structure substantially different from the proline-rich linear extracellular domain of Sdc (Bernfield et al., 1999). The only GAG chains carried by glypicans are HS, involved in the binding of factors essential for the development and morphogenesis. The different way in which syndecans and glypicans are associated to the membrane determines a different metabolic fate for their ligands; in fact, ligands internalised through glypicans can be recycled together with their receptor, while ligands internalised with syndecans go through endocytosis and lysosomal degradation (Fransson et al., 1995; Rosenberg et al., 1997).

### 1.4.5 The syndecan family

The Sdc family, representing the major group of transmembrane heparan sulphate proteoglycans, includes 4 distinct genes in mammals, originated from gene duplication and divergent evolution from a single ancestral gene; syndecan 1 and 3 (Sdc-1 and Sdc-3) and syndecan 2 and 4 (Sdc-2 and Sdc-4) represent subfamilies originated from the ancestral gene (Bernfield et al., 1992). Each gene product is a single type-1 membrane-spanning protein with extracellular domain of varying size containing covalently attached HS chains distal from plasma membrane. *In vivo* experiments have suggested that each Sdc is expressed at specific stages of the development and in specific cell types (Bernfield et al., 1992). All of the Sdc (4 members in mammals and one in *Drosophila* and *Caenorhabditis elegans*) share homologous regions for GAG chain attachment and a putative protease cleavage site in the ectodomain proximal to the membrane (Figure 1-10). Transmembrane and cytoplasmic domains are highly conserved, suggesting a potential biological role for these domains. In fact, syndecans have important roles as cell surface receptors in cell-cell and cell-matrix interactions. Sdc-4 is of particular interest since it is selectively enriched and widespread in focal adhesions (Woods and Couchman, 1994). Members of the Sdc family can form dimers or oligomers resistant to SDS treatment upon binding of specific ligands followed by phosphorylation of the cytoplasmic region (Pierce et al., 1992). In particular, recombinant Sdc-3 core protein forms stable non-covalent multimers through the transmembrane domain and the ectodomain flanking region (Asundi and Carey, 1995). Also, recombinant proteins of Sdc-2 and Sdc-4 form SDS-resistant multimers, even in the absence of the cytoplasmic domain (Longley et al., 1999; Oh et al., 1997a; Oh et al., 1997b). The formation of multimers can create specialised membrane domains able to mediate the interactions between cells and surrounding ECM by binding specific ligands and transmitting the signal to the cytosol or the cytoskeleton (Essner et al., 2006).



### **1.4.5.1 Syndecan-1**

Sdc-1 is expressed really early during development and it is mainly found on epithelia and mesenchymal-cell condensations associated with tissue morphogenesis (Couchman, 2003). Defects in Sdc-1 expression lead to a phenomenon called epithelial-mesenchymal transition, where the cells of interest assume fibroblastic morphology (Bernfield et al., 1992). This transition is correlated to tumorigenesis and severity of neck and cervical carcinoma (Anttonen et al., 1999; Rintala et al., 1999). It is possible that Sdc-1 acts regulating the cell-surface level of the tumour suppressor E-cadherin, since the loss of Sdc-1 is associated with loss of E-cadherin (Leppa et al., 1996), but the mechanism relating the two molecules is still unknown.

Sdc-1 is also involved in cell-cell adhesion, in fact it can bind several members of the Ig super-family of cell-adhesion molecules (CAM), in particular PECAM-1 and N-CAM. Sdc-1 mediated adhesion has heterophilic nature, with a molecule of Sdc-1 on the cell surface binding a counter-receptor on an adjacent cell (Stanley et al., 1995). It has been shown that human myeloma cells lose the ability to adhere to each other after the loss of Sdc-1; normal levels of cell-cell adhesion can be restored by re-introducing Sdc-1 by cell transfection (Stanley et al., 1995); interestingly, cell-cell adhesion can also be restored by transfection with Sdc-4 cDNA, but not with re-introduction of other members of the Sdc family.

### **1.4.5.2 Syndecan-2**

Sdc-2 is mainly expressed in mesenchymal tissue, but it is also found in liver and neuronal cells (Couchman, 2003); the expression of Sdc-2 is limited to sites of cell-cell and cell-matrix interactions (David, 1993). Sdc-2 is the member of Sdc family with the highest expression in fibroblasts, even though its function is still not fully elucidated (David et al., 1992). In particular Sdc-2 has been shown to be involved in signalling, cell-adhesion and angiogenesis (Beauvais and Rapraeger, 2004; Tkachenko et al., 2005), these abilities also link Sdc-2 to tumorigenesis. Sdc-2 has been found to be over-expressed in several cancers, such as lung and colon cancer, where it determines the establishment of a less adhesive phenotype and loss of contact inhibition, thus enhancing the metastatic potential (Gulyas and Hjerpe, 2003; Park et al., 2002).

The C1 domain of the cytoplasmic region interacts with proteins of the ER family, implicated in the organisation of the cortical actin cytoskeleton and in the activation of FAK, thus underlying the role of the receptor in cell adhesion and communication with the actin cytoskeleton (Granes et al., 2000). The C2 domain is also linked to communication with the cytoskeleton; in fact it binds Type II PDZ domain proteins involved in vesicle transport, synaptic transmission, axonal migration and development of cancer metastasis (Beauvais and Rapraeger, 2004; Essner et al., 2006). The V domain contains two residues (Ser197 and Ser198) which can be phosphorylated by activated protein kinase C  $\gamma$  (PKC $\gamma$ ); upon phosphorylation, Sdc-2 is able to mediate the response to vitellogenin 1 (Vg1), a member of the transforming growth factor  $\beta$  (TGF $\beta$ ) family of signalling molecules involved in cell-cell communication (Kramer et al., 2002). Vg1-mediated signalling is of vital importance in the gastrulation process, where it regulates the formation of the right-left axis leading to asymmetric heart and viscera development (Couchman, 2003). Summarising, there are several functions ascribed to Sdc-2, related to the expression in specific cell types and in the composition of the HS chains, which can in turn influence the ability to bind specific ligands (Essner et al., 2006).

#### **1.4.5.3 Syndecan-3**

The expression of Sdc-3 is predominantly related to neural cells, although a certain level of expression can also be detected in musculoskeletal tissue (Couchman, 2003). Sdc-3 has a really high expression in the early postnatal period, when it is involved in cell-matrix adhesion in the developing nervous system (Carey, 1997). In this process, Sdc-3 acts as a receptor for the growth factor pleiotrophin, whose expression is also correlated with the development of the central nervous system (Raulo et al., 1994); once bound to Sdc-3 pleiotrophin promotes neurite outgrowth from embryonic or early post-natal cortical neurons. It has been demonstrated that the binding of pleiotrophin to Sdc-3 (Kd  $\approx$  0.4 nM) is mediated by the HS chains of the proteoglycan, and, in particular, by 2-O-sulphated iduronic acid residues contained in the chains.

#### **1.4.5.4 Syndecan-4**

Differently from the other members of the Sdc family, Sdc-4 is widely expressed through all the stages of the development and it is a constitutive component of focal adhesions (FA) of adhering cells, where it contributes to FA formation and cytoskeletal reorganisation

linked to cell spreading (Couchman et al., 2001; David et al., 1992). The role in FA formation is related to the presence of an intact V region in the cytoplasmic domain; this region in fact contains a core sequence (KKPIYKK) which binds phosphatidylinositol (4,5) bisphosphate (PIP<sub>2</sub>) (Couchman et al., 2002). This sequence is not present in other members of the family and Sdc-4 is the only Sdc binding phospholipids. After binding, PIP<sub>2</sub> stabilises the cytoplasmic domain in dimeric form, and may also be involved in promoting the formation of higher order oligomers forming specialised microdomains in the plasma membrane (Oh et al., 1997a). The complex of Sdc-4 and PIP<sub>2</sub> can then bind and activate PKC $\alpha$ , essential component of FA involved in the phosphorylation of cytoskeletal components (Couchman et al., 2001). C1 domain can also be phosphorylated at a specific Tyr residue (Horowitz and Simons, 1998), and this occurs in situations of growth inhibition; the kinase responsible for C1 phosphorylation is PKC $\gamma$ , the same involved in the phosphorylation of Sdc-2 V domain; this seems to have an antagonistic effect on the activation of PKC $\alpha$  (Couchman, 2003).

Another cytosolic partner of Sdc-4 is syndesmos, which requires both C1 and V region for the interaction; syndesmos acts as an adaptor protein for paxillin, a protein involved in FA formation (Baciu et al., 2000). There is also experimental evidence for Sdc-4 interaction with cytoskeletal components such as  $\alpha$ -actinin, involved in the formation of actin bundles (Greene et al., 2003). The signalling related to Sdc-4 seems to mediate the activation of the small GTPase RhoA (Saoncella et al., 1999) even though the mechanism is still not fully understood but the two main hypothesis consist in a direct interaction of PKC $\alpha$  with RhoA (Slater et al., 2001) or the separate, but equally important action of PKC family members and RhoA (Defilippi et al., 1997). Active RhoA can then regulate cytoskeletal reorganisation either via activating Rho kinases (ROCK), which lead to microfilament contraction promoted by myosin, or modulating actin polymerisation by regulating the activity of diaphanous (Bishop and Hall, 2000).

When plated on fibronectin, primary fibroblasts interact with FN with 2 main cell surface receptor families: integrins and cell surface HSPG, in particular Sdc-4; the two signals are both necessary to regulate focal adhesions and stress fibres formation (Couchman et al., 2001; Couchman and Woods, 1999). Integrin interaction with FN leads to the activation of several signalling molecules, including FAK; this is only sufficient for attachment and spreading. In order to have cytoskeletal and membrane reorganisation, to form stress fibres

and focal adhesion, an additional stimulus is needed, which comes from the heparin binding (HB) domain of FN interacting with Sdc-4 (Saoncella et al., 1999).

#### **1.4.6 Syndecan-4 in tissue injury and wound healing**

Tissue repair process following injury is a complex event which includes interaction of cells with the surrounding ECM -mainly mediated by  $\beta_1$  integrins and Sdc-4- leading to the formation of a new tissue. The importance of Sdc-4 in the wound healing process has been investigated in animal models; Sdc-4  $-/-$  or Sdc-4  $+/-$  mice resulted to have a reduced rate of wound healing compared to wild type mice (Echtermeyer et al., 2001). Mice with no or reduced expression of Sdc-4 in fact showed a reduced formation of granulation tissue, which represent the base for the migration of new cells repopulating the wounded area; this is linked to the delayed contraction of the wound (Echtermeyer et al., 2001). Moreover, the new tissue formed by Sdc-4  $-/-$  and  $+/+$  mice was less vascularised compared to the same tissue in wild type mice; the three groups showed a similar amount of blood vessels per unit area, but the decreased expression of Sdc-4 determined a reduction of their size (Echtermeyer et al., 2001). Elenius and co-workers have also reported that, after skin injury, Sdc-4 expression is transiently decreased in keratinocytes migrating into the wound, whereas it is increased in the keratinocytes proliferating at the wound margin and in the fibroblasts (Sdc-4) within the forming granulation tissue (Elenius et al., 1991). The induction seems to be induced by antimicrobial peptides (i.e. PR-39) released into the wound by inflammatory cells, in fact there is no increased expression in foetal skin, that heals without scarring and without extensive inflammation (Gallo et al., 1996).

## ***Chapter 2: Materials and Methods***

### ***2.1 Materials***

#### ***2.1.1 Cell culture***

##### **2.1.1.1 Reagents**

Dulbecco's Modified Eagles Medium DMEM (12-614F), DMEM/HAM's F12 medium (D6421) and MEM non-essential amino acids solution (M7145) were from Sigma-Aldrich. Penicillin/Streptomycin mix, L-Glutamine, and trypsin solution, were purchased from Cambrex bioscience Ltd.

Heat-inactivated foetal calf serum (FCS) was purchased from BioSera.

Fungizone, was from Invitrogen Corporation.

##### **2.1.1.2 Plastic ware**

All sterile plastic were supplied by Sarstedt, except for:

- Cell scrapers and 8 well glass chamber slides (Lab-Tek II), Thermo Fisher Scientific.
- Cryotube vials (Nalgene), SLS-Scientific Laboratory Supplies.

#### ***2.1.2 Laboratory reagents***

##### **2.1.2.1 Peptides**

RGD peptide (H-Gly-Arg-Gly-Asp-Thr-Pro-OH) and RAD peptide (H-Gly-Arg-Ala-Asp-Thr-Pro-OH), purity  $\geq 97\%$ , were from Calbiochem. A 10 mg/ml stock solution was prepared in DMEM containing 2.5 mg/ml bovine serum albumine (BSA); aliquots were stored at  $-80^{\circ}\text{C}$ .

P3 peptide (WTATVVDQDCTLSLQLTT) (Hang et al., 2005), purity  $\geq 95\%$ , was from Activotec. A 10 mg/ml stock solution was prepared in sterile distilled water; aliquots were stored at  $-80^{\circ}\text{C}$ .

### 2.1.2.2 Enzymes

Chondroitinase ABC (from *Proteus vulgaris*) and heparitinase (from *Flavobacterium heparinum*) were from Seikagaku Corporation. A 10 U/ml stock solution of chondroitinase ABC was prepared in 100mM Tris-HCl, pH 8; aliquots were stored at -80°C. A 1 U/ml stock solution was prepared in 50 mM Tris, pH 7.4 containing 0.1% (w/v) BSA; aliquots were kept at -20°C.

Dispase (from *Bacillus polymyxa*) was from Invitrogen Corporation. A 10 mg/ml stock solution was prepared in sterile PBS, filtered and kept at 4°C.

Guinea pig liver transglutaminase-2 was from Sigma-Aldrich or Zedira GmbH. A 1 mg/ml stock solution was prepared in distilled water; aliquots were stored at -20°C.

### 2.1.2.3 Antibodies

Primary antibody	Company
Monoclonal mouse anti human fibronectin	Sigma-Aldrich
Monoclonal mouse anti human integrin $\beta$ -1 (mab1965)	Chemicon International Inc.
Monoclonal mouse anti human vinculin (hVin-1)	Sigma-Aldrich
Monoclonal mouse anti transglutaminase 2 (Cub 7402)	Abcam
Monoclonal mouse anti transglutaminase 2 (TG100)	Abcam
Monoclonal mouse anti $\beta$ -tubulin	Sigma-Aldrich
Polyclonal goat anti transglutaminase 2 (ab 10445)	Abcam
Polyclonal goat anti-type III collagen	Southern Biotech.
Polyclonal rabbit anti cyclophilin A	Abcam
Polyclonal rabbit anti focal adhesion kinase (p125),	Sigma-Aldrich
Polyclonal rabbit anti focal adhesion kinase (pY397)	Abcam.
Polyclonal rabbit anti phosphotyrosine	BD biosciences
Polyclonal rabbit anti syndecan-4	Zymed laboratories Inc
Polyclonal rabbit anti syndecan-4 (H-140)	Santa Cruz Biotechnology Inc
Polyclonal rabbit anti transglutaminase 2 (ab2972)	Abcam

<b>Secondary antibody</b>	<b>Company</b>
Goat anti-mouse IgG rhodamine Red <sup>TM</sup> -X-conjugated	Invitrogen Corporation
Polyclonal goat anti mouse Ig Horseradish Peroxidase	DakoCytomation
Goat anti rabbit IgG HRP-conjugated	Sigma-Aldrich
Sheep anti mouse IgG FITC-conjugated	Sigma-Aldrich
Goat anti mouse IgG AlexaFluor <sup>®</sup> 488	Invitrogen Corporation

#### **2.1.2.4 Molecular biology reagents**

##### *2.1.2.4.1 Antibiotics*

Kanamycin and ampicillin were from Invitrogen Corporation.

Tetracycline was from Sigma-Aldrich.

G418 was from PAA laboratories GmbH.

##### *2.1.2.4.2 Cloning and Expression vectors*

pGEM<sup>®</sup>-3Zf(+) cloning vector was from Promega Corporation

pSG5 expression vector was from Agilent Technology UK Limited

pEGFP-N1 expression vector was from BdBioscience Clontech

pcDNA<sup>TM</sup> 3.1(+) expression vector (invitrogen) was kindly donated by Prof. R Rees and Dr M. Mathieu, Nottingham Trent University, UK.

##### *2.1.2.4.3 PCR primers*

All DNA primers were provided by Sigma-Genosys (Sigma-Aldrich).

Liofilized primers were resuspended in Tris-EDTA (TE) buffer (10 mM Tris-HCl, pH 7.5 and 1 mM EDTA) at a concentration of 100  $\mu$ M and stored at -20°C. These stock solutions were diluted in TE buffet at 20  $\mu$ M concentration to generate working solutions used to prepare PCR reactions (2.2.10.12).

Target	Primers pair (5'→3'), name and sequence	AT (°C)
Full length human TG2 cDNA	pSG5S: atcagaattcatggccgaggagctggtcttagagagg pSG5AS: atcagaattccggcggggccaatgatgacattccgg	56
Mouse TG2 +/+	TGS1: tactccagcttctgttctg TGA1: tcctgacctgagtcctctgc	56
Mouse TG2 -/-	TGN1: atcatctcgtcttgttctc TGA1: tcctgacctgagtcctctgc	56
Mouse Sdc-4 +/+	EX3S: atgacacggaggagcccaggc EX4AS: ccttacctgccaagacctcag	61
Mouse Sdc-4 -/-	NeoS: atgacacggaggagcccaggc EX4AS: ccttacctgccaagacctcag	68
Mouse GAPDH	GAPDHS: actccactcacggcaaattc GAPDHAS: ccttcacaatgccaagtt	55

**Table 2-1 Primers used for PCR reactions on genomic DNA.** *The annealing temperature (AT) used for PCR amplification is indicated for any primers pair.*

Target	Primers pair (5'→3'), name and sequence	AT (°C)
Mouse Sdc-1	mSdc-1FW: attctttctccccccacagcc mSdc-1RV: aataaggtctgctgggctctgaac	56
Mouse Sdc-2	mSdc-2FW: ctctccccttctgtgactgac mSdc-2RV: agccccctacctccctctctac	56
Mouse Sdc-4	mSdc-4FW: gggggcattctaagtccagtga mSdc-4RV: tatcccgtatccccctacattat	56
Human Sdc-4	hSdc-4FW: tgcaggaattgccatggccc hSdc-4RV: gcgtagaactcattgggtgggg	54
Mouse TG1	mTG1FW: tgagtcctctgatggcattg mTG1RV: tcgccaatctgtgcttctgt	60
Mouse TG2	mTG2FW: agtatgagcatgggcaacga mTG2RV: atacaggggatcgaaagtg	60
Mouse TG3	mTG3FW: tggcagtaggcaaagaagtc mTG3RV: cacatcaatcttaggctgc	60
Mouse TG5	mTG5FW: ctteccctcaaccagtgat mTG5RV: gagtgatgctggctttgtga	60
Mouse TG6	mTG6FW: atatgtggactcttatggccg mTG6RV: tccacacttagcagtttctca	60
Mouse TG7	mTG7FW: catcgctgaggtgaagagac mTG7RV: ccttgtagcctttgatctcc	60
Mouse GAPDH	mGAPDHFw: tggaaagctgtggcgtgat mGAPDHRV: ccctgttctgtagccgtat	55

**Table 2-2 Primers used for PCR reactions on cDNA.** The annealing temperature (AT) used for PCR amplification is indicated for any primers pair.

#### 2.1.2.5 Chemicals

Biotin cadaverine (N-(5-aminopentyl) biotinamide trifluoroacetic acid salt, Invitrogen Corporation. A 50 mM stock solution was prepared in DMSO and stored at 4°C.

DAPI (4',6-diamidino-2-phenylindole), Sigma-Aldrich. A 1 mg/ml solution was prepared in H<sub>2</sub>O, aliquots were stored at -80°C.

Fluorescein cadaverine, Sigma-Aldrich. A 1 mg/ml stock solution was prepared in dimethyl sulfoxide (DMSO); aliquots were kept at -80°C.

Heparin (sodium salt from porcine intestinal mucosa, average molecular weight ~ 3 kDa), Sigma-Aldrich. A 20 mg/ml stock solution was prepared in H<sub>2</sub>O, aliquots were stored at -20°C.

Heparan sulphate (sodium salt from porcine intestinal mucosa, average molecular weight ~ 12 kDa) MW, Celsus company. A 20 mg/ml stock solution was prepared in H<sub>2</sub>O, aliquots were stored at -20°C.

TG inhibitor R283 was synthesized by R. Saint and I. Coutts, Nottingham Trent University. A 100mM stock solution was prepared in distilled water; aliquots were stored at -80°C.

Surfen (bis-2-methyl-4-amino-quinolyl-6-carbamide) was kindly donated by Prof. J Esko (University of California, USA). A 30 mM stock solution was prepared in DMSO; aliquots were stored at -20°C.

All general chemicals were obtained from Sigma-Aldrich unless otherwise stated.

<b>Chemical</b>	<b>Company</b>
EZ-ECL Chemiluminescence detection kit	Geneflow
Protein G Agarose	Insight Biotechnology Ltd
Protein A Agarose	Roche Diagnostics Ltd
Vectashield mounting medium	Vector Laboratories Ltd
Vectashield mounting medium with propidium iodide	Vector Laboratories Ltd
Full-range Rainbow molecular weight markers	Amersham Biosciences.
Nitrocellulose for Western blotting, 0.22 µm	Anachem
Tissue-Tek O.C.T. <sup>TM</sup> compound	Sakura Finetek Europe

### 2.1.3 Laboratory equipment

<b>Instrument</b>	<b>Company</b>
3000 Biacore system and CM4 sensor chips,	GE Healthcare
AE 6450 Atto Vertical Dual Mini Slab Kit,	Genetic research Instr. Ltd
Biochrom30 Amino Acid Analyser	Biochrom Ltd
Bio-Rad mode 680 microplate reader	Bio-Rad Laboratories Ltd.
Bio-Rad Power Pack 300	Bio-Rad Laboratories Ltd
Blood Tube rotator SB1	Jencons PLS
Digital Net Camera DN100	Nikon Corporation
Electrophoresis tank Multi SUB Mini	Geneflow
Eppendorf refrigerated centrifuge 5417R	Eppendorf UK Ltd
Fujifilm intelligent dark box	Fujifilm Life Sciences
Gene Genius Bioimaging System with UV	Syngene
Harrier 18/80 refrigerated centrifuge	Sanyo Gallenkamp PCL
Heating block QBT4	Grant Instruments Ltd
Leica CLMS confocal laser microscope	Leica
Leica CM1850 UV cryostat	Leica
Neubauer hemocytometer	Hawksley
Nucleofector Device (Amaxa)	Lonza Cologne AG
Optical inverted microscope Olympus CK2	Olympus
Optima TLX-120 Ultracentrifuge	Beckman Coulter
Pellet Pestle	Sigma-Aldrich
Rotor-Gene™ 6000	Corbett Research UK
Soniprep 150 sonicator	MSE UK Ltd
Termocycler TC-3000	Techne UK Ltd
Walker class II microbiological safety cabinet	Walker safety cabinets Ltd.
Water bath SUB14	Grant Instruments Ltd

### 2.1.4 Companies

<b>Company</b>	<b>Address</b>
Abcam	Cambridge, UK
AbD Serotech, Serotech Ltd	Oxford, UK
Activotec	Cambridge, UK
Agilent Technology UK Limited	Santa Clara, Ca, USA
Amersham Biosciences	Bucks, UK.
Anachem	Luton, UK
BdBioscience Clontech	Oxford, UK
Beckman Coulter	High Wycombe, UK
Biochrom Ltd	Cambridge, UK
Bio-Rad Laboratories Ltd.	Hemel Hempstead, UK
BioSera	Ringmer, UK
Calbiochem	Darmstadt, Germany
Cambrex bioscience Ltd.	Wokingam, Berkshire, UK
Celsus Inc.	Cincinnati, Oh, USA
Chemicon International Inc.	Temecula, Ca, USA
Corbett Research UK	Eaton Socon, UK
DakoCytomation	Glostrup, Denmark
Eppendorf UK Ltd	Cambridge, UK
Fujifilm Life Sciences Products	Sheffield, UK
GE Healthcare	Bucks, UK
Geneflow	Fradley, UK
Genetic Research Instr. Ltd	Rayne Braintree, UK
Grant Instruments Ltd	Cambridge, UK
Hawksley	Lancing, UK
Insight Biotechnology Ltd	Wembley, UK
Invitrogen Corporation	Paisley, UK
Jencons PLS	Redhill, UK
Leica	Solms, Germany
Lonza Cologne AG	Cologne, Germany
MSE UK Ltd	London, UK

Nikon Corporation	Tokyo, Japan
Olympus	Watford, UK
PAA laboratories GmbH	Pasching Austria
Promega Corporation	Southampton, UK
Roche Diagnostics Ltd	Burgess Hill, UK
Sakura Finetek Europe	Zoeterwoude, The Netherlands
Santa Cruz Biotechnology Inc	Santa Cruz, Ca, USA
Sanyo Gallenkamp PCL	Leicester, UK
Sarstedt	Leicester, UK
Seikagaku Corporation	Tokyo, Japan
Sigma-Aldrich	Poole, UK
SLS-Scientific Laboratory Supplies	Nottingham, UK
Southern Biotech	Birmingham, UK
Syngene	Cambridge, UK
Techne UK Ltd	Newcastle, UK
Thermo Fisher Scientific	Loughborough, UK
Upstate	Lake Placid, NY, USA
Vector Laboratories Ltd	Peterborough, UK
VWR International	Lutterworth, UK
Walker safety cabinets Ltd.	Glossop, UK
Zedira GmbH	Darmstadt, Germany
Zymed laboratories Inc	San Francisco, Ca, USA

## **2.2 Methods**

### **2.2.1 Cell culture**

#### **2.2.1.1 Cell lines**

Primary mouse dermal fibroblasts (MDF) were isolated from wild type (Sdc-4 +/+) and Sdc-4 null (Sdc-4 -/-) mice (Ishiguro et al., 2000) donated by Takashi Muramatsu, Nagoya University, Japan as described in paragraph 2.2.1.7.

Primary mouse embryonic fibroblasts (MEF) from wild type (TG2 +/+) and TG2 null (TG2 -/-) mice (De Laurenzi and Melino, 2001) were donated by Gerry Melino, Leicester University, UK.

Primary human osteoblasts (HOB) obtained from femoral heads (Scotchford et al., 1998) were donated by S. Downes, University of Nottingham, UK. Human osteoblasts permanently transfected to over express TG2, clone 10 and 14 (HOB-TG2-10 and HOB-TG2-14) (Verderio et al., 2001) were provided by Dr Elisabetta Verderio, Nottingham Trent University, UK.

3T3 fibroblasts with tetracycline-regulated expression of TG2 (3T3-TG2) (Verderio et al., 1998) were provided by Dr. Elisabetta Verderio, Nottingham Trent University, UK.

#### **2.2.1.2 Cell culture conditions**

MDF Sdc-4 +/+, MDF Sdc-4 -/-, MEF TG2 +/+ and MEF TG2 -/- were maintained in DMEM nutrient mixture F12 HAM supplemented with 10% (v/v) heat-inactivated FCS, 2mM L-glutamine, 100 U/ml penicillin and 100 µg/ml streptomycin and non essential amino acid mixture.

HOB, HOB-TG2-10 and HOB-TG2-14 were maintained in Dulbecco's Modified Eagle's Medium (DMEM) supplemented as described above with exception for non essential aminoacid mixture, not added.

3T3-TG2 cells were maintained in the same medium used for HOB further supplemented with 250 µg/ml xanthine, 10 µg/ml mycophenolic acid, 400 µg/ml G418, HAT supplement (Sigma-Aldrich) and 2 µg/ml tetracycline. In these conditions the cells express a low basal

level of TG2; to induce exogenous TG2 expression, cells were cultured in the absence of tetracycline for 72 hours.

#### **2.2.1.3 Sub-culture of cells**

Cells were sub-cultured at about 90% confluence; the cells were washed with serum-free culture medium and then incubated with 0.25% (w/v) trypsin in 5 mM EDTA in PBS, pH 7.4 at 37°C. After complete detachment of the cells, trypsin was inactivated with serum containing culture medium (10% serum) and cells were collected by centrifugation at 300g x 5 minutes. Cell pellet was resuspended in complete culture medium and re-seeded.

#### **2.2.1.4 Cell counting**

Cell counting was performed using a hemocytometer (1 mm<sup>2</sup> depth chamber). Two separate counts of 25 fields (0.04 mm<sup>2</sup>) were performed for every cell suspension using light microscopy at x 10 magnification. The final cell concentration, expressed as cell number/ml was calculated using the following formula:

$$\text{Cell concentration} = \text{average cell number in 25 fields} \times 10^4$$

#### **2.2.1.5 Cryo-preservation of cells**

Confluent cell monolayers were trypsinised and collected as described in 2.2.1.3; the cell pellet was then resuspended in heat inactivated FCS containing 10% (v/v) dimethyl sulfoxide (DMSO). The cells were initially frozen at -70°C for 24 hours prior to long-term storage in liquid nitrogen.

#### **2.2.1.6 Resuscitation of cryo-preserved cells**

Vials of frozen cells were removed from liquid nitrogen storage and quickly thawed at 37°C. The cell suspension was then carefully transferred into 25 cm<sup>2</sup> tissue culture flask containing 5 ml complete growth medium and incubated for 12 hours before changing the medium.

#### **2.2.1.7 Isolation of primary dermal fibroblasts**

Primary fibroblasts were isolated from three months old C57BL/6J mice and Sdc-4 null mice (Ishiguro et al., 2000) following a method optimised by P. Kotsakis (Nottingham Trent University) (Kotsakis, 2005). The animals were sacrificed by neck dislocation,

### 2.2.1.8 Cell transfection

Cell transfection was performed by electroporation using Nucleofector<sup>®</sup> Kit (Amaxa GmbH). Low passage cells were grown until 80-90% confluence level, trypsinized (2.2.1.3) and divided in aliquots containing specific amounts of cells (Table 2-3). After centrifugation (2.2.1.3), the appropriate nucleofector solution (100  $\mu$ l) and DNA (5  $\mu$ g) were added to the cell pellet and the cells were transferred to the electroporation cuvette, that was then inserted in the Nucleofector.

Cell type	Cells	Nucleofector solution	Program
MEF TG2 -/-	$1 \times 10^6$	VPI-1006 (MEF starter kit)	U23
MDF Sdc-4 +/+ and Sdc-4 -/-	$5 \times 10^5$	VPI-1002 (Basic kit for fibroblasts)	A24

**Table 2-3 Parameters for cell transfection using Nucleofector Kit, Amaxa.**

After performing the cell-specific electroporation, the cuvette was removed from the machine and the content was gently resuspended in 500  $\mu$ l complete medium with serum before transferring to a 6 well plate well containing 3 ml complete medium with serum. Unless differently stated, the cells were incubated at 37 °C, 5% (v/v) CO<sub>2</sub> for 48 hours before checking gene expression.

The efficiency of transfection was estimated examining by fluorescence microscopy cells transfected with the control plasmid pmaxGFP<sup>®</sup> (Amaxa). Average efficiency was 80% for MEF and 60% for MDF.

## ***2.2.2 Preparation of matrices for cell adhesion***

Matrices of fibronectin (FN) and TG2-FN were prepared as described by Verderio et al. (2003).

### **2.2.2.1 Fibronectin coating**

Tissue culture plastic surfaces or chamber slides were incubated for 16 hours at 4°C with the appropriate amount of 5  $\mu$ g/ml human fibronectin (Sigma Aldrich) in 50 mM Tris-HCl, pH 7.4 (Tris buffer). 50  $\mu$ l/well of the solution were used for 96 well plates, 110  $\mu$ l/well for 8 well chamber slides and 3 ml/dish for 5 cm diameter Petri dishes. The surfaces were then washed once with Tris buffer and blocked with 3% (w/v) BSA in 50 mM Tris-HCl for 1 hour at room temperature. The surfaces were washed with Tris buffer and serum-free cell culture medium prior to cell seeding.

### **2.2.2.2 Preparation of TG2-FN matrices**

Fibronectin coated surfaces were blocked as indicated in 2.2.2.1, then washed twice with 50 mM Tris-HCl, pH 7.4 and incubated for 1 hour at 37°C with purified guinea pig liver TG2 (gpTG2, Sigma Aldrich) (20  $\mu$ g/ml) in PBS, pH 7.4, containing 2 mM EDTA. 100  $\mu$ l of the solution were used for 96 well plates, 220  $\mu$ l for 8 well chamber slides and 6 ml for 5 cm diameter Petri dishes. The gpTG2 solution was then removed and surfaces were washed twice with Tris buffer and once with serum-free medium before cell seeding.

### **2.2.3 Immunocytochemistry**

Cells were harvested and resuspended in complete medium with or without serum as indicated for every single experiment. The cells were then seeded on 8-well chamber slides ( $1.5 \times 10^4$  cells/ well) and incubated at 37°C, 5% CO<sub>2</sub> for 3 hours, unless otherwise stated; the medium was removed and adherent cells were gently washed with PBS. Cells were fixed in 3.7% (w/v) paraformaldehyde in PBS, pH 7.4 for 15 minutes at room temperature and washed three times with PBS. Permeabilization was performed by incubating the cells for 15 minutes at room temperature with 0.1% (v/v) Triton-X100 in PBS; after that, cells were washed again with PBS for 3 times.

Non specific binding of antibodies was prevented by blocking with 3% (w/v) bovine serum albumin (BSA) in TBS for 1h at room temperature with gentle shaking; after blocking, cells were incubated overnight at 4°C in humidified chamber with the primary antibody diluted in blocking buffer. After washing 3 times for 5 minutes with TBS, the cells were incubated for 2 hours at 37°C in humidified chamber with the secondary antibody conjugated with a fluorescent dye (FITC or TRITC) diluted in blocking buffer. A second series of washes was performed, as after the incubation with primary antibody, and the slide was air dried and mounted with Vectashield fluorescence mounting media (containing or not propidium iodide for nuclei visualization).

In selected experiments, nuclear staining was performed with 4',6-diamidino-2-phenylindole (DAPI); after incubation with secondary antibody, cells were incubated for 3 minutes with 1µg/ml DAPI in PBS. Cells were then washed as described above and coverslips were mounted with Vectashield fluorescent mounting media.

### **2.2.4 Detection of actin stress fibres**

8-well chamber slides were coated with FN or TG2-FN as indicated in 2.2.2.1 and 2.2.2.2. Cells were serum-starved for 16 hours before the experiment, then harvested and resuspended in serum-free medium. In selected experiments, aliquots of  $1.5 \times 10^4$  cells were pre-incubated for 10 minutes at 37°C with RGD or RAD peptide (100 µg/ml) or, in control samples, with serum-free medium only. The cells were seeded on the coated wells and incubated for 1 hour at 37°C, 5% CO<sub>2</sub>. The medium was removed and the cells were

## ***2.2.5 Preparation of protein extracts for Western blotting***

### **2.2.5.1 Total protein extract**

Cell monolayers 90% confluent were washed twice with PBS and scraped in ice cold lysis buffer [20 mM Tris-HCl pH 7.4, 150 mM NaCl, 5 mM EDTA, 1% (v/v) IGEPAL CA-630, 0.5% (w/v) deoxycholic acid, 0.1% (w/v) SDS and protease inhibitor cocktail]. The homogenate was then sonicated on ice, 3 × 5 seconds, at amplitude 5, and then denatured as indicated in section 2.2.6.2.

### **2.2.5.2 Cell fractionation**

Crude membrane fractions were prepared following the method described by Germack et al. (2006). Briefly, confluent cell monolayers were detached with 2mM EDTA in PBS in order to preserve cell surface proteins, collected by centrifugation and resuspended in lysis buffer (as described in 2.2.5.1). The homogenate was centrifuged for 2 minutes at 900g to eliminate whole cells and nuclei, and then ultracentrifuged for 30 minutes at 170,000g at a temperature of 4°C to separate the cytosolic cell fraction from the membrane fraction (pellet). The pellet was resuspended in lysis buffer and used as a crude membrane extract.

### **2.2.5.3 Determination of protein concentration**

Protein estimation was performed using DC assay (Biorad) based on the Lowry method (Lowry et al., 1951). Standard solution of BSA (purity ≥ 96%) with a concentration of 0-1 mg/ml were used to produce the calibration curve. 5 µl of sample or BSA standard, 25 µl of reagent A and 200 µl of reagent B were incubated in 96 well plate, in triplicate. If the protein extracts were prepared using a lysis buffer containing IGEPAL CA-630, reagent S was added to reagent A before the incubation (20 µl reagent S per 1 ml reagent A). After 15 minutes incubation at room temperature, the absorbance of the plate was measured at

750 nm using a SpectraFluor 96 well plate reader. The calibration curve made with the BSA standards was used to derive concentration values for unknown samples.

## 2.2.6 Denaturing sodium dodecyl sulfate polyacrylamide gel electrophoresis (SDS-PAGE)

### 2.2.6.1 Preparation of polyacrylamide gels

SDS PAGE was performed under reducing conditions using modification of the method described by Laemmli (1970) for use in vertical slabs gels. Polyacrylamide resolving gels (80×60×1.5 mm) were prepared as described in Table 2-4 and cast in the Atto minigel system, covered by a layer of distilled water to provide them with a flat upper surface and prevent contact with the air.

The gels were let to polymerise for 30 min at room temperature, then the upper surface was washed with distilled water and the stacking gel was poured on top, together with the 10 wells comb that forms the sample wells; the stacking gel was let to polymerize for 20 minutes at room temperature. Composition of stacking gels is described in Table 2-5.

Stock solution	Final % (w/v) acrylamide		
	8%	10%	12%
Distilled H <sub>2</sub> O	6.99 ml	6.00 ml	5.01 ml
30% (w/v) Acrylamide/Bis-acrylamide (29:1)	3.96 ml	4.95 ml	5.94 ml
1.5 mM Tris HCl pH 8.8	3.75 ml	3.75 ml	3.75 ml
10 % (w/v) SDS	0.15 ml	0.15 ml	0.15 ml
10 % (w/v) Ammonium persulfate	0.05 ml	0.05 ml	0.05 ml
TEMED	0.10 ml	0.10 ml	0.10 ml

**Table 2-4 Composition of SDS-PAGE resolving gels containing different acrylamide amounts.** *The amounts shown are enough to prepare two 6×8×0.15 cm gels for the Atto minigel system.*

Stock solution	Final % (w/v) acrylamide	
	4%	5%
Distilled H <sub>2</sub> O	3.56 ml	3.40 ml
30% (w/v) Acrylamide/Bis-acrylamide (29:1)	0.67 ml	0.83 ml
1 mM Tris HCl pH 6.8	0.63 ml	0.63 ml
10 % (w/v) SDS	0.05 ml	0.05 ml
10 % (w/v) Ammonium persulfate	0.05 ml	0.05 ml
TEMED	0.01 ml	0.01 ml

**Table 2-5 Composition of SDS-PAGE stacking gels containing different acrylamide amounts.** *The amounts shown are enough to prepare two gels for the Atto minigel system.*

### 2.2.6.2 Separation of samples via SDS-PAGE

Protein samples were diluted in 5× concentrated reducing electrophoresis buffer [300 mM Tris-HCl, pH 6.8; 50% (v/v) glycerol; 10% (w/v) SDS; 3.2% (v/v) β-mercaptoethanol; 0.5% (w/v) bromophenol blue]. Samples were denatured at 95°C for 5 minutes in heating block, cooled on ice and centrifuged for 10 seconds in a bench centrifuge to collect all the proteins. The samples were then loaded into the gel and separated at constant voltage of 160 V in electrophoresis buffer at pH 8.3 [25 mM Tris, 192 mM glycine and 0.1 % (w/v) SDS]. Typically, 30-50 µg of proteins were loaded in each well. The current was stopped when the dye at the front ran out of the bottom of the gel.

### 2.2.7 Western blotting and immunoprobings of proteins

#### 2.2.7.1 Western blotting

Proteins separated by SDS-PAGE were transferred electrophoretically onto a nitrocellulose membrane by Western blotting using Atto Vertical Dual Mini Slab Kit wet system method. Four pieces of filter paper and one piece of nitrocellulose were cut to the same size as the gel and pre-saturated with electroblotting buffer [48.8 mM Tris, 39 mM glycine, 20 % (v/v) methanol, 0.0375 % (w/v) SDS] together with two fibre pads. The “sandwich” was assembled in the following order starting from the negative electrode: fibre pad, filter paper, polyacrylamide gel, nitrocellulose, filter paper, fibre pad. The sandwich was then

submerged in a tank containing electroblotting buffer and an ice pack for the refrigeration and a constant current of 180 mA intensity was applied for 60 minutes.

### 2.2.7.2 Membrane staining with red ponceau

After the protein transfer, nitrocellulose membranes were immersed in 0.1 % (w/v) Ponceau S in 5 % (v/v) glacial acetic acid in dH<sub>2</sub>O for 30 seconds to reveal the total protein bands. The staining was washed away by rinsing the membranes in Tris buffered saline (TBS) (25 mM Tris-HCl, 150 mM NaCl and 2 mM KCl, pH 7.4).

### 2.2.7.3 Immunoprobng

After protein transfer, the membranes were incubated in blocking buffer [5 % (w/v) fat-free powder milk in TBS buffer + 0.1% (v/v) Tween-20] for 1 hour at room temperature to avoid non-specific binding of antibodies. Blocked membranes were incubated overnight at 4°C with the opportune dilution of primary antibodies (see Table 2-6) in blocking buffer.

Primary antibody	Dilution factor
Monoclonal mouse anti human fibronectin	1:1000
Monoclonal mouse anti RhoGAP (p190) (clone D2D6),	1:500
Monoclonal mouse anti $\beta$ -tubulin	1:2000
Polyclonal goat anti transglutaminase 2 (ab 10445)	1:1000
Polyclonal rabbit anti focal adhesion kinase (p125)	1:2000
Polyclonal rabbit anti phosphotyrosine	1:250
Polyclonal rabbit anti syndecan-4 (Zymed Inc)	1:150
Polyclonal rabbit anti Transglutaminase 2 (ab2972)	1:200
Rabbit polyclonal anti cyclophilin A	1:1000

**Table 2-6 Dilution factors for primary antibodies used for protein immunodetection via Western blotting.**

Following three washes of 10 minutes with TBS buffer + 0.1% (v/v) Tween-20 (TBST), the membranes were incubated for 2 hours at room temperature with the HRP-conjugated secondary antibody diluted in blocking buffer (see Table 2-7 for antibody dilutions), then they were washed with TBST.

<b>Secondary antibody HRP-conjugated</b>	<b>Dilution factor</b>
Polyclonal goat anti mouse Ig	1:5000
Goat anti rabbit IgG	1:5000
Rabbit anti goat IgG	1:5000

**Table 2-7 Dilution factors for secondary antibodies used for protein immunodetection in Western blotting.**

#### **2.2.7.4 Enhanced Chemiluminescence (ECL) development system**

ECL was performed using EZ-ECL kit (Geneflow) according to manufacturer's instructions. Briefly, equal volumes of solution A and solution B were mixed to a final volume of 1 ml (for 8×6 cm<sup>2</sup> nitrocellulose membrane), incubated in the dark for 5 minutes and then placed in contact with the membrane for 1 minute. ECL substrate was drained, the nitrocellulose was placed protein-side facing upwards onto a tray in the Fujifilm Intelligent dark box (Fujifilm Life Sciences Products) and exposed for a time varying from 10 seconds to 30 minutes, depending on the protein analysed.

#### **2.2.7.5 Stripping and reprobing membranes**

Stripping procedure eliminates antibodies bound to nitrocellulose and permits monitoring the expression of different proteins from the same extracts. Membrane were submerged in stripping buffer [100 mM β-mercaptoethanol; 2% (w/v) SDS; 6.25 mM Tris-HCl, pH 6.7] and incubated at 50°C for 30 minutes. The membranes were then washed two times, for 10 minutes, in a large amount of TBST, than blocked and re-probed as detailed in section 2.2.7.3.

### 2.2.7.6 Quantification of immunodetected proteins

To allow for quantitative comparison of protein band intensity following Western blotting and immunoprobng, a process of manual band quantification was performed using the Aida Image Analyser v.4.03, according to the manufacturer's guidelines. Equal sized boxes were drawn around bands to be quantified, and figures which represent the number of pixels in each box multiplied by the grey shade value of each pixel were generated for each band; a specific background signal level was subtracted from each band.

### 2.2.8 Protein immunoprecipitation

Confluent cell monolayers (typical cell number  $3 \times 10^6$ ) were detached using 2 mM EDTA in PBS, collected by centrifugation and homogenized in ice cold hypotonic buffer (30 mM Tris HCl pH7.4, 5 mM MgCl<sub>2</sub>, 100 mM NaCl and 1 mM EDTA) supplemented with protease inhibitor cocktail (Sigma Aldrich). In selected experiments, cells were incubated for 1 hour at 37 °C with heparitinase (Seikagaku) (30 mU/ml) in serum free medium or, as a control, in serum free medium without heparitinase before homogenization. Cells were then lysed in ice-cold hypotonic 30 mM Tris-HCl buffer, pH 7.4, with protease inhibitors cocktail (Sigma-Aldrich), and after low speed centrifugation (800g, 10 minutes, to remove remaining whole cells and nuclei), crude plasma membranes were prepared as indicated in 2.2.5.2. Proteins were estimated using DC protein estimation kit (Biorad) as described in 2.2.5.3. Equal amounts of membrane proteins (500 µg) were then solubilised in 500 µl lysis buffer containing 1% (v/v) IGEPAL CA 630, 1% (v/v) Triton-X100, 0.5% (v/v) deoxycholic acid (DOC), protease inhibitors. The samples were pre-cleared through 1 hour incubation in rocking platform (Blood Tube rotator Sb1, with a constant speed of 33 rpm), at 4°C in the presence of 50 µl protein-G agarose suspension (Insight Biotechnology Ltd); after that, the samples were centrifuged at 10,000g for 1 minute to precipitate the protein-G agarose, and the cleared lysates were transferred to new tubes. The crude membrane lysates were then subjected to immunoprecipitation by incubation with 2 µg of rabbit anti-Sdc-4 (Zymed) (against a Sdc-4-endopeptide) or anti-TG2 antibody TG100 (Abcam); in negative controls, the membrane preparations were incubated with 2 µg of rabbit anti-gliadin antibody (Sigma-Aldrich) or without antibody. After 1 hour incubation in rocking platform at 4°C, 50 µl of protein-G agarose suspension were added to the samples and the

After the precipitation of the agarose beads by centrifuging the samples at 10,000g for 1 minute, the denatured and reduced immunocomplexes were analysed by Western blotting. 15 µl of the supernatant were separated by reducing SDS-PAGE on 10% polyacrylamide gel, transferred onto nitrocellulose membrane and immunoprobed with antibodies against either TG2, Sdc-4 or FN (as described in 2.2.7) Following incubation with the appropriate HRP-conjugated secondary antibody, bands were revealed by enhanced EZ-ECL chemiluminescence; densitometry of the bands was conducted by Aida ID/evaluation 3.44.

## **2.2.9 Detection of TG activity**

### **2.2.9.1 Preparation of cell extracts for TG activity assay**

Cell homogenates and fractions for measurement of TG2 activity were prepared according to Balklava et al. (2002). Cells were washed with PBS and scraped in ice cold lysis buffer (0.25 M sucrose and 2 mM EDTA in Tris buffer containing protease inhibitor cocktail from Sigma Aldrich); the total cell homogenate was sonicated on ice, 3 × 5 seconds, at amplitude 5.

Cell fractions were prepared by ultracentrifugation of the total homogenate (30 minutes at 70,000g, 4°C); the supernatant was used as cytosolic fraction, whereas the pellet was resuspended in 50 µl of lysis buffer and used as crude membrane preparation.

### **2.2.9.2 TG activity measurement**

Transglutaminase activity was assessed using a modification of the enzyme-linked sorbent assay (ELSA) based on incorporation of biotinylated cadaverine (BTC) into fibronectin described by (Jones et al., 1997).

Microtitre plates were coated with 100  $\mu$ l/well 5mg/ml FN in 50 mM Tris-HCl (Tris buffer), pH 7.4 for 15 hours at 4°C. The plates were then washed with Tris buffer and blocked in 3% (w/v) BSA in Tris buffer for 1 hour at room temperature. 60  $\mu$ g of total cell extracts or cell fractions were then incubated for 2 hours at 37°C in reaction buffer (5 mM CaCl<sub>2</sub> [or 5 mM EDTA], 10 mM DTT and 0.1 mM BTC in Tris buffer) in a final volume of 100  $\mu$ l; every sample was tested in triplicates. Together with the samples, standard quantities of gpTG2 (0-200 nM) were incubated in reaction buffer and used to produce a standard curve relating absorbance and transamidating activity.

The reaction was terminated by two washes of the plate with PBS containing 10 mM EDTA, prior to other two washes with TBST and one with TBS. 100  $\mu$ l/well of 1:5000 dilution of extravidine peroxidase in blocking buffer were then added, and the plate was incubated at 37°C for 1 hour to reveal the covalently bound BTC. After removing the solution, the plate was washed with TBST/TBS as indicated above, and equilibrated with 100  $\mu$ l/well of sodium acetate buffer, pH 6, for 10 minutes. The plate was then incubated with developing solution (7.5% [w/v] 3,3',5,5'-tetramethylbenzidine [TMB] in 0.05 M phosphate-citrate buffer, containing 0.014% [v/v] H<sub>2</sub>O<sub>2</sub>, pH 5.0), 100  $\mu$ l/well. The development was stopped by adding 50  $\mu$ l/well of 2.5N H<sub>2</sub>SO<sub>4</sub> and the plate was then read using a microplate reader at 450 nm. Absorbance values obtained in presence of EDTA were subtracted to the ones recorded in presence of CaCl<sub>2</sub> to eliminate background.

If cell surface TG2 activity was measured,  $2 \times 10^4$  cells/well (detached with 2 mM EDTA in PBS) were incubated in complete culture medium without serum (DMEM and DMEM F12-HAM contain 1.8 mM CaCl<sub>2</sub>) on FN-coated plates in presence of 0.1 mM BTC as indicated for cell homogenates. After blocking the reaction by washing with 10 mM EDTA in PBS, the cells were detached by incubating the plate with 100  $\mu$ l/well of 0.1 % (w/v) deoxycholate in PBS for 20 minutes at room temperature, with gentle shaking. The plate was washed with TBST/TBS as indicated above and covalently incorporated BTC was detected as described for cell extracts.

### 2.2.9.3 *In situ* TG activity assay

The incorporation of FITC-cadaverine in fibronectin by living cells was previously developed to visualise TG2 activity *in situ* (Verderio et al., 1998).

Wild type and syndecan-4 null MDF were enzymatically detached, collected by centrifugation and resuspended in complete growth medium with serum (as described in 2.2.1.3). Cells were seeded in 8-well chamber slides (15,000 cells/well) in the presence of 0.5 mM fluorescein isothiocyanate conjugated cadaverine (FITC-cadaverine) and incubated for 15 hours at 37°C, 5% CO<sub>2</sub>. In selected experiments, cells were additionally incubated with the active-site directed TG inhibitor R283 (200 µM) (Balklava et al., 2002) to confirm the specificity of the assay. At the end of the incubation, the medium was removed, the cells were washed gently with PBS and fixed in ice-cold methanol for 10 minutes at -20°C; this fixation method is essential to remove the unspecifically bound fluorescent compound. After washing 4 times with PBS the samples were mounted with Vectashield mounting medium containing propidium iodide (for visualization of the nuclei) and the incorporation of FITC-cadaverine was visualised using a Leica CLMS confocal laser microscope equipped with an Argon/Krypton laser. Differences in fluorescence were evaluated measuring the intensity of the emission in 5 non overlapping images using Leica TC-SNT software (Leica).

### ***2.2.10 Molecular biology techniques***

Standard molecular biology methods were performed according to Sambrook and colleagues (Sambrook et al., 1989). When kits were used, the instructions of the manufacturers were followed.

#### **2.2.10.1 Transformation of bacteria with plasmid DNA**

Frozen Subcloning Efficiency DH5α *E. coli* competent cells (Invitrogen life technologies) were thawed on ice; 100 ng of plasmid DNA were mixed with 100 µl aliquots of cells and incubated for 30 minutes on ice. Uptake of DNA from the cells was induced by 20 seconds heat-shock in water bath at 37°C followed by 2 minutes incubation on ice. The cells were allowed to recover by the addition of 900 µl Luria Bertani (LB) medium [1% (w/v) bactotryptone, 0.5% (w/v) yeast extract and 1% (w/v) NaCl in H<sub>2</sub>O] and 1 hour incubation at 37°C, 225 rpm. The suspensions were then centrifuged at 1000 g for 1 minute and, after that, the cell pellet was gently resuspended in 200 µl of LB and plated in LB agar plates [LB medium containing 1.5 % (w/v) agar, that determines the solidification] containing the specific selective antibiotic (ampicillin was used at 75 µg/ml, kanamycin at 50 µg/ml). The

plates were incubated overnight (15 hours) at 37°C and they were examined on the following day for the formation of antibiotic-resistant colonies.

#### **2.2.10.2 Storage of bacteria colonies**

A single bacteria colony isolated from a fresh LB plate was used to inoculate 10 ml of selective LB medium; the cells were then incubated at 37°C in a shaking incubator (225 rpm) for 12-16 hours. Glycerol stocks were prepared by mixing 810 µl of the bacterial culture and 190 µl of sterile 80% (v/v) glycerol in cryovials, that were then stored at -80°C.

To retrieve a bacterial clone, the specific glycerol stock was taken out of the -80°C storage and a portion of it was scraped off using a sterile inoculating loop used to inoculate 3 ml LB medium containing the specific selective agent. This procedure was performed quickly, avoiding the thawing of the glycerol stock, which was then immediately transferred to -80°C.

#### **2.2.10.3 Amplification and extraction of plasmid DNA**

Plasmid Mini preparations (minipreps) were prepared using Wizard<sup>®</sup> Plus SV Minipreps DNA purification system (Promega). A single bacterial colony isolated from a fresh LB plate (see 2.2.10.1) was used to inoculate 10 ml of LB medium containing the same antibiotic used for the selection. The cells were then incubated overnight (12-16 hours) at 37°C in a shaking incubator (225 rpm). After that the bacteria were collected by centrifugation (10 minutes at 10,000 g) and lysed, and the plasmid DNA was extracted following the centrifugation protocol indicated by the manufacturer (yield was approximately 10 µg DNA).

When higher amounts of plasmid DNA were required, MIDI kit (Qiagen) was used; in this case 5 ml of LB medium (containing selective antibiotic) were initially inoculated with the bacterial colony and incubated at 37°C in a shaking incubator (225 rpm) for 8 hours. The bacteria culture was then diluted 1:500 into 100 ml selective LB medium and incubated overnight 37°C in a shaking incubator (300 rpm). The bacteria were then harvested and plasmid DNA was purified following manufacturer's instructions (yield was approximately 100 µg DNA).

The plasmid DNA extracted was highly purified (ratio 260/280  $\geq$  1.8), therefore it was directly used for cell transfection.

#### **2.2.10.4 Agarose gel electrophoresis of DNA**

Gels for electrophoresis were prepared dissolving agarose (typically 1% w/v) in Tris-acetate-EDTA (TAE) buffer [40 mM Tris, pH 7.4; 0.114% (v/v) glacial acetic acid; 1 mM EDTA] and heating the solution in a microwave oven until the agarose was completely dissolved. After cooling, ethidium bromide (0.5  $\mu$ g/ml) was added to the solution, which was poured into a casting plate with the appropriate comb. 50 ml of agarose gel were used for small casting plate (8 wells) and 120 ml were used for large plates (15 wells).

#### **2.2.10.5 Restriction enzyme digestion of plasmid DNA**

Restriction enzyme digestions were performed in 100  $\mu$ l final volume containing: 15  $\mu$ g DNA, 10  $\mu$ l specific 10 $\times$  digestion buffer, 5  $\mu$ l of each 10 U/ $\mu$ l restriction enzyme (Promega), 1  $\mu$ l 100 $\times$  BSA solution, distilled water up to 100  $\mu$ l. Digestion reaction was incubated for 1 hour in water bath at 37 $^{\circ}$ C; 1  $\mu$ l of the product was used for DNA electrophoresis (Paragraph 2.2.10.4) to check the efficiency of the reaction.

#### **2.2.10.6 Dephosphorylation of plasmid DNA**

Dephosphorylation prevents the re-circularization of vectors digested with a single restriction enzyme or with two enzymes that generate compatible ends, enhancing the efficiency of the ligation process. The reaction was performed by adding 11  $\mu$ l of 10 $\times$  dephosphorylation buffer and 1  $\mu$ l of alkaline phosphatase (ALP) (Promega) to the 100  $\mu$ l restriction product (2.2.10.5). Dephosphorylation was carried in water bath at 37 $^{\circ}$ C for 30 minutes, then another 1  $\mu$ l of ALP was added and other 30 minutes of incubation were performed as above.

#### **2.2.10.7 Isolation of DNA from agarose gel**

After restriction enzymes digestion, vector and insert DNA was loaded into 0.7% agarose gel and the band of interest was excised using a scalpel keeping the gel on a UV transilluminator for no more than a minute, since UV light causes DNA damages. DNA was then purified from the band using Costar<sup>®</sup> SpinX<sup>®</sup> columns: the agarose band was placed in the columns and centrifuged for 10 minutes at 10,000g to separate the agarose

from the solution containing DNA. In order to concentrate it, DNA was then precipitated by adding 0.25 volumes of 10 M ammonium acetate and 2 volumes of 100 % ethanol and incubating 15 hours at -20°C (or 1 hour on dry ice). A DNA pellet was obtained by centrifugation at 10,000g for 20 minutes; the DNA was washed in 500 µl 70% (v/v) ethanol to eliminate residual salt, centrifuged at 10,000g for 10 minutes and the ethanol solution was removed. The pellet was allowed to air dry and it was then resuspended in 20 µl sterile water. When the DNA was used for ligation, 1 µl of DNA was loaded on 0.7 % agarose gel together with quantitative DNA ladder (Invitrogen), which, by comparison, permits to quantify DNA fragments.

#### 2.2.10.8 Ligation

Ligation was performed overnight at 16°C in a reaction volume of 10 µl; molar ratios insert/vector of 1:1, 1:3 and 3:1 were used, keeping constant the amount of vector (250 ng). The amount of insert to be used was calculated with the formula:

$$ng\ insert = \frac{ng\ vector \times size\ insert\ (base\ pairs)}{size\ vector\ (base\ pairs)} \times molar\ ratio\ insert/vector$$

Specific amounts of insert and vector were mixed with 1 µl 10× ligation buffer, 0.8 µl (2.5 U) T4 ligase (Promega) and distilled water up to the final volume.

The total ligation product was used to transform an aliquot of *E.coli* competent cells as described in paragraph 2.2.10.1.

#### 2.2.10.9 RNA extraction

RNA was extracted from primary cells using RNeasy kit (Quiagen) following manufacturer's instructions. The RNeasy procedure represents a well-established technology for RNA purification. Briefly, after cell lysis, RNA was allowed to bind a silica membrane in presence of a high salt buffer containing RNases inhibitors; after eliminating cell-contaminants and salts through a series of washes, RNA was eluted from the silica membrane in RNase-free water.

Aliquots of  $1 \times 10^6$  cells were used for the extraction. To avoid RNA degradation, all the instruments and working surfaces were cleaned with RNaseZap® RNase decontamination

solution (Ambion) and rinsed with 0.1% diethylpyrocarbonate (DEPC)-treated water before use; the samples were digested with RNase-free DNase before reverse transcription to minimize the risk of DNA contamination.

#### **2.2.10.10 Quantification of nucleic acids**

Concentration of DNA and RNA samples was determined by using spectrophotometry. The samples were diluted (typically 1:50) in 10 mM Tris-HCl, pH 8.0 and placed in a quartz micro-cuvette; absorbance was measured at 260 and 280 nm to determine nucleotide concentration and grade of purity. When RNA was measured, the cuvette was washed with DEPC-treated water before use to prevent RNA degradation. Considering that at 260 nm an optical density of 1 corresponds to 50 µg/ml for DNA and 44 µg/ml for RNA, nucleotide concentrations were calculated following the formulas indicated below:

*Concentration of DNA sample* = 50 µg/ml x A<sub>260</sub> x dilution factor

*Concentration of RNA sample* = 44 µg/ml x A<sub>260</sub> x dilution factor

#### **2.2.10.11 Reverse transcriptase polymerase chain reaction (RT-PCR)**

RT-PCR was performed using SuperScript™ II Reverse Transcriptase (Invitrogen), enzyme that synthesizes first-strand cDNA starting from RNA template. A reaction containing 1 µl Oligo R<sub>15</sub>, 2 µg RNA, 4 µl dNTP mix and sterile water up to 12 µl was prepared in a nuclease-free microtube, heated at 65°C for 5 minutes and chilled on ice. 4 µl of 5× First-Strand buffer and 2 µl of 0.1 mM DTT were added, the content of the tube was gently mixed and incubated at 42°C for 2 minutes before adding 1 µl (200 units) of SuperScript™ II RT and incubating at 42°C for 50 minutes. The reaction was inactivated by incubating it at 75°C for 15 minutes; 2 µl of the RT-PCR product were used for conventional PCR reactions 2.2.10.12) in a final 50 µl volume.

#### **2.2.10.12 Polymerase chain reaction (PCR)**

PCR was performed using GoTaq® Flexi DNA polymerase kit (Promega) following manufacturer's instructions; reactions were performed in a final volume of 50 µl, using 1 µg DNA. When cDNA was used as template, 2 µl of RT reaction were used (see 2.2.10.11). PCR reactions were prepared in nuclease-free 200 µl tubes kept on ice.

5× Green GoTaq <sup>®</sup> Flexi buffer	10 µl
25 mM MgCl <sub>2</sub>	3 µl
5 mM dNTP mix	8 µl
20 µM Forward primer	1.5 µl
20 µM Reverse primer	1.5 µl
GoTaq <sup>®</sup> Flexi DNA polymerase (5U/µl)	1 µl
DNA (or cDNA)	1 µg (or 2 µl)
Nuclease-free water	up to 50 µl

All the PCR programs used included a initial denaturation step of 5 minutes at 94°C followed by 30 cycles of denaturation (1 minute, 94°C), primer annealing (45 seconds, see Table 2-1 and Table 2-2 for specific annealing temperatures), elongation (72°C, 45 seconds); a final elongation step (5 minutes, 72°C) was performed to complete the synthesis of all the DNA strands, then the samples were kept at 10°C.

### **2.2.11 Subcloning of TG2 and Sdc-4 cDNA into mammalian expression vectors**

Full length TG2 cDNA was amplified by PCR from pSG5TG (Appendix 2) (Gentile et al., 1992) using proof-reading Pwo-DNA polymerase (Roche) and the *EcoRI*-modified primers (5'→3') pSG5S: atcagaattcatggccgaggagctggtcttagagagg (forward) and pSG5AS: atcagaattccgggcggggccaatgatgacattccgg (reverse) listed in Table 2-1. The underlined bases represent *EcoRI* restriction sites; 4 additional bases were added after *EcoRI* sequence to ease the endonuclease digestion. The primers were designed with the purpose of keeping TG2 cDNA sequence in frame with EGFP coding region after insertion of TG2 cDNA into the mammalian expression vector pEGFP-N1. The PCR product and the vector were then digested with *EcoRI*, to generate compatible ends and ligated as indicated in 2.2.10.8. Plasmid DNA from transformed kanamycin-resistant *E. coli* was analysed for the presence and the correct orientation of TG2 cDNA by double restriction with *EcoRV* and *XhoI* (Figure 2-1). Plasmid DNA from clones containing circularised pEGFP-N1 only would generate a single fragment of 4733 bp, while purified plasmid DNA with correct TG2 orientation (pEGFP-TG) was used for transfection of mammalian cells via electroporation as described in 2.2.1.8.

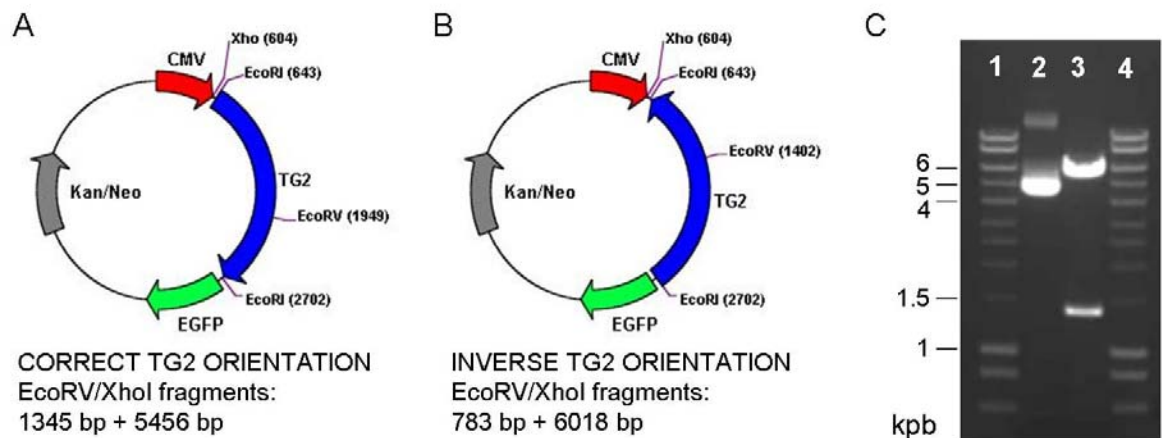


**Figure 2-1 Screening of pEGFP-TG2 construct by double restriction with *EcoRV/XhoI*.** The map of pEGFP-TG2 with correct and inverse orientation of TG2 cDNA is shown in (A) and (B), respectively. Position of restriction site is indicated next to each restriction enzyme. CMV, cytomegalovirus promoter; Kan/Neo, resistance to kanamycin/neomycin. (C) Electrophoretic separation of restriction products: 1 and 4, 1 kb DNA ladder (Promega); 2, uncut pEGFP-TG2; 3, pEGFP-TG2 digested with *EcoRV* and *XhoI*.

Syndecan-4 cDNA was provided by Dr M. Bass (Manchester University, UK) at the *EcoRI/SalI* sites of the cloning vector pBluescript. The plasmid DNA was digested with *EcoRI* and *SalI* (as described in 2.2.10.5) to generate extremes compatible with the ones of the mammalian expression vector pcDNA 3.1 (+). Insert and vector were ligated as described in 2.2.10.8 to generate the construct pcDNAhS4 (Figure 2-2).

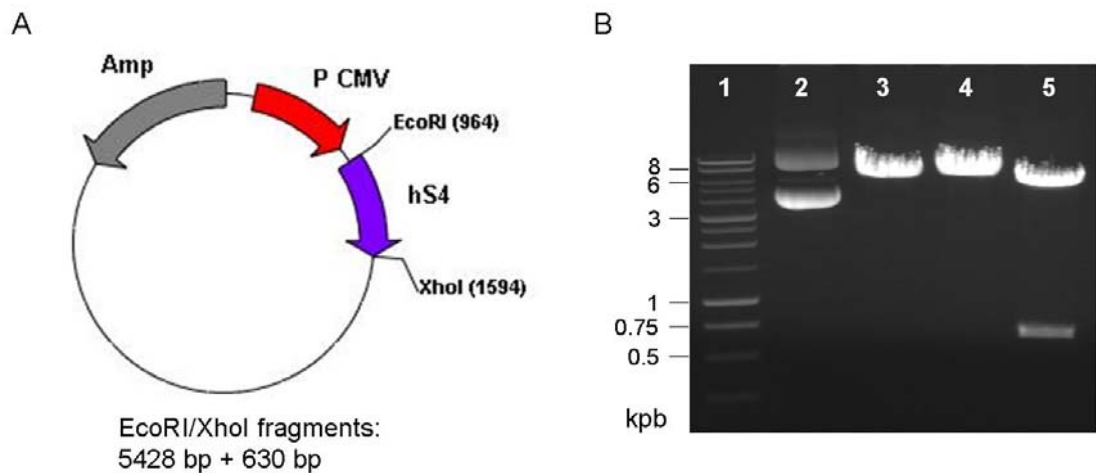


**Figure 2-2 Screening of pcDNAhS4 construct by double restriction with EcoRI/XhoI.** (A) Map of the construct, with indicated the restriction sites for EcoRI and XhoI. CMV, cytomegalovirus promoter; Amp, ampicillin resistance. (B) Electrophoretic separation of restriction products: 1, 1 kb DNA ladder (Promega); 2, uncut pcDNAhS4; 3-4-5, pcDNAhS4 digested with EcoRI, XhoI and EcoRI plus XhoI, respectively.

### 2.2.11.1 Real time PCR

In order to have a precise quantification of gene expression, cDNA samples (2.2.10.11) were analysed by real time PCR using iQ™ SYBR Green Supermix for qPCR (Biorad). All the reactions were prepared in triplicates in micro nuclease-free tubes.

2× iQ™ SYBR Green Supermix	6.25 µl
20 µM Forward primer	0.375 µl
20 µM Reverse primer	0.375 µl
cDNA template	1 µl
Nuclease-free water	up to 12.5 µl

GAPDH was used as housekeeping gene in order to determine the relative expression of the genes of interest. The sequences of the primers used for real time PCR are listed in Table 2.1-2.

An initial denaturation step of 3 minutes at 95°C was followed by 40 cycles of denaturation (94°C, 1 minute), annealing (60°, 1 minute) and elongation (72°C, 1 minute). For the preparation of melting curves, a ramp temperature from 58°C to 95°C was used.

A mean cycle threshold (Ct) value was calculated for every gene of interest from the fluorescence data and the relative gene expression was calculated using the  $2^{-\Delta\Delta Ct}$  (delta-delta Ct) method (Livak and Schmittgen, 2001); the threshold was arbitrarily determined for every reaction, in order to differentiate the fluorescence from the background. Ct is inversely proportional to the logarithmic scale of the initial quantity of template, hence a higher number of cycles (high Ct value) will be required to reach the threshold if the quantity of template is low.

For each gene of interest, a normalized delta Ct ( $\Delta Ct$ ) value, indicating the level of expression of the gene compared to the expression of GAPDH, was calculated as:

$$\Delta Ct \text{ (normalised to GAPDH)} = Ct \text{ (target gene)} - Ct \text{ (GAPDH)}$$

From this value, delta-delta Ct ( $\Delta\Delta Ct$ ) value, representing the difference of expression between the gene of interest and a calibrator, was calculated as:

$$\Delta\Delta Ct = \Delta Ct - \Delta Ct \text{ (calibrator)}$$

The calibrator can be any of the target genes, and it is used as a reference to calculate the expression of the other genes of interest.

For every gene of interest, the relative expression was calculated as  $2^{-\Delta\Delta Ct}$ .

### 2.2.11.2 Mice genotyping

Genomic DNA was extracted from mice for genotyping purposes before isolation of primary dermal fibroblasts (2.2.1.7). Ear biopsies were obtained from 1 month old mice and placed in 500  $\mu$ l DNA extracting buffer (10 mM Tris HCl pH 8, 400 mM NaCl, 100 mM EDTA, 0.6% [w/v] SDS and 0.4 mg/ml proteinase K). The samples were incubated in water bath at 55°C for 2 hours and then mixed by vortex to complete the solubilisation. To precipitate DNA, after adding 500  $\mu$ l of isopropanol the samples were centrifuged at 13,000 g for 10 minutes and the supernatant was discarded. The DNA pellet was resuspended in 30  $\mu$ l Tris-EDTA (TE buffer), pH 8.0 and incubated at 65 °C for 15

## **2.2.12 Transglutaminase-2 binding studies to heparin/HS**

### **2.2.12.1 ELISA-based assay to measure TG2 binding to heparin and heparan sulfates**

#### *2.2.12.1.1 Immobilisation of heparin and fibronectin for solid binding assay*

The ELISA-based assay was developed using BD™ heparin binding plates (BD Biosciences), specially treated with plasma polymerisation to immobilize a wide range of active and unmodified heparin and heparan sulfate (Mahoney et al., 2004).

Low molecular weight heparin (4-6 kDa) or heparan sulfate (12 kDa) were dissolved in PBS at 1.2, 2.3 or 4.6  $\mu\text{M}$  concentration and immobilized on heparin binding plate by 15 hours incubation at room temperature. Fibronectin was dissolved in 50 mM Tris, pH 7.4 at a concentration of 5  $\mu\text{g}/\text{ml}$  and immobilised on conventional microtiter plate by 15 hours incubation at 4°C. Plates were washed three times with PBS and incubated for 1 hour at 37 °C with blocking solution (3% w/v BSA in PBS); after washing three times with PBS, the plates were ready to be used for solid binding assay.

#### *2.2.12.1.2 Solid binding assay*

Guinea pig liver TG2 (0-600 ng/well) was incubated on heparin/HS or FN coated-plate in blocking buffer containing either 2 mM EDTA or 2 mM  $\text{CaCl}_2$  for 2 hours at 37°C, in order to reach binding equilibrium. The plate was then washed with PBS as described above and incubated overnight with anti-TG2 antibody (Cub4701, Abcam; 0.2  $\mu\text{g}/\text{ml}$ ) of in blocking buffer at 4 °C. After washing with PBS, the plate was incubated with 1:5000 dilution of goat anti mouse immunoglobulins-HRP (Sigma-Aldrich) in blocking buffer for 2 hours at room temperature. The plate was developed by using 3,3',5,5' TMB liquid substrate system (Sigma-Aldrich; 200  $\mu\text{l}/\text{well}$ ) according to manufacturer's instructions.

The color reaction was stopped by adding 0.5 M H<sub>2</sub>SO<sub>4</sub> (50 µl/well) and read at 450 nm using a SpectraFluor 96 well plate reader. The strength of the binding was determined via GraphPrism software, which provided an approximate dissociation constant (K<sub>d</sub>). The data were fitted to “one site specific binding model”, described by the equation  $Y = B_{max} * X / [K_d + X]$ , where X is the concentration of the ligand, Y is the binding, B<sub>max</sub> is the maximum binding (in the same unit as Y) and K<sub>d</sub> is expressed in the same unit as X. The equation is based on the consideration that at equilibrium only a small fraction of the ligand is bound to the substrate, so the free ligand concentration is very close to the ligand concentration added at the beginning.

#### 2.2.12.2 Surface Plasmon Resonance (SPR)

SPR was performed at the “Institut de Biologie Structurale” CEA-CNRS-UJF, Grenoble, France, in a collaborative project with Dr. H. Lortat-Jacob, using a 3000 Biacore system.

Size defined heparin (6 kDa), was biotinylated at its reducing end with Biotin-LC-Hydrazide and immobilized on a Biacore sensorchip. For this purpose, two flow cells of a CM4 sensorchip were activated with 50 µL of 0.2 M N-ethyl-N'-(diethylaminopropyl)-carbodiimide and 0.05 M N-hydroxysuccinimide, before injection of 50 µl of streptavidin (0.2 mg/ml in 10 mM acetate buffer pH 4.5). The remaining activated groups were blocked with 50 µl ethanolamine 1M, pH 8.5. Typically, this procedure permitted coupling of approximately 3500 resonance units (RU) of streptavidin. Biotinylated heparin (5 µg/ml) in HBS containing 0.3 M NaCl was then injected across one flow cell to obtain an immobilization level of 50 RU. The other one was left untreated and served as a negative control. For binding assays, 80 µl of purified TG2 (0-586 nM) diluted in HBS-EP buffer [0.01 M HEPES, pH 7.4; 0.15 M NaCl; 3 mM EDTA, 0.005 % (v/v) Surfactant P20] at 25°C were simultaneously injected at a flow rate of 10 µl/min (kinetic mode) across the control and heparin surfaces, after which the formed complexes were washed with running buffer for 5 min. The sensorchip surface was regenerated with a 1 minute pulse of 0.025% (w/v) SDS followed by 5 minutes of 2 M NaCl in HBS-P buffer. Control sensorgrams were subtracted on line from the heparin sensorgrams, and results analyzed using the Biaeval 3.1 software.

### **2.2.12.3 Cell adhesion to heparin/HS-coated plates**

Heparin binding plates (BD Biosciences) were coated with 2.3 or 4.6  $\mu\text{M}$  heparin or 1.2, 2.3, 4.6  $\mu\text{M}$  HS following manufacturer's instructions, as described in section 2.2.12.1.1, then washed and blocked with 3 % (w/v) BSA in PBS for 1 hour at room temperature. Wild type and TG2 null mouse embryonic fibroblasts, serum-starved for 15 hours and allowed to adhere in serum-free medium for 1 hour at 37°C, 5% CO<sub>2</sub> ( $1 \times 10^4$  cells/well). The medium was removed and the attached cells were washed with PBS and fixed in 3.7% (w/v) paraformaldehyde in PBS for 15 minutes at room temperature. The excess fixative was washed away with 3 PBS washes, after that the fixed cells were permeabilized in 0.1% (v/v) Triton X-100 in PBS for 15 minutes at room temperature. After further washing with PBS, the fixed and permeabilised cells were stained with crystal violet solution (0.5% w/v crystal violet in 70% v/v ethanol), extensively washed with distilled water and allowed to air dry before microscope observation. For a precise quantification of cell adhesion, crystal violet stained cells were solubilised in 30% (v/v) acetic acid and the absorbance of the specimens was measured at 540 nm using a microplate reader (Biorad) as previously described (Balklava et al., 2002).

### **2.2.13 Statistical analysis**

All experiments were undertaken at least three times unless specified. Data are expressed as means  $\pm$  standard deviation (SD). Differences between data sets were determined by the Student's t-test (two-tailed distribution, two-sample equal variance). When several data sets had to be compared to each other, One-way Anova was used to determine statistically significant differences.

## ***Chapter 3: Outside-in role of TG2 in cell adhesion: implication of Sdc-4***

### ***3.1 Introduction***

The process of cell adhesion and subsequent spreading requires specific interactions of cell-surface molecules with the adhesion substrate, followed by a signalling cascade which determines a re-organization of the cytoskeleton leading to the formation of focal adhesions (FA) and actin stress fibres (SF). Two main complementary signalling pathways originate from integrins and Sdc-4, as explained in Chapter 1, section 1.2.9.3 (Figure 3-1) (Bass et al., 2007; Morgan et al., 2007; Stephens et al., 2004). Cell attachment, mediated by integrins, involves FAK auto-phosphorylation at Tyr397, but complete activation of the kinase and phosphorylation of other FA components such as paxillin and vinculin is required for the subsequent spreading (Wilcox-Adelman et al., 2002).

Central to cell adhesion is the activation of FAK, occurring via phosphorylation of the enzyme. FAK is initially auto-phosphorylated (Tyr397) upon integrin clustering induced by cell-matrix contact; this process leads to the complete activation of FAK through further phosphorylation (Tyr 576 and Tyr 577) involving Src kinases. Activated FAK, together with driving the formation of FA, determines the regulation of the small GTPase RhoA, which, in turn, is involved in the formation of SF. FAK phosphorylation at Tyr 397 has been shown to be critical for the initial downregulation of RhoA at the beginning of the adhesion process (Ren et al., 1999), leading to efficient cell spreading. According to this, FAK null cells are characterised by RhoA hyper-activity (Ren et al., 2000). In the second phase of cell adhesion FAK contributes to RhoA activation determining full SF formation. Sdc-4 appears to have an important role in the full activation of FAK and cells defective in Sdc-4 have been shown to have impaired FAK activation and retarded cell migration (Gentile et al., 1992; Saoncella et al., 1999). Sdc-4-mediated activation of FAK occurs through the activation of PKC $\alpha$  which, in turn, activates Src kinases responsible for FAK phosphorylation (Simons and Horowitz, 2001).

TG2 has been shown to have different roles in cell adhesion. Firstly, it can modify ECM components via its crosslinking activity thus enhancing the adhesive potential of the matrix; secondly, thanks to the GTP-binding potential, it can contribute to the signalling events involved in cytoskeleton re-organisation (Gentile et al., 1992; Stephens et al., 2004).

In particular, intracellular GTP-bound TG2 is suggested to be involved in the regulation of signal transduction pathway leading to the activation of PLP-C $\delta$ 1, which, in turn, regulates the activity of PKC, involved in FAK activation cascade (Nakaoka et al., 1994). Extracellular TG2, in complex with FN, is involved in a RGD-independent adhesion process which does not depend on its enzymatic activity and which complements integrin-mediated adhesion (Stephens et al., 2004). This process relies on the presence of cell surface HS, and is impaired if the cells are treated with heparitinase (Verderio et al., 2003). Lack of TG2 determines impairment in the spreading process, in fact cells with defects in TG2 expression (via transfection of antisense RNA for TG2) were shown to form focal complexes at the base of actin filaments, but these complexes failed to mature into complete FA; moreover, TG2-deficient cells were shown to have an impairment in SF formation (Jones et al., 1997; Stephens et al., 2004). These TG2-related defects seem to be related to an impairment of FAK phosphorylation/activation. Indeed, even though TG2-deficient cells had values of FAK-P (Y397) similar to control cells, they had significantly lower levels of FAK-P(Y576), implicated in FA and SF formation (Stephens et al., 2004).

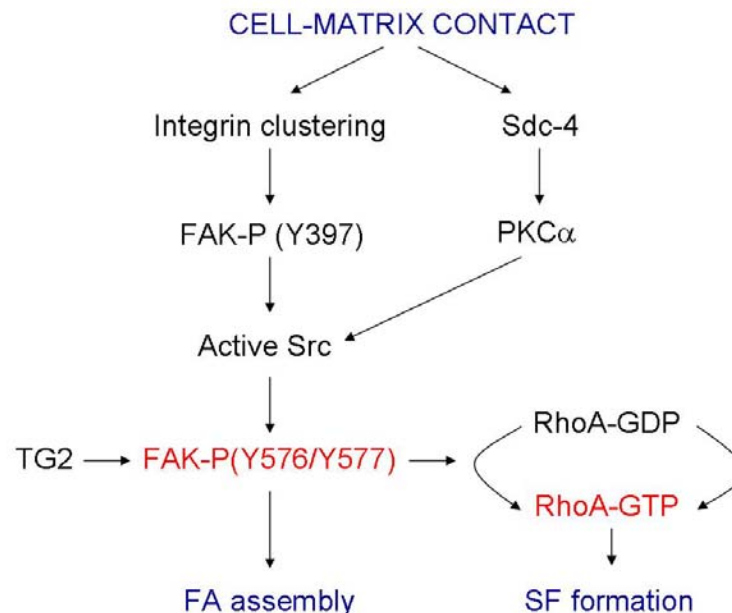


**Figure 3-1** Signalling events leading to FA and SF formation upon cell adhesion to FN.

Given the signalling role of cytosolic TG2 and the role of TG2 associated to FN in RGD-independent cell adhesion, which relies on cell surface HSPG (Verderio et al., 2003), it is possible that TG2 may be involved in FAK activation in the initial stages of cell adhesion in a co-operative way with the HSPG receptor Sdc-4.

The aims of this chapter were (1) to investigate the specific role of extracellular TG2 in the cell adhesion process and FAK activation and (2) to test the hypothesis that Sdc-4 may be involved in TG2-mediated RGD-independent cell adhesion. Primary embryonic fibroblasts with and without deletion of the gene coding for TG2 were the chosen model for the investigation of the role of matrix TG2 in cell adhesion. Primary dermal fibroblasts with and without targeted deletion of Sdc-4 gene were utilised to test the involvement of Sdc-4 in TG2-mediated RGD-independent cell adhesion.

## 3.2 Results

### 3.2.1 TG2 localisation in primary fibroblasts

Transglutaminase-2 localization was investigated in the early stages of cell adhesion on FN, in order to understand whether TG2 externalisation is an early event and hence it can contribute to initial cell adhesion/spreading on FN. Indirect immunofluorescent staining was performed in embryonic fibroblasts (MEF) from wild type mice, using MEF originated from TG2 null mice (De Laurenzi and Melino, 2001) as a negative control.

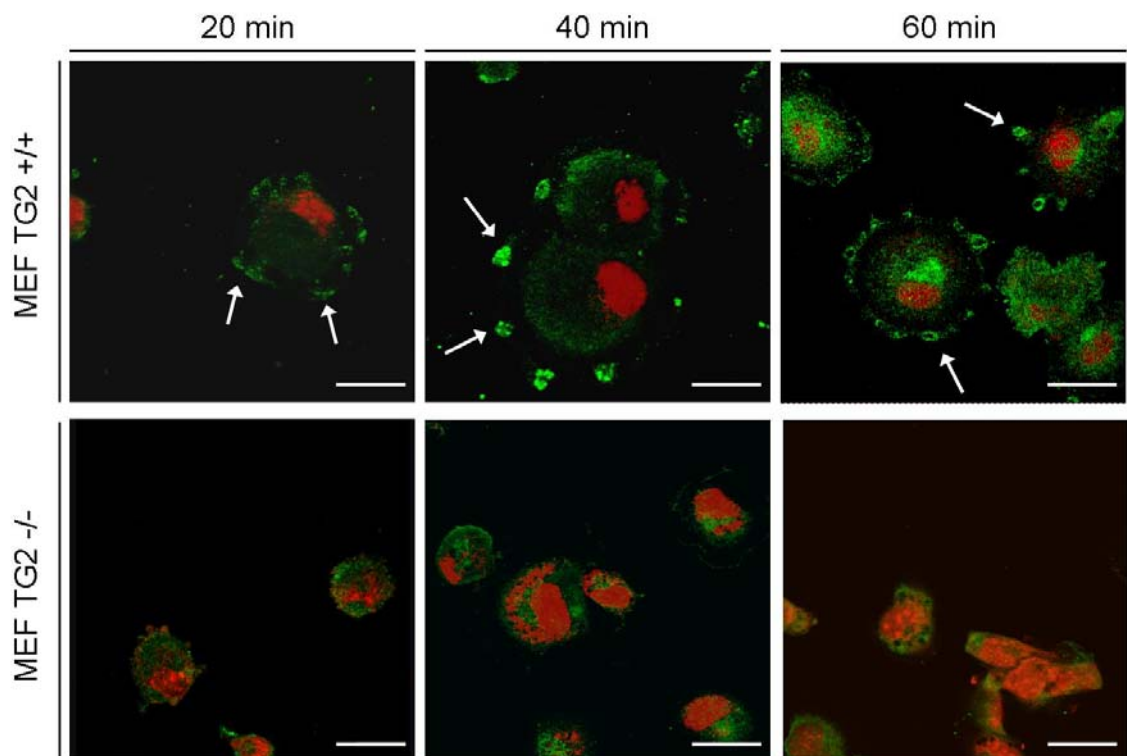


**Figure 3-2** Localization of TG2 in primary fibroblasts adhering on FN. Wild type (TG2+/+) and TG2 null (TG2-/-) MEF were allowed to adhere on FN-coated slides in medium containing serum for 20, 40 and 60 minutes (min). After fixing and permeabilising the cells, TG2 was detected by monoclonal anti-TG2 antibody Cub7402 (1:100) followed by FITC-labelled secondary antibody (1:100); nuclei were stained with propidium iodide. Images were acquired by confocal microscopy. The arrows point at dense areas of TG2 localisation at the basal cell surface. The bar indicates 20  $\mu$ m.

Cells were allowed to adhere on FN-coated slides in complete medium containing serum for 20, 40 and 60 minutes, then fixed, permeabilised and stained for TG2 (Figure 3-2). As shown in Figure 3-2, an increasing level of TG2 was detected at the periphery of wild type cells starting from the early stage of 20 minutes adhesion (arrows). At 40 minutes after seeding, TG2 appeared to be concentrated in punctuate structures at the cell periphery of TG2 *+/+* fibroblasts, resembling cell-matrix adhesion points; this distribution was maintained at 60 minutes adhesion, with an intensification of the signal (pointed by arrows). TG2 also appeared to be localised intracellularly in wild type MEF, with a marked staining in the perinuclear area. A perinuclear staining was detected in TG2 *-/-* cells at 20, 40 and 60 minutes adhesion; this staining could be non specific and/or due to another member of the TG family expressed in TG2 *-/-* MEF.

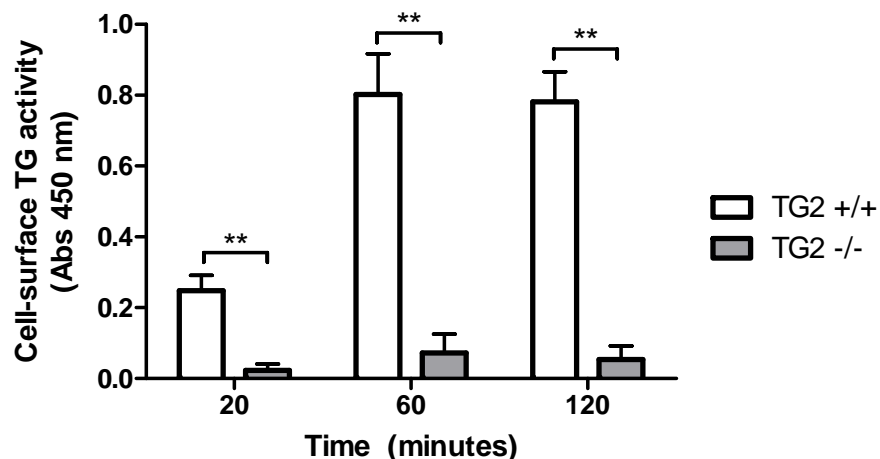


**Figure 3-3 Extracellular TG activity in primary fibroblasts.** Wild type (TG2 *+/+*) and TG2 null (TG2 *-/-*) MEF were allowed to adhere to FN for 20, 60 and 120 minutes in serum-free medium supplemented with biotinylated cadaverine. 2mM CaCl<sub>2</sub> and 5 mM DTT were added to the culture medium to activate the TG-mediated incorporation of the amine substrate into DOC-insoluble FN matrix. *n*=3; \*\* indicates *p*<0.01.

The externalisation of TG2 at early stages of cell adhesion was also monitored by measuring its transamidation activity in fibroblasts adhering on FN-coated microplates (biotin-cadaverine incorporation into DOC insoluble FN matrix), an ELISA-type assay developed by (Jones et al., 1997). This assay, which is performed on whole cells in culture, measures the activity of externalised transglutaminases only; in addition, it is thought to be specific for the activity of TG2 (Verderio et al., 1998). However, TG2 null cells were used as a negative control to confirm the specificity of the assay for TG2. In agreement with the TG2 staining (Figure 3-2), in TG2 +/+ cells it was possible to detect extracellular TG activity starting from 20 minutes cell adhesion (Figure 3-3); the measured activity reached a maximum level at 60 minutes adhesion and then remained constant, as shown by the measurement at 120 minutes. The residual activity found in TG2 -/- cells, was significantly lower compared to that of TG2 +/+ cells at all the time points ( $p < 0.01$ ). By examining the expression of all the members of the TG family in wild type and TG2 -/- cells by RT-PCR, it was found that TG2 is the only member of the family expressed in wild type MEF. However, TG -/- MEF express TG1 (Figure 3-4); this is likely to be a compensatory event which may be responsible for the residual TG activity and was observed before by De Laurenzi and Melino (2001).

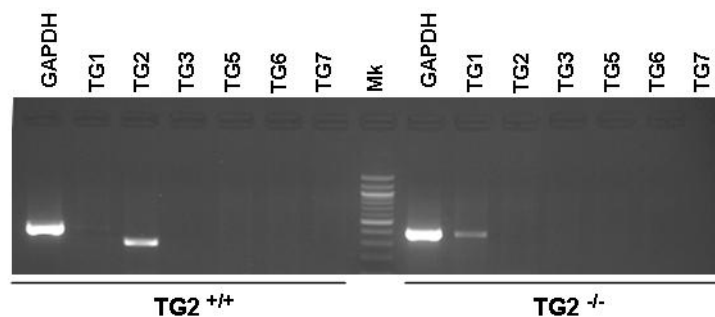


**Figure 3-4 RT-PCR-based study of TG family members in MEF.** *cDNA preparation from wild type (TG2 +/+) and TG2 null (TG2 -/-) MEF were analysed for the presence of various member of the TG family. GAPDH amplification was used as a control for the cDNA quality. The primers used are listed in Table 2-2. Mk, 100 bp DNA ladder.*

The distribution of TG2 in primary fibroblasts was also monitored by Western blotting. Crude membrane extracts and cytosolic fractions were prepared from TG2  $+/+$  and TG2  $-/-$  MEF and analysed for the presence of TG2. The membrane fraction of wild type cells showed a 77 kDa immunoreactive band corresponding to the molecular weight of TG2 (Figure 3-5, arrowheads) and, as expected, no immunoreactivity was detected in the crude membrane extracts of TG2  $-/-$  cells (Figure 3-5). The cytosolic fraction of wild type cells showed the 77 kDa TG2 band (Figure 3-5, arrowhead) but, in addition to that, two lower molecular weight bands (approximately 67 kDa and 55 kDa) (Figure 3-5, arrows). The lower bands were also present in the cytosolic fraction of TG2  $-/-$  cells, suggesting lack of specificity. Densitometric analysis showed that approximately 47% of the detected TG2 was located in the membrane fraction and 53% in the cytosolic fraction of TG2  $+/+$  cells.

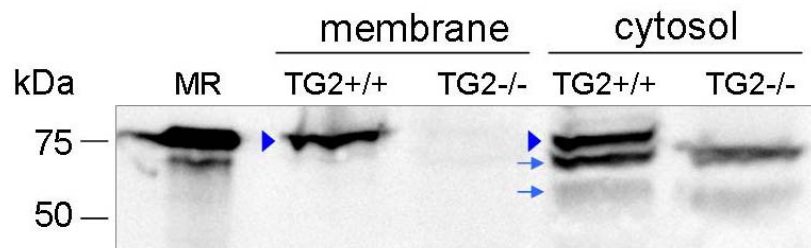


**Figure 3-5 TG2 distribution in MEF.** TG2 was detected by Western blotting in membrane and cytosolic fractions from wild type (TG2  $+/+$ ) and TG2 null (TG2  $-/-$ ) MEF; 25  $\mu$ g proteins were loaded. TG2 was detected by polyclonal anti TG2 antibody ab10445 followed by secondary antibody HRP-conjugated. MR indicates gpTG2 standard, 100 ng. Arrowhead, 77 kDa TG2; arrows, additional immunoreactive bands at 67 and 55 kDa.

### 3.2.2 Role of TG2 in the early stages of cell adhesion

The early externalisation of TG2 during fibroblasts adhesion supports the idea of a specific role for matrix TG2 in FA and actin SF formation, opening events in the cell adhesion/spreading process. To investigate the role of externalised TG2, the formation of FA and actin SF was monitored in TG2  $+/+$  and TG2  $-/-$  cells adhering on FN, and rescue experiments with either TG2 cDNA or extracellular TG2 were carried out.

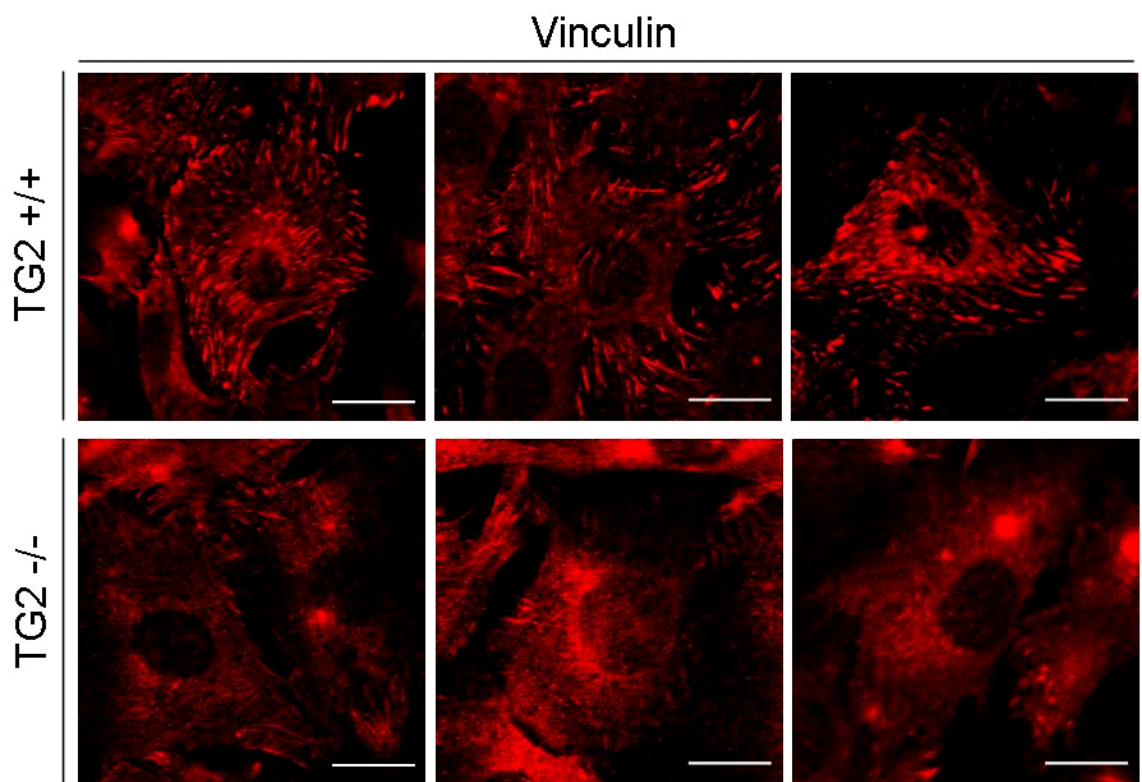


**Figure 3-6 Lack of TG2 impairs vinculin FA formation.** Staining of vinculin-containing FA in fixed and permeabilised wild type (TG2  $+/+$ ) and TG2 null ( $-/-$ ) MEF after 45 minutes adhesion on FN coated slides in serum-free medium. The cells were serum starved (0.1 % serum) for 16 hours before the experiment. Vinculin was detected with monoclonal anti human-vinculin antibody followed by incubation with secondary antibody conjugated with Red X Rhodamine. Images were acquired by fluorescent confocal microscopy. Three random fields per cell type are shown. The bar indicates 20  $\mu$ m.

As shown in Figure 3-6, after 45 minutes of adhesion on FN wild type cells formed sharp vinculin-containing FA, distributed in defined sites at the cell surface; on the contrary, TG2  $-/-$  cells showed diffused vinculin staining. The staining of actin SF via FITC-labelled phalloidin, which binds filamentous actin, revealed a dense network of mature actin fibres crossing the cell body of TG2  $+/+$  cells (Figure 3-7). Cells lacking TG2 failed to form a complete actin cytoskeleton, but they formed thin actin fibres which did not appear to end at FA as in wild type cells (Figure 3-7). These findings indicate that lack of TG2 leads to a disruption in SF formation.

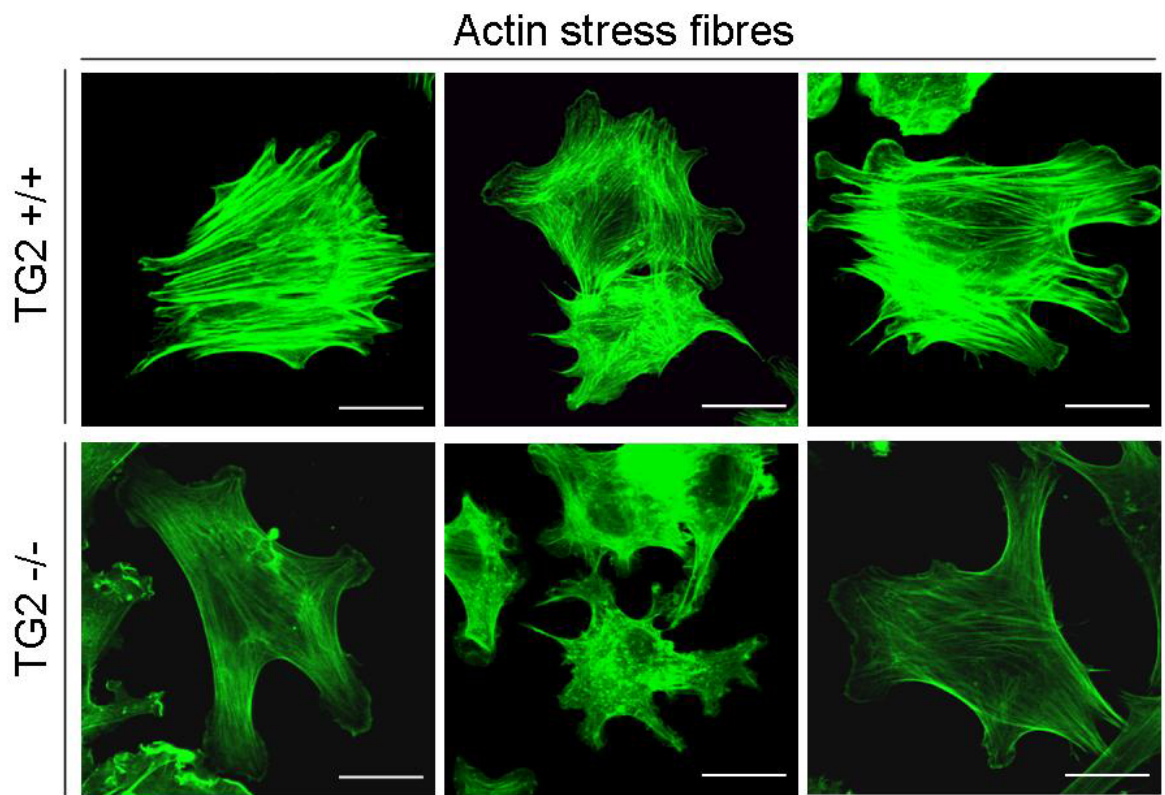


**Figure 3-7 Lack of TG2 impairs actin SF formation.** *Staining of actin SF in wild type (TG2  $+/+$ ) and TG2  $-/-$  MEF after 45 minutes adhesion on FN coated slides in serum-free medium. The cells were serum starved (0.1 % serum) for 16 hours before the experiment. Actin stress fibres were detected by incubating fixed and permeabilised cells with FITC-labelled phalloidin. Images were acquired and presented as described in Figure 3-6. The bar indicates 20  $\mu$ m.*

Add-back experiments were carried out to confirm the role of TG2. TG2 cDNA was amplified by PCR from pSG5TG (Gentile et al. 463-74) using proof-reading DNA polymerase and *EcoRI* modified primers. The cDNA was cloned into the mammalian expression vector pEGFP-N1 in frame with the sequence codifying for the fluorescent protein EGFP (construct pEGFP-TG2, Figure 2-1). To verify the expression of EGFP-tagged TG2 (where EGFP is localised at the C-terminal of TG2) and to make sure that the TG2 codified by pEGFP-TG2 plasmid was not altered by the conjugated EGFP, TG2  $-/-$  fibroblasts were transfected with pEGFP-TG2 and the cell extracts were analysed by Western blotting with anti-TG2 antibody. The transfection was performed by electroporation using Nucleofector System (Amaxa), which in the system analysed gives a typical efficiency of ~80%. As shown in Figure 3-8.A, transfected cells expressed a level of TG2 comparable to cells transfected with the control plasmid pSG5-TG2 (shown in Appendix 2), which encodes for untagged TG2. The molecular weight of the EGFP-TG2 band (~ 100 kDa) was, as expected, higher than the one of TG2 (77 kDa), given the additional mass of EGFP (28 kDa). The negative control homogenate prepared from non transfected (NT) TG2  $-/-$  cells, did not show a band (Figure 3-8. A). The same cell extracts were also analysed for TG2-dependent transamidation using a plate assay based on Jones et al. (1997). TG2  $-/-$  cells transfected with pEGFP-TG2 showed an activity level comparable to the one of pSG5-TG2 transfected cells. Both extracts exhibited a significantly higher ( $p < 0.001$ ) transamidation level compared to non transfected cells (Figure 3-8 B). These data indicate that the biochemical properties of TG2 were not changed by the conjugated protein EGFP. Therefore TG2  $-/-$  MEF were transfected with the pEGFP-TG2 construct and the successfully transfected cells were identified by the EGFP fluorescence concomitant with TG2 expression. Re-introduction of TG2 via electroporation rescued to a large extent the formation of vinculin-containing FA in TG2  $-/-$  cells adhering on FN (Figure 3-9, arrows), confirming that lack of TG2 was responsible for the defects in FA formation.

To investigate whether the externalised TG2 was responsible for the correct formation of vinculin-containing FA specifically, exogenous TG2 was provided to TG2  $-/-$  fibroblasts by seeding them onto a matrix of TG2 immobilised on FN (TG2-FN) (Verderio et al. 42604-14). As shown in Figure 3-10, TG2  $-/-$  MEF seeded onto TG2-FN matrix displayed vinculin containing FA similarly to TG2  $+/+$  MEF adhering on FN, as pointed by the white arrows. TG2 $-/-$  MEF also formed better defined SF when seeded on TG2-FN compared to

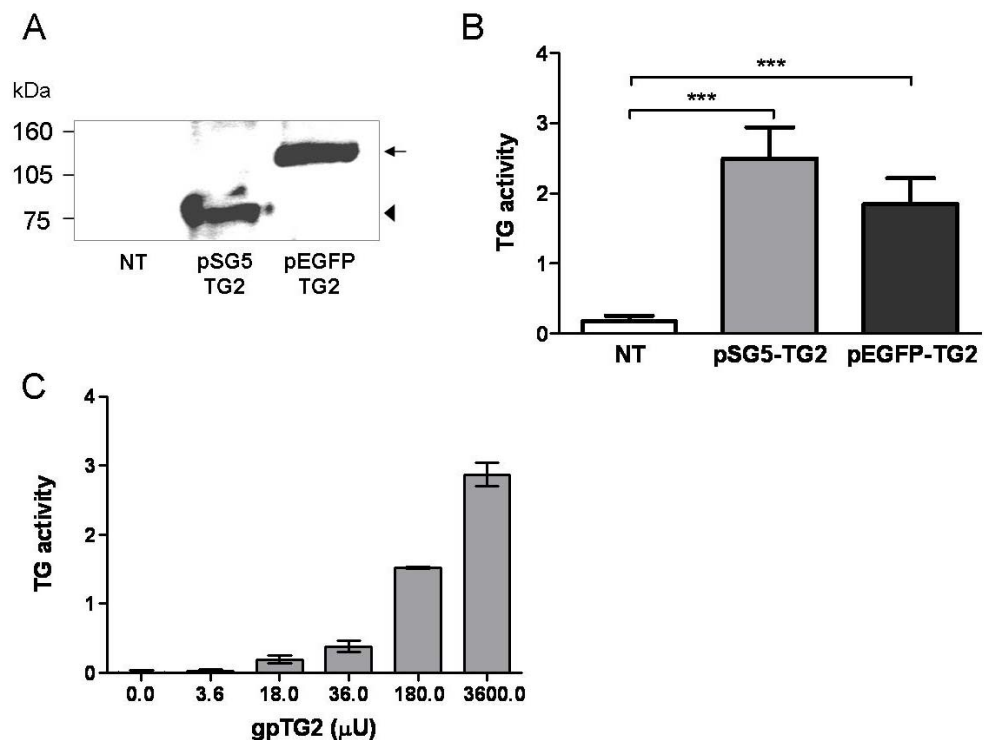


**Figure 3-8 Biochemical characterisation of pEGFP-TG2 construct.** *TG2 null MEF* were transfected with *pEGFP-TG2* or *pSG5-TG2* plasmid (positive control); non transfected (NT) cells were used as negative control. Cell lysates (50  $\mu$ g) were analysed by Western blotting with monoclonal anti TG2 antibody Cub7402 followed by HRP-conjugated secondary antibody (A) or tested for transamidating activity (TG activity) (measured as Abs 450 nm) (B). The arrowhead points to 77 kDa TG2; the arrow points to TG2 fused to EGFP. \*\*\* indicates  $p < 0.001$ . (C) Standard curve for TG activity measured on purified *gpTG2*, measured as absorbance at 450 nm.

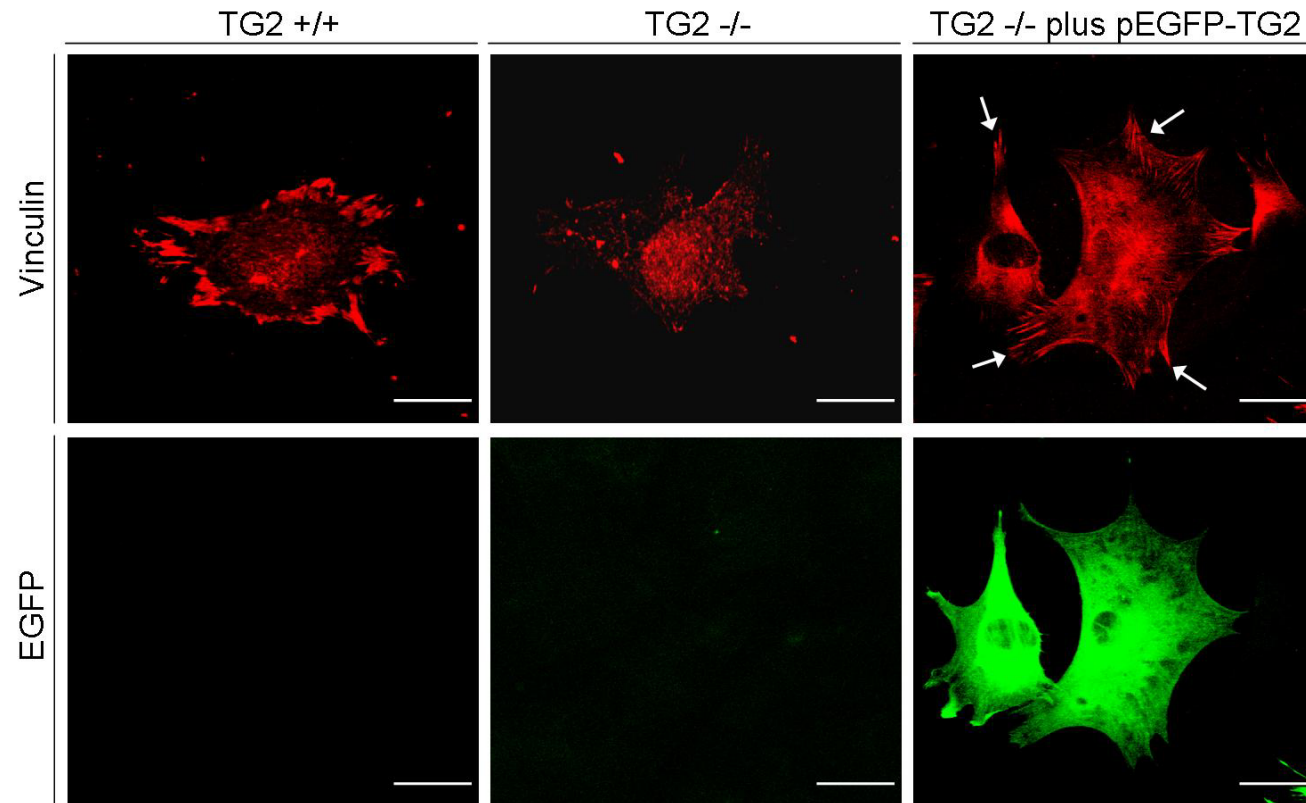


**Figure 3-9 Vinculin-containing FA formation is rescued by re-expression of TG2 cDNA.** *TG2 null cells (TG2 -/-) were transfected with the pEGFP-TG2 construct. After 48 hours, cells were allowed to adhere on FN coated slides for 45 minutes in serum-free medium. Untransfected wild type and TG2 -/- cells were also similarly seeded on FN as positive and negative controls. Transfected cells were identified by the expression of EGFP conjugated to TG2. Vinculin staining was performed as in Figure 3-6. The arrows point at restored FA. The bar indicates 20  $\mu$ m.*

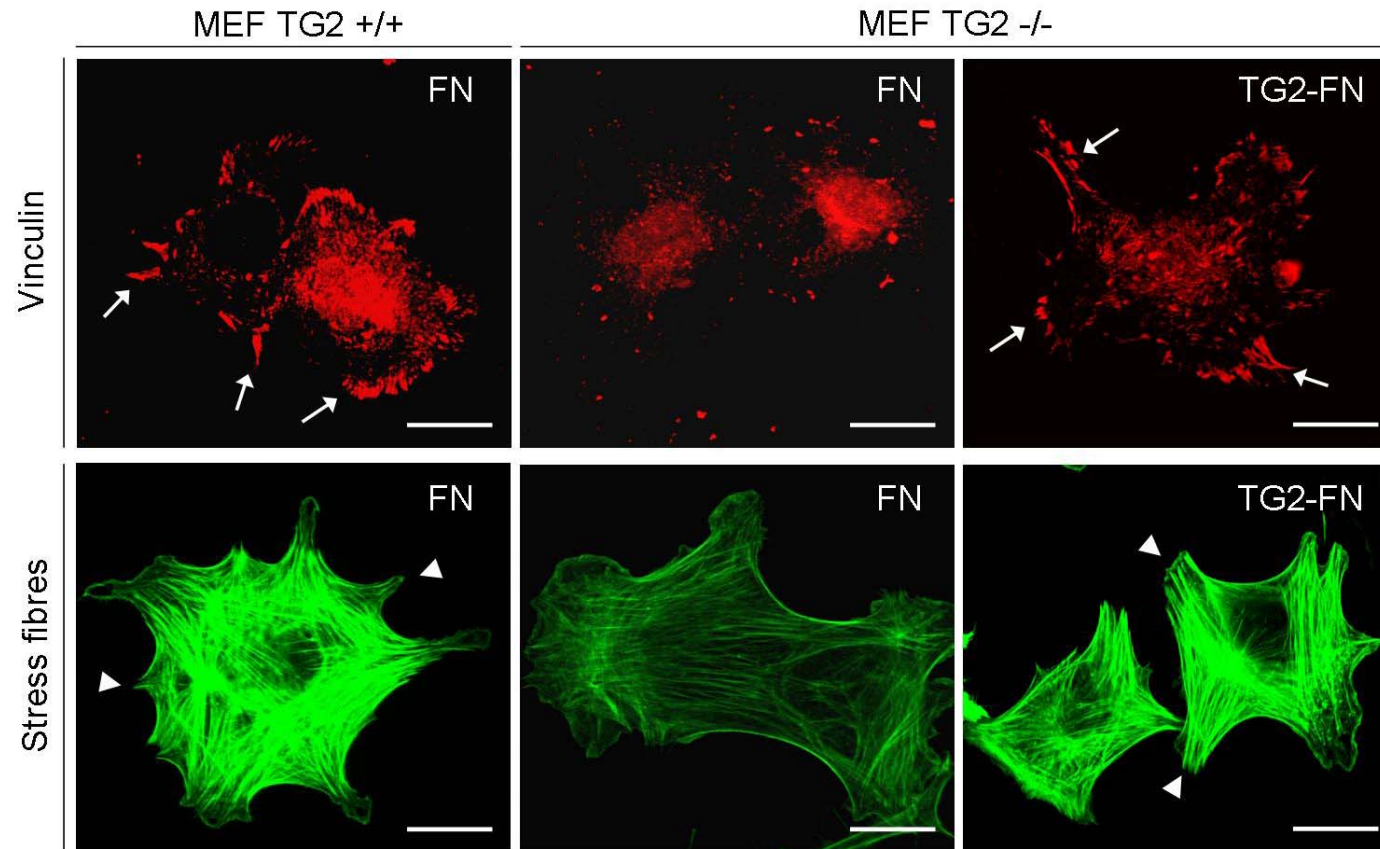


**Figure 3-10 FA formation of TG2  $-/-$  MEF is rescued by extracellular TG2.** TG2 null cells (TG2  $-/-$ ) were allowed to adhere for 45 minutes on FN or TG2-FN coated slides for 45 minutes in serum-free medium. The cells were serum starved (0.1 % serum) for 16 hours before the experiment. Wild type cells adhering on FN are shown as positive control. Vinculin and actin SF were detected as in Figure 3-6 and Figure 3-7, respectively. The arrows point at vinculin-containing FA; the arrow heads at SF ending at FA. The bar indicates 20  $\mu$ m.

### 3.2.3 Matrix-Transglutaminase-2 has an RGD-independent role in FAK activation

Next, the role of TG2 in focal adhesion kinase (FAK) activation was investigated, by measuring FAK phosphorylation at Tyr 397 (Y397) -the first residue to be phosphorylated upon extracellular ligand binding (Mitra et al., 2005)- in wild type and TG2  $-/-$  MEF. FAK activation was measured at 45 minutes cell adhesion on FN in serum-free medium. Cells were serum-starved for 15 hours before the experiment, in order to exclude serum-induced effects on cell adhesion.

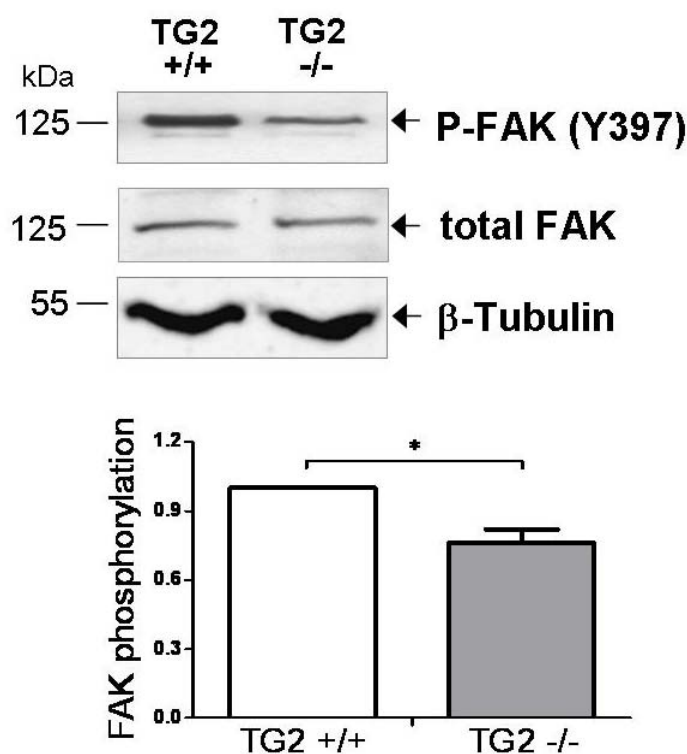


**Figure 3-11 Lack of TG2 impairs early FAK phosphorylation.** Wild type (TG2  $+/+$ ) and TG2 null (TG2  $-/-$ ) MEF were serum starved for 15 hours and left to adhere on FN-coated plates for 45 minutes in serum-free medium. The level of phosphorylated FAK in the cell extracts (50  $\mu$ g) was determined by Western blotting using an anti phosphor-FAK (Y397) antibody followed by HRP-conjugated secondary antibody. For normalisation of the data, blots were stripped and re-probed with anti total FAK and anti  $\beta$ -tubulin antibodies. Three separate experiments were performed and a typical blot is shown. The mean values of FAK phosphorylation relative to total FAK are shown, normalised considering TG2  $+/+$  values as 1. \* indicates  $p < 0.05$ .

Following cell adhesion, cell homogenates were prepared and analysed by Western blotting using an antibody against phosphorylated FAK (Y397). In order to confirm equal loading, the membrane were stripped and re-probed with antibodies against total FAK and  $\beta$ -tubulin. A small but significantly lower level of FAK phosphorylation (-25%;  $p < 0.05$ ), calculated by densitometric analysis as ratio between P-FAK and the total FAK protein (125 kDa), was revealed in TG2  $-/-$  MEF compared to TG2  $+/+$  MEF (Figure 3-11). This finding suggests that lack of TG2 impairs initial FAK signalling.

FN-associated TG2 has been shown to support RGD-independent FAK-phosphorylation (Verderio et al., 2003). To determine if extracellular FN-bound TG2 was sufficient to restore FAK phosphorylation in TG2  $-/-$  fibroblasts, TG2  $-/-$  MEF were allowed to adhere on either FN or TG2-FN prior to analysis of FAK phosphorylation by Western blotting. BSA-coated wells were used as a negative control. As shown in Figure 3-12 A, the adhesion of TG2 null MEF on TG2-FN enhanced the level of FAK phosphorylation (+ 25%;  $p < 0.05$ ) compared to FN matrix.

To investigate whether FAK phosphorylation driven by FN-bound TG2 was RGD-independent, TG2 null MEF were allowed to adhere on TG2-FN in the presence of soluble RGD peptide, at a concentration which competes with integrin receptors for binding to the RGD cell-binding domain of FN (Verderio et al., 2003). Inactive RAD peptide was utilised as a negative control. As shown in Figure 3-12 B, in TG2  $-/-$  MEF adhering on FN, FAK-P (Y397) level was further reduced in the presence of RGD peptide compared to RAD peptide (150  $\mu\text{g/ml}$ ). However, if TG2 null MEF were allowed to adhere on TG2-FN the phosphorylation level of FAK was significantly increased ( $p < 0.01$ ) in the presence of RGD peptide (Figure 3-12 B), confirming that matrix TG2 mediates RGD-independent FAK activation. As a negative control for the effect of TG2, cells were allowed to adhere on FN with a stoichiometric amount of BSA; unlike TG2-FN, BSA-FN did not reconstitute RGD-independent FAK phosphorylation in TG2  $-/-$  MEF (Figure 3-13).

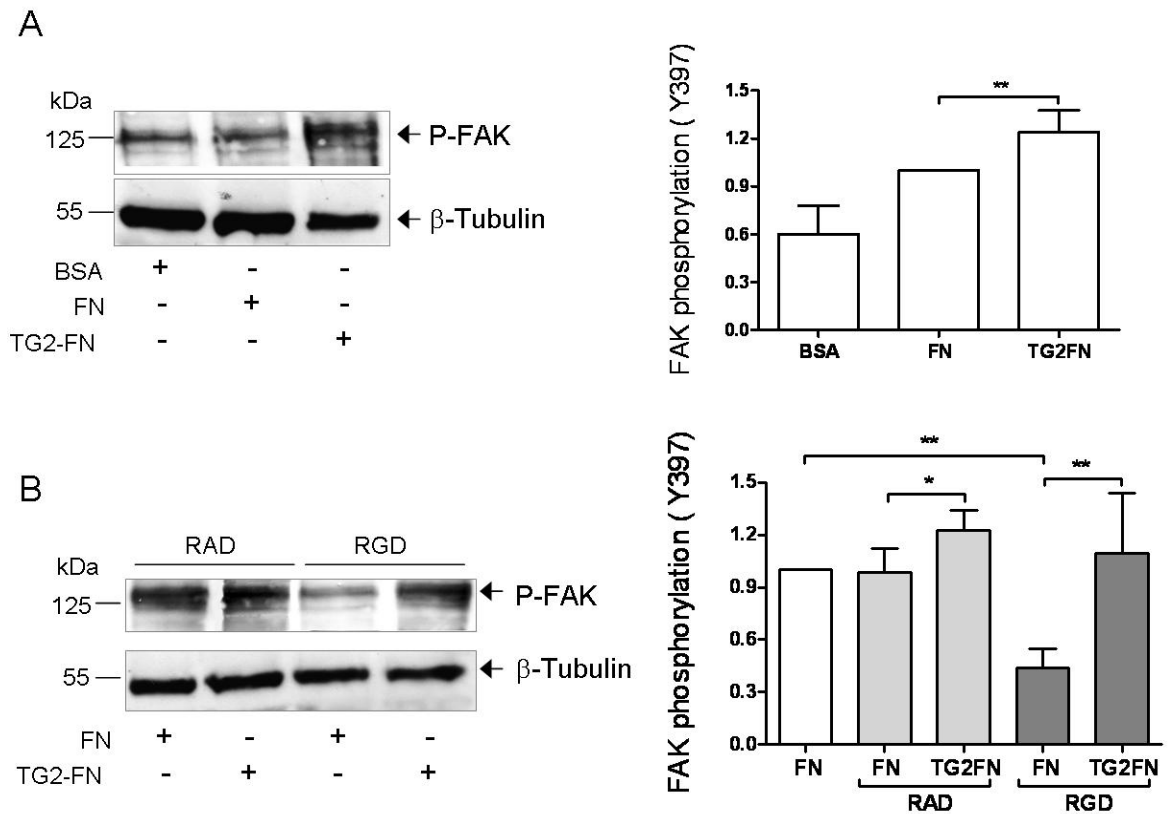


**Figure 3-12 Adhesion to FN-bound TG2 promotes FAK phosphorylation (Y397) in TG2<sup>-/-</sup> MEF in a RGD-independent way.** TG2 null (TG2<sup>-/-</sup>) fibroblasts were serum starved for 15 hours and let to adhere on BSA, FN or TG2-FN coated plates for 45 minutes in serum-free medium (A); in selected experiments adhesion was performed in the presence of 150  $\mu\text{g/ml}$  RGD peptide or control RAD peptide (B). Cell extracts were analysed by Western blotting as described in Figure 3-11; since a single cell line was used,  $\beta$ -tubulin was used for normalisation. Three separate experiments were performed and one typical blot is shown. The mean values of FAK phosphorylation in three experiments, relative to  $\beta$ -tubulin, are displayed; \* indicates  $p < 0.05$ , \*\* indicates  $p < 0.01$ .

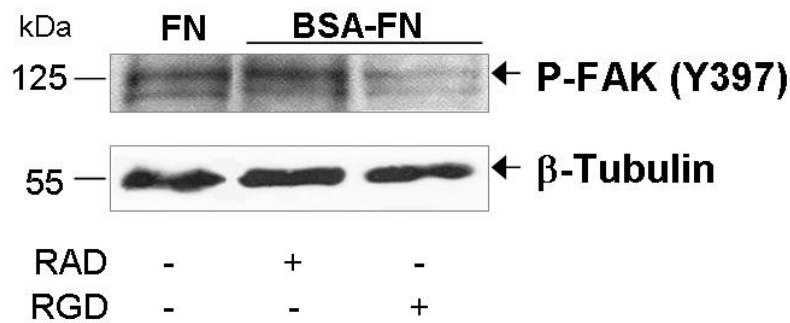


**Figure 3-13 Adhesion to FN-bound BSA does not induce RGD-independent FAK phosphorylation (Y397).** *TG2 null (TG2 <sup>-/-</sup>) fibroblasts were serum starved for 15 hours and let to adhere to either FN or BSA-FN coated plates for 45 minutes in serum-free medium, in the presence or absence of 150 µg/ml RAD or RGD peptide. Cell extracts were analysed by Western blotting as indicated in Figure 3-11; β-tubulin was used as a control for equal loading.*

### 3.2.4 Importance of Sdc-4 in RGD-independent FAK phosphorylation induced by matrix TG2

The presence of cell-surface heparan sulphate (HS) chains, such as the ones of heparan sulphate proteoglycan (HSPG), has been shown to be essential in the RGD-independent cell-adhesion process mediated by matrix TG2 (Verderio et al., 2003). Therefore, after demonstrating the role of matrix TG2 in RGD-independent FAK activation, the hypothesis of the involvement of HSPG Sdc-4 in outside-in signalling induced by matrix TG2 was tested. To this aim, primary dermal fibroblasts were isolated from mice lacking Sdc-4 (MDF Sdc-4 <sup>-/-</sup>) (Ishiguro et al., 2000) as described in Chapter 2 (2.2.1.7). Control Sdc-4 <sup>+/+</sup> MDF were isolated from wild type C57BL/6 mice. Firstly, the ability of Sdc-4 null MDF to support TG2-mediated RGD-independent cell adhesion was investigated. Wild type and Sdc-4 null MDF were allowed to adhere to either FN or TG2-FN in the presence or absence of RGD peptide before measuring the level of FAK phosphorylation (Y397) by Western blotting. As shown in Figure 3-14, matrix TG2 failed to mediate RGD-independent FAK activation in Sdc-4 <sup>-/-</sup> MDF compared to wild type MDF, suggesting the involvement of Sdc-4 in the mechanism. Interestingly, a small but significant reduction of FAK-P was associated with Sdc-4 deletion at 45 minutes cell adhesion.

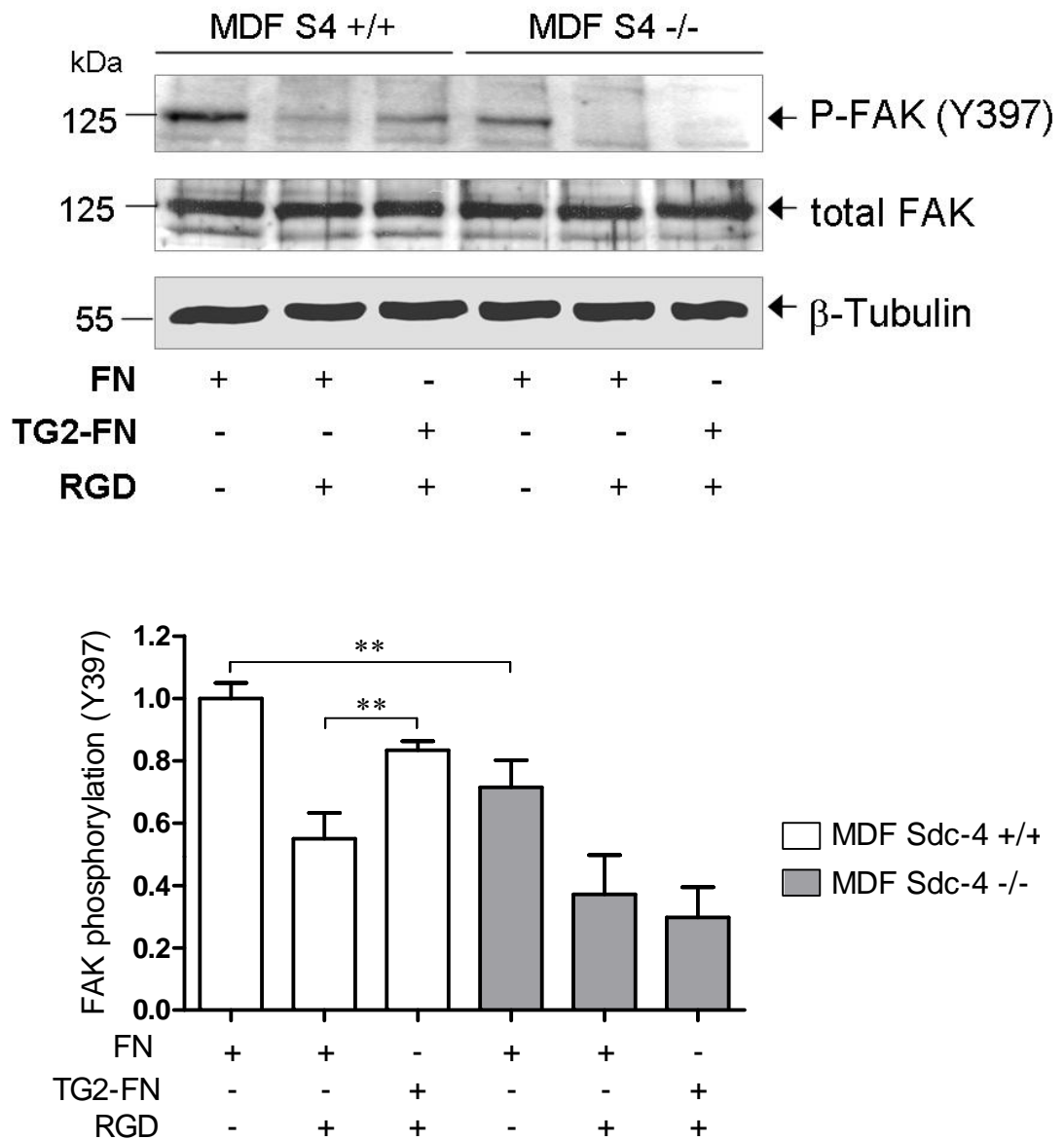


**Figure 3-14 Co-operation of Sdc-4 and TG2 in RGD-independent FAK phosphorylation.** Wild type (*Sdc-4* +/+) and *Sdc-4* -/- fibroblasts were serum starved for 15 hours and let to adhere on FN or TG2-FN coated plates for 45 minutes in serum-free medium; in selected experiments adhesion was performed in the presence of 150  $\mu$ g/ml RGD peptide. Cell extracts were analysed by Western blotting as indicated in Figure 3-11; FAK phosphorylation is expressed as ratio between P-FAK (Y397) and total FAK.  $\beta$ -tubulin was used as a control for protein equal loading.  $n=3$ ; \* indicates  $p<0.05$ , \*\* indicates  $p<0.01$ .

In order to investigate the specificity of action of Sdc-4 in extracellular TG2-mediated adhesion, a construct expressing human Sdc-4 (pcDNAhS4) was created by cloning human Sdc-4 cDNA (hS4) into the mammalian expression vector pcDNA 3.1. Preparation of the construct is described in the Material and Methods section, paragraph 2.2.11. The vector was used to add back Sdc-4 to Sdc-4  $-/-$  cells by cell electroporation. As illustrated in Figure 3-15, RT-PCR of human Sdc-4 (hS4) showed that Sdc-4  $-/-$  cells transfected with pcDNAhS4 expressed human Sdc-4 at 48 hours from cell transfection. The negative controls, represented by both non transfected (NT) Sdc-4  $-/-$  MDF and Sdc-4  $-/-$  MDF transfected with pcDNA, did not show expression of any Sdc-4. As expected, wild type MDF showed expression of endogenous murine Sdc-4 (mS4) instead of hS4.

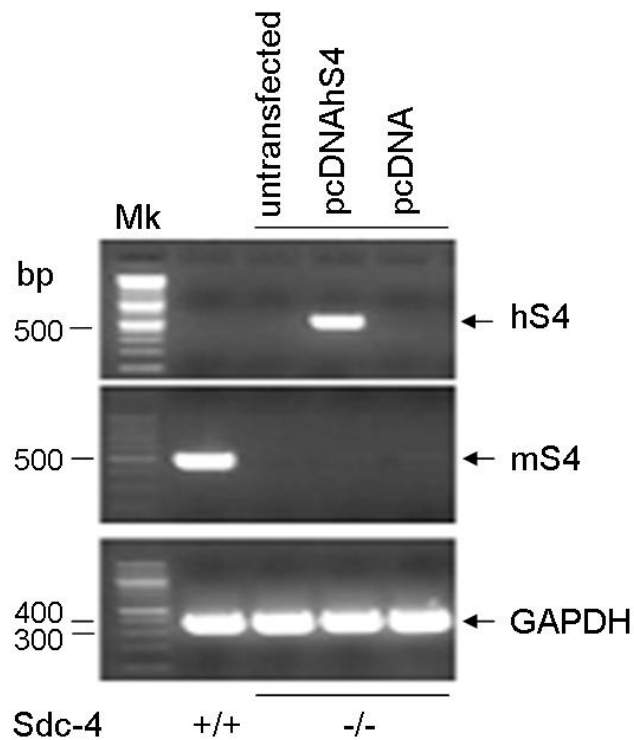


**Figure 3-15 Controls on the expression of pcDNAhS4 vector in Sdc-4  $-/-$  cells.** RNA was extracted from wild type (Sdc-4  $+/+$ ) and Sdc-4  $-/-$  cells (untransfected and transfected with pcDNAhS4 or pcDNA) and analysed for the presence of mouse and human Sdc-4 (mS4 and hS4) by RT-PCR. GAPDH expression was used as a positive control. Mk, molecular weight markers (100 bp DNA ladder). Primers' sequences are shown in Table 2-2.

At this stage, Sdc-4 null MDF with added back Sdc-4 were tested for RGD-independent FAK-phosphorylation mediated by TG2. As shown in Figure 3-16, the re-introduction of Sdc-4 via pcDNAhS4 largely restored RGD-independent FAK activation induced by cell adhesion to TG2-FN, which was lost in Sdc-4  $-/-$  MDF transfected with the empty vector. Sdc-4 null cells transfected with the vector only (pcDNA) showed the same profile of FAK phosphorylation previously observed in non transfected Sdc-4  $-/-$  cells (Figure 3-14). This result confirms that Sdc-4 is implicated in TG2-mediated outside-in signalling leading to FAK phosphorylation (Y397) in a RGD-independent way.

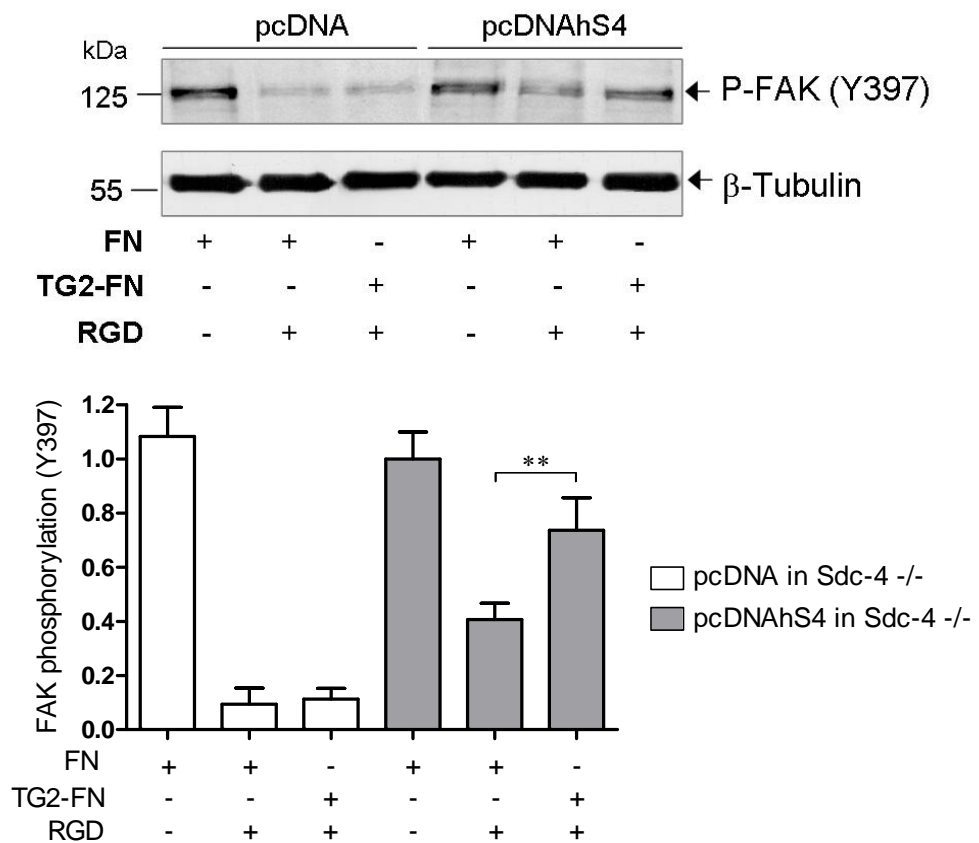


**Figure 3-16 Add-back of Sdc-4 rescues TG2-mediated RGD-independent FAK phosphorylation in Sdc-4  $-/-$  MDF.** Sdc-4  $-/-$  fibroblasts were transfected with either pcDNAhS4 or pcDNA. After 48 hours, cells were serum starved for 15 hours and let to adhere on FN or TG2-FN coated plates for 45 minutes in serum-free medium; in selected experiments adhesion was performed in the presence of 150  $\mu$ g/ml RGD peptide. Cell extracts were analysed as indicated for FAK-P(Y397) by Western blotting as indicated in Figure 3-11; FAK phosphorylation was expressed as ratio between P-FAK and  $\beta$ -tubulin.  $n=3$ ; \*\* indicates  $p<0.01$ .

It was noted that the rescue of Sdc-4 (pcDNAhS4) in Sdc-4 *-/-* MDF did not increase the level of FAK-P on FN compared to cells transfected with pcDNA vector (Figure 3-16). This suggests that the decrease in FAK-P observed in Sdc-4 null cells (Figure 3-14) may not be due to the lack of Sdc-4. Alternatively, the added back Sdc-4 could not be enough to re-stimulate FAK-P.

The involvement of Sdc-4 in RGD-independent adhesion was also investigated by monitoring actin SF formation. Staining with FITC-phalloidin revealed that the absence of Sdc-4 does not inhibit SF formation, even though Sdc-4 *-/-* cells displayed thinner SF compared to wild type cells when adhering on FN (Figure 3-17). The actin cytoskeleton of both wild type and Sdc-4 null cells was disrupted when the cells were allowed to adhere on FN in the presence of RGD peptide, and it was not possible to identify correctly formed SF. When wild type MDF were plated on FN-bound TG2 in the presence of RGD peptide they still formed SF which were morphologically similar to those formed on FN in the absence of RGD peptide (Figure 3-17). This finding agrees with previous data showing that matrix TG2 supports RGD-independent SF formation (Verderio et al., 2003). However, Sdc-4 null MDF failed to form actin SF when plated on TG2-FN in the presence of RGD peptide, suggesting the important role of Sdc-4 in TG2-mediated RGD-independent cell adhesion.

Examination of SF formation in Sdc-4 *-/-* cells transfected with pcDNAhS4 revealed that the re-introduction of Sdc-4 can restore actin SF formation in Sdc-4 *-/-* fibroblasts adhering on TG2-FN in the presence of RGD peptide, as shown by the white arrows in Figure 3-18 A. The specificity of Sdc-4 effect was demonstrated by the absence of RGD-independent SF formation in Sdc-4 *-/-* cells transfected with pcDNA vector only (Figure 3-18 A). The level of SF formation was also quantified in non transfected (NT) Sdc-4 *-/-* cells and Sdc-4 *-/-* cells transfected with either pcDNAhS4 or pcDNA demonstrating that re-introduction of Sdc-4 significantly increased ( $p < 0.01$ ) SF formation in RGD-independent cell adhesion on TG2-FN (Figure 3-18 B). As previously shown in the selection of pictures presented in Figure 3-17 and Figure 3-18 A, the transfection with pcDNA vector did not affect the formation of SF in Sdc-4 null cells and (Figure 3-18 B). These results indicate that it was the specific re-introduction of Sdc-4 that drove the RGD-independent formation of SF when cells were plated on TG2-bound FN, since SF were not formed in untransfected Sdc-4 null MDF or in Sdc-4 null MDF transfected with pcDNA vector (Figure 3-18 B).

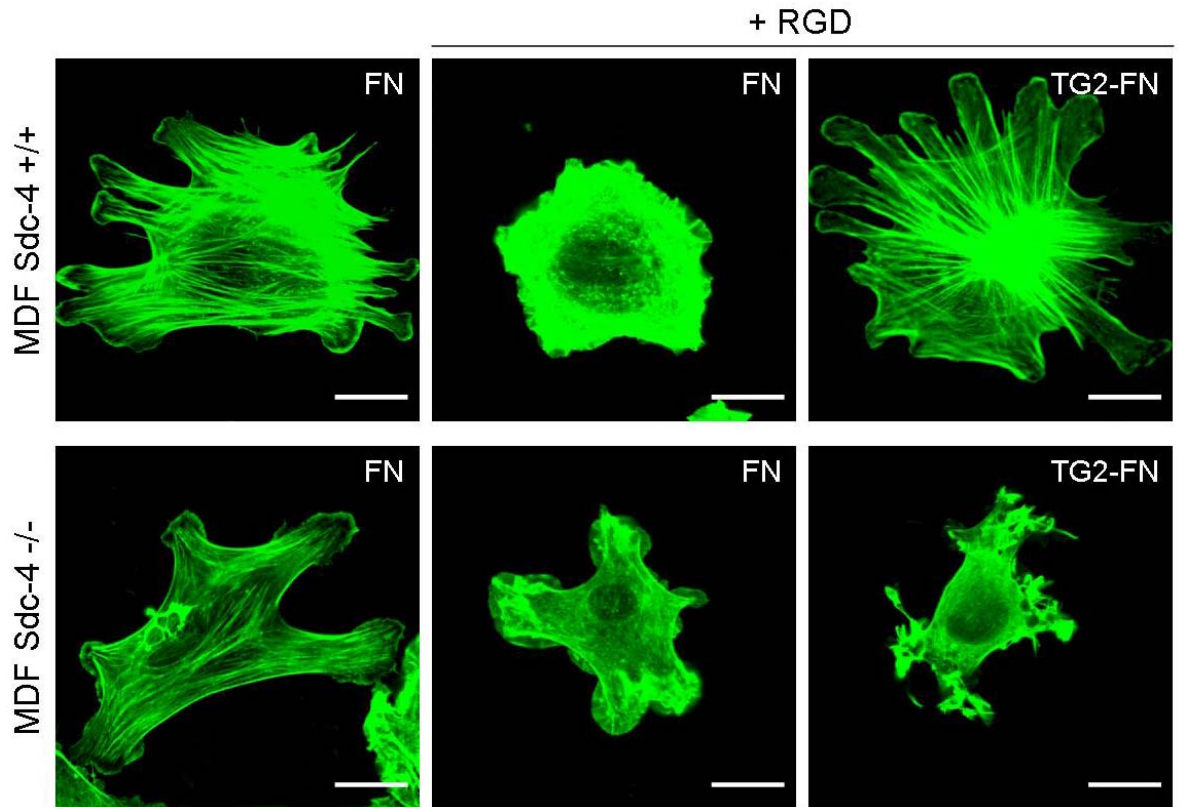


**Figure 3-17 Co-operative role of Sdc-4 and TG2 in SF formation during RGD-independent cell adhesion.** Wild type (*Sdc-4* +/+) and *Sdc-4* -/- cells were plated on FN or TG2-FN in the presence or absence of RGD peptide (150  $\mu\text{g/ml}$ ). Cells were allowed to adhere for 45 minutes in serum-free medium. Actin SF were detected as described for Figure 3-6. The bar indicates 20  $\mu\text{m}$ .

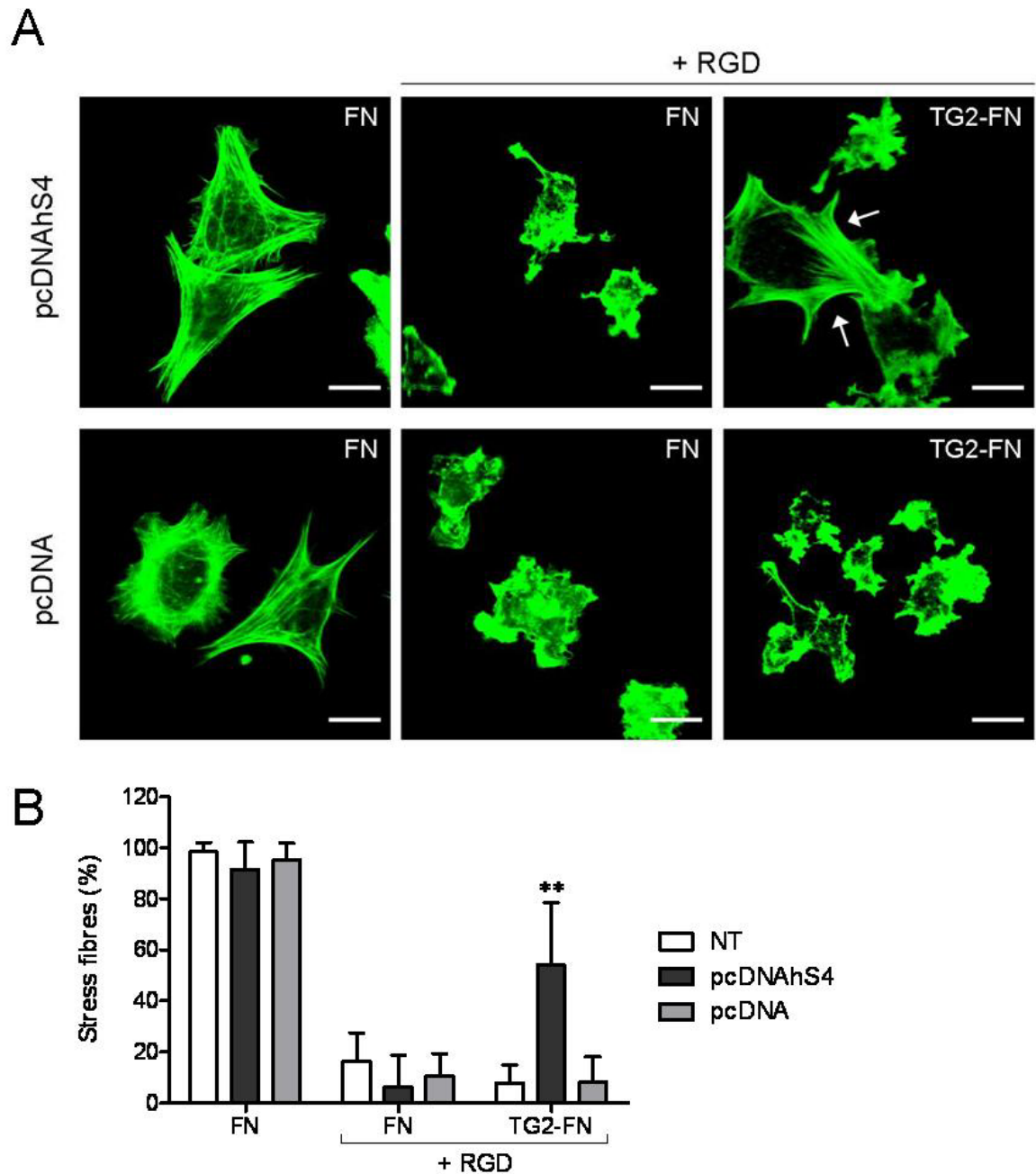


**Figure 3-18 Re-introduction of Sdc-4 in Sdc-4<sup>-/-</sup> MDF restores TG2-mediated RGD-independent SF formation.** A) Sdc-4<sup>-/-</sup> cells transfected with pcDNAhS4 or pcDNA only were seeded on FN or TG2-FN in the presence or absence of RGD peptide (150  $\mu$ g/ml). Cells were allowed to adhere for 45 minutes in serum-free medium. Actin SF were detected as described for Figure 3-6. The white arrows point at the restored SF in Sdc-4<sup>-/-</sup> cells after re-introduction of Sdc-4. The bar indicates 20  $\mu$ m. B) SF formation was quantified in three separate experiments by image analysis (three non-overlapping fields per experiment). Mean % of cells with SF ( $\pm$ SD) is plotted. \*\* indicates  $p < 0.01$ .

### 3.3 Discussion

In this study the role of extracellular TG2 in the early stages of cell adhesion on FN was analysed for the first time using a cell system of primary fibroblasts derived from wild type and TG2 null mice (De Laurenzi and Melino, 2001). The availability of embryonic fibroblasts isolated from mice where TG2 was disrupted by homologous recombination (De Laurenzi and Melino, 2001) provided a useful control for both the specificity of TG2 detection and for studying the role of TG2 in cell adhesion.

The first set of experiments addressed the issue of whether TG2 was externalised and how early in the cell adhesion process. Extracellular TG2 was detected by both immunocytochemistry and measurement of cell-surface TG activity; both experiments were performed in a time course fashion, analysing TG2 externalisation at 20, 40 and 60 minutes cell-adhesion on FN-coated plates. In agreement with a possible role for TG2 in early cell adhesion, it was possible to detect TG2 antigen starting from 20 minutes of adhesion to FN. TG2 was mainly localised in cell-matrix adhesion structures at the cell periphery. TG2 was also detected in the cytosol, concentrated in the perinuclear area; the diffused cytosolic signal was absent in TG2 *-/-* cells, however the perinuclear staining was also present in TG2 null cells, suggesting its non specificity. The results obtained by immunocytochemistry were confirmed by measurement of cell-surface TG activity by incorporation of biotinylated cadaverine onto FN. Transamidating activity was detectable starting from 20 minutes adhesion, and it reached a plateau at 40 minutes adhesion, supporting the idea of a role for TG in the early stages of cell adhesion. In order to determine which part of the cell-surface transamidation activity measured was attributable to TG2, a study of expression of the different members of the TG family was performed on wild type and TG2 null primary fibroblasts. The study revealed that TG2 is the member with the highest expression level in primary fibroblasts; the only other member expressed is TG1, which is localised intracellularly (Mehta, 2005; Zhang et al., 2009), but its level is significantly lower. However, in TG2 *-/-* cells the level of TG1 was found to be significantly increased (possibly for compensatory effect). This finding was previously described by (De Laurenzi and Melino, 2001), who also did not report a parallel increase in transamidation activity. The conclusion is that the activity measured in the considered cell system is mainly due to TG2.

TG2 has been mainly described as a cytosolic enzyme (Fesus and Piacentini, 2002), and this was often seen in disagreement with TG2 externalisation and involvement in cell adhesion. The analysis of TG2 distribution by Western blotting presented in this study has revealed that in our cell system the enzyme has a comparable level in the cytosol and in the cell membrane, together with being externalised and localised at cell-matrix adhesions. To my knowledge, this is the first study showing TG2 distribution in primary fibroblasts. TG2 concentration at the cell surface and in the cell membrane, at matrix adhesion sites, is consistent with its role in cell-matrix interactions.

In the present study, the formation of FA and SF during cell adhesion on FN has been monitored in the presence and absence of TG2. Lack of TG2 inhibited the formation of correct FA and SF compared to wild type cells, as previously shown in cells with inhibited TG2 expression via antisense RNA (Jones et al., 1997; Stephens et al., 2004). TG2 was re-introduced in TG2 null cells by either transfecting them with a pEGFP-TG2 construct or by seeding TG2 null cells on a TG2-FN matrix. The enhanced TG2 level largely rescued the formation of FA and stress fibers in both cases, confirming the essential role of extracellular TG2 in the early adhesion process.

Previously, FN-bound TG2 has been shown to contribute to RGD-independent cell adhesion on FN, leading to RGD-independent formation of SF (Verderio et al., 2003). TG2-FN has also been shown to promote RGD-independent FAK phosphorylation (Y397) in human osteoblasts (Verderio et al., 2003). Having identified a specific role for extracellular TG2 in early cell adhesion, the outside-in signalling events induced by TG2 were also investigated. The first outcome was that the absence of TG2 causes a decreased level of FAK-P at Tyr 397, which is likely to be responsible for altered FA and SF formation, since extracellular TG2 compensated both the defects in FAK-P and that of FA formation. Although increased expression of TG2 has been linked to FAK phosphorylation (Akimov and Belkin, 2003), FAK-P (Y397) was previously shown to be unaltered in fibroblasts where TG2 was silenced by antisense RNA (Stephens et al., 2004), even though these cells presented alterations in FA and SF formation. The differences in FAK-P (Y397) measured in the present study results from the analysis of primary cell lines of fibroblasts, contrary to previous experiments where TG2 effects on cell adhesion were measured on immortalised clones of fibroblasts where TG2 expression was altered by stable cell transfection with TG2 antisense RNA (Stephens et al., 2004). Thus, the results presented

here are more indicative of the possible role of TG2 in physiological systems of adhering fibroblasts.

In this study, it was confirmed that TG2-mediated FAK phosphorylation is RGD-independent. This finding suggests a role for externalised TG2 in situations of cell stress or wound healing, when FN matrix is fragmented (Davis et al., 2000) and the ordinary cell adhesion mechanism mediated by integrin binding to FN is not sufficient to sustain full cell adhesion/spreading (Jeong et al., 2001). A previous study performed in human osteoblasts has shown that the role of TG2 in mediating RGD-independent cell adhesion relies on the presence of cell surface HS, as the process is inhibited by pre-treating cells with heparitinase (Verderio et al., 2003). Cell surface HSPG mainly consist of glypicans and syndecans, each of the families containing members with specific tissue and development-related expression. In the current study, Sdc-4 was chosen as a candidate HSPG-receptor for mediating the RGD-independent extracellular TG2 role since, contrary to the other syndecans, it is a widespread component of FA and it has an active role in mediating the cell spreading events (Echtermeyer et al., 1999). The role of Sdc-4 was investigated by studying TG2-induced SF formation and FAK phosphorylation in primary dermal fibroblasts isolated from wild type and Sdc-4 null mice (Ishiguro et al., 2000). It emerged that the presence of Sdc-4 is essential for TG2-mediated events in RGD-independent cell adhesion, and the essential role of Sdc-4 was confirmed by rescue experiments performed by transfecting Sdc-4 null cells with pcDNAhS4. Interestingly, Sdc-4 deletion did not result into a significant reduction in SF formation. This is in agreement with previous reports where it was shown that Sdc-4 null cells can form FA on FN (Bass et al., 2007; Ishiguro et al., 2000) and only when the heparin-binding fragment of FN is missing from the cell surface, then Sdc-4 deletion affects cell spreading (Ishiguro et al., 2000).

Since both TG2 and Sdc-4 have been involved in cell spreading events, it was important to clarify whether the action of TG2 and Sdc-4 is synergistic or simply additive. Since no increase in RGD-independent cell spreading (Figure 3-18), SF assembly (Figure 3-17) and FAK-P (Figure 3-14) was observed in Sdc-4 null cells plated on TG2-FN matrix compared to FN, these findings suggest that the effect of TG2 is not simply additive to that of Sdc-4 but synergistic (both molecules are required to mediate RGD-independent cell adhesion).

The results of this study have identified Sdc-4 as a possible receptor in RGD-independent cell adhesion mediated by TG2, a process which is likely to occur in situations of



## ***Chapter 4: Investigation on TG2 binding to Sdc-4***

### ***4.1 Introduction***

#### **4.1.1 Interactions of proteins with Heparin/HS**

Given the structure of heparin/HS (general introduction, paragraph 1.2), strong ionic interactions can take place between basic side chains of protein bound Arg, Lys and His and negatively charged sulphate groups (Fromm et al., 1997). There are also other types of interactions taking place between heparin/HS and partner molecules: van der Waals forces, hydrogen bonds and hydrophobic interactions with the carbohydrate backbone (Gandhi and Mancera, 2008). Affinity of protein-heparin binding can be enhanced by polar amino acids which provide minimal steric constraints and good flexibility, thus facilitating the interaction with GAG chains (Caldwell et al., 1996).

X-Ray crystallography studies have provided several information on heparin-binding, such as protein fold, periodicity of basic amino acids and sulphate clusters, and sulphation level required for protein-GAG interaction (Hileman et al., 1998). These studies have also permitted the identification of amino acids consensus sequences involved in heparin-binding. From comparison of several heparin-binding sites, it has emerged that the typical sequences XBBXB, XBBBXXB or XBBBXXBBBXXBBX (where B is Lys or Arg and X is a “hydrophobic residue”, most commonly Asn, Ser, Ala, Gly, Ileu, Leu and Tyr) are involved in heparin/HS-binding (Cardin and Weintraub, 1989; Sobel et al., 1992). Examples of heparin-binding domains and corresponding predicted secondary structures have been reviewed by Hileman et al. (1998) and are shown in Figure 4-1. These binding sites can also be formed by residues which are distant in the amino acid sequence, but are brought in spatial proximity by the protein folding, and the binding usually involves a portion of 6-12 monosaccharides in the GAG chain. The distribution of sulphated groups in GAG chains can determine the structure of GAG-binding sites on the protein surface by neutralising inhibitory charge repulsion of residues present in a specific spatial arrangement (Sibille et al., 2006). The relative proportion of N- and O-sulphated groups in heparin and HS, together with the presence of N-linked acetyl groups, can also influence the interaction with proteins (Kuschert et al., 1999).



TFPI	<sup>212</sup> GKCRPFKYSGCGNENNFTSKQECLRACKKGF <sup>243</sup> ---ttttttttt--tttt-ttttααααttttβ
AAMP	<sup>14</sup> RRLRMESESES <sup>25</sup> ααααααααttt
IGFBP-5	<sup>221</sup> RKGFYKRKQCKPSRGRKR <sup>238</sup> ttt-----ttttttt
IGFBP-3	<sup>215</sup> KKGFYKKQCRPSKGRKR <sup>232</sup> ttt-----ttttttt
HB-EGF	<sup>21</sup> KRKKKGKGLGKKRDPCLRKYK <sup>41</sup> ttt--tttt----tttt---t

**Figure 4-1 Heparin binding proteins with predicted secondary structure.** Heparin binding regions and predicted secondary structure of different proteins are shown (Hileman et al., 1998).

#### 4.1.2 TG2 affinity for heparin

TG2 has been known to have a certain affinity for heparin for a long time; in fact Signorini et al. (1988) have developed a method for the purification of TG2 from human erythrocytes involving heparin-Sepharose affinity chromatography as the last step. Interestingly, amino acid analysis of TG2 from human erythrocytes has shown that the enzyme has a lower proportion of basic amino acids compared to TG2 from guinea pig liver (Signorini et al., 1988), thus suggesting that the latter enzyme, which is used in the present investigation, could present higher affinity for negatively charged heparin and HS. More recently Gambetti et al. (2005) described that binding of TG2 to heparin does not affect TG2 accessibility to substrates of transamidation reaction, but it protects the enzyme from thermal unfolding and proteolytic degradation, enhancing the potential cross-linking activity of the enzyme. However, the binding affinity of TG2 for heparin and the kinetics of the interaction have never been addressed. As illustrated in Figure 4-1, ECM glycoproteins as fibronectin, vitronectin and laminin, known to be TG2 substrates (Nardacci et al., 2003; Sane et al., 1988) are heparin binding proteins (Hileman et al., 1998). Sane and colleagues (1990) have demonstrated that TG2-mediated transamidation activity on vitronectin can be increased by the presence of highly sulphated GAG chains, suggesting that heparin could enhance TG2 accessibility to its substrates either by immobilising it on the cell surface or by increasing the concentration of available substrates in particular spatial disposition.

The aim of this chapter was to measure for the first time the affinity of TG2 for heparin and HS employing *in vitro* systems and cells in culture.

## 4.2 Results

### 4.2.1 Affinity of TG2 for heparin/HS

The first step to test the interaction of TG2 with GAG chains was the development of an ELISA-based solid binding assay aimed to study the affinity of TG2 for heparin/HS. For this study, heparin-binding microtiter plates previously developed by (Mahoney et al., 2004) were utilised. Since the ELISA detection of TG2 bound to heparin was conducted as previously described for the detection of TG2 bound to FN (Verderio et al., 2003), control binding studies were firstly performed on either immobilised FN or, as a control, BSA. TG2 was allowed to bind immobilized molecules in the presence of the  $\text{Ca}^{2+}$  chelator EDTA (2 mM) to prevent TG2 auto-transamidation, after that, bound TG2 was detected by ELISA using the monoclonal anti-TG2 antibody Cub7402. Under these settings, TG2 showed a dose-dependent binding to FN (Figure 4-2). Since the binding was saturable, it was also possible to obtain some information on the strength of TG2 binding to FN, even though there was variability in estimated dissociation constant between separated experiments. The best fitting ( $R^2=0.8820$ ) of the absorbance data was obtained using the “one site specific binding” model of GraphPad Prism. The estimated dissociation constant for TG2 bound to FN was approximately 20 nM when calculated from three independent experiments, confirming high affinity binding.

Deleted: negative

Deleted: informations

Deleted: kinetic

Deleted: 19.47±6.92 nM

Deleted: The binding to the negative control BSA was not saturable, and was significantly lower than the binding to FN at any measured point ( $p<0.002$ ) (Figure 4-2). ¶

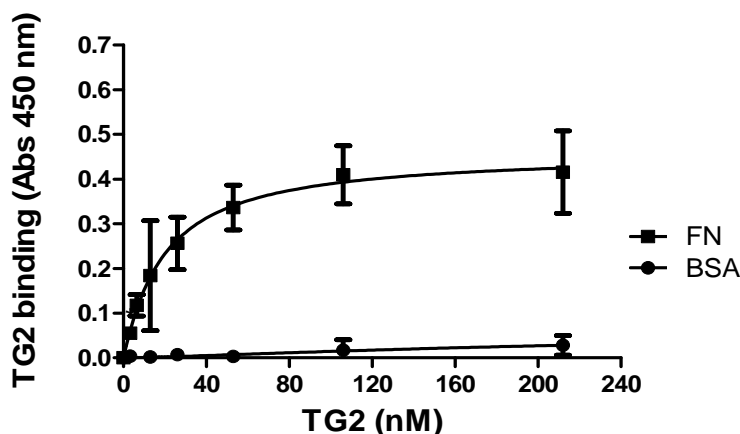


**Figure 4-2** TG2 binding to immobilised FN. *In this control experiment* TG2 (0-212 nM) was allowed to bind immobilised FN (5 µg/ml) or, as a negative control, BSA (5 µg/ml) in the presence of 2 mM EDTA. Binding was performed at 37°C for 2 hours.  $K_d$  for FN was  $19.47 \pm 6.92$  nM.  $n=3$ .

Formatted: Font: Not Bold, Italic

Deleted: \*\* indicates  $p < 0.002$ .

The same approach was then used for binding studies of TG2 to heparin and HS. Heparin, representative for the sulphated protein-binding regions of heparan sulphate, was initially used as a model for the HS chains of Sdc-4, given the structural similarity and the ready availability. As shown in Figure 4-3, TG2 displayed a saturable concentration-dependent binding to low molecular weight heparin (4-6 kDa); as for the binding to FN, the best fitting was obtained applying a one site specific binding model ( $R^2=0.9785$ ). The estimated affinity of TG2 for heparin was in the low nM range, with a  $K_d$  of approximately 20 nM ( $23.20 \pm 1.84$  nM) estimated from three independent experiments, similar to the value obtained for FN-binding.

Deleted:

Since the binding of TG2 to HS chains in physiological conditions occurs in presence of  $Ca^{2+}$ , the ELISA was also performed in a buffer containing 2 mM  $Ca^{2+}$  (Figure 4-3); under this condition, the binding was still saturable and fitted with a model of one site specific binding ( $R^2=0.9722$ ). However, the affinity of TG2 for heparin in the presence of  $Ca^{2+}$  (approximate  $K_d = 40$  nM estimated from three independent experiments) resulted slightly lower than the one measured in the presence of EDTA. It has to be considered that this  $K_d$

Deleted:  $0.33 \pm 3.75$

is an estimated value and, although lower than the value measured for the binding in the presence of EDTA, it is still in the low nM range. In order to see whether it was the  $\text{Ca}^{2+}$ -bound conformation of TG2, as opposed to the GTP-bound conformation, to be responsible for the lower affinity for heparin, the experiment was also conducted in the presence of GTP $\gamma$ S, a non hydrolysable form of GTP. Even in this condition the affinity of TG2 for heparin was slightly lower than when measured in the presence of EDTA only, with a Kd of approximately 40 nM (39.75 $\pm$ 11.63 nM) estimated from three independent experiments (Figure 4-3). In this case the fitting with the one site specific binding model was not as good as for the other conditions ( $R^2=0.86$ ). This finding, however, suggests that the lower Kd measured with  $\text{Ca}^{2+}$  compared to that measured with EDTA does not depend on the  $\text{Ca}^{2+}$ -induced conformation of TG2.

Deleted: , although

Deleted: a calculated

Deleted: ;

Deleted: the fitting was not improved if the data were analyzed according to the other binding models available in GraphPad tools, suggesting a more complex binding mechanism.

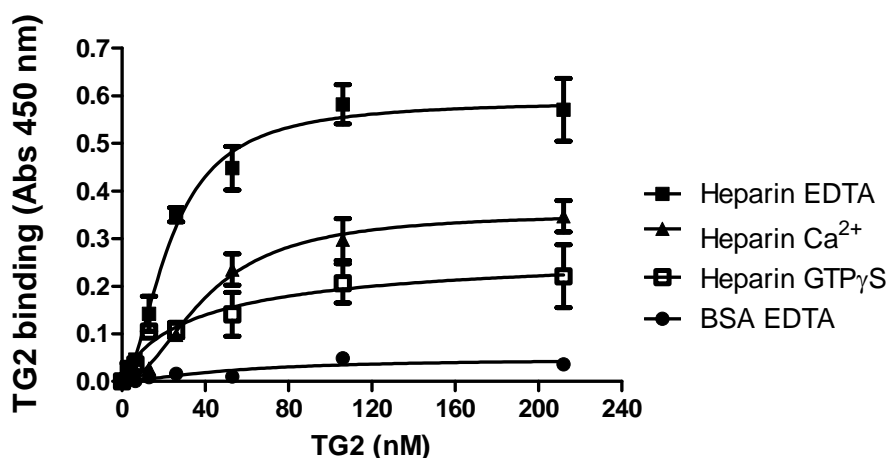


**Figure 4-3 TG2 binding to heparin.** TG2 (0-212 nM) was allowed to bind immobilised heparin (4.6  $\mu\text{M}$ ) or, as a negative control, BSA (5  $\mu\text{g/ml}$ ) in the presence of either 2 mM EDTA, 2 mM  $\text{Ca}^{2+}$ , or 2 mM EDTA plus 150  $\mu\text{M}$  GTP $\gamma$ S at 37 $^{\circ}\text{C}$  for 2 hours. Kd values were 23.20 $\pm$ 1.84 nM, 40.33 $\pm$ 3.75 nM and 39.75 $\pm$ 11.63 nM, respectively. n=3.

Since the decreased TG2 binding to heparin in the presence of  $\text{Ca}^{2+}$  could also be due to the formation of  $\text{Ca}^{2+}$ -dependent TG2 oligomers via TG2 auto-crosslinking activity, the binding reaction was monitored at the end of the 2 hours incubation time by analyzing the reagents through Western blotting using anti-TG2 antibody. As shown in Figure 4-4 (arrowheads), the presence of  $\text{Ca}^{2+}$  was accompanied by the formation of TG2 oligomers generated by auto-crosslinking activity of the enzyme. The presence of TG2 oligomers was absent in the control (TG2 not incubated at  $37^\circ\text{C}$ ) and it was significantly lower in TG2 incubated in the presence of either EDTA or EDTA plus  $\text{GTP}\gamma\text{S}$ . However, the formation of TG2 oligomers did not seem to reduce the amount of free monomeric TG2 in a considerable way (Figure 4-4, arrow) suggesting that it may not significantly affect TG2 binding to heparin..

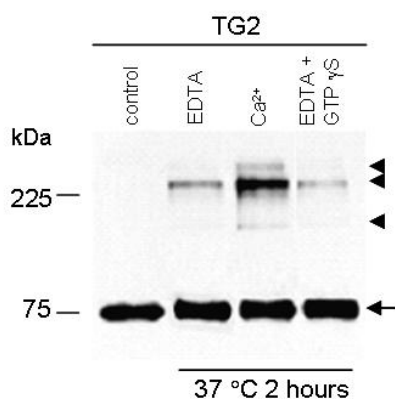


**Figure 4-4 Western blot analysis of TG2-heparin binding reaction.** *The TG2-heparin binding reaction was performed in a test tube in identical conditions to the solid binding assay (Figure 4-3). After the 2 hours incubation at  $37^\circ\text{C}$ , the reagents were analysed by Western blotting using monoclonal anti-TG2 antibody TG100. Secondary antibody was goat anti mouse-HRP. The arrow indicates the TG2 monomer (77-80 kDa) and the arrow heads indicate TG2 oligomers (approximately 155, and 310 kDa).*

The decreased binding in the presence of  $\text{Ca}^{2+}$  could also be a consequence of an interaction of positively charged ions with heparin. For this reason, TG2-heparin binding was also studied in the presence of ions of similar properties such as  $\text{Mg}^{2+}$  and  $\text{K}^+$ . As illustrated in Figure 4-5, by performing the assay in the presence of either 2 mM  $\text{Ca}^{2+}$ , 2 mM  $\text{Mg}^{2+}$  or 4 mM  $\text{K}^+$ , the  $K_d$  values were, respectively,  $40.33 \pm 3.70$  nM,  $43.05 \pm 5.96$  nM and  $54.85 \pm 7.57$  nM; the best fitting model for all the conditions was the one site specific binding ( $R^2$  values were 0.9722, 0.9563 and 0.9762, respectively). Since the  $K_d$  were not significantly different, these results indicated that the decreased TG2-heparin affinity recorded in the presence of  $\text{Ca}^{2+}$  compared to EDTA could be a consequence of ionic interference in TG2 binding to heparin rather than  $\text{Ca}^{2+}$ -dependent conformational change of the enzyme or  $\text{Ca}^{2+}$ -induced oligomerisation.

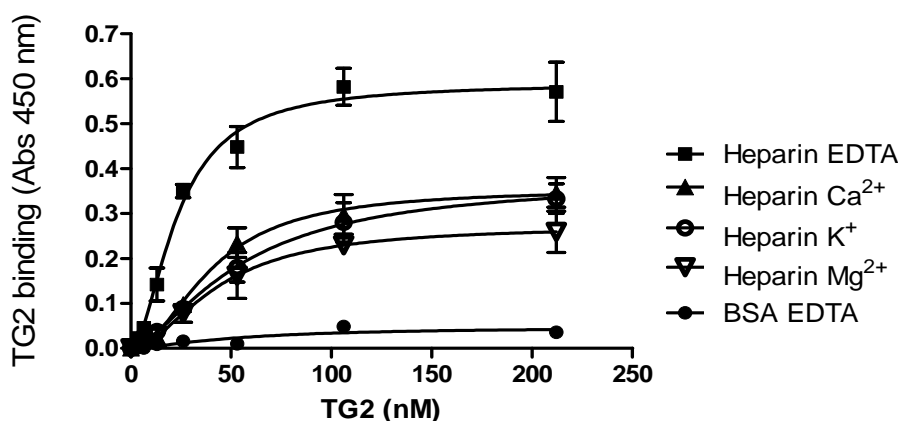


**Figure 4-5 Interference of positively charged ions on TG2-binding to immobilised heparin.** TG2 (0-212 nM) was allowed to bind immobilised heparin (4.6  $\mu\text{M}$ ) or, as a negative control, BSA (5  $\mu\text{g}/\text{ml}$ ), in the presence of either 2 mM EDTA, 2 mM  $\text{Ca}^{2+}$ , 2 mM  $\text{Mg}^{2+}$  or 4 mM  $\text{K}^+$ . Binding was performed at 37°C for 2 hours.  $n=3$ .  $K_d$  values for  $\text{Mg}^{2+}$  and  $\text{K}^+$  were  $43.05 \pm 5.96$  nM and  $54.85 \pm 7.57$  nM, respectively. TG2 binding in the presence of EDTA and  $\text{Ca}^{2+}$  is the same previously shown in Figure 4-3, with  $K_d$  values of  $23.20 \pm 1.84$  nM and  $40.33 \pm 3.75$  nM, respectively.

Since the GAG chains of HSPG are mainly HS, and heparin is a highly sulphated form of HS, the ELISA-based assay was repeated in the same way using equimolar concentrations of purified HS. Figure 4-6 shows that TG2 displayed a dose-dependent binding to HS (4.6  $\mu\text{M}$ ), as previously recorded using heparin. Analogously to the TG2 binding studies to heparin, the best fit of the TG2 binding curve to HS was obtained using a one site specific binding model ( $R^2 = 0.9394$ ), and the binding was saturable. The calculated  $K_d$  was  $19.47 \pm 2.76$  nM, indicating high affinity of TG2 for HS.

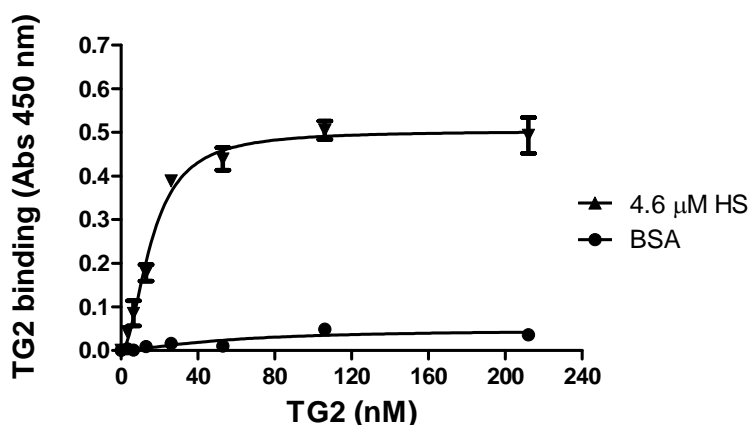


**Figure 4-6 Binding of TG2 to HS.** TG2 (0-212 nM) was allowed to bind immobilised HS (4.6  $\mu\text{M}$ ) or, as a negative control, BSA (5  $\mu\text{g/ml}$ ) in the presence of 2 mM EDTA for 2 hours at 37°C as shown in Figure 4-3.  $K_d$  for HS was  $17.03 \pm 2.76$  nM.  $n=3$ .

After showing that TG2 binds either heparin or HS with similar high affinity, the interaction of TG2 with heparin was further investigated in real time by using surface plasmon resonance (SPR). For this study heparin was immobilised on a Biacore sensorchip, thus mimicking the cell surface presentation of HSPG, and TG2 was perfused above this surface in a buffer containing 2 mM EDTA. Injection of a range of TG2 concentrations (51-586 nM) over a sensorchip activated with 50 RU of heparin gave rise to the binding curves shown in Figure 4-7. The data were fitted with the Langmuir 1:1 model,

which explains the simplest way an analyte (A) (TG2) can interact with an immobilised ligand (B), in our case heparin ( $A+B \rightleftharpoons AB$ ).

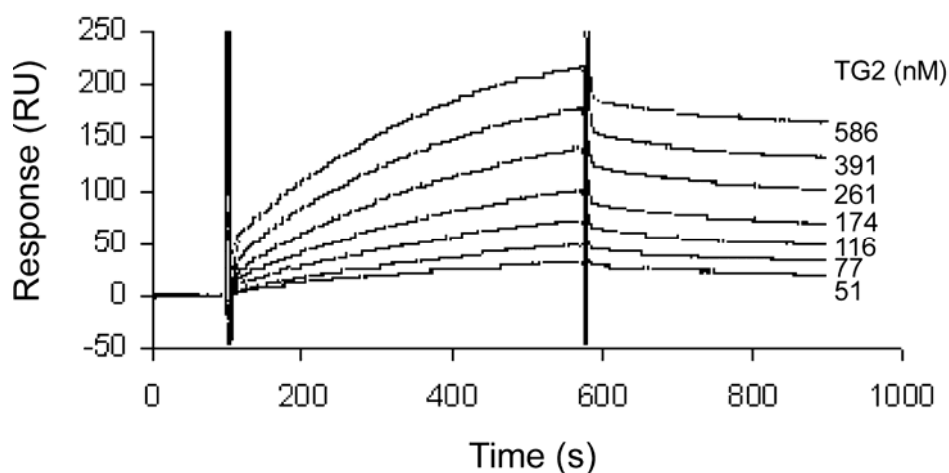
The fitting of the data with the Langmuir model returned a  $\chi^2$  value (which describes the closeness of the fit) of 4.5; fitting the data with other binding models did not improve the closeness (data not shown). Following data fitting, it was possible to calculate:

$k_{\text{off}}$  (rate of dissociation) =  $4.95 \times 10^{-4} \text{ s}^{-1}$  and

$k_{\text{on}}$  (rate of association) =  $5.5 \times 10^3 \text{ M}^{-1} \text{ s}^{-1}$

leading to an average  $K_d$  ( $k_{\text{off}}/k_{\text{on}}$ ) of  $92.7 \pm 4.7 \text{ nM}$ .

Within the limit of the  $\chi^2$  this finding confirmed a nM-range affinity of TG2 for HS, as shown by the solid binding assay.

Deleted:  $K_1$ Deleted:  $M^{-1}$ Deleted:  $K_2$ Deleted:  $\cdot$ Deleted:  $K_2$ Deleted:  $K_1$ 

**Figure 4-7 SPR analysis of TG2 affinity for heparin.** TG2 (51-586 nM) was injected over a heparin activated surface for 8 min at a flow rate of  $10 \mu\text{l}/\text{min}$ , after which running buffer was injected, and the response in RU was recorded as a function of time. Sensorgrams were analysed with Biaeval 3.1 software.

#### 4.2.2 Cell-surface TG2 interacts with heparin and HS chains

After establishing a strong affinity of purified gp1, TG2 for heparin and heparan sulphate, the affinity of endogenous cell-surface TG2 for heparin/HS was explored. Since wild type MEF externalise TG2 starting from early stages of cell-adhesion (see Chapter 3), reaching a peak of externalisation after 1 hour post-seeding, they were used as a source of cell-surface TG2. The TG2-heparin binding was investigated by monitoring the cell-attachment to heparin/HS of wild type MEF compared to the one of TG2 null MEF.

As shown in Figure 4-8, cells presenting TG2 at the cell surface (TG2 +/+) had a significantly higher level of adhesion on both heparin and heparan sulphate compared to TG2 -/- cells ( $p < 0.001$ ). Wild type cells showed a  $\approx 60\%$  level of adhesion to wells coated with  $2.3 \mu\text{M}$  heparin and  $\approx 100\%$  adhesion to wells coated with  $4.6 \mu\text{M}$  heparin. When the adhesion of wild type MEF was performed on HS-coated plates, there was  $\approx 65\%$  adhesion on  $1.3 \mu\text{M}$  HS and  $\approx 100\%$  adhesion on both  $2.3$  and  $4.6 \mu\text{M}$  HS. Cells lacking TG2 (TG2 -/-) cells displayed a significantly lower adhesion level (20-30%) compared to wild type cells on heparin/HS, suggesting that TG2 is critical for heparin/HS binding. Both TG2 +/+ and TG2 -/- cells displayed a similar level of cell adhesion on control FN, although differences in the spreading level were noticeable, with wild type cells showing a more homogeneous distribution and a flatter morphology (Figure 4-8). The level of cell adhesion on BSA-coated plates was significantly lower for both the cell lines compared to FN, and was estimated to be lower than 10% compared to the positive FN control.

Deleted: 1

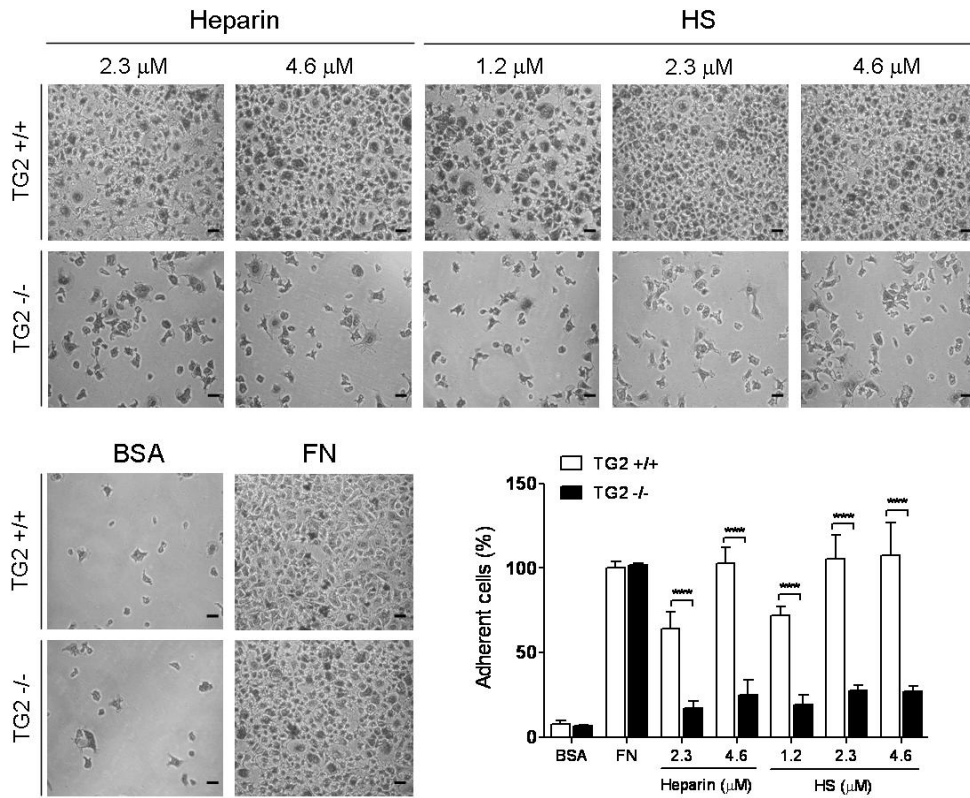


**Figure 4-8 Cell adhesion studies on heparin/HS-coated plates.** Wild type (TG2 +/+) and TG2 -/- MEF were serum-starved and allowed to adhere on plates coated with either heparin (2.3 or 4.6  $\mu$ M) or HS (1.2, 2.3 or 4.6  $\mu$ M) for 1 hour in serum-free medium. Plates coated with BSA or FN (5  $\mu$ g/ml) were used as negative and positive control, respectively. Adherent cells were quantified and normalised considering cell adhesion of TG2 +/+ cells on FN as 100%. The bar indicates 20  $\mu$ m. n=3. \*\*\* indicates  $p < 0.001$ .

### 4.2.3 Direct co-association of TG2 and HS chains of Sdc-4 at the cell surface

After establishing the association of TG2 to GAG chains through affinity measurements, the biological significance of this binding was investigated by co-immunoprecipitation studies of TG2 and Sdc-4. Sdc-4 was chosen among the others HSPG given its significant role in TG2-mediated RGD-independent cell adhesion, as shown in Chapter 3. Given the transmembrane localization of Sdc-4, co-immunoprecipitation experiments were performed on crude membrane preparations. It was decided to undertake the co-immunoprecipitation experiments using a cell line particularly rich in both HSPG and TG2; for this reason human osteoblasts (HOB) (Scotchford et al., 1998) were chosen, since they are rich in HSPG (Gronthos et al., 1997) and express cell-surface TG2 (Heath et al., 2001; Verderio et al., 2001). Moreover, stably transfected HOB over-expressing human TG2 (HOB-TG14) (Verderio et al., 2001) were available for the study.

As a preliminary study, the expression of Sdc-4 was tested in membrane extracts from HOB cells by Western blotting. In order to distinguish the glycosylated forms from the core protein of Sdc-4, untreated extracts were compared to heparitinase-treated extracts. Heparitinase catalyses the cleavage of  $\alpha$ -N-acetyl-D-glucosaminide linkage (either 6-sulphated or non-sulphated) in heparan sulphate, reducing or eliminating the glycosylation level of the Sdc-4 core protein. Western blotting analysis revealed a strong band at ~200 kDa and other high molecular weight bands in the untreated sample (Figure 4-9, asterisk); these bands were markedly reduced after heparitinase treatment, indicating their glycosylated nature. Heparitinase treatment also resulted in the intensification of the band at ~44 kDa, which should correspond to Sdc-4 core protein SDS-insoluble homodimer (Echtermeyer et al., 1999; Longley et al., 1999) (Figure 4-9, arrow).

Next, membrane extracts obtained from HOB and HOB-TG14 cells were immunoprecipitated with anti-Sdc-4 antibody and analysed by Western blotting for the presence of TG2. As shown in Figure 4-10 A (arrow head), a band of 77 kDa, corresponding to TG2 was detected in both HOB and HOB-TG14 Sdc-4-immunoprecipitates (S4), which was not detected in the negative controls, represented by immunoprecipitation with beads only (B) and with anti gliadin antibody (G1); this finding suggests association of TG2 with Sdc-4.

The above described immunoprecipitates were also examined for the presence of Sdc-4, to test the efficiency and the specificity of the immunoprecipitation process. As shown in Figure 4-10 B, Sdc-4 immunoprecipitates displayed high molecular weight bands corresponding to the glycosylated core protein of Sdc-4 (in particular a band of ~200 kDa, indicated by the asterisk) together with a large band of 35-45 kDa which may include Sdc-4 core protein homodimer and other glycosylated Sdc-4 isoforms. The band of 50-55 kDa, detected in both immunoprecipitates with anti-gliadin and anti-Sdc-4 antibody corresponds to the heavy chain (Hc) of the rabbit antibody used for the immunoprecipitation, reacting with anti-rabbit IgG secondary antibody (Figure 4-10 B, Hc).

To verify the association of TG2 and Sdc-4, membrane extracts from HOB and HOB-TG14 were also immunoprecipitated with anti-TG2 antibody and analysed by Western blotting for the presence of Sdc-4. As shown in Figure 4-11 A (left panel), both glycosylated Sdc-4 (asterisk) and other lower Mr Sdc-4 oligomers were detected in the TG2-immunoprecipitates. The Sdc-4 band profile in TG2 immunoprecipitates was analogue to the one detected in membrane protein extracts from HOB cells (Figure 4-9). To verify the identity of the bands detected by the anti Sdc-4 antibody, the TG2-immunoprecipitates were treated with heparitinase before Western blotting (Figure 4-11 A, right panel). Treatment of TG2-immunoprecipitates with heparitinase determined the loss of high molecular weight bands and the intensification of the band corresponding to Sdc-4 core protein homodimer (Figure 4-11 A, right panel, arrow). This time the antibody heavy chain was not detectable, since the antibody used for immunoprecipitation was a mouse monoclonal and the secondary antibody used for the Western blotting was an anti-rabbit IgG from mouse. Control Western blotting for TG2 revealed that TG2 was correctly immunoprecipitated in both HOB and HOB-TG14 extracts (Figure 4-11 B, arrow head).

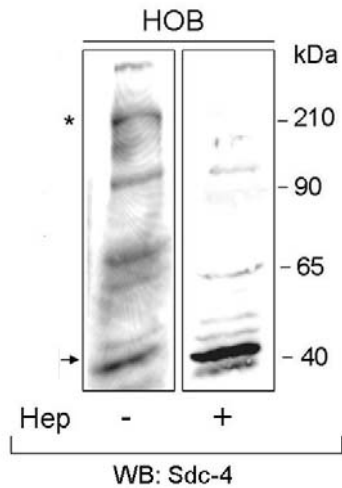


**Figure 4-9 Sdc-4 detection in total membrane extract from HOB.** 30  $\mu$ g of untreated or heparitinase (Hep)-treated membrane protein extract from HOB were separated by reducing SDS-PAGE (10% polyacrylamide gel) and analysed by Western blotting.. Sdc-4 was detected by anti-Sdc-4 antibody followed by secondary antibody, HRP-conjugated. The arrow points at Sdc-4 core protein dimers (~44 kDa). The asterisk indicates the predominant band of glycosylated Sdc-4 (~200 kDa). Positions of molecular weight markers are shown on the right hand side of the blot.

Formatted: Font: Symbol

Deleted: (Zymed)

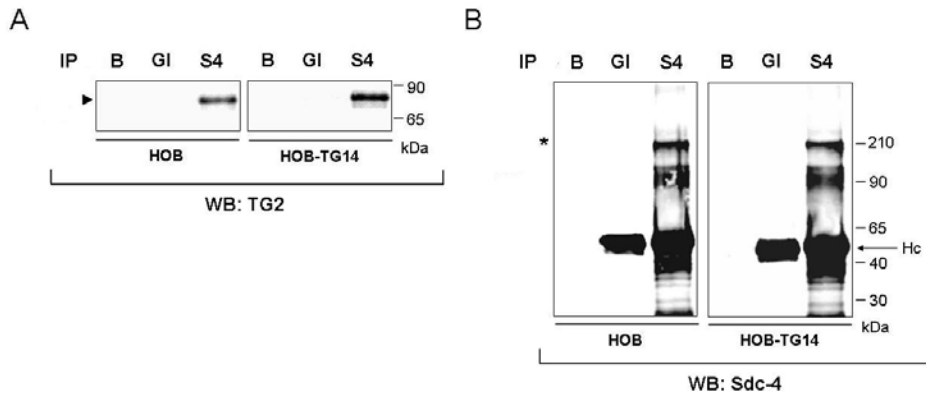


**Figure 4-10 TG2 detection in Sdc-4 immunoprecipitates from HOB and HOB-TG14.** Membrane preparations (500  $\mu$ g) from HOB and HOB over-expressing human TG2 (HOB-TG14) were immunoprecipitated with anti-Sdc-4 antibody [S4] (2 $\mu$ g) and after that the immunoprecipitates were subjected to Western blot analysis for TG2 (A) and, as a control, for Sdc-4 (B). Control immunoprecipitations were performed with beads only [B] and anti gliadin antibody [GI] (2  $\mu$ g). Hc represents the heavy chain of the antibody used for immunoprecipitation. \*, glycosylated Sdc-4 (~200 kDa); arrow head, TG2 (~77 kDa).

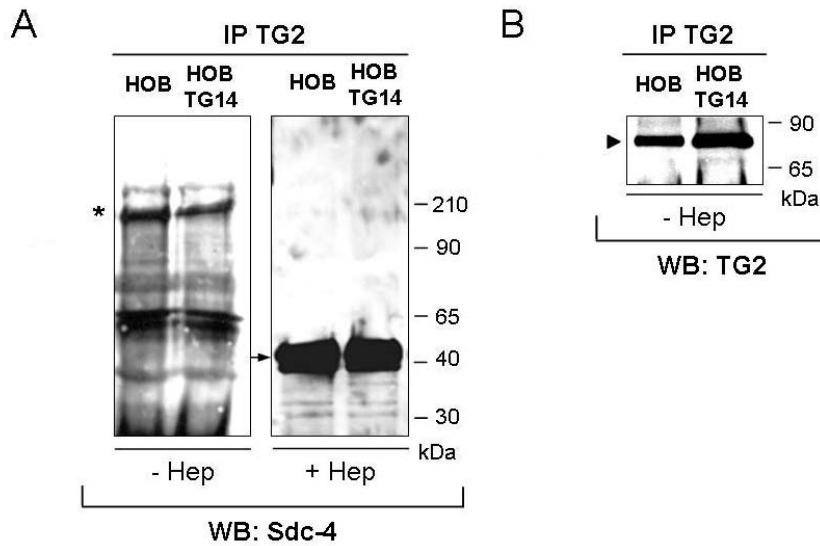


**Figure 4-11 Sdc-4 detection in TG2 immunoprecipitates from HOB and HOB-TG14.** Membrane preparations (500  $\mu$ g) from HOB and HOB overexpressing human TG2 (HOB-TG14) were immunoprecipitated with anti-TG2 antibody (2 $\mu$ g) and after that the immunoprecipitates were subjected to Western blot analysis for Sdc-4 (A) and, as a control, for TG2 (B) before and after heparitinase (Hep) treatment. \*, glycosylated Sdc-4 (~200 kDa); arrow, Sdc-4 core protein dimer (~44 kDa); arrow head, TG2 (~77 kDa).

To investigate whether TG2-Sdc-4 association was also present in the fibroblast cell type, a Swiss 3T3 cell line (clone TG3) with tetracycline-regulated inducible expression of TG2 was used (Verderio et al., 1998). A band corresponding to TG2 (~77 kDa) was present in the Sdc-4-immunoprecipitates (S4) from TG3 Swiss 3T3 cells + tet (expressing endogenous level of TG2), which intensified in the Sdc-4 immunoprecipitates from cells overexpressing TG2 (TG3 Swiss 3T3 – tet) (Figure 4-12). A faint TG2 band could also be detected in the control immunoprecipitation performed by incubating the protein preparation with protein G agarose only, indicating aspecific binding to protein G agarose beads. However, the intensity of aspecific binding was much lower compared to the intensity of TG2 bands in Sdc-4 immunoprecipitates.

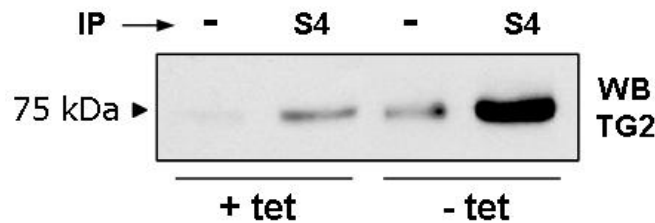


**Figure 4-12 TG2 detection in Sdc-4 immunoprecipitates from Swiss 3T3 cells with inducible expression of TG2.** Membrane preparations (500  $\mu$ g) from Swiss 3T3 cells control (+tet) or with induced TG2 expression (-tet) were immunoprecipitated with anti Sdc-4 antibody (S4) (2  $\mu$ g) or with protein G agarose beads (-) and analysed by Western blotting with anti TG2 antibody. The band corresponding to TG2 is indicated by the arrow head.

The experiments described in section 4.2.1 demonstrated the binding affinity of TG2 for heparin and heparan sulphate. To investigate if TG2 associates with Sdc-4 via binding of Sdc-4 HS chains, the cell suspensions of HOB and Swiss 3T3 cells were incubated with protease-free heparitinase (to selectively clear HS chains) prior to immunoprecipitation of Sdc-4 using an antibody directed against the core protein.

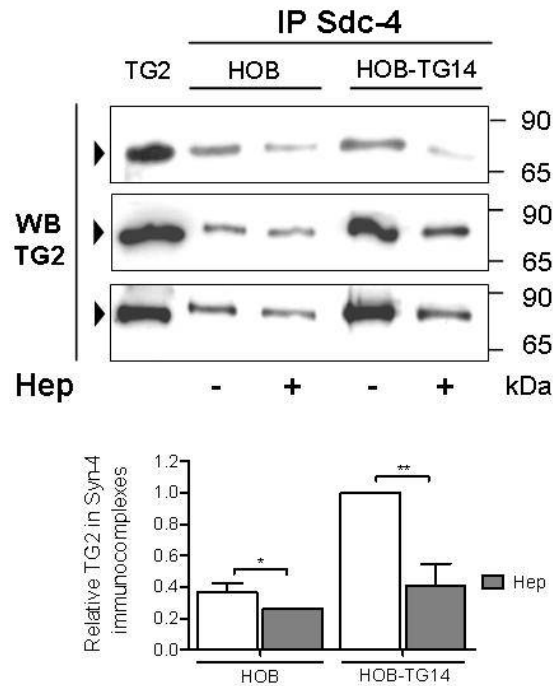


**Figure 4-13 Immunoprecipitation of TG2 and Sdc-4 largely relies on Sdc-4 HS chains (1).** Membrane extracts prepared from HOB and HOB overexpressing human TG2 (HOB-TG14) were digested or not with heparitinase (Hep) (30 mU/ml) to remove HS chains. The membrane preparations (500 µg) were then immunoprecipitated with anti Sdc-4 antibody (S4) (2 µg) and analysed by Western blotting against TG2. Three independent experiments and their densitometric analysis are shown (data are expressed as the mean ± SD); data were normalised considering HOB-TG14 value without Hep as 1. gpTG2 (200 ng) was used as a control and for normalisation of data. \* indicates  $p < 0.05$ ; \*\* indicates  $p < 0.002$ .

Deleted: n

The removal of HS significantly reduced the amount of TG2 associated with Sdc-4 in both HOB and HOB-TG14 cells (Figure 4-13) and Swiss 3T3 cells by a 40-50% value (Figure 4-14). This range is in agreement with the effect of heparitinase treatment on HOB cells, that, if measured by flow cytometry, shows a digestion level of HS chains of ~ 50% (previous work by E. Verderio, Nottingham Trent University).

These results give information on the way TG2 interacts with Sdc-4, which largely occurs through the HS chains of Sdc-4.

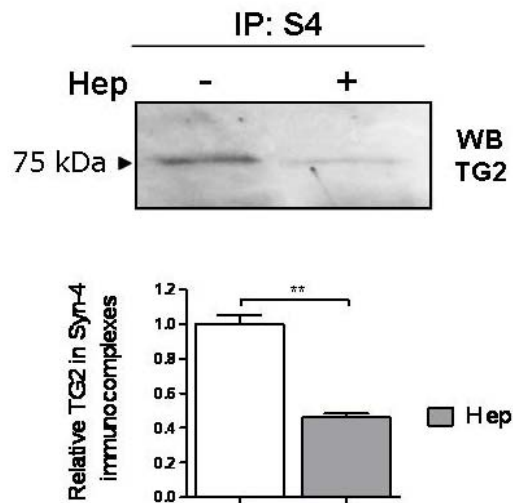


**Figure 4-14 Immunoprecipitation of TG2 and Sdc-4 largely relies on Sdc-4 HS chains (2).** Membrane extracts were prepared from Swiss 3T3 cells control (+tet) digested or not with heparitinase (Hep) (30 mU/ml). Membrane preparations (500 µg) were immunoprecipitated with anti Sdc-4 antibody (S4) (2 µg) and analysed by Western blotting against TG2. Densitometric analysis of two independent experiments is shown; data are normalised considering sample -Hep equal to 1. \*\* indicates  $p < 0.002$

Deleted: n

#### 4.2.4 Binding of TG2 to Sdc-4 is not mediated by fibronectin

Fibronectin is known to interact with HS chains of Sdc-4 through its high affinity Hep II binding domain (Woods et al., 2000); since FN has also elevated affinity for TG2, it was important to demonstrate that the binding of TG2 to the HS chains of Sdc-4 at the cell surface was direct and not mediated by FN. For this purpose TG2 binding to FN was inhibited by using a peptide (P3 peptide, Hang et al., 2005) which mimics FN binding site within TG2, and thus binds FN in competition with TG2 (Figure 4-15).

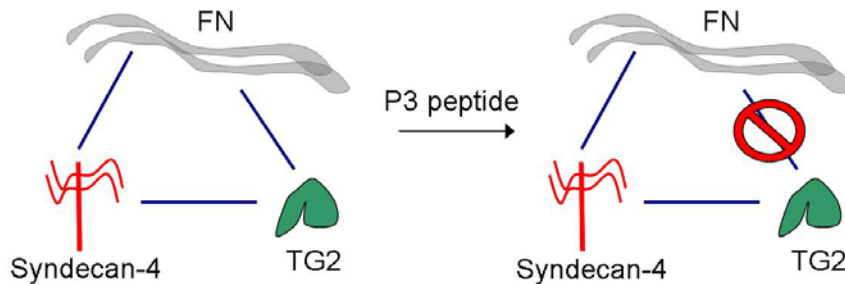


**Figure 4-15 Scheme of triangular association of TG2, Sdc-4 and FN.** The triangular association of the three molecules is shown, together with the inhibitory action of P3 peptide (Hang et al., 2005), which interferes with TG2 binding to FN by mimicking FN binding region of TG2.

In order to confirm the inhibitory action of P3 peptide on TG2 binding to FN, a plate assay was performed, measuring the binding of TG2 to FN in the presence of increasing concentrations (0-150  $\mu\text{M}$ ) of P3 peptide (Figure 4-16). The FN-binding of TG2 at both 20 nM and 50 nM was significantly reduced if 100  $\mu\text{M}$  P3 peptide was present; this result validated the use of 100  $\mu\text{M}$  P3 peptide in subsequent immunoprecipitation experiments to interfere with TG2-FN association.

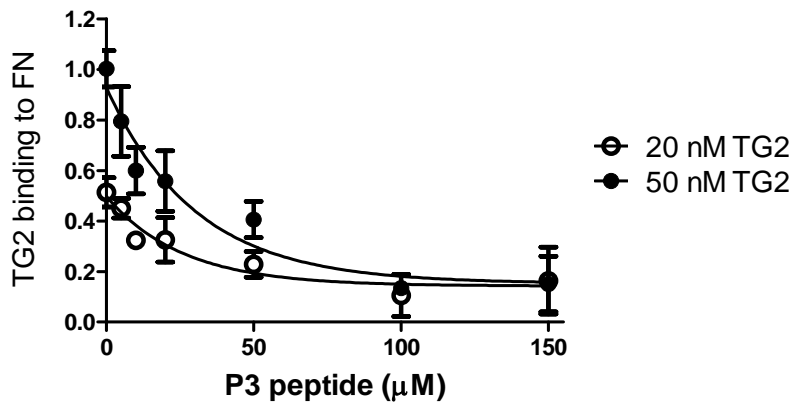


**Figure 4-16 Inhibition of TG2 binding to FN using P3 peptide.** Inhibition of TG2-FN binding, assayed by ELISA using 20 nM and 50 nM purified gpTG2 allowed to bind FN-coated microtiter plates (5  $\mu\text{g}/\text{ml}$ ) for 1 hour in the presence of increasing concentrations of P3 peptide (0-150  $\mu\text{M}$ ). Data (mean absorbance values  $\pm$  SD from three independent experiments) have been normalised considering the binding of 50 nM TG2 to FN in the absence of P3 peptide equal to 1.

At this stage HOB cells were plated on a FN matrix pre-incubated with P3 peptide (100  $\mu$ M) in order to saturate the TG2 binding sites on FN; after one hour, both adherent and not adherent cells were collected and membrane preparations were subjected to immunoprecipitation with anti Sdc-4 antibody followed by Western blotting against TG2 and FN (Figure 4-17). The pre-incubation of FN with P3 peptide did not reduce the amount of TG2 co-immunoprecipitated with Sdc-4 (Figure 4-17, top panel), suggesting that the binding is direct and not mediated by FN. As a control, FN was also detected in the Sdc-4 immunoprecipitates, showing that the amount of FN associated with Sdc-4 was not reduced by the action of P3 peptide (Figure 4-17, bottom panel) (densitometric values for FN with and without P3 peptide were  $1.2 \pm 0.2$  and  $1.0 \pm 0.1$ , respectively;  $p=0.32$ ).

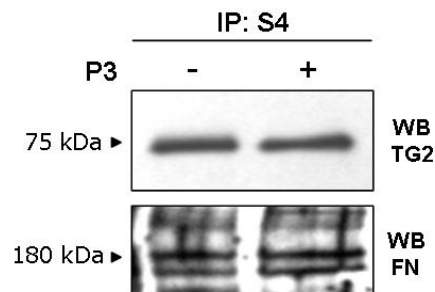


**Figure 4-17 Immunoprecipitation of TG2 and Sdc-4 in the presence of competitive concentrations of P3 peptide.** HOB cells were let to adhere on FN matrices pre-incubated (+) or not (-) with P3 peptide (Hang et al., 2005) (100  $\mu$ M) before preparation of membrane extracts. Membrane preparations (500  $\mu$ g) were immunoprecipitated with anti-Sdc-4 antibody (S4) (2  $\mu$ g) and analysed by Western blotting against TG2 and FN. The arrow heads point at TG2 (top panel) and FN (bottom panel).

#### 4.2.5 Visualisation of TG2-Sdc-4 association by fluorescence microscopy

Association of TG2 with Sdc-4 was further investigated by using indirect double fluorescent labelling of HOB allowed to adhere for 2 hours on tissue culture plastic in serum-containing medium. A combination of secondary antibody conjugated to different fluorescent dyes was chosen in order to avoid overlapping emission signals, and to make sure that any co-staining of TG2 and Sdc-4 was effectively due to co-localisation of the two molecules. To this purpose, the primary antibodies mouse anti-TG2 and rabbit anti-Sdc-4 were revealed by sheep anti mouse IgG FITC and donkey anti rabbit IgG AlexaFluor568, respectively. As shown in Figure 4-18, the two molecules appeared to co-localise, in particular at the cell borders and in correspondence of cell-cell contacts, as pointed by the arrows.

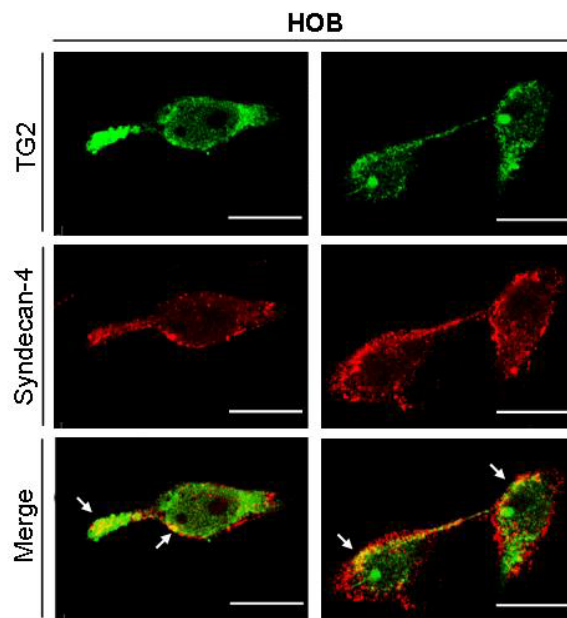


**Figure 4-18 Co-localisation of TG2 and Sdc-4 in HOB.** Fixed and permeabilised HOB were stained with anti-TG2 and anti-Sdc-4 antibodies and revealed with anti mouse-FITC and anti rabbit-AlexaFluor 568 secondary antibodies, respectively. Images were acquired by laser confocal microscopy and represent sections of the cellular basal surface. Two different fields are shown. The arrows point at areas of co-localisation. The bar indicates 20  $\mu$ m.

### 4.3 Discussion

After showing the involvement of Sdc-4 in TG2 mediated RGD-independent adhesion (Chapter 3), in the present chapter the investigation was focused on the physical interaction between TG2 and Sdc-4. Solid binding assays were developed to measure for the first time the affinity of purified TG2 for heparin and HS. A strong binding affinity was measured, with a  $K_d$  of  $\approx 20$  nM. Considering that so far FN has been considered the main extracellular binding partner for TG2, this value is surprisingly high if compared to the measured affinity of TG2 to the 42 kDa gelatin binding domain of FN, which was estimated as 8-10 nM (Jeong et al., 1995; Radek et al., 1993) and, more recently, using SPR, as 180 nM (Hang et al., 2005). Since the estimated affinity of TG2 for HS measured in this thesis is similar to the measured affinity of TG2 for FN, the results shown in this thesis show that FN may not be the only extracellular high-affinity binding partner for TG2, especially in cell systems with a high expression of HSPG.

Deleted: T

It was of interest that the estimated affinity of TG2 for heparin and HS was slightly lower in the presence of physiological extracellular concentration of  $Ca^{2+}$  compared to EDTA, even though both affinities were in the low nM range. Given that TG2 is catalytically active outside the cell and  $Ca^{2+}$  changes TG2 conformation (Li et al., 2002), TG2 auto-crosslinking was considered at first as an interfering factor on heparin-binding. Western blot analysis in reducing conditions showed that even though a certain amount of TG2 is present in oligomeric form in the presence of  $Ca^{2+}$ , the majority of the enzyme is still in monomeric form, so auto-crosslinking can not be the cause of the reduced binding to heparin in the presence of  $Ca^{2+}$ . The presence of  $Ca^{2+}$  is not supposed to interfere with heparin and HS binding to the plates used for the assay (Mahoney et al., 2004), but, given its positive charge,  $Ca^{2+}$  could interfere with negatively charged heparin and HS, thus potentially lowering the binding of TG2 (Rudd et al., 2007). Solid binding assays were also performed in the presence of positive ions with similar properties to  $Ca^{2+}$ . The apparent affinity of TG2 for heparin was not significantly different in the presence of either  $Ca^{2+}$ ,  $Mg^{2+}$  or  $K^+$ . This suggests that the slightly lower binding recorded in the presence of  $Ca^{2+}$  compared to EDTA was not due to a change in conformation of the enzyme, but more likely to altered heparin accessibility (Rudd et al., 2007).

Deleted: measured

Deleted: ( $\approx 40$  nM)

Deleted: .

A lower apparent binding affinity of TG2 to heparin was also measured in the presence of GTP $\gamma$ S (150  $\mu$ M); however, there is no documented evidence of GTP/GDP interaction with heparin/HS. Therefore, it can not be excluded that a lower binding of TG2 to heparin/HS in the presence of GTP $\gamma$ S could be the consequence of the GTP-induced conformation of the enzyme (Lorand and Graham, 2003; Smethurst and Griffin, 1996), which may have a lower affinity for heparin/HS.

The estimated affinity of TG2 for HS obtained with solid binding assay was confirmed by monitoring TG2 binding to heparin with SPR. Here the binding was measured in real time and not at equilibrium, after 2 hours of TG2 interaction with heparin, as in the solid-binding assay. The estimated Kd in this case was  $\approx$  90 nM, a value of similar range to what obtained with solid binding, although suggesting a slightly lower affinity. It has to be mentioned that the  $\chi^2$  value obtained for this analysis (indicating the goodness of the fitting) was 4.5, a value higher than the limit normally considered for a meaningful fitting ( $\chi^2 = 2$ ). Therefore the SPR result can be regarded as indicative of a high affinity but with some limitations, due to the complexity of the system.

Deleted: results of TG2-HS

Deleted: were

Deleted: calculated

Deleted: However, the analysis of the binding results with models different from Langmuir 1:1 did not improve the fitting, t

Deleted: s

At least one of the heparin-binding motif described by Cardin and Weintraub (1989), XBBXB (see 4.1.1) can be found in human TG2 (position 261-265), and appears to be accessible on the enzyme surface (personal communication by Lortat-Jacob, Institut De Biologie Structurale, Grenoble). Interestingly this domain is not only conserved in TG2 from different species (rat, mouse, human, guinea pig) (Figure 4-19) but it is also specific for TG2, since it is not present in TG1, TG3, TG5, TG6, TG7 and FXIIIa so it may be a good candidate for the specific interaction of TG2 with HSPG (Verderio et al., 2008).

Deleted: ¶

Next, to find out if cell-surface TG2 as opposite to purified TG2 could interact with immobilized heparin/HS, and thus support the physiological relevance of the binding, the adhesion of wild type MEF to heparin/HS was compared to that of TG2 null MEF. As shown in Chapter 3, wild type MEF display cell-surface TG2. The study revealed that the presence of cell surface TG2 is essential for the interaction of primary fibroblasts with heparin/HS. Interestingly, the absence of cell surface TG2 did not alter cell adhesion to immobilized FN, in accordance with the fact that TG2 inhibition via antisense RNA affects cell spreading but not cell attachment on FN (Stephens et al., 2004).



**Figure 4-19 Putative heparin-binding site conserved in TG2 from different species (Verderio et al., 2008).** Multiple sequence alignment (ClustalW) of rat, mouse, human and guinea pig liver TG2, showing a conserved putative heparin-binding site based on the motif XBBXB, where X is an hydrophobic amino acid and B is either Arg (R) or Lys (K).  $\square$ =fully conserved;  $\square$ =non conserved;  $\square$ =conserved;  $\square$ =similar.

Co-immunoprecipitation studies performed on cell membrane preparations from different cell lines (osteoblasts and fibroblasts) revealed that TG2 and Sdc-4 are physically associated at the cell surface, and that this association is largely mediated by HS chains of Sdc-4, since it was significantly reduced by heparitinase cleavage of HS chains. The physical association was confirmed by dual labeling, revealing an overlapping signal for TG2 and Sdc-4 in correspondence of cell-cell contacts and at the cell surface. The TG2-Sdc-4 association resulted to be direct and not mediated by the mutual interaction of TG2 and Sdc-4 with the high affinity partner FN, since the level of TG2 co-precipitated with Sdc-4 was not altered by a previously characterized peptide that inhibits the binding of FN to the N-terminal  $\beta$ -sandwich domain of TG2 (Hang et al., 2005).

A recent study has shown that the extracellular domain of  $\alpha 5 \beta 1$  integrins is able to bind heparin/HS (Faye et al., 2009). Since TG2 has been shown to have a high affinity for this class of integrins (Akimov et al., 2000), the reciprocal binding of  $\alpha 5 \beta 1$  integrins to HS chains could mediate the association of TG2 to heparin/HS. However, in the study by Faye and colleagues (2009), the interaction of integrins with heparin/HS was performed using purified molecules, which may interact in a different way compared to a cell system. The study also shows no difference in cell attachment on immobilized  $\alpha 5 \beta 1$  integrins (measured by SPR) between control chinese hamster ovary (CHO) cells and CHO cells which do not present sulfated GAG at the cell surface (Faye et al., 2009), thus confirming

Deleted: ¶

**Deleted:** Next, to find out if cell-surface TG2 as opposite to purified TG2 could interact with immobilized heparin/HS, and thus support the physiological relevance of the binding, the adhesion of wild type MEF to heparin/HS was compared to that of TG2 null MEF. As shown in Chapter 3, wild type MEF display cell-surface TG2. The study revealed that the presence of cell surface TG2 is essential for the interaction of primary fibroblasts with heparin/HS. Interestingly, the absence of cell surface TG2 did not alter cell adhesion to immobilized FN, in accordance with the fact that TG2 inhibition via antisense RNA affects cell spreading but not cell attachment on FN (Stephens et al., 2004).¶

Deleted: TG2

Deleted: FN

the hypothesis that the interaction between integrins and Sdc-4 may not occur under physiological conditions.

In conclusion, this study has revealed for the first time that TG2 has high affinity for heparin/HS, that the association is direct and physiologically relevant.

## ***Chapter 5: Role of Sdc-4 in the trafficking and cell-surface localization of TG2***

### ***5.1 Introduction***

#### **5.1.1 Insight on TG2 cell-surface trafficking**

Since TG2 is a multifunctional enzyme whose action can lead to permanent protein modifications, and since TG2 influences intracellular signalling, its cell-surface trafficking needs to be highly regulated. Several mechanisms have been proposed as regulators of cell-surface/ECM adhesion-related TG2 functions. Belkin and colleagues have suggested a model of TG2 release involving proteolysis of cell-surface TG2, mediated by membrane-anchored and soluble metalloproteases (Belkin et al., 2001; Belkin et al., 2004). Another model describes inside-out regulation of TG2-mediated cell-matrix adhesion by the Ras-Raf-MEK1-ERK1 signalling pathway (Akimov and Belkin, 2003). More recently, a novel mechanism of TG2 regulation has been proposed, involving TG2 internalisation and degradation in the lysosomes (Zemskov et al., 2007). This process is mediated by the low density lipoprotein receptor-related protein 1 (Zemskov et al., 2007) and seems to be related to TG2 association to the binding partners FN and  $\beta 1/\beta 3$  integrins, which are also internalised in an analogous way.

The mechanism of TG2 externalisation remains to be elucidated as numerous evidence justify a possible unconventional export. In fact, TG2 lacks of a hydrophobic leader sequence or the post-translational modifications, which would indicate processing by endoplasmic reticulum and Golgi apparatus leading to externalisation (Lorand and Graham, 2003). Interestingly, even though TG2 shows important extracellular functions, it presents some characteristics typical of cytosolic proteins, such as the absence of disulfide bridges and the lack of glycosylation (Ikura et al., 1989), thus strengthening the idea of non-conventional secretion. A common feature of TG2 and Factor XIIIa, both secreted members of the TG family, is the modification of the N-terminal domain by removal of the terminal Met and acetylation of the adjacent Ala (Ikura et al., 1989; Takahashi et al., 1986). This modification could represent a signal for TG2 externalisation. So far, it has been shown that TG2 externalisation is affected by the conformation of the Cys-containing active site and by the N-terminal FN-binding  $\beta$ -sandwich domain

(Balklava et al., 2002; Gaudry et al., 1999). More recently, transamidating activity was shown not to affect TG2 secretion, since the process was shown to occur even in the presence of the TG inhibitor R283 (Telci et al., 2009). Although TG2 externalisation is enhanced by situations of cell-stress (Lorand and Graham, 2003; Thomazy and Fesus, 1989), this process does not seem to be a passive event following cell damage, since it occurs in the absence of leakage of intracellular components, when the cells are still viable (Skill et al., 2004).

Work by Peng et al. (1999) has demonstrated that TG2 is also translocated in the nucleus, and this process is mediated by importin  $\alpha$ -3, a nuclear transport protein (Lorand and Graham, 2003).

### **5.1.2 Possible role of HS in mediating the cell-surface biological action of TG2.**

Recent evidence have ascribed a role to HSPG in both membrane secretion and endocytosis (MacArthur et al., 2007), raising the hypothesis of the current study, that HSPG could influence cell trafficking of TG2 through the high affinity binding of TG2 for HS.

HSPGs are specialised glycoproteins with a core protein linked to one or more HS glycosaminoglycan chains, which are linear polysaccharides consisting of alternating N-acetylated or N-sulphated glucosamine units, and uronic acids (Bishop et al. 2007). The assembly of HS chains on core proteins, which is catalysed by enzymes of the Golgi, leads to a wide structural heterogeneity (e.g. chain size and length, extent of sulphation, spatial distribution of negatively charged groups). Interestingly, adhesive ECM glycoproteins such as FN and vitronectin, and growth factors such as midkine, which all serve as substrates for TG2 transamidation, are also heparin-binding proteins (Table 4-1). In some cases, the TG2-mediated protein transamidation can be even augmented by GAGs such as heparin (Sane et al., 1990), suggesting that heparin could help immobilise TG2 on these target substrates.

The aim of this chapter is to test the possible influence of TG2 binding to HS on its cell-surface localisation and activity.

## 5.2 Results

### 5.2.1 Role of Sdc-4 in the cell-surface localisation of TG2 in primary fibroblasts

Given the association of TG2 and Sdc-4 at the cell surface, proven by co-immunoprecipitation and double immunofluorescence (Chapter 4), a set of experiments was carried out in order to determine whether Sdc-4 was involved in TG2 extracellular localisation.

In a first set of experiments, TG2 was detected by indirect immunofluorescence on fixed and permeabilised mouse dermal fibroblasts expressing or not Sdc-4 (Sdc-4  $+/+$  or Sdc-4  $-/-$ ) adhering on FN-coated slides and visualised by confocal microscopy. As shown in Figure 5-1 (arrows), TG2 was found to be predominantly located in patches at the cell periphery of wild type cells, where contacts between cells and the ECM take place. A similar TG2 staining was detected in FN-adhering MEF (Chapter 3, 3.2.1). A diffused cytosolic signal was also present, and a marked perinuclear signal, which was, however, also visible in cells lacking TG2 (Chapter 3, Figure 3-1). In the absence of Sdc-4, TG2 appeared to be mainly located in the cytosol, and its presence at the cell periphery was negligible (Figure 5-1). This aspect has been further investigated in Chapter 3. In order to gain more insights on the cellular localisation of TG2, firstly wild type and Sdc-4  $-/-$  cells were further visualised by double phase contrast microscopy and ordinary confocal microscopy. Pictures taken at the basal cell surface confirmed that TG2 is predominantly located at cell-matrix adhesions in wild type cells (Figure 5-2, arrows) and that in the absence of Sdc-4 TG2 is mostly localised in the cytosol/perinuclear area (Figure 5-2). TG2 was also co-stained with actin stress fibres, in order to visualise the location of TG2 in relation to the actin cytoskeleton. As shown in Figure 5-3 (arrowheads), in wild type MDF anti-TG2 antibody stained peripheral cell structures at the basal surface, most of which appeared to be connected with the end of actin stress fibres; TG2 was also localised in the pericellular matrix, as indicated by the small arrows. As previously shown, TG2 staining was restricted to the perinuclear and cytosolic regions of Sdc-4 null cells (Figure 5-3).

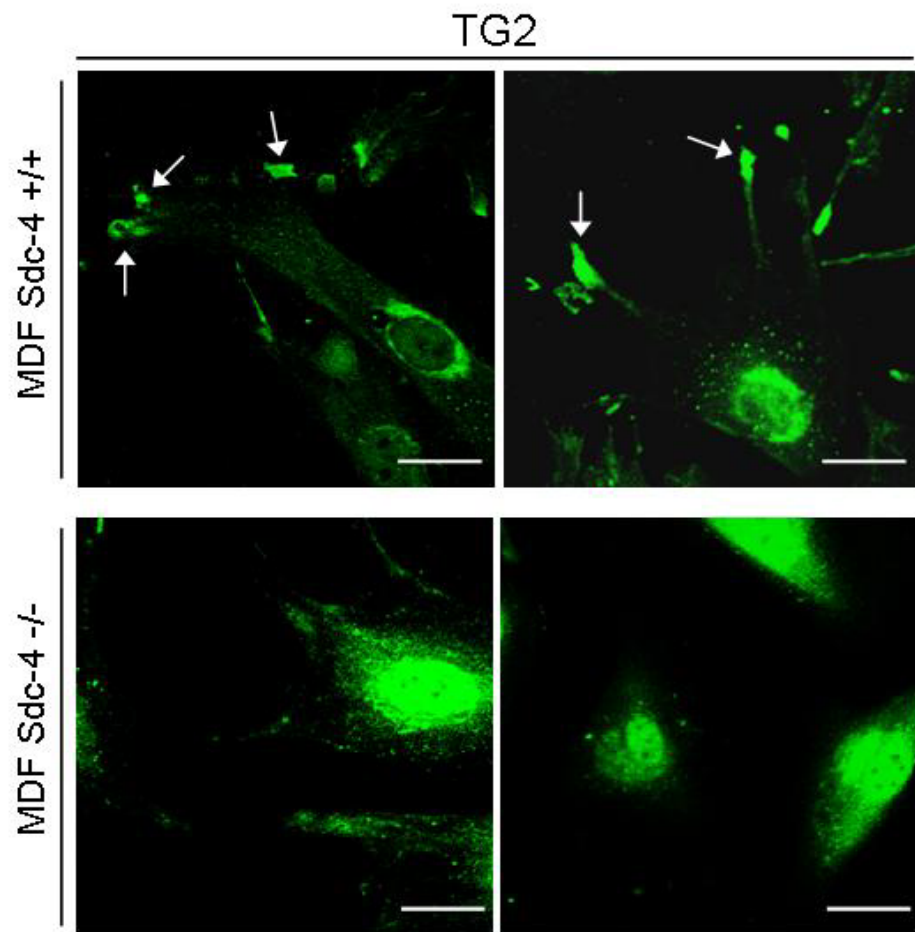


**Figure 5-1** TG2 staining in wild type and Sdc-4 null MDF. Wild type (*Sdc-4* +/+) and *Sdc-4* -/- MDF were allowed to adhere for 2 hours in complete serum-containing medium. TG2 was detected in fixed and permeabilised cells by monoclonal anti-TG2 antibody Cub7402 and revealed by FITC-conjugated secondary antibody. Two representative fields are shown. The arrows point at TG2 at the cell periphery in *Sdc-4* +/+ cells. The bar corresponds to 20  $\mu\text{m}$ .

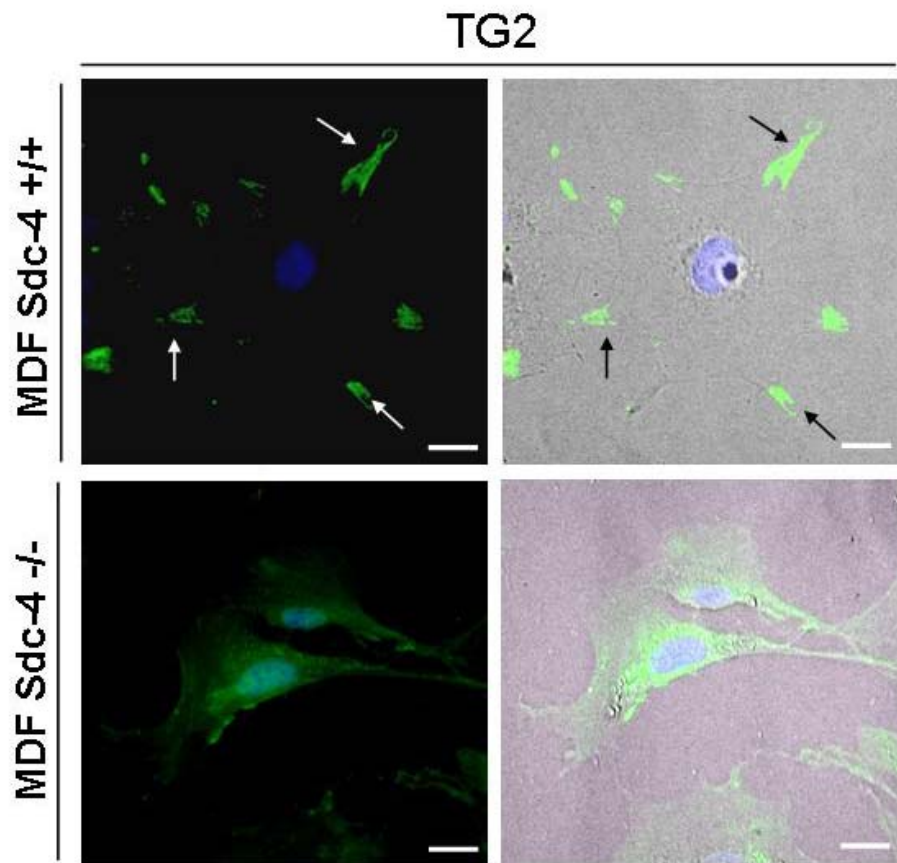


**Figure 5-2** Visualisation of TG2 by dual phase contrast confocal microscopy. *TG2* was detected in wild type (*Sdc-4* +/+) and *Sdc-4* -/- MDF as described in Figure 5-1. Cells were visualised with fluorescent confocal microscopy (left panel) and phase-contrast microscopy (right panel). Nuclei were stained with DAPI. The arrows point at *TG2* localised at cell-matrix adhesions in *Sdc-4* +/+ cells. The bar corresponds to 20  $\mu\text{m}$ .

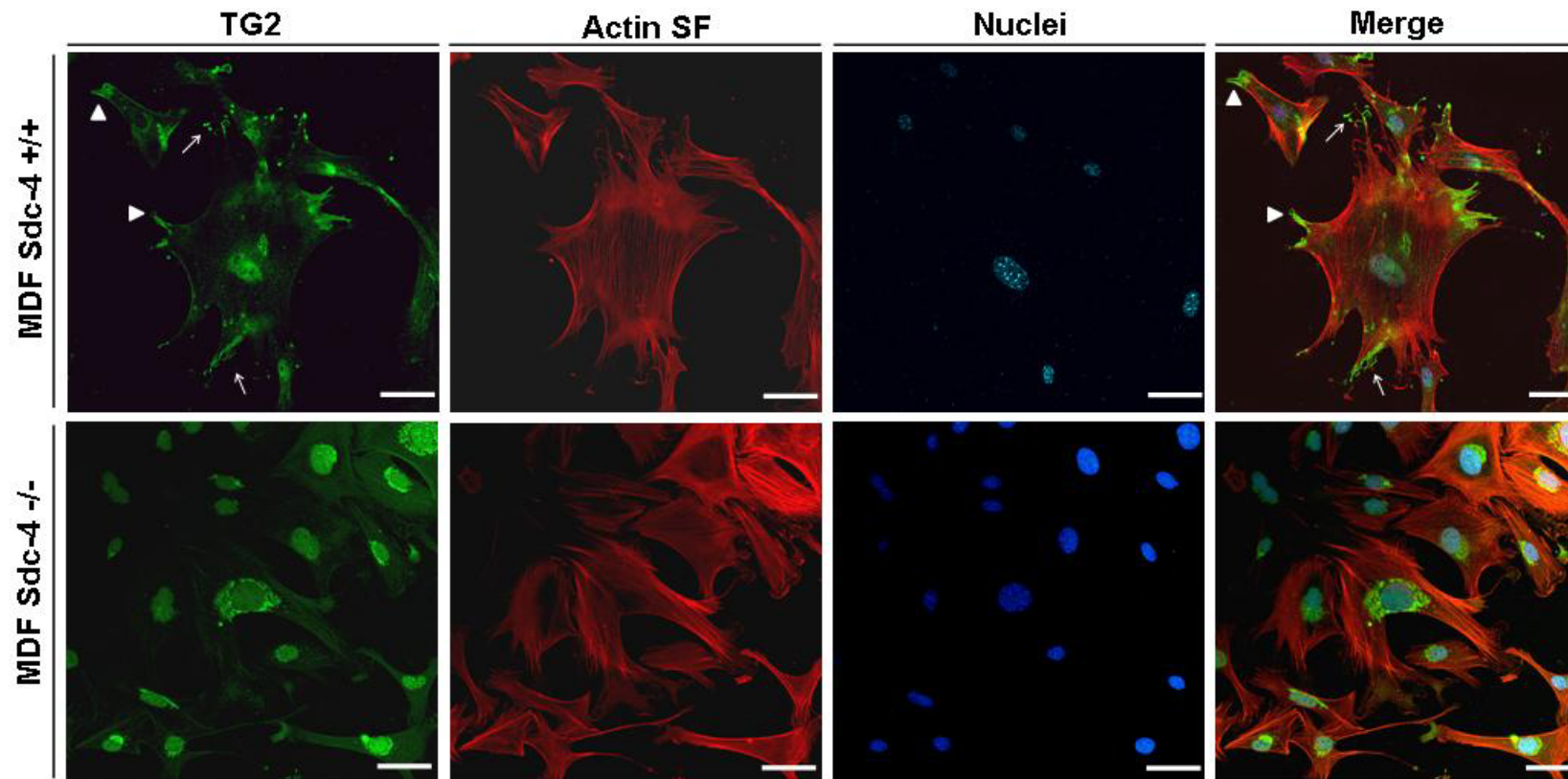


**Figure 5-3 Co-staining of TG2 and SF in wild type and Sdc-4 null MDF.** *TG2 and SF were detected in fixed and permeabilised Sdc-4 +/+ and Sdc-4 -/- MDF after 2 hours adhesion in complete serum-containing medium as described in Figure 5-1. Cells were stained with anti-TG2 antibody Cub7402 followed by 488Alexafluor-conjugated secondary antibody. SF were detected by TRITC-conjugated phalloidin. Nuclei were stained with DAPI. The arrowheads point at TG2 at cell-matrix adhesions. The small arrows point at TG2 in the pericellular matrix. The bar corresponds to 20  $\mu$ m.*

TG2 and actin stress fibres co-staining was also performed on MDF adhering on FN-coated slides, in order to simulate cell adhesion on a mature extracellular matrix. As shown in Figure 5-4, the same pattern of TG2 previously observed in cells adhering on uncoated slides (Figure 5-3) was produced in both wild type and Sdc-4  $-/-$  fibroblasts. However, a noticeable difference could be spotted in S4  $+/+$  cells, where TG2 was present in diffuse patches at cell-matrix contacts (Figure 5-4, pointed by arrows) as if those were the sites from where TG2 is released into the ECM.

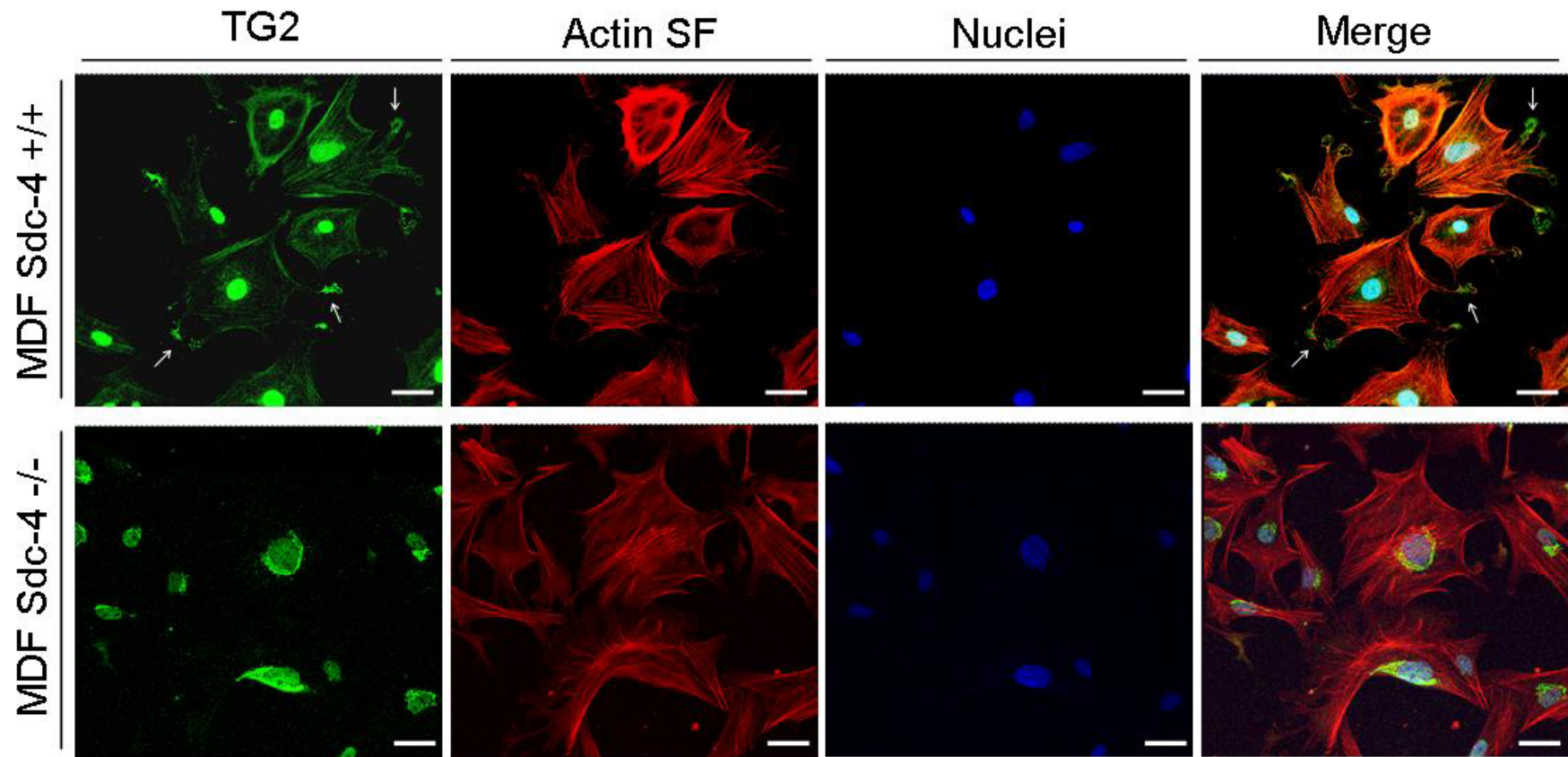


**Figure 5-4** TG2 localisation in wild type and Sdc-4 null MDF adhering on FN. TG2 and stress fibres were detected in wild type (*Sdc-4* +/+) and *Sdc-4* -/- MDF allowed to adhere on FN for 2 hours in complete serum-containing medium. All the stainings were performed as described in Figure 5-3. The arrows point at TG2 at cell-matrix adhesion. The bar corresponds to 20  $\mu$ m.

The data shown so far suggest that TG2 is predominantly located at cell-matrix adhesions and that the absence of Sdc-4 alters the pattern of TG2 localisation. The association of TG2 and Sdc-4 in MDF was also examined by double immunostaining, as previously done in osteoblasts (Chapter 4, paragraph 4.2.5). The results (Figure 5-5) showed that TG2 and Sdc-4 co-localise at cell-matrix adhesions, as pointed by the arrows. Only a faded Sdc-4 signal was detected in Sdc-4  $-/-$  cells, confirming the specificity of the antibody used for the staining. As previously shown in Figure 5-1 to 5-3, TG2 was absent from cell adhesion structures in cells lacking Sdc-4 (Figure 5-5).

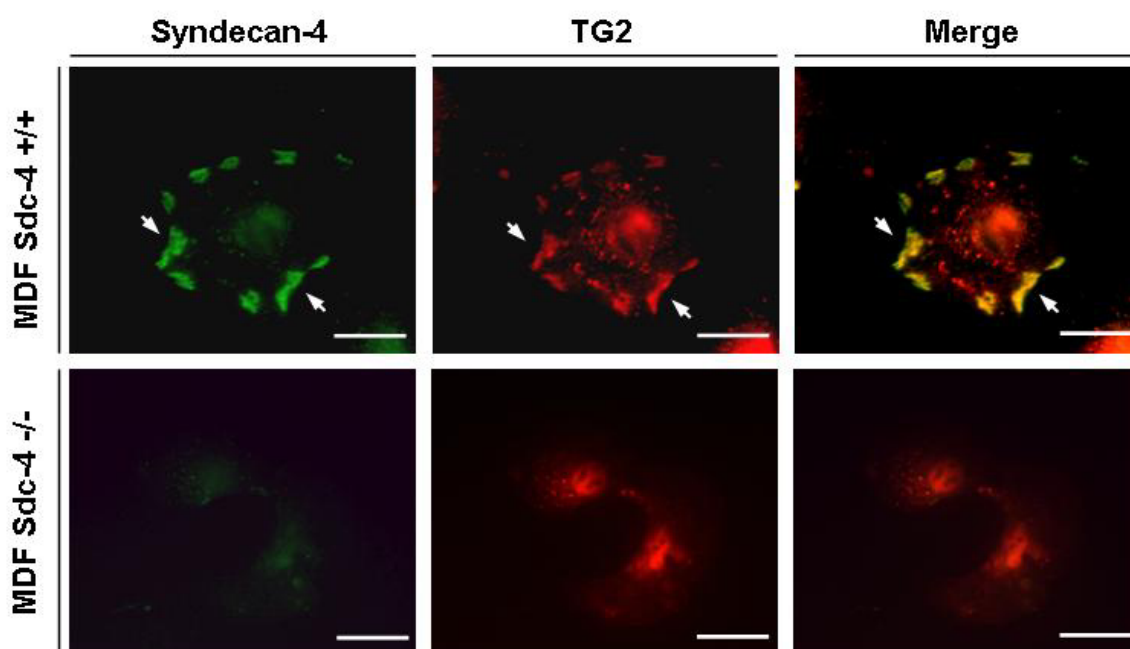


**Figure 5-5 Co-staining of TG2 and Sdc-4 in MDF.** *The staining was performed on fixed and permeabilised wild Sdc-4 +/+ and Sdc-4 null -/- MDF after 2 hours adhesion in complete serum-containing medium. Sdc-4 was detected by rabbit anti-syndecan-4 antibody and TG2 was detected by mouse anti-TG2 antibody Cub7402; secondary antibodies were goat anti rabbit IgG Alexafluor488 and goat anti mouse IgG Rhodamine RedX, respectively. The arrows point at cell-matrix adhesion sites where TG2 and Sdc-4 co-localise. The bar indicates 20  $\mu$ m.*

Next, the cellular distribution of TG2 distribution in wild type MDF compared to Sdc-4 null MDF was studied by Western blotting. Equal amounts of crude membrane (M) and cytosolic (C) fractions prepared from wild type and Sdc-4 *-/-* cells were separated by reducing SDS-PAGE and analysed by Western blotting for the presence of TG2. Protein equilading was verified by probing blots of membrane extracts with antibody towards Na<sup>+</sup>/K<sup>+</sup>ATPase (a membrane marker) and the blots of cytosolic extracts with antibody against  $\beta$ -tubulin (a cytosolic marker) (Figure 5-6).

As shown in Figure 5-6, TG2 antigen was significantly higher ( $p < 0.05$ ) in membrane fractions from wild type MDF compared to S4 *-/-* MDF; on the contrary, Sdc-4 *-/-* cytosolic extracts presented a significantly higher level of TG2 compared to wild type cells ( $p < 0.05$ ). There was not a significant difference in the total level of TG2 in wild type and Sdc-4 *-/-* cells when calculated as the sum of M and C (Figure 5-6).

After studying the cellular distribution of TG2 by immunofluorescence and Western blotting, the distribution of TG2 activity in different cell compartments was also studied by measuring Ca<sup>2+</sup>-dependent transamidation (TG activity) in membrane and cytosolic cell extracts from wild type and Sdc-4 null dermal fibroblasts.

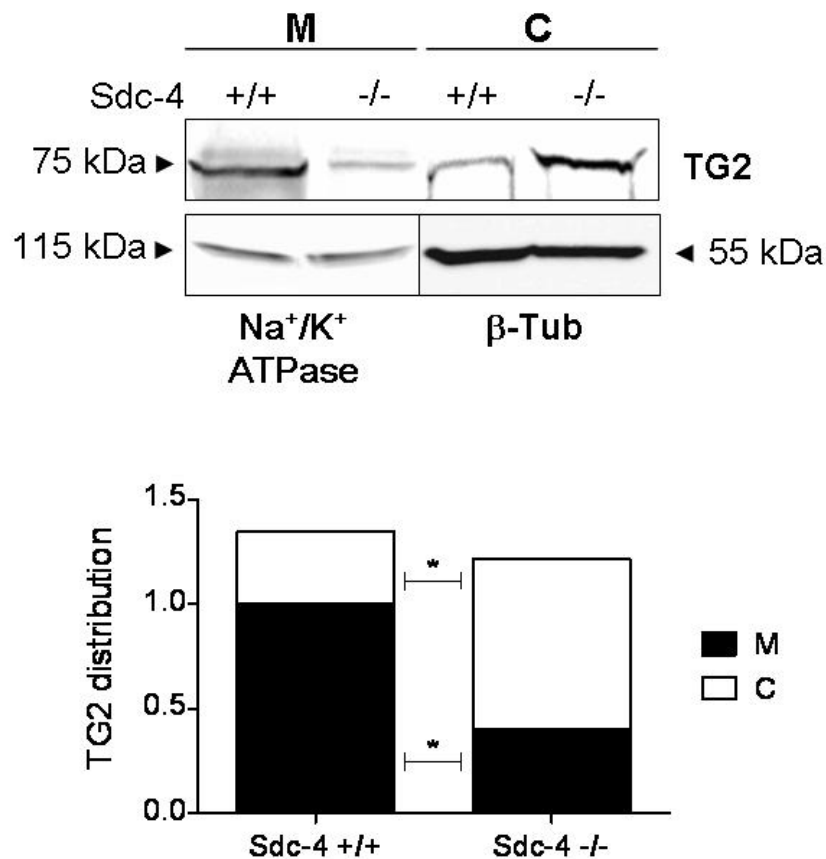


**Figure 5-6 Analysis of TG2 distribution in cell compartments of wild type and Sdc-4 null MDF.** The distribution of TG2 in crude membrane (M) and cytosol (C) of Sdc-4 +/+ and Sdc-4 -/- fibroblasts was analysed by Western blotting. Proteins (50  $\mu$ g) were separated by reducing SDS-PAGE (10% polyacrylamide gel) and immunoblotted with anti-TG2 polyclonal antibody Ab10445. The equilading was verified on a parallel blot of membrane and cytosolic extracts using, respectively, anti Na<sup>+</sup>/K<sup>+</sup> ATPase and anti  $\beta$ -Tubulin ( $\beta$ -Tub). The arrow heads point at TG2 (77 kDa), Na<sup>+</sup>/K<sup>+</sup> ATPase (113 kDa) and  $\beta$ -tub (55 kDa). Densitometric analysis of three independent blots is shown in the histogram below the blots; data were normalised considering Sdc-4 +/+ M equal to 1. \* indicates  $p < 0.05$ . There was no significant difference between the total (M+C) level of TG2 in Sdc-4 +/+ and Sdc-4 -/- cells ( $p > 0.05$ ).

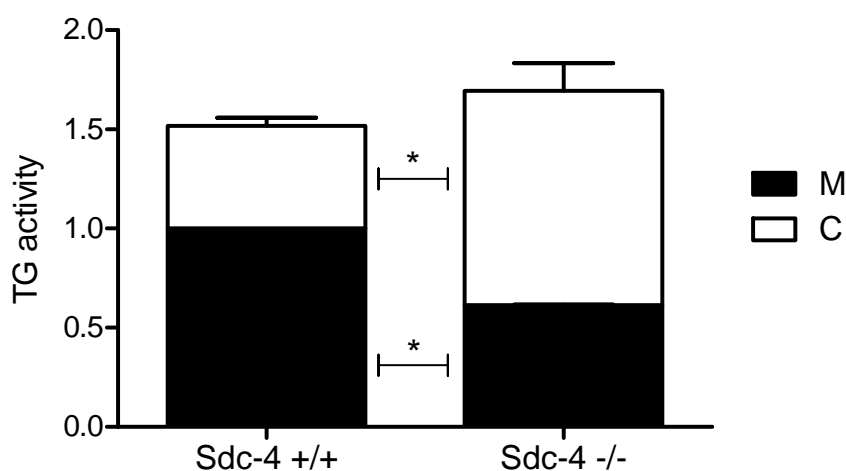


**Figure 5-7 Cellular distribution of TG activity in wild type and Sdc-4 null MDF.** *Sdc-4 +/+* and *Sdc-4 -/-* fibroblasts were fractionated into membrane (M) and cytosolic (C) fractions. TG activity was measured in the cell fractions through incorporation of biotinylated cadaverine into FN. The histogram shows the mean values  $\pm$  SD of three independent experiments performed in triplicate. Data (Abs 450 nm) were normalised considering *Sdc-4 +/+* M fraction equal to 1. \* indicates  $p < 0.05$ . There was no significant difference between the total (M+C) activity level of *Sdc-4 +/+* and *Sdc-4 -/-* cells ( $p > 0.05$ ).

In wild type cells, TG2 activity was predominantly present in the membrane fraction; on the contrary, Sdc-4 null cells exhibited a higher level of TG2 activity in the cytosolic fraction compared to the membrane fraction. Considering the total level of TG activity as the sum of membrane plus cytosol activity, no significant differences were measured between wild type and Sdc-4 null cells ( $p > 0.05$ ) (Figure 5-7). This finding was consistent with the cell distribution of TG2 detected by Western blotting (Figure 5-6). As a further control, the specificity for TG2 of the total TG activity assay used in this study (Balklava et al., 2002) was confirmed by testing cell extracts lacking TG2. The results (Figure 5-8) showed that the  $\text{Ca}^{2+}$ -dependent transamidation was close to zero in TG2 null MEF and was significantly lower than the signal measured in wild type MEF ( $p < 0.01$ ), indicating that the TG activity is predominantly due to TG2.

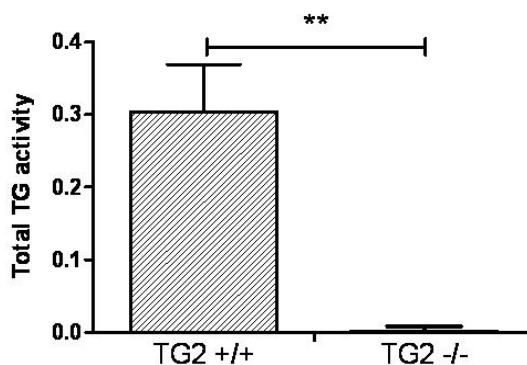


**Figure 5-8 Total TG activity measurement in wild type and TG2 null MEF.** *TG activity was measured on total cell lysates from TG2 +/+ and TG2 null (-/-) MEF. Data presented are the mean values (Abs 450 nm ± SD) of 3 independent experiments performed in triplicates. \*\* indicates  $p < 0.01$ .*

Next, the analysis of TG2 cellular distribution was completed by examining the level of secreted TG2. TG2 is known to be secreted and to bind ECM components, however it is not easily found free in the culture medium (Balklava et al., 2002; Gaudry et al., 1999). Therefore, the level of extracellular TG2 was analysed by using an immunofluorescence-based protocol designed to specifically detect matrix-bound TG2 (Verderio et al., 1998). TG2 was detected by incubating wild type and Sdc-4 null cells with anti-TG2 antibody before cell fixation, as described in the Material and Methods section; the cells were then fixed and the primary antibody was detected by FITC-conjugated secondary antibody. The resulting staining showed a much lower level of matrix TG2 in cells lacking Sdc-4 compared to wild type (Figure 5-9). Quantitative analysis of matrix-TG2 revealed that the difference between wild type and Sdc-4 -/- cells was statistically significant ( $p < 0.01$ ), thus suggesting a role for Sdc-4 in TG2 externalisation.

At this stage, a series of controls on TG2 expression was performed in order to make sure that the differences in TG2 expression/externalisation between wild type and Sdc-4 null cells were due to the presence/absence of Sdc-4 rather than to different TG2 expression in the two cell lines. Firstly, RNA was extracted from wild type and Sdc-4 null cells, retro-transcribed into cDNA and analysed by real-time PCR for the expression of TG2 and



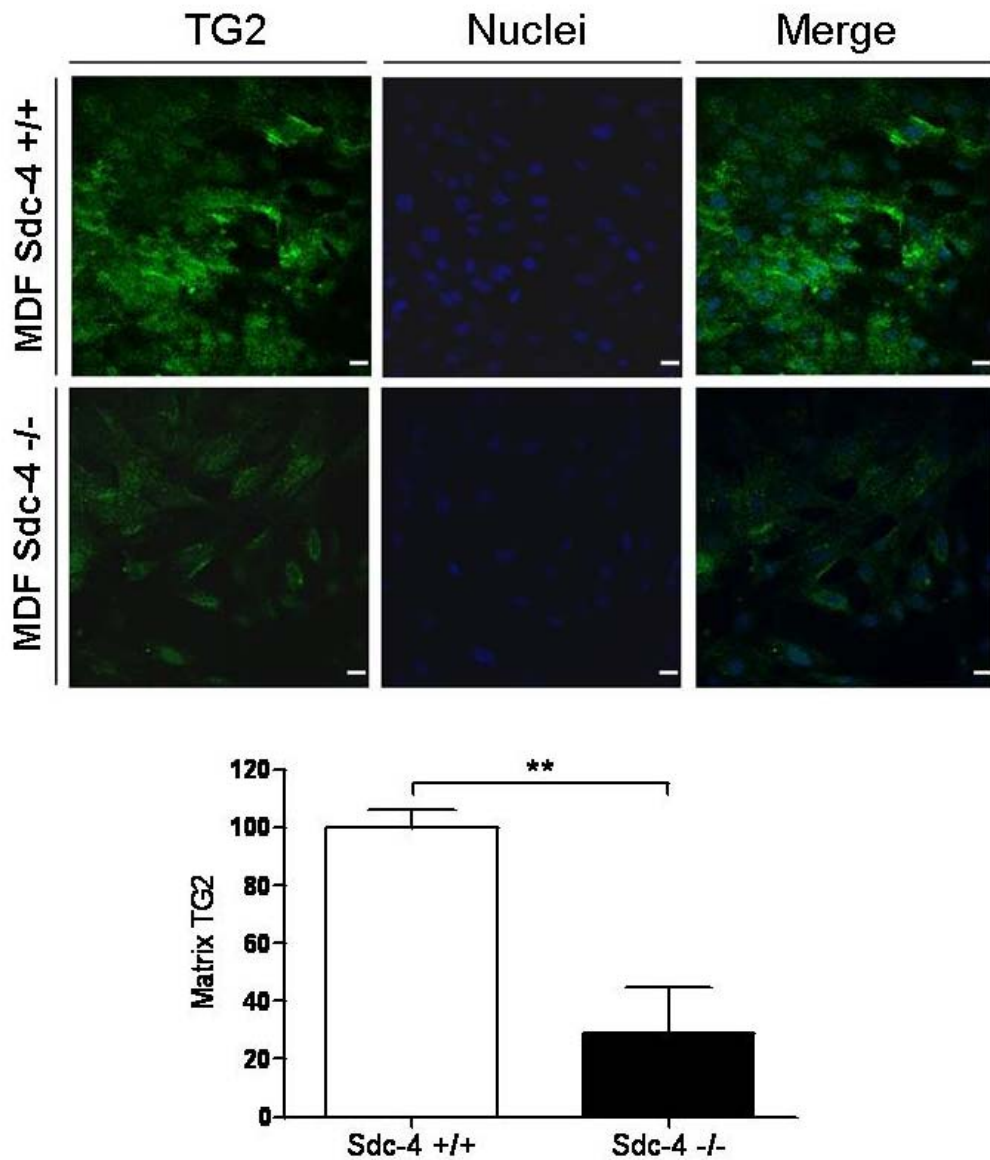


**Figure 5-9 Matrix-TG2 distribution in wild type and Sdc-4 null cells.** *Matrix TG2 was detected in Sdc-4 +/+ and Sdc-4 null -/- MDF by culturing them in the presence of anti-TG2 antibody Cub7402 for 2 hours before cell fixation and incubation with FITC-conjugated secondary antibody. Nuclei were stained with DAPI, The bar indicates 20  $\mu$ m. The average fluorescence of 5 random fields was quantified with Leica TCSNT image processing and represents matrix TG2 signal per number of nuclei; data were normalised considering Sdc-4 +/+ matrix TG2 as 100. n=5. \*\* indicates  $p < 0.01$ .*

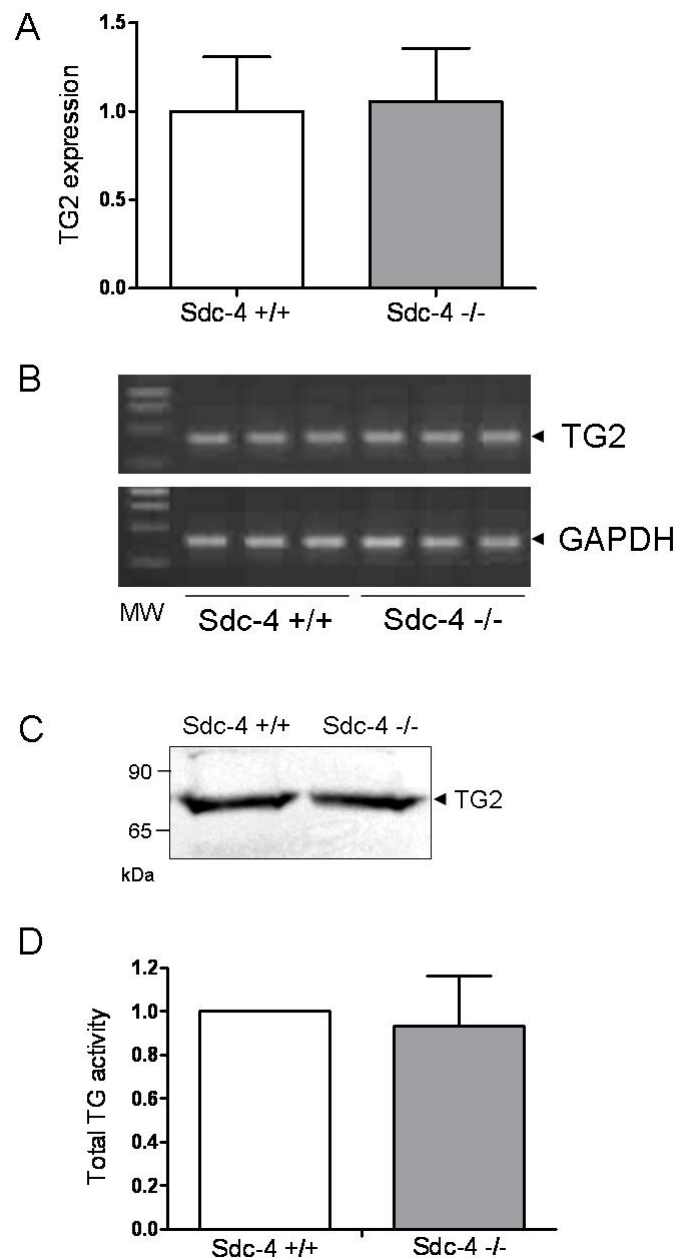


**Figure 5-10 Analysis of TG2 expression in primary fibroblasts.** (A) *TG2* expression was analysed by real time PCR in extracts from *Sdc-4* +/+ and *Sdc-4* -/- MDF; analysis was performed in triplicate. Values presented in the histogram are the mean changes of *TG2* expression versus control *GAPDH* expression ( $2^{-\Delta\Delta C_t}$ ). (B) Real-time PCR products were analysed by gel electrophoresis. MW, 1 kb DNA ladder. (C) Western blot analysis of *TG2* expression in total cell extracts (30  $\mu$ g) from *Sdc-4* +/+ and *Sdc-4* -/- MDF. *TG2* was detected by anti *TG2* antibody Ab10445. (D) *TG* activity was measured in total cell extracts from *Sdc-4* +/+ and *Sdc-4* -/- MDF as incorporation of biotinylated cadaverine into FN. The histogram shows the mean  $\pm$  SD of three independent performed in triplicate; data were normalised considering *Sdc-4* +/+ activity (Abs 450 nm) as 1.

### 5.2.2 Sdc-4 influences TG2 activity at the cell-surface.

The biological significance of the altered TG2 distribution at the cell surface was analysed in terms of TG2 transamidation activity, the main TG2 activity that takes place in the extracellular environment. To test this, the effects caused by interference with the heparan sulphate (HS) chains of HS proteoglycans, in particular those of Sdc-4, were studied. Two different approaches were used to interfere with HS chains, the first was heparitinase digestion, and the second consisted in the cell-treatment with surfen (bis-2-methyl-4-amino-quinolyl-6-carbamide), an antagonist of HS function (Schuksz et al., 2008). To test the consequences of lack of Sdc-4 on TG2 activity, Sdc-4 null MDF were also used.

Measurement of extracellular TG transamidation was carried out by using a previously developed assay involving biotinylated-cadaverine incorporation into FN by whole cells in serum-free culture medium (Jones et al., 1997). The transamidation level of wild type cells was significantly lowered by treating the cells with heparitinase or surfen, indicating that an interference with cell surface HS chains is correlated with a decreased cell-surface TG2 activity (Figure 5-11). The IC<sub>50</sub> value for surfen-mediated cell-surface TG activity inhibition was calculated from the titration curve showed in Figure 5-12, and corresponded to 6.8  $\mu$ M surfen. To rule out an effect of surfen on the transamidation potential of TG2, the activity of purified gpTG2 was tested in the presence of surfen (6 and 12  $\mu$ M). The presence of surfen did not determine a significant change in TG2 transamidation compared to the untreated control ( $p > 0.05$ ) (Figure 5-13). This confirms that the effect on cell-surface TG2 activity is due to surfen antagonism for HS chains function.

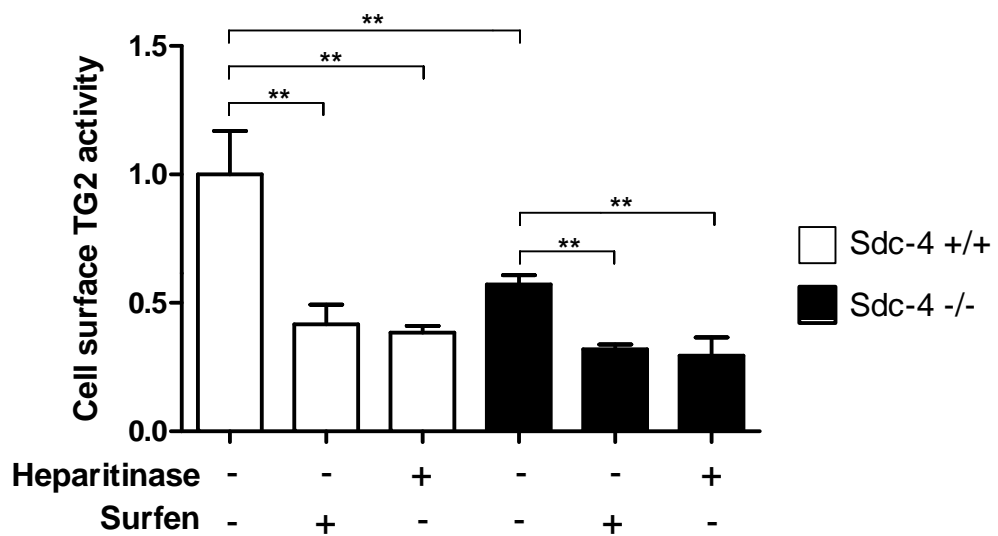


**Figure 5-11 Cell surface HS affect extracellular TG2 activity of MDF adhering on FN.** Cell-surface TG activity was measured in Sdc-4 +/+ and Sdc-4 -/- MDF through the incorporation of BTC into FN. Where indicated, cells were pre-treated with heparitinase (Hep, 30mU/ml), surfen (12  $\mu$ M) or medium only for 1 hour at 37°C; afterwards cells were seeded on FN in the presence of either Hep or surfen. The histogram shows the mean values  $\pm$  SD of 3 independent experiments performed in triplicate; data were normalised considering activity of untreated Sdc-4 +/+ cells as 1. \*\*,  $p < 0.01$ .

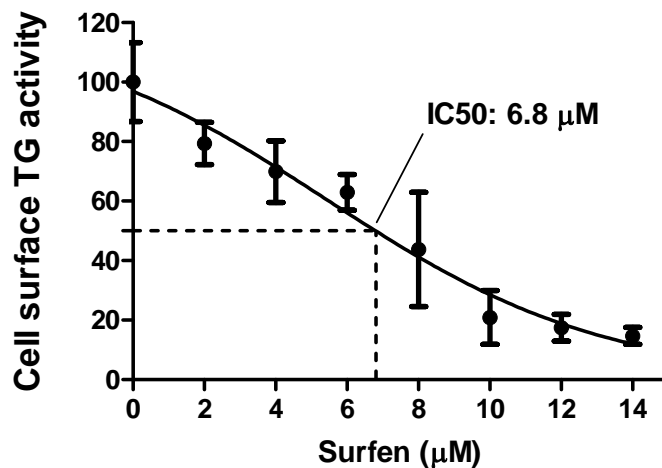


**Figure 5-12 Titration of TG2-activity inhibition by surfen.** Dose response curve of TG2 activity in the presence of increasing concentrations of surfen (1-14  $\mu\text{M}$ ). Cell-surface TG activity of wild type MDF was measured through the incorporation of biotinylated cadaverine into FN. The mean  $\pm$  SD of two independent experiments performed in triplicate is shown; data presented are normalised considering TG activity in the absence of surfen as 100. The calculated IC50 was 6.8  $\mu\text{M}$ .

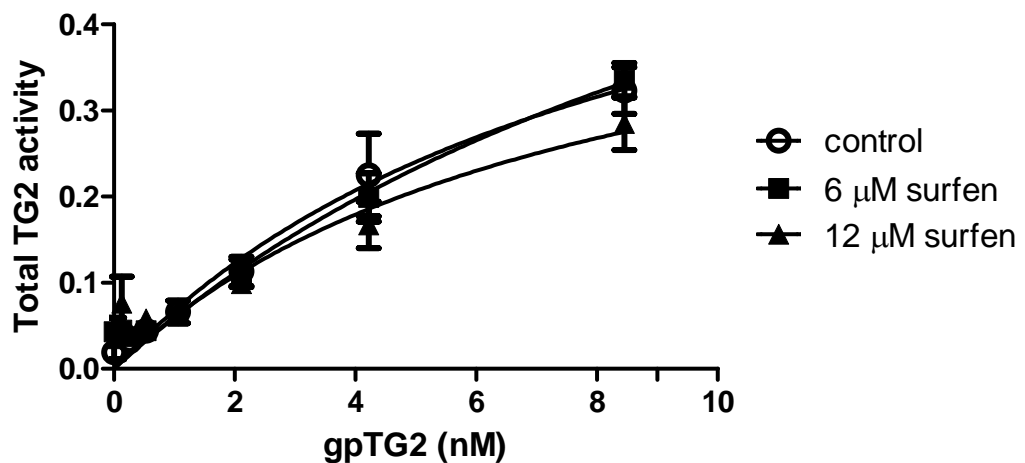


**Figure 5-13 Dose-response curves of TG2 in the presence of surfen.** TG activity of purified gpTG2 (0-8.5 nM) was measured through the incorporation of biotinylated cadaverine into FN in the absence (control) or presence of surfen (6 or 12  $\mu\text{M}$ ). The data shown are the mean Abs 450 nm  $\pm$  SD of three independent experiments performed in triplicate. Differences were not statistically significant ( $p > 0.05$ ).

A significantly lower level of cell-surface TG2 activity was also measured in Sdc-4 null cells compared to wild type ( $p < 0.01$ ) (Figure 5-11). However, as noticed in Figure 5-10, the total level of TG2 expression and activity was unchanged between the two cell lines, thus confirming that the differences noticed on cell-surface activity were not due to different enzyme levels. The treatment of wild type fibroblasts with heparitinase and surfen determined a lower transamidation activity compared to Sdc-4 null cells Figure 5-11. Moreover, interference with HS chains significantly reduced the TG activity of Sdc-4  $-/-$  cells (Figure 5-11). Together, these data indicate that HS are important for the transamidation activity of TG2 at the cell-surface. They also show that even though Sdc-4 appears to be the main player in determining TG2 cell-surface transamidation activity, other HSPG are likely to be involved in TG2 presentation at the cell-surface.

To confirm that the observed changes in TG2 were related to the lack of Sdc-4, a series of add-back experiment was performed. The re-introduction of Sdc-4 in Sdc-4 null cells using pcDNAhS4 determined a total rescue of cell-surface TG2 transamidation (Figure 5-14), which, as noticed for wild type and non transfected Sdc-4 null cells, was significantly reduced by treating the cells with heparitinase or surfen.

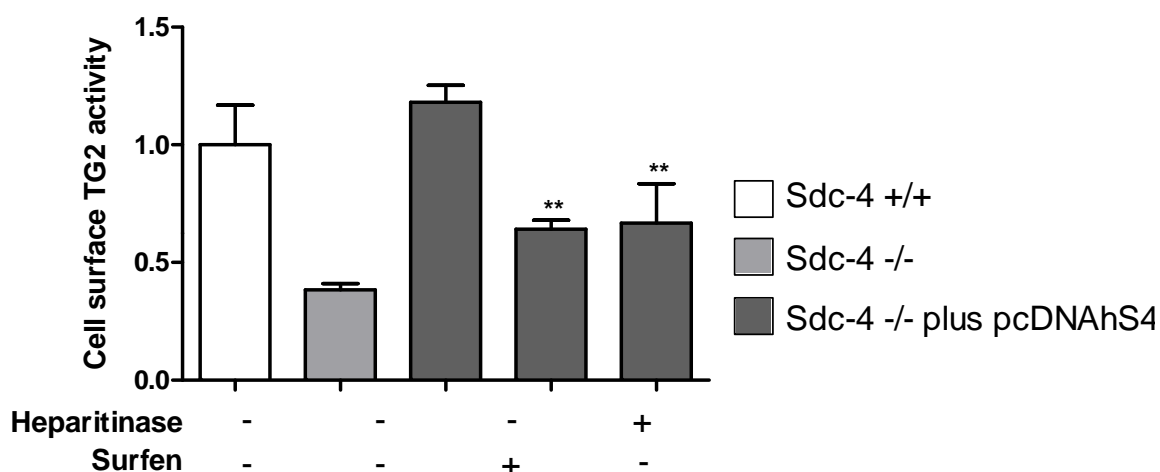


**Figure 5-14 Sdc-4 rescues the level of extracellular TG2 activity in primary fibroblasts.** Cell-surface TG2 activity was measured in Sdc-4  $-/-$  MDF with added back Sdc-4 through transfection with pcDNAhS4; TG2 activity was measured as described in Figure 5-11. Wild type fibroblasts (Sdc-4  $+/+$ ) are shown as a control. The histogram shows the mean values  $\pm$  SD of three independent experiments performed in triplicate; data were normalised considering activity of untreated S4  $+/+$  cells as 1. \*\*,  $p < 0.01$ .

Since the assay used to measure cell-surface transamidation activity is based on the incorporation of biotinylated cadaverine into FN and presupposes cell-FN contacts taking place, the effect of either surfen or lack of Sdc-4 on cell adhesion on FN was tested. This was important to determine if the decreased transamidation was really due to interference with TG2 presentation or simply to a reduced cell-contact with the substrate. For the adhesion assay, cells in suspension were incubated for 1 hour at 37°C in serum-free medium with or without surfen (6 or 12  $\mu$ M). The cells were then seeded onto FN-coated plates for 2 hours as in the cell-surface TG activity protocol (Jones et al., 1997). BSA coated plates were used as negative control for cell adhesion. As shown in Figure 5-, the presence of surfen neither interfered with the level of cell-adhesion on FN, nor with the morphology of adhering cells. Quantitative analysis (Figure 5-, histogram) revealed that there was no significant difference in cell adhesion on FN between wild type and Sdc-4 null cells ( $p>0.05$ ), as well as between untreated wild type cells and cells treated with surfen ( $p>0.05$ ), thus confirming the suitability of the TG2 assay.

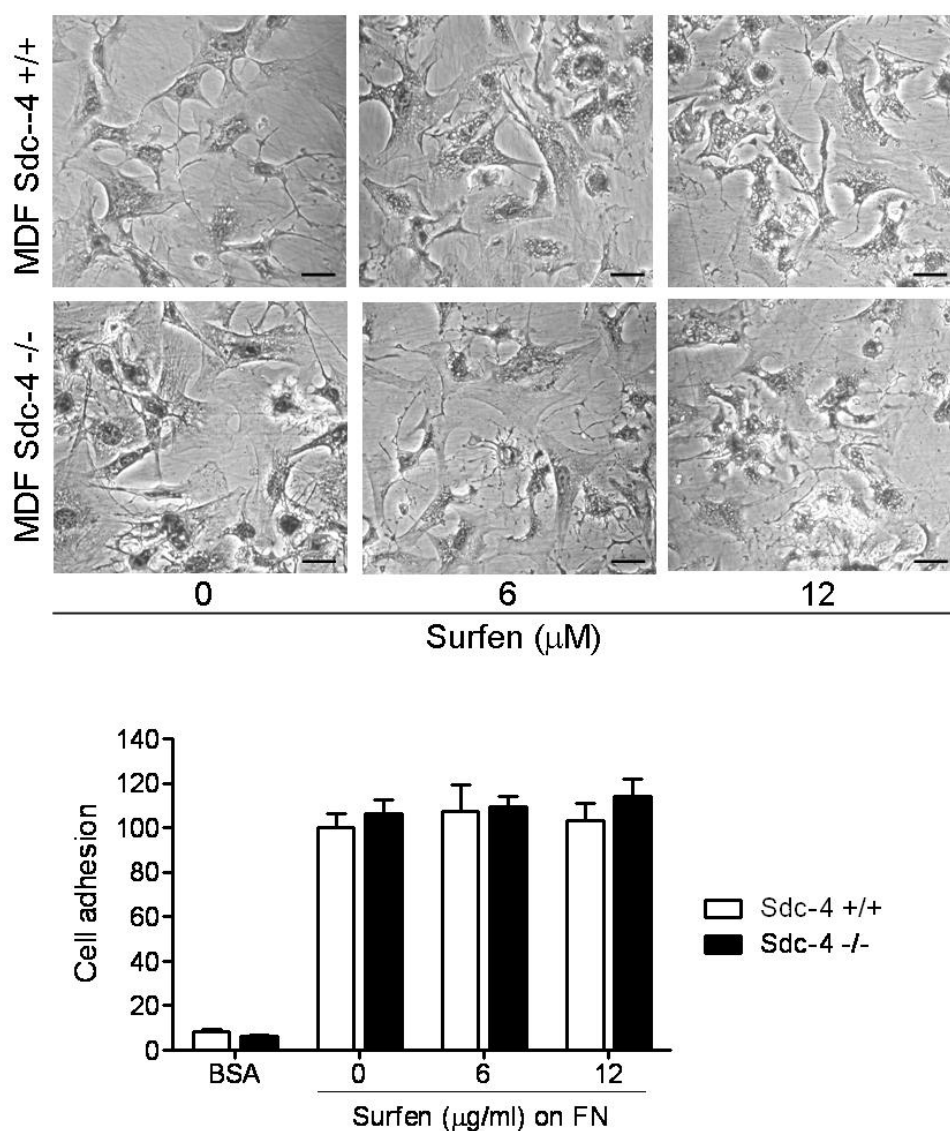


**Figure 5-15 Analysis on surfen effect on cell-adhesion on FN.** *Sdc-4 +/+* or *Sdc-4 -/-* MDF were incubated for 1 hour at 37°C in serum-free medium with surfen (6 or 12 μM) or in serum-free medium only prior to seeding on BSA or FN coated microplates (in the absence or presence of surfen, as indicated). After 2 hours adhesion, cells were stained with crystal violet and cell adhesion was quantified spectrophotometrically after dissolving the attached cells in acetic acid. Absorbance data were normalised considering attachment of *Sdc-4 +/+* cells in the absence of surfen as 100. Values are the mean ± SD of three independent experiments. The bar indicates 20 μm. There was not a significant difference in cell adhesion on FN between untreated and surfen- treated cells ( $p > 0.05$ ).

The extracellular transamidation activity of TG2 was also measured by an *in situ* assay based on the incorporation of FITC-cadaverine into endogenous cellular substrates. The fluorescent substrate permeates the cells, however it has been previously shown to be predominantly incorporated in extracellular substrates, given the high  $\text{Ca}^{2+}/\text{GTP}$  ratio in the extracellular environment (Balklava et al., 2002; Verderio et al., 1998). Cells were incubated for 15 hours in complete serum-containing medium supplemented or not FITC-cadaverine before being fixed and analysed by confocal microscopy. In negative controls, either an active-site inhibitor of TG activity (R283, 200  $\mu\text{M}$ ) (Balklava et al., 2002), or no FITC-cadaverine were added. In Figure 5-16 representative pictures of wild type and Sdc-4 null cells incubated in the different conditions are shown; the fluorescent amine was found to be predominantly cross-linked in cell-matrix glutaminyI substrates and in the pericellular matrix of wild type fibroblasts. Quantification of the average fluorescent signal per cell showed that the absence of Sdc-4 determined a significantly lower level of extracellular TG activity compared to wild type cells ( $p < 0.01$ ) (Figure 5-16). The specificity of TG-mediated incorporation was proven by the almost total inhibition of the reaction by TG inhibitor R283 (Figure 5-16) (Balklava et al., 2002). The specificity of the *in situ* assay for TG2 was tested by using TG2-null MEF as shown in Figure 5-17; no FITC-cadaverine incorporation was detected in TG2 null cells compared to wild type cells.

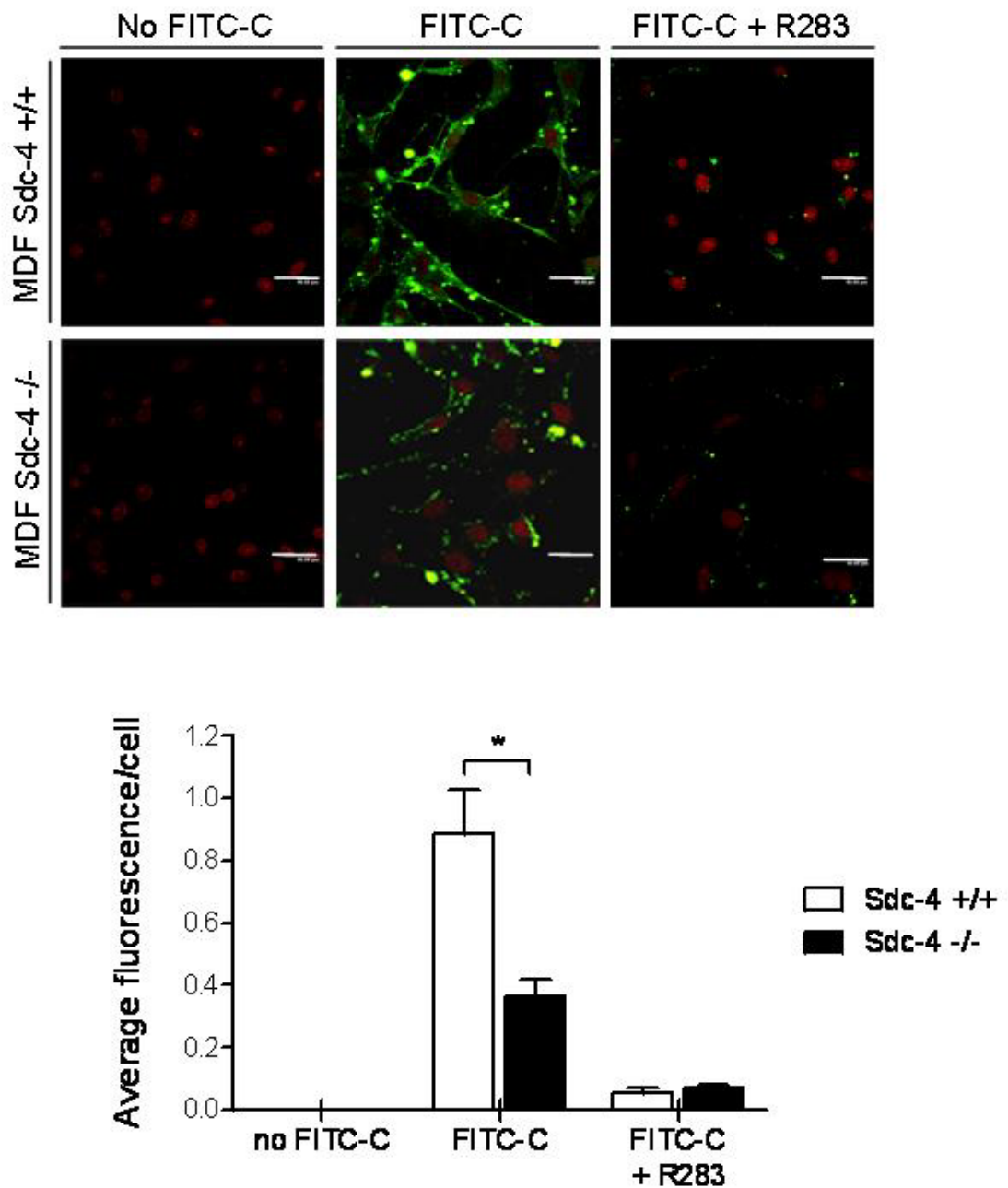


**Figure 5-16** *In situ* measurement of extracellular TG2 activity. *In situ* TG activity of Sdc-4 +/+ and Sdc-4 null -/- MDf was visualised by the incorporation of FITC-labelled cadaverine into endogenous substrates. R283 (200  $\mu$ M), a specific TG inhibitor, was used as a control for the reaction. Nuclei were stained with propidium iodide. The bar indicates 20  $\mu$ m. The average fluorescence/cell of 5 random fields (as those shown in the image) was quantified with Leica TCSNT image processing; data  $\pm$  SD are presented in the histogram. \* indicates  $p < 0.01$ .

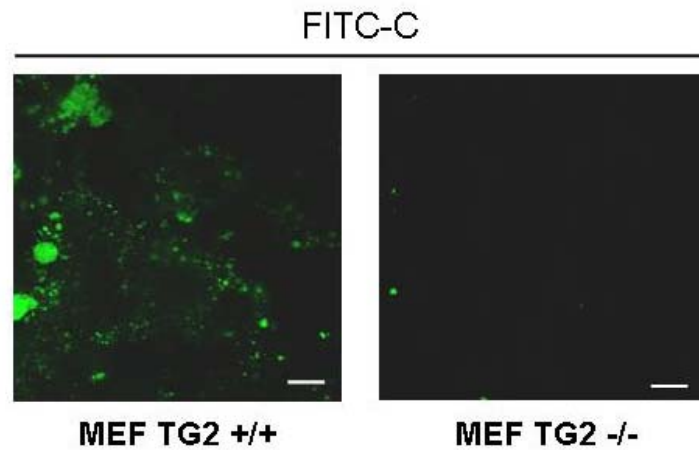


**Figure 5-17 Validation of FITC-cadaverine incorporation as TG2 activity assay for primary fibroblasts.** *In situ TG activity of TG2 +/+ and TG2 -/- MEF was visualised by the incorporation of FITC-labelled cadaverine into endogenous substrates. The bar indicates 20  $\mu$ m.*

At this stage it was important to test whether heparin and HS had a direct effect on TG transamidation activity to investigate whether the effect of HSPG, and in particular that of Sdc-4, was also due to an action on TG2 enzymatic activity. To this purpose, the enzymatic assay was performed on purified TG2 (0-8.5 nM) in the presence of 2.3 or 4.6  $\mu$ M heparin (same concentrations used for the solid-binding assay showed in Chapter 3). The results, shown in Figure 5-18, indicated that at these concentrations heparin does not affect the enzymatic activity of TG2 per se, since no differences were recorded between TG2 assayed with or without the presence of heparin. Therefore, this finding suggests that HS affects the biological activity of TG2 indirectly by altering its cell-surface localisation.

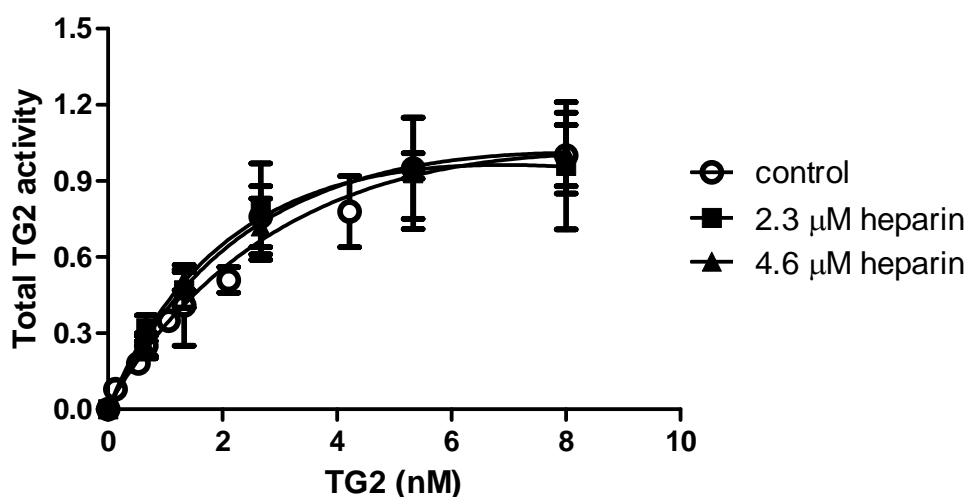


**Figure 5-18 Study of heparin-binding effect on TG2 activity.** TG activity of purified TG2 (0-8.5 nM) was measured through the incorporation of biotinylated cadaverine into FN in the absence (control) or presence of heparin (2.3 or 4.6  $\mu$ M). The data shown are the mean Abs 450 nm  $\pm$  SD of three independent experiments performed in triplicate. Differences were not statistically significant ( $p > 0.05$ ).

### 5.3 Discussion

The experiments presented in this chapter were aimed to investigate the role of Sdc-4 on the cell-surface trafficking of TG2 in primary fibroblasts.

The physical association of TG2 and Sdc-4 at the cell surface was confirmed by co-staining of the two molecules in large peripheral cell-matrix adhesions. These structures, which determine the cell shape, have been reported by Longley et al. (1999) and Zamir and Geiger (2001). The absence of Sdc-4 determined a drastic reduction of the amount of TG2 present at these cell-surface structures, and a parallel accumulation of TG2 in the cytosol. Interestingly, when the staining was performed on cells adhering on FN, the patches corresponding to TG2 staining became larger, as if the TG2 was externalised from these cell-matrix contacts. Western blot analysis and TG2 activity assays performed on membrane and cytosolic fractions confirmed that in the absence of Sdc-4 TG2 is mostly retained intracellularly. This finding suggests a possible role for Sdc-4 in the cell-surface trafficking of TG2 and it is supported by the observation that heparin/HS does not influence the Ca<sup>2+</sup>-dependent transamidation activity of purified TG2.

The results of the previous chapter showed a direct interaction of TG2 and Sdc-4 mediated by the HS chains of Sdc-4. The results of this chapter support this data, as lack of Sdc-4 is shown to lower cell-surface TG2, which is rescued by adding back Sdc-4. However, since perturbation of all cell-surface HS chains by either heparitinase or surfen (Schuksz et al., 2008), determined an even lower cell surface activity in Sdc-4 null cells, it is possible that Sdc-4 may not be the only HSPG receptor involved in the trafficking of TG2. A possible candidate for this role is Sdc-2, the Sdc family member with the highest expression at cell-matrix contact points in fibroblasts (David et al., 1992; David, 1993).

The role of HSPG in the externalization of unconventionally secreted proteins has been suggested and HSPG are essential factors in the export of FGF-2, (Zehe et al., 2006). It is therefore possible that the HS chains of Sdc-4 and other HSPG may be involved in the externalization of TG2 in a similar way.

However, HS are also involved in endocytosis of extracellular components (MacArthur et al., 2007), therefore they could affect the cell-surface trafficking of TG2 influencing its internalization. This possibility is particularly intriguing, since Zemskov and colleagues

(2007) have demonstrated that internalization of TG2 requires the endocytic receptor LRP1, and this receptor has been shown to act in concert with HSPG (Mahley and Ji, 1999). Although the possible double action of HSPG receptors in externalization and internalization of TG2 can not be excluded, even though the model used for the investigation presented in this thesis (Sdc-4 null cells) is not adequate to clarify the effect of lack of Sdc-4 in TG2 internalisation since these cells are not able to externalize TG2.

In conclusion, this study has shown for the first time that cell-surface HSPG like Sdc-4 influence the activity of extracellular TG2 by driving its location at cell-matrix adhesions.

## ***Chapter 6: Physiological significance of Transglutaminase-2 binding to Syndecan-4 in kidney fibrosis***

### ***6.1 Introduction***

#### **6.1.1 TG2 and kidney fibrosis**

Since kidneys are organs constantly subjected to injuries, they are regarded a good model for studying wound repair. There are several factors responsible for kidney insults, such as drugs, dietary compounds, environmental factors and diseases. Under normal conditions the repair processes take place without being noticed, but when the insult becomes chronic (eg glomerulosclerosis, diabetic nephropathy) or the repair process is aberrant, the diseased condition becomes evident (El Nahas et al., 1997; Verderio et al., 2004). This abnormal state is characterized by a continuous remodelling process, which leads to kidney scarring and fibrosis and carries on until the kidney loses functionality. In particular, a non-resolving inflammatory response takes place, together with fibroblasts proliferation and over expression/accumulation of ECM components, leading to loss of functionality and destruction of the kidney (Johnson et al., 2002; Johnson et al., 2003; Johnson et al., 1997). Despite being the main factor in determining renal failure, the matrix accumulation and the changes in cells-ECM interaction typical of this process are only partially understood and their improved understanding would support the development of new selective therapies.

Experimental studies on the association of TG2 with progressive kidney fibrosis have shown a considerable increase in TG2 expression and externalisation. Extracellularly, given the high  $\text{Ca}^{2+}$  and low GTP/GDP concentrations, TG2 catalyses the formation of  $\epsilon$ -( $\gamma$ -glutamyl) lysine crosslinks, characteristic of kidney fibrosis (El Nahas et al., 2004; Johnson et al., 1997; Johnson et al., 1999). It is possible to distinguish different stages in the development of renal conditions where TG2 is involved. In the initial stage, there is an increased level of TG-mediated cross-links in the expanding ECM; this process seems to be correlated with either the externalisation of existing TG2, or to the involvement of other members of the TG family, since the overall renal TG level remains constant (Skill et al., 2001). With the progression of the disease state, TG2 levels increase in tubular epithelial and mesangial cells (El Nahas et al., 2004; Johnson et al., 2004; Johnson et al., 2003). This new pool of TG2 is released in the ECM, where it further contributes to the crosslinking of

ECM proteins. In vitro studies have shown a marked reduction in matrix accumulation when TG2 activity is blocked, thus confirming the direct role of the enzyme on the development of fibrotic diseases (Skill et al., 2004). As a consequence, understanding of the regulation of TG2 externalisation and activity is important in the development of an effective therapy against kidney fibrosis.

### **6.1.2 Sdc-4 and renal diseases**

The role played by Sdc-4 in the regulation of cell-matrix interactions and the variety of ligands that the HS chains can bind, determine the involvement of Sdc-4 in several types of diseases. In particular, given the high expression of Sdc-4 in kidney, compared to other tissues/organs, its role in the development of renal diseases is of particular interest. Kidneys isolated from Sdc-4 deficient mice are functionally and structurally normal (Ishiguro et al., 2000), but they react differently from wild type kidneys if exposed to artificial stress or diseases. For example, induction of obstructive nephropathy via intraperitoneal injection of  $\kappa$ -carrageenan (polysaccharide which accumulates in the collecting ducts) leads to high mortality in Sdc-4 null mice but not in wild type mice (Ishiguro et al., 2001). Kidneys from Sdc-4  $-/-$  mice injected with  $\kappa$ -carrageenan showed a high level of dilation of the renal tubules and of the inner medulla, where the compound was accumulated and determined obstruction of the collecting ducts. This obstruction led to high level of blood urea nitrogen in Sdc-4  $-/-$  mice, which was responsible of the higher mortality compared to wild type animals. It has been suggested a role for Sdc-4 in preventing carrageenan accumulation in the collecting ducts, but the mechanism behind it is still unknown.

It has been demonstrated that Sdc-4 is up-regulated in progressive proliferative kidney diseases, such as IgA nephropathy, but not in non-proliferative diseases such as thin-membrane nephropathy (Yung et al., 2001). Sdc-4 was increased at both the mRNA and protein level, and interestingly, there was a correlated up-regulation of microfilament-associated proteins such as vinculin,  $\alpha$ -actinin and paxillin. These proteins, in particular  $\alpha$ -actinin, have been shown to form stable complexes with Sdc-4 in vitro, thus suggesting a possible role for Sdc-4 in cytoskeletal reorganisation which occurs during the development of proliferative diseases (Yung et al., 2001).

As reported in paragraph 6.1.1, TGF $\beta$ 1 is an important factor in the wound healing process and fibrotic response, and TG2 plays a role in the regulation of TGF $\beta$ 1 activation (Nunes et al., 1997; Telci et al., 2009; Verderio et al., 1999). Sdc-4 has been shown to be an essential factor in mediating cytoskeletal re-organisation in response to TGF $\beta$ 1 (Chen et al., 2005). These data, together with the *in vitro* evidence of the essential role of cell surface HS for TG2-mediated RGD-independent cell adhesion (Verderio et al., 2003) suggest a possible connection between TG2 (which is also over-expressed in kidney fibrosis) and Sdc-4 signalling in the development of fibrotic diseases.

### 6.1.3 TG2 and HSPG in kidney fibrosis

Chronic kidney diseases lead to kidney fibrosis, characterised by accumulation of ECM components, fibroblasts proliferation and tubular atrophy (Johnson et al., 2003; Johnson et al., 1997); this process ultimately determines kidney failure. TG2, which has a high expression level in several kidney cell types (tubular epithelial cells and mesangial cells) plays an important role in the development of kidney fibrosis, as demonstrated by *in vivo* studies on experimental renal scarring models (Johnson et al., 1999). TG2 involvement in kidney fibrosis requires externalisation and translocation to the ECM, and it has been demonstrated that the level of extracellular TG2 is significantly increased in biopsies from fibrotic kidneys (Johnson et al., 2003). However, it is still unclear how TG2 is translocated to the cell-surface and ECM, as previously mentioned (Chapter 1, paragraph 1.2.9.6.3). In the previous chapters new evidence have been provided for the high affinity of TG2 and cell-surface HSPG *in vitro*, which has a significant impact on cell-surface trafficking of TG2. Therefore, HSPG may act as modulators of TG2 extracellular functions also *in vivo*.

HSPG are key components of the tubular basement membrane and play an essential role for the proliferation of renal fibroblasts by facilitating the interaction of FGF with its cell-surface receptor (Clayton et al., 2001). Moreover, cell-surface HSPG have been shown to participate to the unconventional mechanism of FGF translocation through the plasma membrane, mediated by FGF binding of HS chains of the receptors (Zehe et al., 2006). HSPG are upregulated in chronic kidney diseases characterised by tissue fibrosis (Fisher et al., 2009). These cell surface receptors have been implicated in kidney fibrosis by creating gradients of pro-fibrotic factors. Given the length and flexibility of their HS chains they

could also present the bound pro-fibrotic factors to cell types that do not secrete them, thus amplifying the response of those HS-binding molecules.

The results presented in this thesis so far have highlighted a role for Sdc-4 in the regulation of cell-surface TG2 localisation and biological activity. Given the importance of TG2 activity as a pro-fibrotic factor in the establishment of scarring and fibrosis, the analysis of the co-operation between Sdc-4 and TG2 was investigated *in vivo*. Unilateral ureteral obstruction (UUO) was used as an experimental model of kidney fibrosis, firstly to assess the role of Sdc-4 in the development of kidney fibrotic disease, and secondly to investigate whether TG2 and Sdc-4 cooperate in this process.

## 6.2 Materials and Methods

### 6.2.1 Experiment design

The minimum number of animals to use for the in vivo study was determined using an online power calculator (<http://www.stat.ubc.ca/~rollin/stats/ssize/n2.html>). The parameters used for the algorithm ( $\mu$  78 vs 36,  $\sigma$  19, Power 0.99,  $\alpha$  0.05) were derived from a previous study on the effect of lack of TG2 in unilateral ureteral obstruction (UUO) development (Mohammed et al., 2006). The power calculator returned a value of 8, for that reason 8 or more (wild type or Sdc- null) animals were chosen for each time point considered as shown in Table 6-1. Both kidneys from control animals (untreated) were analysed. UUO was typically induced in the left kidney and the right kidney from animals with UUO induction was also analysed (it is indicated as untreated kidney in UUO).

Time point	Sdc-4 +/+ control	Sdc-4 +/+ UUO	Sdc-4 -/- control	Sdc-4 -/- UUO
7 days	8	8	10	8
14 days	8	8	8	10
21 days	8	8	8	10

**Table 6-1 Experimental design for in vivo study on Sdc-4 and TG2 contribution to kidney fibrosis.** *The table shows the number of animals used in every experimental group.*

### 6.2.2 Induction of UUO

Experimental unilateral ureteric obstruction (UUO) was performed by the Department of Histopathology, Northern General Hospital (Sheffield) in wild type and Sdc-4 -/- mice (Ishiguro et al. 5249-52). Anaesthesia was induced with 5% fluorothane and maintained by 2% fluorothane during all the surgical process. The procedure consisted in the ligation of the left ureter of each animal with a legating clip (Hemoclip Plus, Weck Closure Systems), which was placed one-third of the way down the ureter from the pole of the kidney (Ophascharoensuk et al., 1998). The peritoneum was flooded with ADEPT (4 % Icodextrin solution), in order to prevent post-surgical adhesions prior to closing. The muscle wall was closed with single cross-over stitching using dissolvable stitches. After UUO was

performed, all mice were provided with Buprenorphine (10 mg/kg) for 40 hours for analgesic purpose. The mice were allowed to recover and were given free access to food and water. At days 7, 14 and 21, the kidneys ( $n \geq 8$ ) were retrieved, weighed and then sectioned into four equal parts to be used for the different analytical techniques. All procedures were carried out under license according to regulations laid down by Her Majesty's Government, United Kingdom (Animals Scientific Procedures Act, 1986).

### **6.2.3 Preparation of kidney paraffin sections**

Paraffin sections were prepared by the Department of Histopathology, Northern General Hospital (Sheffield). Kidneys were fixed in neutral buffered formalin then embedded in paraffin and, after solidification, cut at a thickness of 4  $\mu\text{m}$ .

### **6.2.4 Preparation of kidney cryosections**

Cryosections were prepared from kidney tissues stored in liquid  $\text{N}_2$ . Tissues were mounted on tissue holders using Tissue-Tek O.C.T.<sup>TM</sup>, a compound made of water soluble glycols and resins, providing an excellent specimen for cryostat sectioning at temperatures  $\leq -10^\circ\text{C}$ . After embedding, the tissues were placed inside the cryostat, at a temperature of  $-16^\circ\text{C}$ , for 20 minutes, in order for the embedding resin to solidify completely and for the tissue to reach the same temperature of the cryostat chamber. After that, 14 mm thick sections were cut and, with the help of a fine brush, placed on Superfrost<sup>®</sup> Plus microscope slides, suitable for tissue staining procedures and microscopy. Cryosections were immediately used for in situ enzymatic activity assay (6.2.8).

### **6.2.5 Masson's trichrome staining on kidney tissues**

Masson's trichrome staining was performed by the Department of Histopathology, Northern General Hospital (Sheffield) to stain in blue/green any collagen present and in red/pink nuclei, fibers, erythrocytes and elastin. Paraffin sections were de-waxed in xylene for 10 minutes, serially re-hydrated in 100%, 95% and 75% (v/v) ethanol, and then washed in distilled water prior to staining in Weigert's iron hematoxylin working solution [0.5% (w/v) hematoxylin, 47.5% (v/v) ethanol, 0.6% (w/v) ferric chloride, 0.5% (v/v) concentrated hydrochloric acid] for 10 minutes. Sections were rinsed in distilled water, stained in Biebrich scarlet-acid fuchsin solution [0.9% (w/v) biebrich scarlet, 0.1% (w/v)

### **6.2.6 Multiphase image analysis**

Multiphase analysis consents to quantify the percentage of coverage of a specific colour in a specific image. The analysis was performed using Analysis™ 3.2 software (Soft Imaging Systems, Germany), considering 10 images of non overlapping regions for each kidney sample. For each image, a distinct phase was allocated to a defined colour shade, representing a specific component of the tissue (i.e. one phase was representative of the blue/green colour of collagen after Masson's Trichrome staining). The phases were allocated in order to have a minimum total phase coverage of 95%.

### **6.2.7 Measurement of Hydroxyproline by Amino Acid Analyser.**

Kidney tissue was homogenised in four times its volume of homogenising buffer (50 mM Tris HCl, pH 7.4 containing 0.25 M sucrose, 10 mM EDTA and proteases inhibitor cocktail) using a motor-driven pellet pestle (Sigma Aldrich). Total proteins were assessed as described in Chapter 2 (section 2.2.5.3) after dissolving 10 µl of the homogenate in 10 µl homogenation buffer supplemented with 0.2% (w/v) SDS in order to solubilise all the proteins present. 1.4 mg of proteins from the homogenate were hydrolysed in 1.5 ml of 6M HCl at 110°C for 18 hours. The samples were then freeze-dried for 8 hours and resuspended in 200 µl lithium citrate loading buffer (0.2 M, pH 2.2) for amino acid analysis. 40 ml of the preparation were loaded onto a Biochrom30 Amino Acid Analyser (available at Sheffield University) using a partial fill loop. The fractionation was performed using 96361 LiHP control program and analysis package, and the readings of Ninhydrin derivatised peaks at 440nm were recorded. The estimated hydroxyproline

concentration in the volume loaded was calculated by reference to the 10 nmol/20  $\mu$ l Biochrom calibration standard.

### 6.2.8 Detection of *in situ* TG activity in kidney tissues

Determination of *in situ* TG activity was performed on kidney cryosections with a thickness of 14  $\mu$ m. Unfixed sections were rehydrated in reconstitution buffer [5% (v/v) donkey serum; 10 mM EDTA; 0.1 (v/v) Triton X-100 in 50 mM Tris-HCl, pH 7.4 containing protease inhibitor cocktail] for 30 minutes at room temperature, then washed twice with washing buffer [10 mM EDTA in PBS containing protease inhibitor cocktail]. Kidney sections were incubated for 1 hour at 37°C in reaction buffer containing the TG substrate Texas Red cadaverine [5 mM CaCl<sub>2</sub>; 5 mM DTT, 0.1 mM Texas Red cadaverine in 50 mM Tris-HCl, pH 7.4 containing protease inhibitor cocktail]. The TexasRed fluorochrome was specifically chosen instead of FITC used in the original protocol, which emits at a frequency similar to the auto-fluorescence of kidney tissue. In negative controls, 10 mM EDTA was used instead of 5 mM CaCl<sub>2</sub> in the reaction buffer. After the incubation, sections were washed 3 times with washing buffer, fixed in ice cold acetone for 5 minutes at -20°C and air dried. Slides were mounted with Vectashield fluorescence mounting media and visualised using Leica TCS-NT confocal microscope. The level of TG *in situ* activity was determined subtracting the fluorescence level of negative control (10 mM EDTA) to the level of samples containing CaCl<sub>2</sub>. Non overlapping fields of the same size were quantified for each kidney sample using the Leica confocal image analysis software. Data were expressed as TexasRed emission versus auto-fluorescent emission.

## 6.3 Results

### 6.3.1 Lack of Sdc- is protective against the development of kidney fibrosis

Impaired kidney function results from remodelling in the kidney and excess ECM deposition, leading to renal fibrosis. Wild type and Sdc-4 null mice were subjected to UUO as described in section 6.2.2. Masson's trichrome staining was used to assess the overall level of scarring in normal and fibrotic kidney tissue harvested at 7, 14 and 21 days after the induction of UUO. The scarring level, represented by accumulation of collagen (blue staining), was quantified by using multiphase image analysis, as described in section 6.2.6; for each sample the scarring index was expressed as the average ratio of blue signal to red signal (non collagen staining) in order to correct the values for the area of tissue analysed.

As shown in Figure 6-1 normal kidney sections from both wt and Sdc-4  $-/-$  mice showed almost absence of blue/green colour and a tight association of tubules (index of renal functionality) in the cortical region of the kidneys. No differences were registered in the scarring level, with a measured value of  $0.015 \pm 0.004$  for Sdc-4  $+/+$  and  $0.016 \pm 0.006$  for Sdc-4  $-/-$  kidneys (Figure 6-2). There was a progressive accumulation of tubulo-interstitial collagen in both Sdc-4  $+/+$  and Sdc-4  $-/-$  kidneys after the induction of UUO, reaching the maximum level at 21 days post UUO induction. The induced fibrosis also disrupted the association of tubules, with the creation of gaps among them filled by ECM components. Starting from day 7 after UUO induction, it was possible to detect collagen deposition in the tubulointerstitial space and in the area surrounding the glomeruli (Bowman's capsule) in kidneys from wild type mice. At the same time point, sections taken from Sdc-4  $-/-$  mice showed a significantly lower amount of collagen deposition compared to the sections from wild type mice ( $p < 0.05$ ), and the association between the tubules did not appear to be altered. The scarring index was  $0.117 \pm 0.059$  for the wild type and  $0.030 \pm 0.012$  for the Sdc-4 null kidneys (Figure 6-2).

At 14 days after the induction of UUO the blue signal indicating collagen deposition was more diffused compared to the previous time point in wild type cells ( $0.221 \pm 0.081$ ), and the association between tubules also started to be compromised (Figure 6-1). The scarring index was also increased in Sdc-4  $-/-$  kidney tissues ( $0.133 \pm 0.058$ ), but in these samples the tubular structure was maintained. Even though wild type kidneys displayed a higher

The trend observed after 21 days of UUO was consistent with what observed at the previous time points, with a higher level of collagen deposition in wild type kidneys compared to Sdc-4 <sup>-/-</sup> kidneys (Figure 6-1). At this time point the structure of Sdc-4 null kidneys was also altered, with an accumulation of blue-stained collagen in the tubulo-interstitial space compromising the contact between tubules. The scarring index values calculated at 21 days were  $0.3167 \pm 0.171$  for Sdc-4 <sup>+/+</sup> tissues and  $0.133 \pm 0.087$  for Sdc-4 <sup>-/-</sup> tissues ( $p < 0.05$ ).

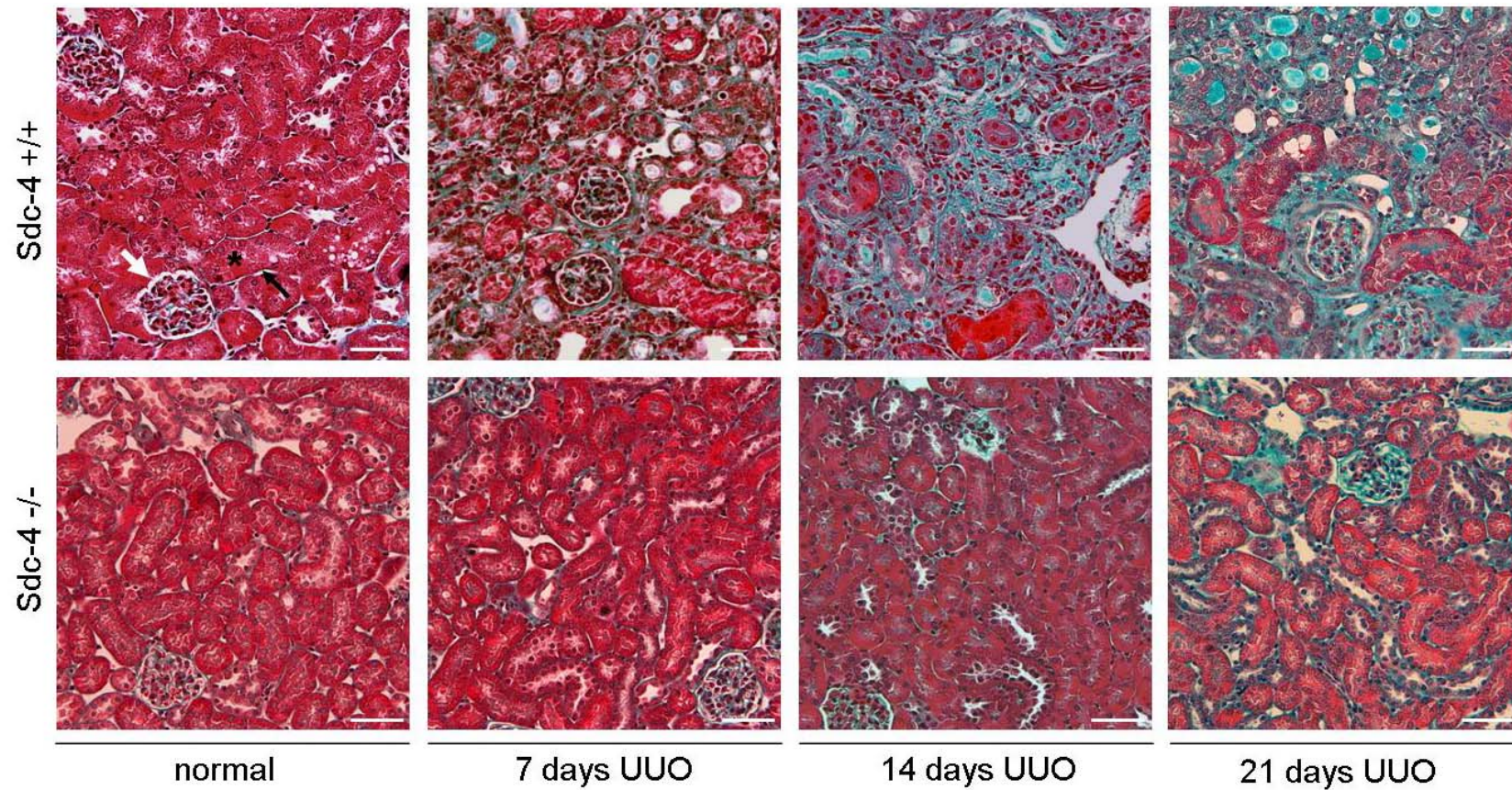


**Figure 6-1 Extracellular matrix accumulation after induction of kidney fibrosis-Masson's Trichrome staining.** *Paraffin sections from normal and UUO (7, 14 and 21 days) kidneys from Sdc-4 +/+ and Sdc-4 -/- mice were stained to evaluate renal scarring. Collagen is stained in blue/green; nuclei, fibers and elastin in red/pink. White arrow: glomerulus; asterisk: tubular lumen; black arrow: peritubular space. The bar indicates 50  $\mu$ m.*

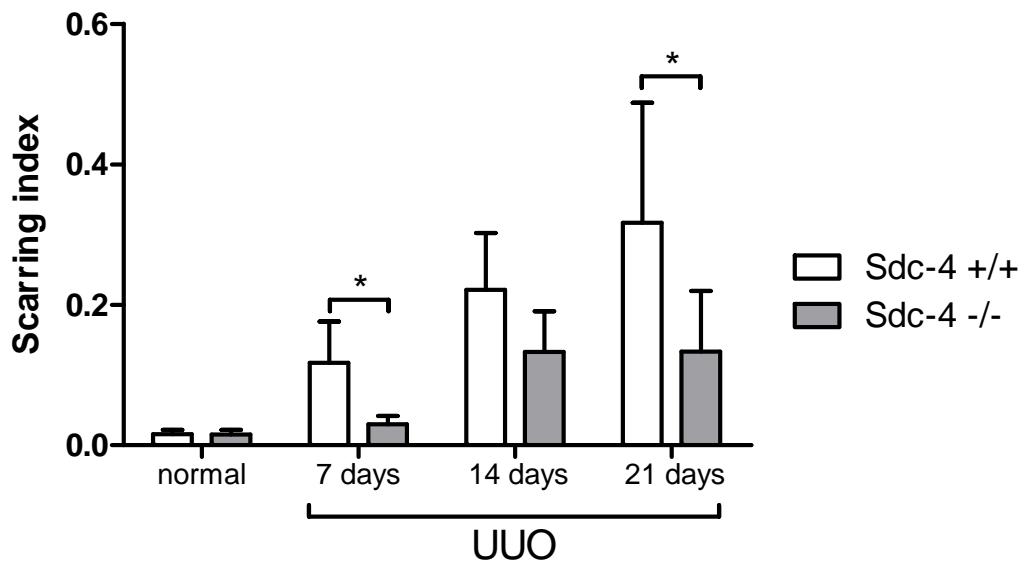


**Figure 6-2 Quantification of scarring index in normal and fibrotic (UUO) kidneys.**

The data represent the average values obtained from multiphase analysis of 4 to 10 kidneys from *Sdc-4 +/+* and *Sdc-4 -/-* mice at 7, 14 and 21 days after UUO induction; scarring index of normal kidneys is shown as a control. 10 images taken from non-overlapping fields were analysed for each kidney sample. Average scarring index  $\pm$  SD is shown. \* indicates  $p \leq 0.05$ . Normal kidneys,  $n=48$ . UUO kidneys,  $n=8$ .

To have a clearer idea of the localisation of the collagen staining, kidney sections were analysed at 400X magnification and separate pictures were taken for proximal tubules and glomeruli. Figure 6-3 displays collagen accumulation in the proximal tubules of the kidney cortex. It is possible to see that, with the progression of the disease, there is an expansion of the matrix surrounding the tubules, with a loss of the compact structure observed in normal tissue. As presented in Figure 6-1, the blue staining appeared to be higher in wild type kidneys compared to *Sdc-4 -/-*. A similar analysis was performed on the glomeruli, the functional units of the kidney (Figure 6-4). A progressive collagen accumulation is evident in the space surrounding the glomerulus (Bowman's capsule), indicating glomerulosclerosis, characteristic of renal fibrotic diseases.

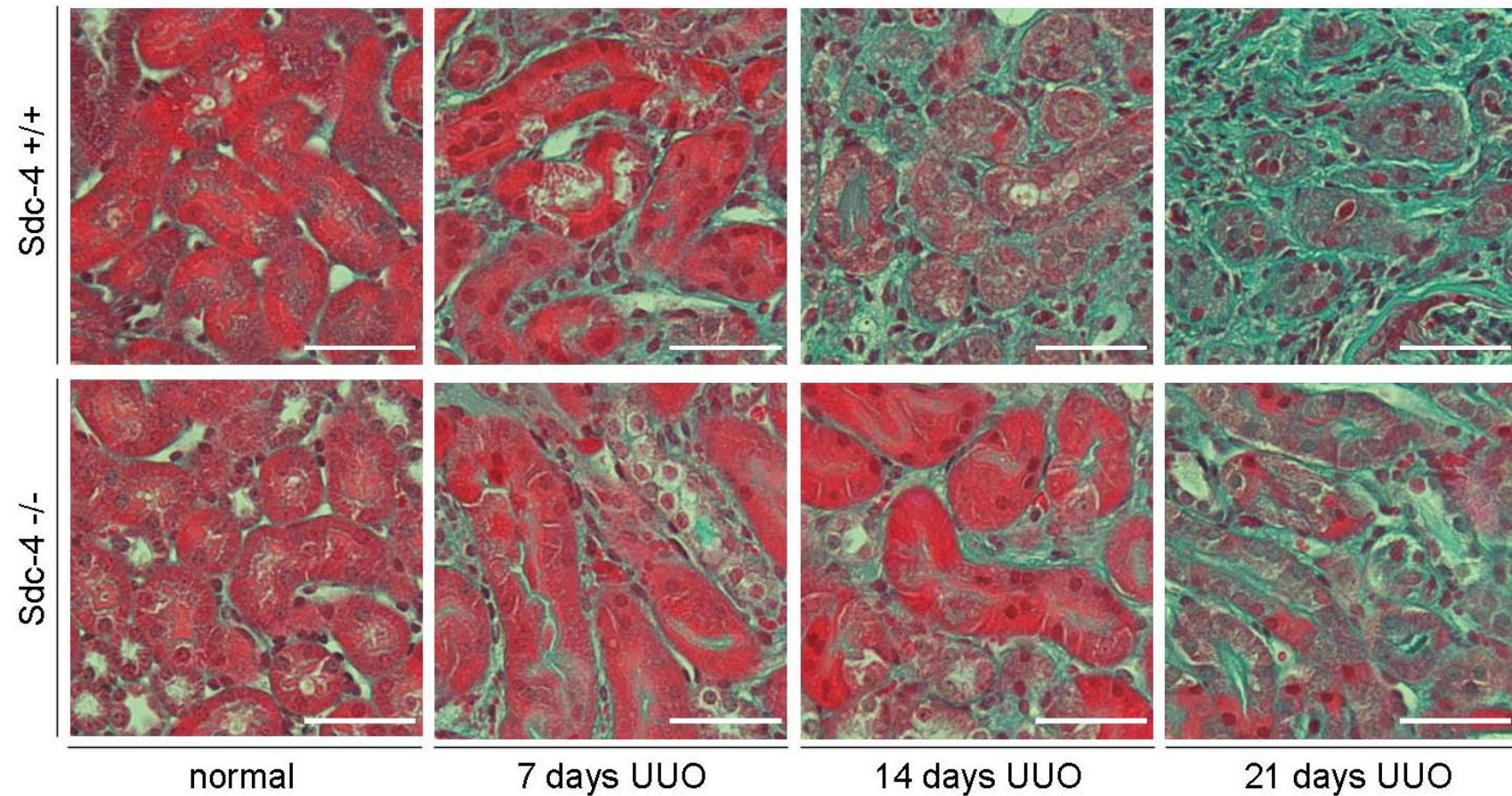


**Figure 6-3 Collagen accumulation in the proximal tubules after UUO induction.** *Progressive collagen accumulation was monitored after UUO induction (7, 14 and 21 days) in the proximal tubules of Sdc-4 +/+ and Sdc-4 -/- kidneys. Collagen was detected using Masson's trichrome staining. The bars correspond to 50  $\mu$ m.*

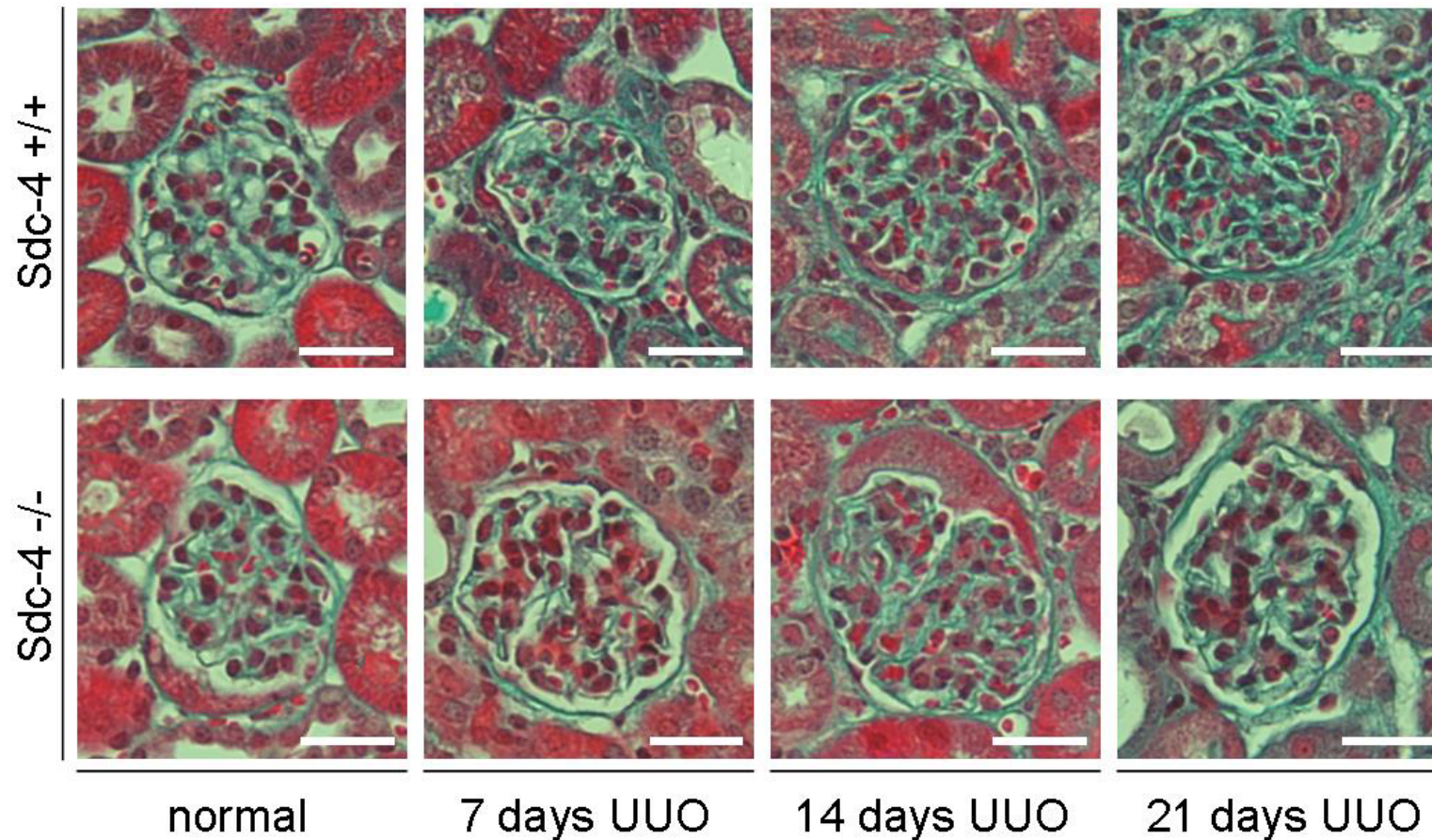


**Figure 6-4 Collagen accumulation in the glomeruli after UUO induction.** *Progressive collagen accumulation was monitored after UUO induction (7, 14 and 21 days) in the periglomerular area of Sdc-4 +/+ and Sdc-4 -/- kidneys. Collagen was detected using Masson's trichrome staining. The bars correspond to 50  $\mu$ m.*

The scarring index was also assessed in untreated kidneys of animals which had UUO induced in the left kidney, in order to determine if compensatory effects were taking place. The results presented in Figure 6-5 show that at the three time points considered there was not a significant difference between kidneys from normal mice and untreated kidneys from UUO mice ( $p>0.05$ ) even though a general increase in scarring index could be measured in untreated kidneys from UUO mice at the higher stages of UUO development (Figure 6-5).

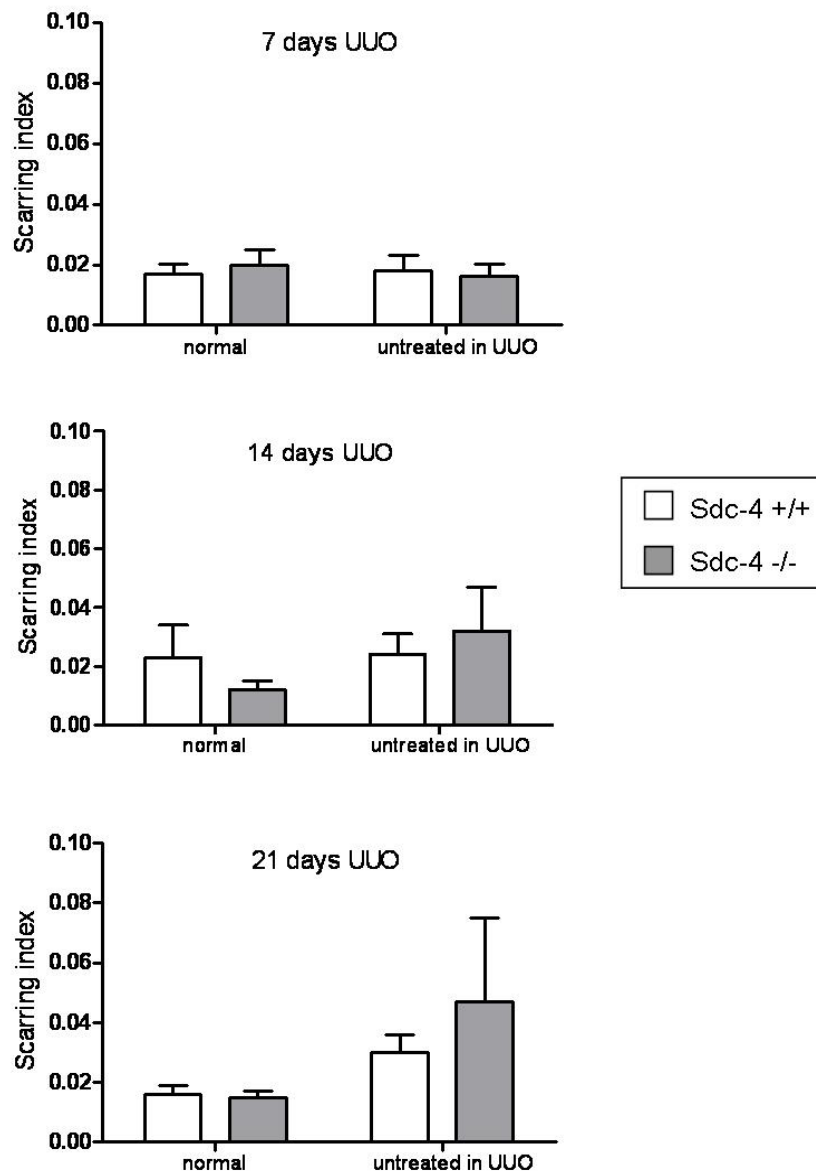


**Figure 6-5 Quantification of scarring index in the untreated kidneys of mice with UUO induction.** Scarring index was quantified as described in Figure 6-2. Normal kidneys ( $n=16$ ) and untreated kidneys from UUO mice ( $n=8$ ) were compared at every time point (7, 14 and 21 days) for wild type and Sdc-4 mice.

The effect of the gender in the development of kidney fibrosis was investigated by analysing separately the scarring index values relative to male and female individuals. Normal kidneys from either wild type (Figure 6-6 A) or Sdc-4 null (Figure 6-6 B) displayed similar values of scarring index at the three time points considered and no significant differences were detected between male (M, shown in blue) and female (F, shown in red) samples.

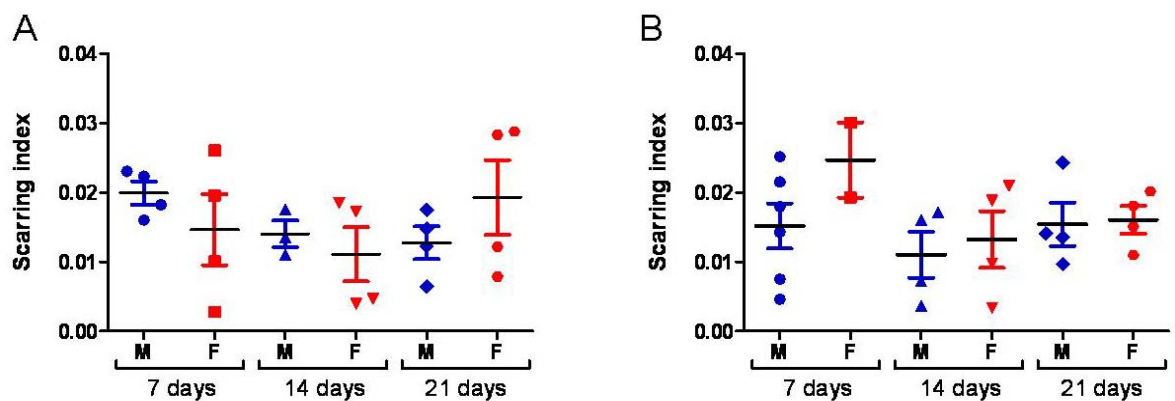


**Figure 6-6 Effect of gender on scarring index of normal kidneys.** *Kidney scarring index (quantified with Masson's trichrome staining) was compared between normal male (M, blue) and female (F, red) at 7, 14 and 2 days. Quantification of wild type samples is shown in A, Sdc-4 null samples is presented in B.*

Wild type kidneys affected by UUO showed a progressive increase in scarring index, but no significant differences could be identified between males and females at the three time points considered (Figure 6-7 A). Sdc-4 null samples displayed a lower level of scarring index compared to wild type samples, as already shown in Figure 6-1, but, as wild type samples, there was no difference between male and females at the three time points considered (Figure 6-7 B).

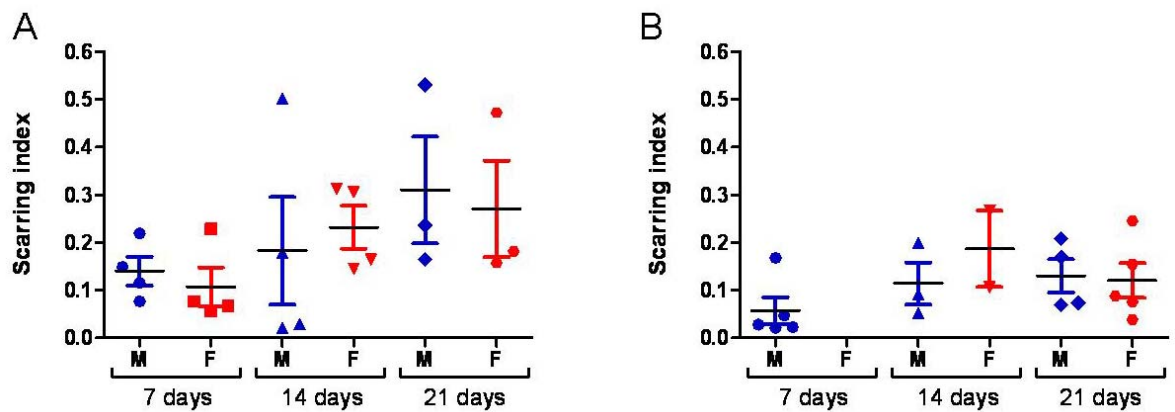


**Figure 6-7** Effect of gender on scarring index on kidneys subjected to UUO. *Kidney scarring index (quantified with Masson's trichrome staining) was compared between UUO male (M, blue) and female (F, red) at 7, 14 and 21 days. Quantification of wild type samples is shown in A, Sdc-4 null samples are presented in B.*

Collagen accumulation during UUO was also monitored by measuring the level of hydroxy-Pro, a major component of collagen. Hydroxy-Pro gives a more precise measurement of collagen deposition compared to Masson's trichrome staining, which can be altered by urine infiltration in kidneys subjected to UUO. As shown in Figure 6-8, a significantly higher value of the hydroxyl-Pro was detected in wild type samples after 21 days UUO compared to Sdc-4 null samples. No significant differences were measured between wild type and Sdc-4 null normal samples. The analysis validated what previously determined with Masson's trichrome quantification.

In conclusion, these data have shown that Sdc-4 is involved in the development of experimental renal fibrosis. Since previous work has shown that TG2 is also implicated in this process, we next tested whether the interaction of TG2 with Sdc-4 could affect TG2 activity also *in vivo*.

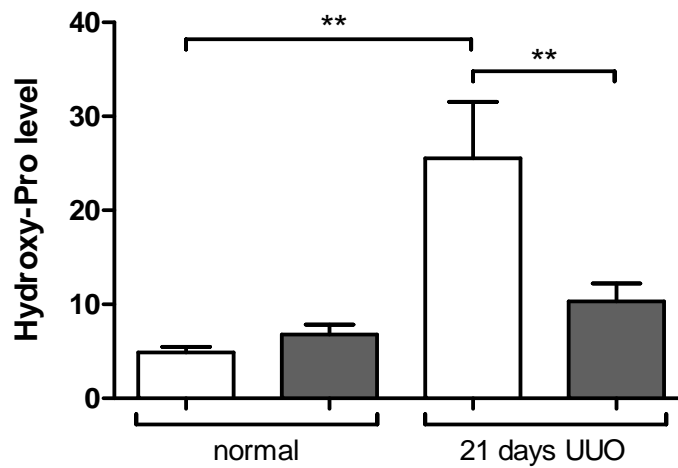


**Figure 6-8 Hydroxy-Pro quantification in normal and fibrotic kidneys.** *The total level of hydroxyproline was quantified in normal and UUO (21 days) kidney homogenates from Sdc-4 +/+ and Sdc-4 -/- mice, as described in section 6.2.7. \*\*,  $p < 0.01$ .  $n \geq 3$ . Normal kidneys,  $n = 24$ . UUO kidneys,  $n = 8$*

### 6.3.2 Lack of Sdc-4 leads to lower *in situ* Transglutaminase activity

*In situ* TG activity was assayed on kidneys from wild type and Sdc-4 null mice through the incorporation of Texas Red labelled cadaverine into unfixed cryosections, either normal or post UUO. Since the TG-reaction is Ca<sup>2+</sup>-dependent, reaction buffer containing EDTA was used as a negative control. The green auto-fluorescence of the kidney tissue was used as a normaliser for the area of tissue considered (kidney cortical area).

As shown in Figure 6-9 and Figure 6-10, TG *in situ* activity was hardly detectable in normal kidneys from wild type and Sdc-4 <sup>-/-</sup> mice. At 7 days after the induction of UUO there was a clear distribution of TG activity in the space surrounding the tubules of wild type kidneys, as pointed by the arrow in Figure 6-9. The signal measured in Sdc-4 <sup>-/-</sup> kidneys at the same time point was significantly lower ( $p < 0.05$ ), as shown in Figure 6-10 and quantified in the histogram of Figure 6-11. At 14 days after UUO induction, the peritubular signal was increased in wild type kidneys compared to the previous time point (Figure 6-9 and Figure 6-11), with a pattern analogue to the collagen distribution measured with Masson's trichrome (Figure 6-1). At the same time, a similar pattern of TG activity was detected in Sdc-4 null kidneys, as pointed by the arrow in Figure 6-10, even though the activity level was significantly lower ( $p < 0.01$ ) than what measured in wild type kidneys. TG *in situ* activity was still significantly higher ( $p < 0.05$ ) in wild type kidneys compared to Sdc-4 null kidneys at 21 days UUO. At this late time point post UUO, the kidney integrity was also compromised, so it was difficult to have a clear idea of TG activity localisation (Figure 6-9).

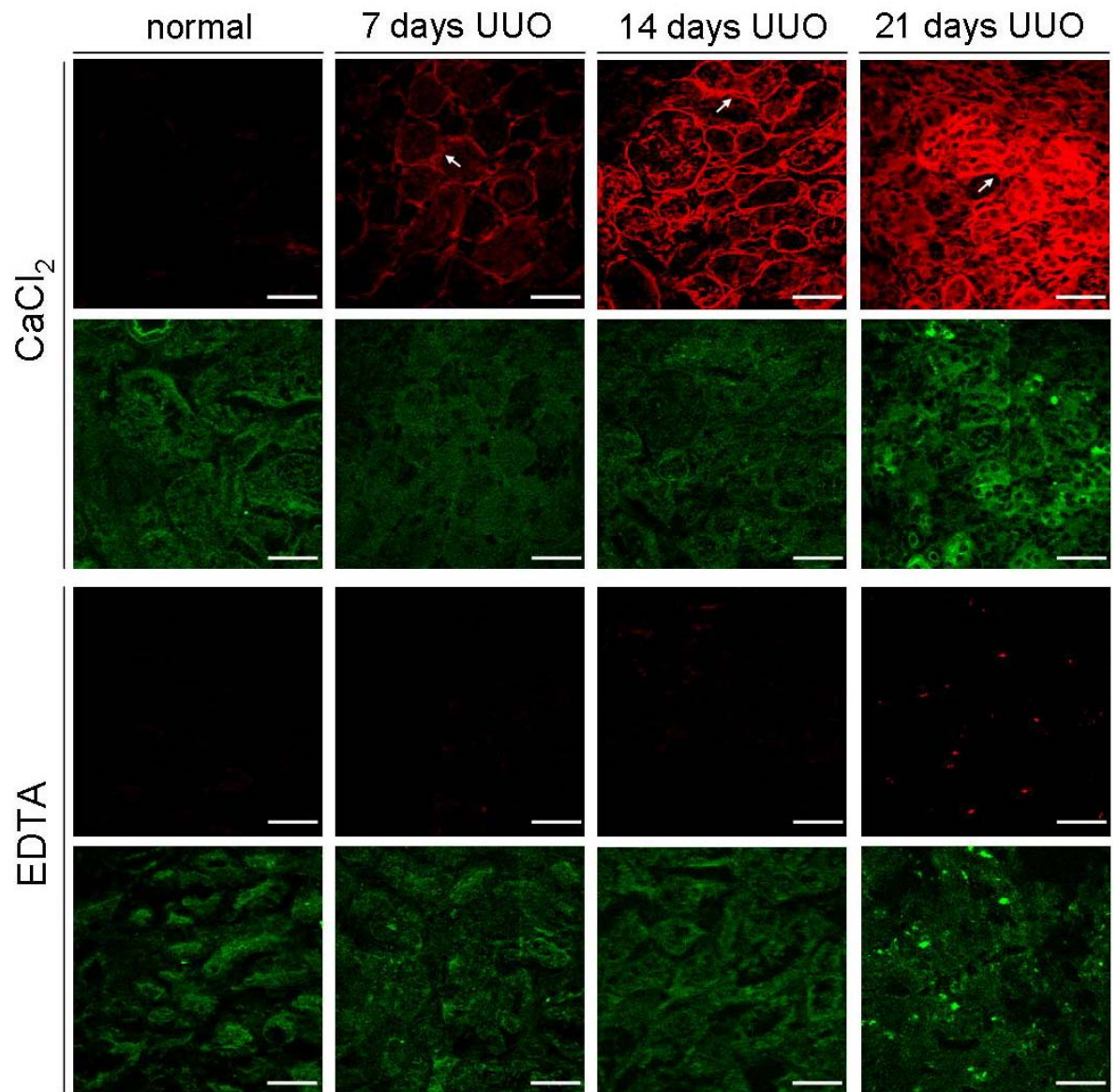


**Figure 6-9 Measurement of TG activity in situ in normal and fibrotic (UUO) kidneys from wild type mice.** *TG activity was measured in cryosections produced from normal and UUO (7, 14 and 21 days) kidneys from wild type mice via the incorporation of TexasRed-cadaverine into endogenous substrates in the presence of either 5 mM CaCl<sub>2</sub> or, as a negative control, 10 mM EDTA. The green auto-fluorescence of the kidney tissue was used as a area normaliser. 3 non-overlapping images acquired by confocal microscopy were quantified for each kidney sample. Normal kidneys, n=48. UUO kidneys, n=8. The arrows point at the TG distribution in the ECM surrounding tubules and glomeruli. The bar indicates 50  $\mu$ m.*

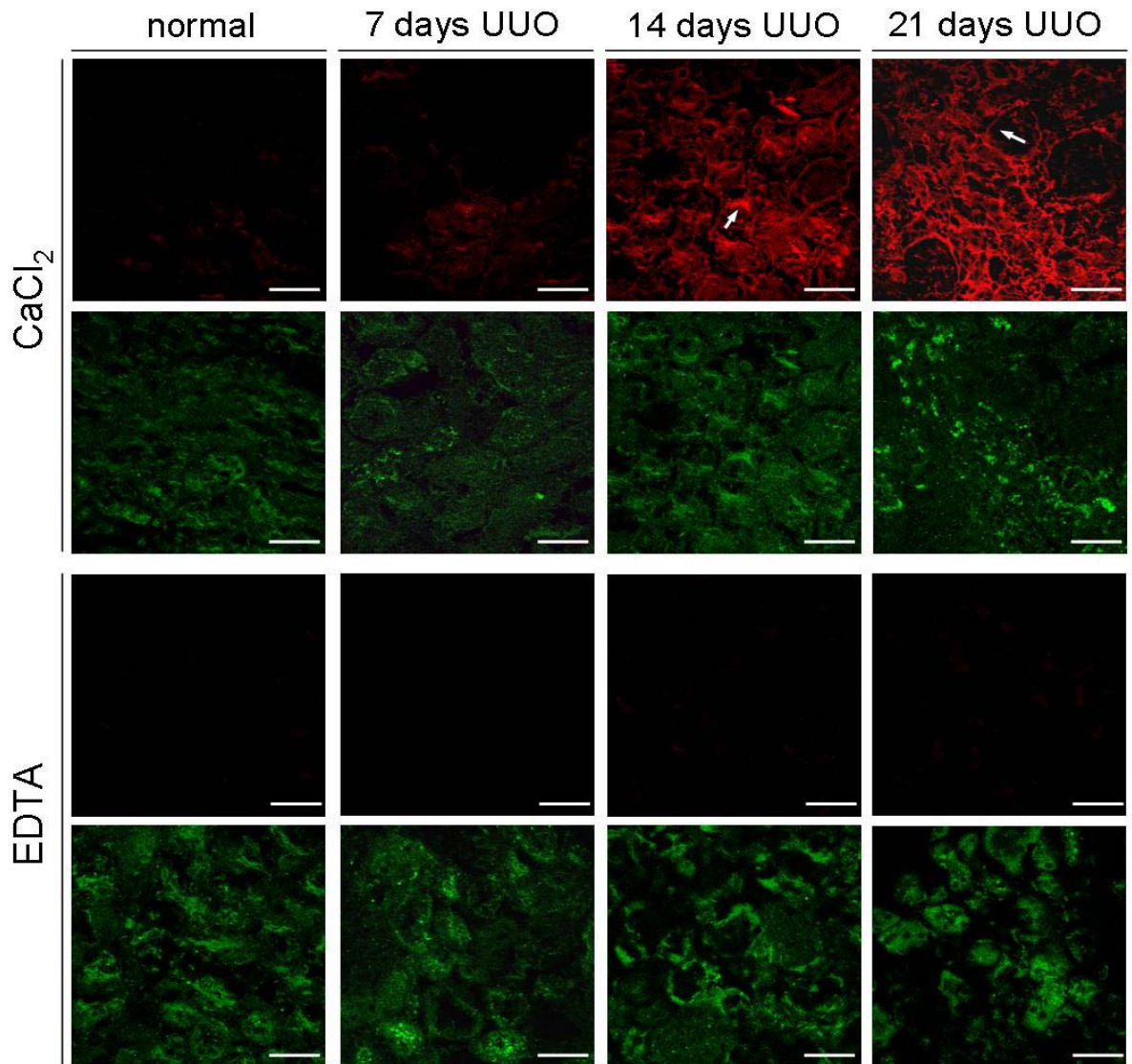


**Figure 6-10** Measurement of TG activity in situ in normal and fibrotic (UUO) kidneys from *Sdc-4*<sup>-/-</sup> mice. The staining was performed on normal and UUO (7, 14 and 21 days) from *Sdc-4* null mice as described in the legend of Figure 6-9. Normal kidneys, n=48. UUO kidneys, n=8. The arrows point at the TG distribution in the ECM surrounding tubules and glomeruli. The bar indicates 50  $\mu$ m.

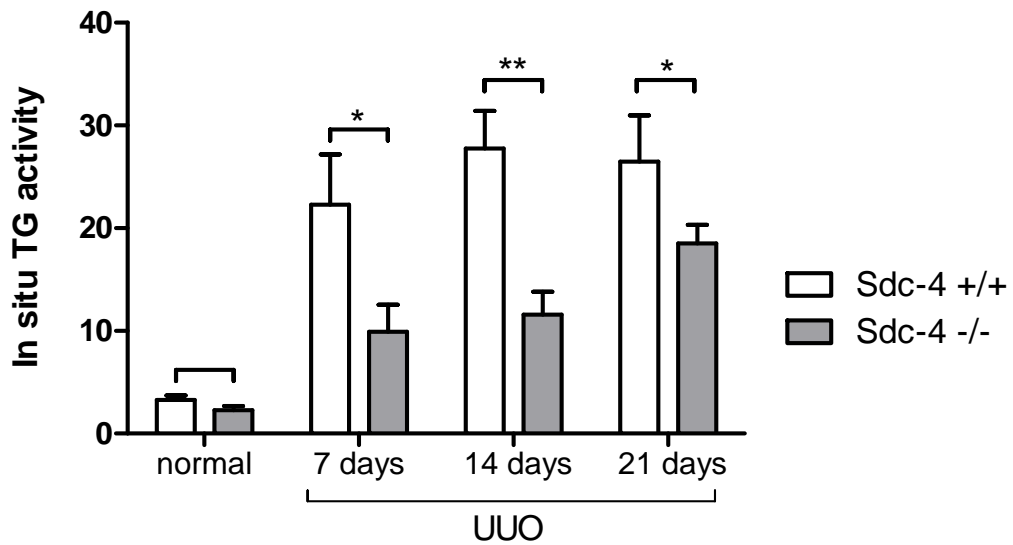


**Figure 6-11 Quantification of TG in situ activity in normal and fibrotic (UUO) kidneys.** The data represent the average values obtained from quantification of the fluorescent signal of 4 to 10 kidneys from wild type (*Sdc-4 +/+*) and *Sdc-4 -/-* mice at 7, 14 and 21 days after UUO induction. TG activity of normal kidneys is shown as a control. 5 images taken from non-overlapping fields were analysed for each kidney sample. Average in situ activity  $\pm$  SD is shown. Normal kidneys,  $n=48$ . UUO kidneys,  $n=8$ . \*,  $p \leq 0.05$ ; \*\*,  $p < 0.01$ .

Linear correlation (Pearson's correlation) between renal scarring (estimated with Masson's trichrome quantification) and *in situ* TG activity was determined using GraphPad software. The analysis revealed a coefficient of linear correlation ( $r$ ) equal to 0.6532 when measured considering Masson's trichrome as scarring index (Figure 6-12); the linear correlation resulted statistically significant ( $p < 0.0001$ ). It has to be considered that the large number of samples analysed can determine a low  $p$  value and significant correlation even though from the graph many samples do not appear to fit with the correlation line.

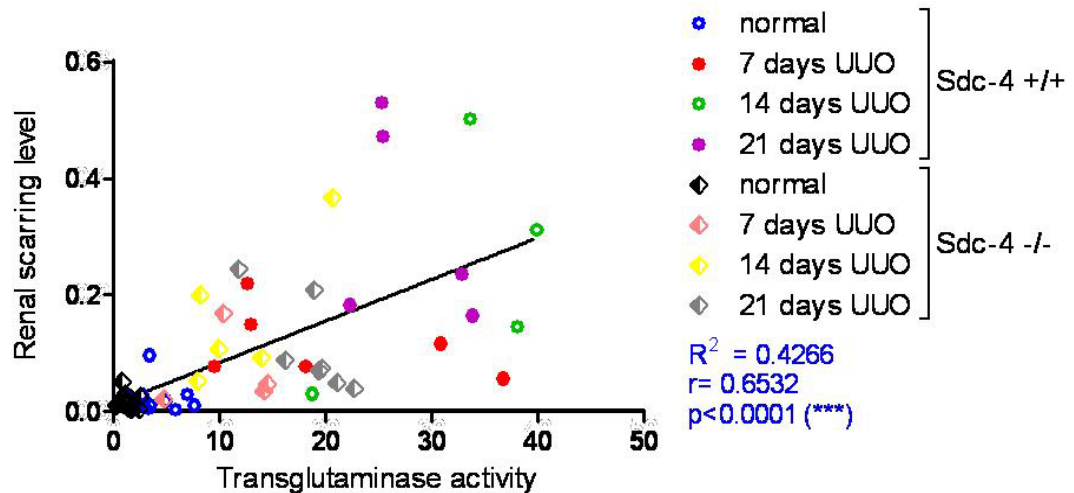


**Figure 6-12 Correlation between TG activity and renal scarring index after the induction of UUO.** Correlation was determined between *in situ* TG activity and scarring index (measured with Masson's trichrome staining) using GraphPad Prism software. Values relative to all the samples used in the study (normal and UUO kidneys from wild type and Sdc-4 null mice) are plotted.  $R^2$  indicates the fitting with the regression line.  $r$ , Pearson's coefficient of linear correlation;  $p$  is relative to positive correlation.

Linear correlation was also estimated separately for wild type and Sdc-4 samples (normal and UUO). The data in Figure 6-13 show clearly that in wild type samples the levels of both TG activity and scarring index are higher compared to Sdc-4 null samples. In both wild type and Sdc-4 -/- there was a positive correlation between TG activity and scarring index ( $r = 0.6355$  and  $r = 0.5318$ , respectively) and the correlation was statistically significant ( $p = 0.0001$  and  $p = 0.003$ , respectively). It is interesting to see how the values of TG activity start to increase before the scarring index in UUO samples compared to normal samples (Figure 6-13). This observation is consistent with a role of TG activity in the development of the fibrotic status, where the accumulation of ECM is a consequence of TG activity.

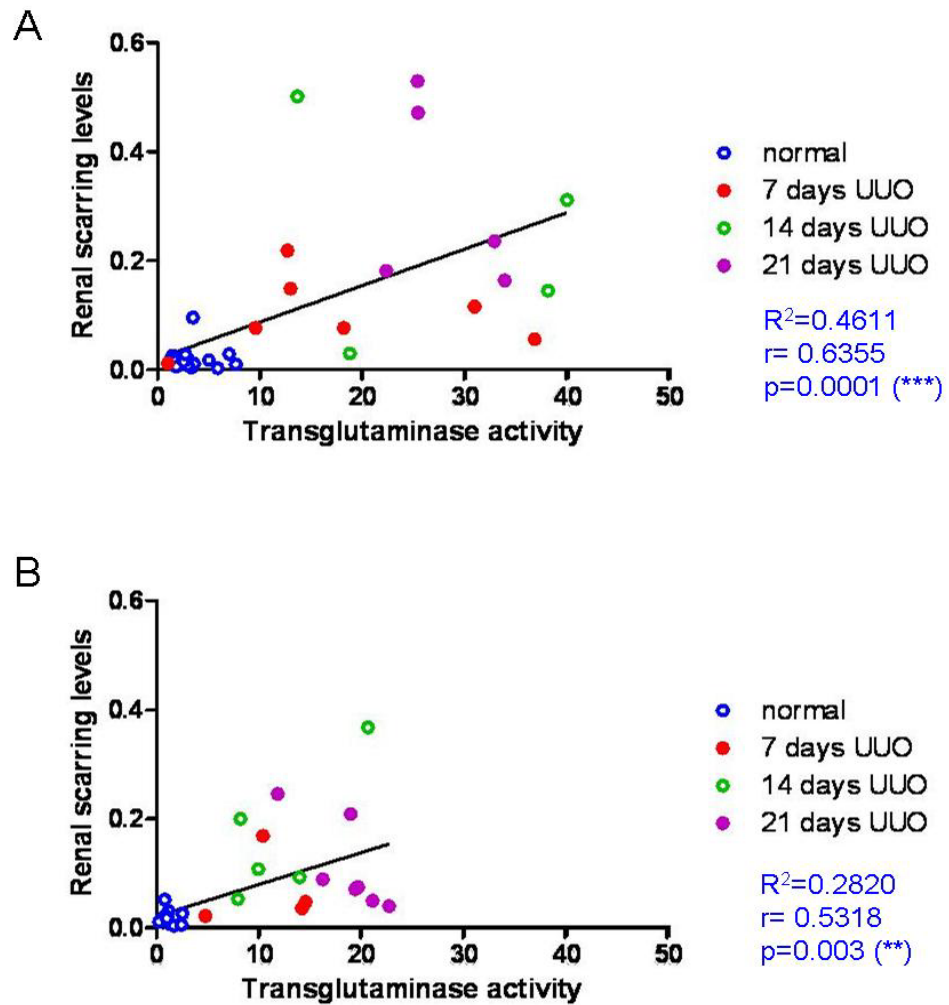


**Figure 6-13 Effect of Sdc-4 on the correlation between TG in situ activity and scarring index.** Correlation was determined between in situ TG activity and scarring index (measured with Masson's trichrome staining) using GraphPad Prism software. Values relative to wild type samples (normal and UUO) are presented in A; values relative to Sdc-4 null samples (normal and UUO) are shown in B.  $R^2$  indicates the fitting with the regression line.  $r$ , Pearson's coefficient of correlation;  $p$  is relative to positive correlation.

Controls on TG2 expression level were performed by Western blotting on normal and 21 days UUO kidney sample from wild type and Sdc-4  $-/-$  animals. The results presented in Figure 6-14 show that there was no significant difference in the level of TG2 expression in normal kidneys from wild type and Sdc-4 null mice. The level of TG2 was increased in an analogous way in wild type and Sdc-4 null kidneys at 21 days after the induction of UUO,

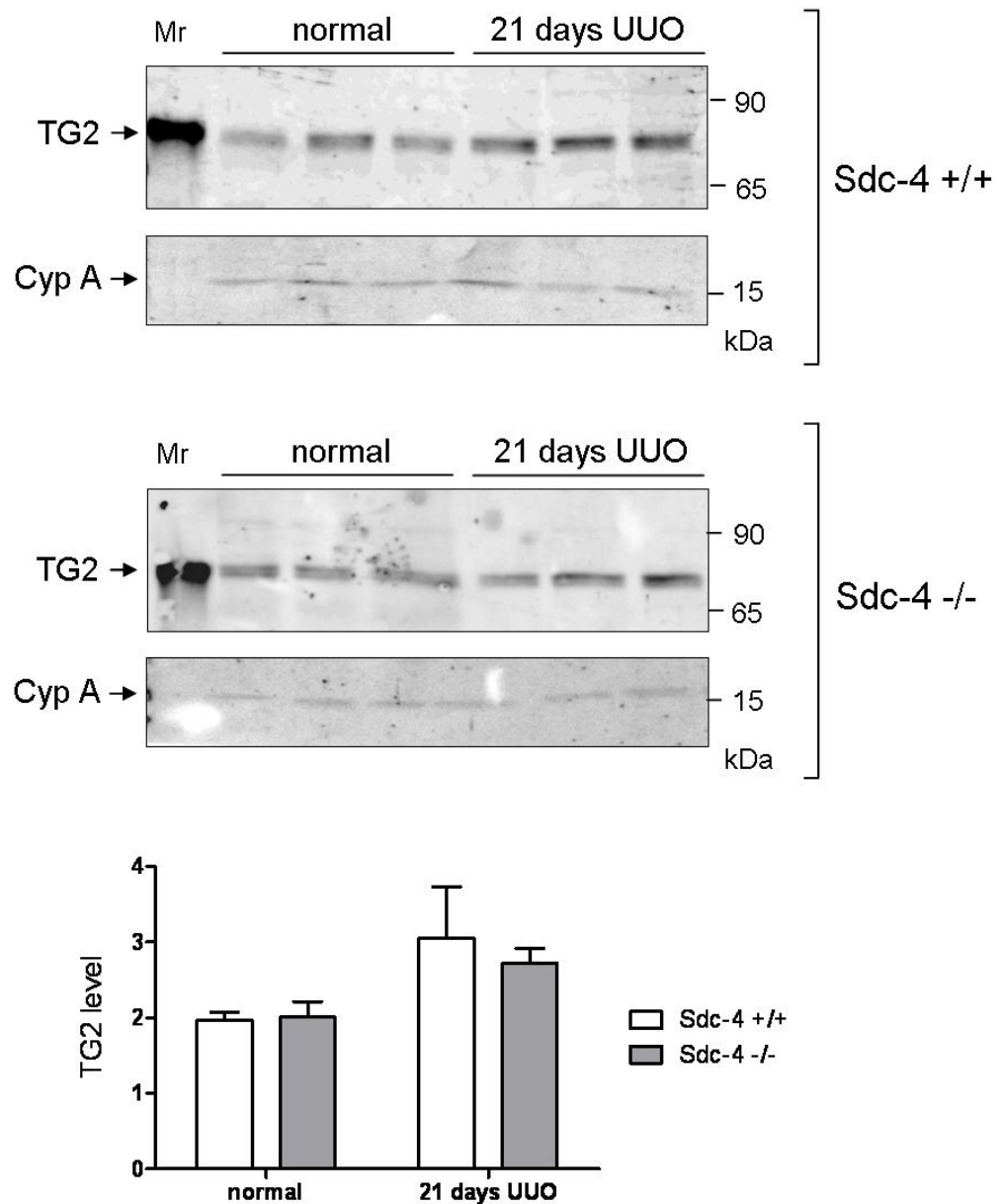


**Figure 6-14** TG2 level in kidney extracts from wild type and Sdc-4 null mice. TG2 expression was measured by Western blotting in protein extracts of normal and UUO kidneys from Sdc-4<sup>+/+</sup> and Sdc-4<sup>-/-</sup> mice. 25  $\mu$ g protein extract were loaded; three separate samples were analysed for each condition. TG2 was detected by anti-TG2 polyclonal antibody Ab10445 and revealed by incubation with HRP-conjugated secondary antibody. Cyclophilin A (CypA) was used as a control for equilloading. The histogram shows TG2 level expressed as ratio TG2/CypA. Mr, indicates gpTG2 standard, 100 ng.

Kidney fibrosis, characterised by glomerular sclerosis accompanied by interstitial fibrosis is a common consequence of several renal diseases of different aetiology. For this reason, understanding the mechanisms regulating the development of kidney fibrosis is particularly important in order to develop specific therapies aimed to the reduction of fibrotic diseases progression. UUO was chosen as experimental model for progressive proliferative renal fibrosis since it is a well established model for rodents which permits the development of fibrotic state in a relatively short time without the use of exogenous toxins and without the development of uremia (Chevalier et al., 2009). Moreover, UUO gives the advantage of the availability of the contralateral kidney as a control. The use of UUO as a fibrotic model is also particularly significant considering that in infants and children the obstruction of the urinary tract due to congenital factors is the principal cause of kidney failure (Seikaly et al., 2003). One important disadvantage of this model is that, since the urinary tract is blocked, it is not possible to perform studies on renal functionality (i.e. analysis on urine samples). On the other side, given the high correlation between UUO-induced renal insufficiency and interstitial fibrosis (Schainuck et al., 1970), UUO represent a valid experimental model for fibrotic studies.

The first step of the investigation consisted in the measurement of changes in ECM deposition (collagen) in wild type and Sdc-4 null kidneys after the induction of UUO. Quantification of Masson's trichrome staining, which allows an estimation of collagen fibres deposition, revealed a significantly higher level of scarring in wild type kidneys compared to the Sdc-4 *-/-* at all the time points considered, suggesting a protective role for Sdc-4 against the development of kidney fibrosis. This finding was confirmed by the measurement of hydroxyl-Pro in kidney homogenates, directly correlated to the amount of collagen. Samples prepared from UUO Sdc-4 null kidneys displayed a significantly lower level of the amino acid compared to the wild type at 21 days UUO. Being kidney fibrosis related to an un-regulated tissue repair process, this result is in accordance with the involvement of Sdc-4 in wound healing and the reported delay in wound healing in Sdc-4 *-/-* mice (Echtermeyer et al., 2001). Our findings of a protective role of Sdc-4 in kidney fibrosis appeared to be in contrast with a previous study focused on the role of Sdc-4 in kidney diseases induced by unilateral nephrectomy (UNX). In the reported study, the absence of Sdc-4 determined an increased level of glomerulosclerosis after UNX, which was however correlated to the compensatory overexpression of Sdc-2 in Sdc-4 *-/-* kidneys

(Cevikbas et al. 42-52). Indeed, Sdc-2 promotes the activity of pro-fibrotic TGF- $\beta$ 1, a key mediator of glomerulosclerosis (Chin et al., 2001; Gagliardini and Benigni, 2006). Moreover, Cevikbas and colleagues did not show any significant changes in wild type kidneys after UNX. The UUO model used in the current study analyses the effect of Sdc-4 knock out from a different perspective compared to UNX model, where one of the kidneys is eliminated and the remaining kidney is subjected to glomerular hyperfiltration. This may explain the differences observed in the development of renal fibrosis between the present study and the one reported by Cevikbas et al. (2008), where no interstitial fibrosis was detected.

Several studies have been published on gender effect in the susceptibility to renal diseases such as ischemia/reperfusion injury (Hu et al., 2009), polycystic kidney disease (Stringer et al., 2005) and diabetic nephropathy (Tomiyoshi et al., 2002). When the effect of gender was investigated in the current study, no significant differences were detected in the development of kidney fibrosis after UUO induction, suggesting that hormonal levels do not influence this experimental model of kidney fibrosis. However, the analysis of a higher number of samples would be required in order to have a more representative study on gender effect on kidney fibrosis.

Given the direct association of TG2 and Sdc-4 demonstrated in this study, next the role of Sdc-4 in the regulation of TG activity was studied in normal and fibrotic kidneys. TG activity was found to be distributed in the same regions where collagen deposition was detected, in particular in the periglomerular area and in the extracellular space surrounding the tubules. The amount of *in situ* TG activity was found to be increased with the progression of the disease in both wild type and Sdc-4 ko kidneys, in accordance with previous reports (Fisher et al., 2009). At any time point considered (7, 14 and 21 days post UUO induction) TG2 activity was always significantly higher in wild type kidneys compared to Sdc-4 *-/-*. TG2 *in situ* activity was also positively correlated with the collagen deposition quantified by Masson's trichrome staining. Since the TG activity level was comparable in normal wild type and Sdc-4 *-/-* kidneys, as well as the level of TG2 expression, these data suggest a possible role for Sdc-4 in the regulation of extracellular TG2 activity correlated with the development of kidney fibrosis. Expression analysis of TG2 antigen failed to show a significantly increased TG2 level in wild type kidneys compared to Sdc-4 null kidneys at 21 days UUO. This finding suggests that the reduced

TG2 activity observed in Sdc-4 <sup>-/-</sup> kidneys post UUO may be due to the involvement of Sdc-4 in TG2 externalisation, as reported *in vitro* in this study (Chapter 5). The analysis also failed to show a significant difference in TG2 antigen between normal and post UUO samples, both wild type and Sdc-4 <sup>-/-</sup>. This finding is surprisingly, given that previous reports have shown an increased level of TG2 expression in kidney fibrotic diseases (El Nahas et al. 2004; Johnson et al., 2003; Johnson et al., 1999).

In conclusion, these data suggest that the role of Sdc-4 is not directly related to the activation of TG2 expression, but it may involve the translocation of the enzyme in the extracellular environment, where the conditions are favourable for the Ca<sup>2+</sup>-dependent transamidating activity.

## ***Chapter 7: General discussion***

TG2 plays an important role in the ECM, regulating cell-matrix interactions in physiological conditions and in situations of cell stress/wound healing by influencing cell adhesion and matrix stabilisation. The results presented in the first part of this thesis aimed to investigate the specific role of extracellular TG2 in the early stages of cell adhesion to FN, which was studied in primary fibroblasts for the first time. In order for TG2 to mediate extracellular events, the enzyme needs to be externalised and presented at the cell surface. This concept has been clearly demonstrated by the results presented in Chapter 3, showing FA formation in TG2  $-/-$  MEF with or without added-back matrix TG2. Moreover, it is known that extracellular TG2 combined to FN mediates a novel adhesion mechanism, independent from integrin binding to FN (RGD-independent cell adhesion) (Verderio et al., 2003). This mechanism plays an important role in mediating cell survival in situations of cell stress, when the ECM is fragmented and RGD-dependent adhesion is impaired (Davis et al., 2000; Verderio et al., 2003). However, even though TG2 is known to be externalised, the mechanism regulating its cell-surface trafficking is still not fully understood. TG2-mediated RGD-independent cell-adhesion relies on the presence of cell-surface HS chains (Verderio et al., 2003), moreover, TG2 has been known for a long time to have a certain affinity for heparin (analogue of HS) (Gambetti et al., 2005; Signorini et al., 1988). In this study HSPG like Sdc-4 were investigated as possible receptors for TG2 at the cell surface.

These results presented in Chapter 3 are in accordance with previous reports describing the presence of TG2, in association with FN, in the pericellular matrix and in the ECM of Swiss 3T3 fibroblasts (Gaudry et al., 1999; Verderio et al., 1998). In fact both TG2 antigen and activity could be detected at the cell surface of primary fibroblasts starting from 20 minutes of cell adhesion on FN. TG2 localisation at cell-matrix contacts supported the idea of a role for the enzyme in early cell adhesion. Further studies aimed to investigate the role of externalised TG2 in cell adhesion were based on the use of primary cells isolated from mice where TG2 was disrupted by homologous recombination (De Laurenzi and Melino, 2001). TG2 was selectively re-introduced on these cells either by cell transfection with a pEGFPTG construct or by plating the cells on a matrix of TG2 bound to FN. Cell adhesion was evaluated by monitoring FAK activation (phosphorylation of Tyr 397), actin cytoskeleton morphology and formation of vinculin-containing FA. Cells lacking TG2

displayed a significantly lower level of FAK-P in the early stages of cell adhesion, moreover they failed to form correct actin SF and vinculin-containing FA. These observations suggested a role for TG2 in the initial activation of FAK, showing that TG2 is involved in this step of FAK activation together with participating to the following activation by phosphorylation at Tyr 576 and Tyr 577 as previously described by Stephens et al. (2004).

Syndecans and glypicans are the two families of membrane-bound proteoglycans, and both carry HS chains (Bernfield et al., 1992). The difference between the two families is that syndecans are type-1 transmembrane receptors, while glypicans are linked to the cell surface by a C-terminal GPI anchor (Bernfield et al., 1992). Since the current work aimed to understand the mechanism which regulates TG2 externalisation and biological activity at the cell surface, the attention was focused on syndecans for a number of reasons. Firstly, given their transmembrane and cytosolic domains, they can be involved in cell membrane trafficking. Secondly, TG2-mediated RGD-independent cell adhesion has been shown to be repressed by a specific inhibitor of PKC $\alpha$  (Go6976) (Verderio et al., 2003) and Sdc-4 mediates PKC $\alpha$  activation (Defilippi et al., 1997; Slater et al., 2001). Thirdly, Sdc-4 is a widespread component of FA (Echtermeyer et al., 1999; Woods and Couchman, 1994), a site where TG2 was also found to be localised (Chapter 3 and Chapter 5). In order to investigate the role of Sdc-4 in TG2-mediated RGD-independent cell adhesion, experiments were performed on primary MDF isolated from mice lacking Sdc-4 (Ishiguro et al., 2000) using wild type MDF as a control. It is well known that, following initial cell attachment to FN via  $\alpha 5\beta 1$  integrins, Sdc-4 is essential for the formation of actin SF (Baciu and Goetinck, 1995; Woods and Couchman, 1994; Woods and Couchman, 2001). However, the results showed in this thesis indicated that Sdc-4  $-/-$  primary fibroblasts can still spread and form stress fibers when plated on FN. Anyway, SF of Sdc-4 null cells appeared to be less thick compared to those of wild type fibroblasts, indicating impairment in the spreading process. This hypothesis fits with the results obtained on the phosphorylation level of FAK. FAK phosphorylation at Tyr397 is an early event in FA formation. Results showed that Sdc-4  $-/-$  MDF have a significantly lower amount of activated FAK compared to wild type cells; this could be the justification for the defects in actin cytoskeleton assembly, since FAK has a role in the modulation of stress fibers formation mediated by the small GTPase RhoA (Arthur and Burridge, 2001). This observation is in accordance with what previously published, stating that lack of Sdc-4

only affects cell spreading when the cell-binding domain of FN is missing (Ishiguro et al., 2000). Measurements of FAK phosphorylation and SF formation revealed that the lack of Sdc-4 impairs TG2-mediated RGD-independent focal adhesion, which was rescued when Sdc-4 was added back to Sdc-4 null cells via transfection with pcDNAhS4 construct. While this study was being conducted, a parallel work stating the importance of Sdc-4 in FN-bound TG2-mediated RGD-independent cell adhesion was published (Telci et al., 2008). The cited work did not explore the contribution of Sdc-4 to TG2-mediated RGD-independent FAK activation, which is an original outcome of the studies presented in this thesis.

Syndecans are constituted by a transmembrane protein which carries GAG chains (predominantly HS) on the extracellular domain; these chains, spanning outside the cell surface, are mostly responsible for binding properties of syndecans (Bernfield et al., 1992). For these reasons, binding studies were performed using purified TG2 and heparin (highly sulphated analogue of HS) or HS. Both SPR and solid-binding assays revealed a high binding affinity of TG2 for heparin/HS, estimated to be in the nM range. The apparent affinity of TG2 for both heparin and HS was measured, with a Kd of approximately 20 nM, when estimated with solid binding assay; the apparent affinity of TG2 for heparin was 90 nM when measured by SPR. It is interesting to notice that the affinity of TG2 for heparin/HS is slightly higher of the measured affinity of TG2 for FN (Kd= 180 nM, measured by SPR), which, so far, has been considered the main binding partner for TG2 (Hang et al., 2005). However, given the high affinity of TG2 for both FN and HS and, in turn, the affinity of FN for HS chains, collectively these data suggest a possible triangular association of TG2, HS chains of Sdc-4 and FN at cell-matrix contacts. Janiak et al. (2006) proposed an association of TG2 and  $\beta$ 1 integrins at the cell surface, leading to integrin-mediated signalling involved in cell adhesion. Our results lead to the hypothesis that TG2 may exist in complex with Sdc-4 and FN at the cell surface. It is tempting to propose that TG2 may mediate the cross-talking between integrins and Sdc-4 leading to full adhesion and spreading (Saoncella et al., 1999).

The work was carried on by showing that endogenous TG2 secreted by primary fibroblasts can interact with immobilised extracellular heparin/HS, indicating the possibility of a physiological role for the interaction of TG2 with HSPG, as already introduced in the work by Verderio et al (2003). This hypothesis was validated by studies on the physical

association of TG2 and Sdc-4 *in vitro*, which revealed a direct association of the two molecules at the cell surface of different cell types when analysed by co-immunoprecipitation studies. In a parallel work exogenous FN-bound TG2 has been shown to co-immunoprecipitate with Sdc-4 (Telci et al., 2008). The work by Telci and colleagues however did not investigate the association of endogenous TG2 and Sdc-4. On the contrary, the results presented in this thesis (Chapter 4) show for the first time that cell-secreted TG2 is associated with Sdc-4 at the cell surface and the interaction involves TG2-binding of Sdc-4 HS chains.

In this study, the extracellular localization and the cell-surface activity of TG2 were found to be regulated by Sdc-4 in primary fibroblasts, since MDF lacking Sdc-4 failed to show TG2 antigen and activity on the cell surface and the enzyme appeared to be retained intracellularly. In addition, added back Sdc-4 restored TG2 cell-surface activity in Sdc-4 null cells. Further studies showed that the interference with cell-surface HS chains, either via heparitinase treatment or the HS antagonist surfen, significantly decreased the level of cell-surface TG2 activity. Since the HS chains did not appear to alter the intrinsic transamidation activity of TG2, these findings collectively demonstrated that HS chains of Sdc-4 influence cell-surface TG2 activity by controlling the localisation of the enzyme and not by affecting its transamidating activity.

TG2 externalisation is enhanced in situations of cell stress and TG2 activity assumes an important role in the wound repair process, where it contributes to cell adhesion and to the stabilisation of the ECM. When the wound repair mechanism is altered, or when the insult causing the wound becomes chronic, there is the development of a fibrotic condition, characterised by an excess of ECM deposition leading to block of function of the interested organ (Singer and Clark, 1999). The involvement of TG2 in kidney fibrosis has been already described (El Nahas et al., 1997; Haroon et al., 1999; Johnson et al., 1999), and experiments performed on animal models have shown that lack of TG2 is protective against the development of renal fibrosis (Johnson et al., 2003). Therefore TG2 may be regarded as a novel therapeutic target for the cure of kidney fibrosis; consequently, current work in the field is aimed to find a way to regulate TG2 externalisation and activity (Johnson et al., 2007).

After studying the interaction of TG2 and Sdc-4 *in vitro* and defying a role for Sdc-4 HS chains in the localisation of TG2 biological activity, further studies were performed in

order to see if Sdc-4 regulates TG2 activity *in vivo*. Using an experimental model of kidney fibrosis (UUO) it was shown that the absence of Sdc-4 is protective against the development of kidney fibrosis. This data is in accordance with data previously published illustrating the role of Sdc-4 in the wound repair process and showing that wound repair is delayed in Sdc-4 null mice (Echtermeyer et al., 2001). TG activity was measured *in situ* in normal and fibrotic kidneys from wild type and Sdc-4 mice and its level was found to be positively correlated to the level of ECM accumulation. Even though normal kidneys from wild type and Sdc-4 null mice displayed the same level of *in situ* TG activity, this was found to be significantly lower in Sdc-4  $-/-$  kidneys subjected to UUO compared to wild type kidneys. This result is reminiscent of what obtained with MDF isolated from wild type and Sdc-4 null mice, with wild type cells showing a higher level of cell-surface TG2 activity compared to Sdc-4 null MDF. Therefore it is possible that Sdc-4 may also be involved in TG2-mediated ECM accumulation in fibrotic diseases (Verderio et al., 2008).

In recent years much research in the area focused on the development of inhibitors of TG activity, in order to block TG2 action and therefore the progression of the fibrotic disease (Johnson et al., 2007). The major problem in designing these inhibitors is the lack of specificity. In fact, aiming the TG conserved catalytic site, they interfere with the activity of all the members of the TG family causing severe side effects such as problems in blood coagulation (FXIIIa) and in maintenance of skin integrity (TG1 and TG3) (Huang et al., 2009). In order to achieve a higher level of specificity, new inhibitors have been designed in order to target only externalised transglutaminases (Huang et al., 2009), however, even though these inhibitors have a more limited target, the side effects related to the inhibition of FXIII, another member of the TG family to be externalised, are still present. Given the problems related to the use of TG inhibitors, it would be of great interest to have a better understanding on the mechanism of TG2 localisation, in order to control the secretion of the enzyme and hence its extracellular role.

In conclusion, this study has shown that the association of TG2 with Sdc-4 could have several key roles. In fact Sd-4 is involved in TG2 cell-surface trafficking (Figure 7-1 point 1) and, therefore, it indirectly regulates TG2 transamidation in the ECM (Figure 7-1 point 2). Moreover, by acting as a cell surface receptor, Sdc-4 regulates TG2-mediated signalling in cell adhesion events in co-operation with integrins (Figure 7-1 point 3). In situations of cell stress, when integrin-mediated adhesion is inhibited and ECM is fragmented,

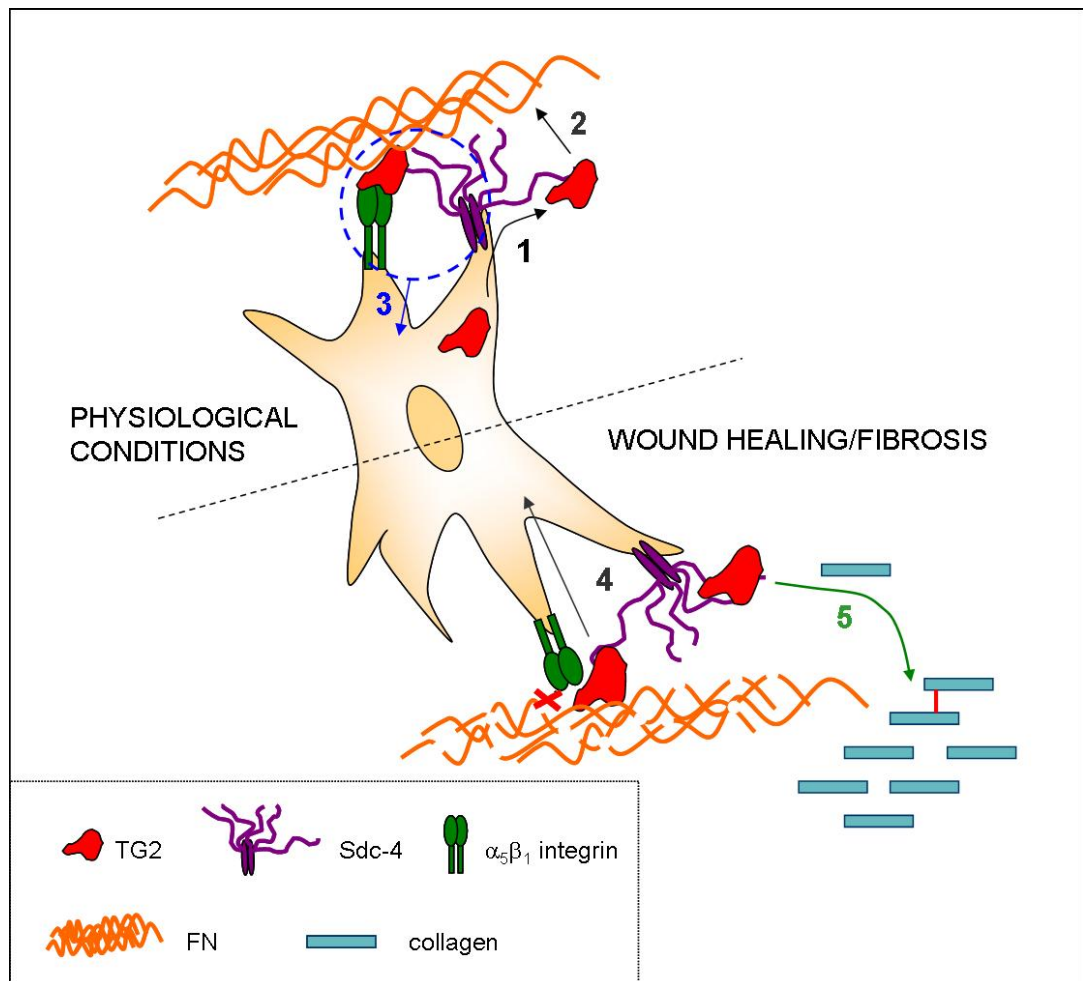


**Figure 7-1** Events mediated by TG2 association with Sdc-4. 1) Sdc-4 regulates TG2 cell-surface trafficking. 2) Extracellular TG2 associates to and stabilises FN. 3) Signalling from FN-associated TG2 in co-operation with Sdc-4 and integrins promotes cell adhesion and migration. 4) Externalised FN-bound TG2 mediates RGD-independent cell adhesion in a Sdc-4 dependent way 5) In fibrotic diseases, extracellular TG2 promotes ECM accumulation in a Sdc-4 dependent mechanism.

---

## Bibliography

- Achyuthan, K. E. and Greenberg, C. S.** (1987). Identification of a guanosine triphosphate-binding site on guinea pig liver transglutaminase. Role of GTP and calcium ions in modulating activity. *J. Biol. Chem.* 262, 1901-1906.
- Aeschlimann, D. and Paulsson, M.** (1991). Cross-linking of laminin-nidogen complexes by tissue transglutaminase. A novel mechanism for basement membrane stabilization. *J. Biol. Chem.* 266, 15308-15317.
- Aeschlimann, D. and Paulsson, M.** (1994). Transglutaminases: protein cross-linking enzymes in tissues and body fluids. *Thromb. Haemost.* 71, 402-415.
- Aeschlimann, D., Kaupp, O. and Paulsson, M.** (1995). Transglutaminase-catalyzed matrix cross-linking in differentiating cartilage: identification of osteonectin as a major glutaminy substrate. *J. Cell Biol.* 129, 881-892.
- Aeschlimann, D., Koeller, M. K., Ien-Hoffmann, B. L. and Mosher, D. F.** (1998). Isolation of a cDNA encoding a novel member of the transglutaminase gene family from human keratinocytes. Detection and identification of transglutaminase gene products based on reverse transcription-polymerase chain reaction with degenerate primers. *J. Biol. Chem.* 273, 3452-3460.
- Aeschlimann, D. and Thomazy, V.** (2000). Protein crosslinking in assembly and remodelling of extracellular matrices: the role of transglutaminases. *Connect. Tissue Res.* 41, 1-27.
- Afford, S. and Randhawa, S.** (2000). Apoptosis. *Mol. Pathol.* 53, 55-63.
- Ahvazi, B., Boeshans, K. M., Idler, W., Baxa, U., Steinert, P. M. and Rastinejad, F.** (2004). Structural basis for the coordinated regulation of transglutaminase 3 by guanine nucleotides and calcium/magnesium. *J. Biol. Chem.* 279, 7180-7192.
- Akimov, S. S., Krylov, D., Fleischman, L. F. and Belkin, A. M.** (2000). Tissue transglutaminase is an integrin-binding adhesion coreceptor for fibronectin. *J. Cell Biol.* 148, 825-838.
- Akimov, S. S. and Belkin, A. M.** (2003). Opposing roles of Ras/Raf oncogenes and the MEK1/ERK signaling module in regulation of expression and adhesive function of surface transglutaminase. *J. Biol. Chem.* 278, 35609-35619.
- Anderson, R. G.** (1998). The caveolae membrane system. *Annu. Rev. Biochem.* 67, 199-225.
- Antonyak, M. A., Miller, A. M., Jansen, J. M., Boehm, J. E., Balkman, C. E., Wakshlag, J. J., Page, R. L. and Cerione, R. A.** (2004). Augmentation of tissue transglutaminase expression and activation by epidermal growth factor inhibit doxorubicin-induced apoptosis in human breast cancer cells. *J. Biol. Chem.* 279, 41461-41467.
- Anttonen, A., Kajanti, M., Heikkila, P., Jalkanen, M. and Joensuu, H.** (1999). Syndecan-1 expression has prognostic significance in head and neck carcinoma. *Br. J. Cancer* 79, 558-564.
- Asundi, V. K. and Carey, D. J.** (1995). Self-association of N-syndecan (syndecan-3) core protein is mediated by a novel structural motif in the transmembrane domain and ectodomain flanking region. *J. Biol. Chem.* 270, 26404-26410.

- Baciu, P. C., Saoncella, S., Lee, S. H., Denhez, F., Leuthardt, D. and Goetinck, P. F.** (2000). Syndesmos, a protein that interacts with the cytoplasmic domain of syndecan-4, mediates cell spreading and actin cytoskeletal organization. *J. Cell Sci.* 113 Pt 2, 315-324.
- Backhaus, R., Zehe, C., Wegehngel, S., Kehlenbach, A., Schwappach, B. and Nickel, W.** (2004). Unconventional protein secretion: membrane translocation of FGF-2 does not require protein unfolding. *J. Cell Sci.* 117, 1727-1736.
- Baek, K. J., Kang, S., Damron, D. and Im, M.** (2001). Phospholipase Cdelta1 is a guanine nucleotide exchanging factor for transglutaminase II (Galpha h) and promotes alpha 1B-adrenoreceptor-mediated GTP binding and intracellular calcium release. *J. Biol. Chem.* 276, 5591-5597.
- Bailey, C. D., Tucholski, J. and Johnson, G. V.** (2005). Transglutaminases in neurodegenerative disorders. *Prog. Exp. Tumor Res.* 38, 139-157.
- Balklava, Z., Verderio, E., Collighan, R., Gross, S., Adams, J. and Griffin, M.** (2002). Analysis of tissue transglutaminase function in the migration of Swiss 3T3 fibroblasts: the active-state conformation of the enzyme does not affect cell motility but is important for its secretion. *J. Biol. Chem.* 277, 16567-16575.
- Ballestar, E., Abad, C. and Franco, L.** (1996). Core histones are glutaminy substrates for tissue transglutaminase. *J. Biol. Chem.* 271, 18817-18824.
- Barsigian, C., Stern, A. M. and Martinez, J.** (1991). Tissue (type II) transglutaminase covalently incorporates itself, fibrinogen, or fibronectin into high molecular weight complexes on the extracellular surface of isolated hepatocytes. Use of 2-[(2-oxopropyl)thio] imidazolium derivatives as cellular transglutaminase inactivators. *J. Biol. Chem.* 266, 22501-22509.
- Bass, M. D., Morgan, M. R. and Humphries, M. J.** (2007). Integrins and syndecan-4 make distinct, but critical, contributions to adhesion contact formation. *Soft. Matter* 3, 372-376.
- Baumgartner, W., Golenhofen, N., Weth, A., Hiiragi, T., Saint, R., Griffin, M. and Drenckhahn, D.** (2004). Role of transglutaminase 1 in stabilisation of intercellular junctions of the vascular endothelium. *Histochem. Cell Biol.* 122, 17-25.
- Beauvais, D. M. and Rapraeger, A. C.** (2004). Syndecans in tumor cell adhesion and signaling. *Reprod. Biol. Endocrinol.* 2, 3.
- Begg, G. E., Holman, S. R., Stokes, P. H., Matthews, J. M., Graham, R. M. and Iismaa, S. E.** (2006). Mutation of a critical arginine in the GTP-binding site of transglutaminase 2 disinhibits intracellular cross-linking activity. *J. Biol. Chem.* 281, 12603-12609.
- Begg, G. E., Carrington, L., Stokes, P. H., Matthews, J. M., Wouters, M. A., Husain, A., Lorand, L., Iismaa, S. E. and Graham, R. M.** (2006). Mechanism of allosteric regulation of transglutaminase 2 by GTP. *Proc. Natl. Acad. Sci. U. S. A* 103, 19683-19688.
- Belkin, A. M., Akimov, S. S., Zaritskaya, L. S., Ratnikov, B. I., Deryugina, E. I. and Strongin, A. Y.** (2001). Matrix-dependent proteolysis of surface transglutaminase by membrane-type metalloproteinase regulates cancer cell adhesion and locomotion. *J. Biol. Chem.* 276, 18415-18422.
- Belkin, A. M., Zemskov, E. A., Hang, J., Akimov, S. S., Sikora, S. and Strongin, A. Y.** (2004). Cell-surface-associated tissue transglutaminase is a target of MMP-2 proteolysis. *Biochemistry* 43, 11760-11769.

- Bernfield, M., Kokenyesi, R., Kato, M., Hinkes, M. T., Spring, J., Gallo, R. L. and Lose, E. J.** (1992). Biology of the syndecans: a family of transmembrane heparan sulfate proteoglycans. *Annu. Rev. Cell Biol.* 8, 365-393.
- Bernfield, M., Gotte, M., Park, P. W., Reizes, O., Fitzgerald, M. L., Lincecum, J. and Zako, M.** (1999). Functions of cell surface heparan sulfate proteoglycans. *Annu. Rev. Biochem.* 68, 729-777.
- Bishop, A. L. and Hall, A.** (2000). Rho GTPases and their effector proteins. *Biochem. J.* 348 Pt 2, 241-255.
- Bishop, J. R., Schuksz, M. and Esko, J. D.** (2007). Heparan sulphate proteoglycans fine-tune mammalian physiology. *Nature* 446, 1030-1037.
- Bungay, P. J., Owen, R. A., Coutts, I. C. and Griffin, M.** (1986). A role for transglutaminase in glucose-stimulated insulin release from the pancreatic beta-cell. *Biochem. J.* 235, 269-278.
- Bures, D. M. and Goldsmith, L. A.** (1978). Localization of transglutaminase in adult chicken epidermis. *Arch. Dermatol. Res.* 262, 329-332.
- Caldwell, E. E., Nadkarni, V. D., Fromm, J. R., Linhardt, R. J. and Weiler, J. M.** (1996). Importance of specific amino acids in protein binding sites for heparin and heparan sulfate. *Int. J. Biochem. Cell Biol.* 28, 203-216.
- Candi, E., Tarcsa, E., Idler, W. W., Kartasova, T., Marekov, L. N. and Steinert, P. M.** (1999). Transglutaminase cross-linking properties of the small proline-rich 1 family of cornified cell envelope proteins. Integration with loricrin. *J. Biol. Chem.* 274, 7226-7237.
- Candi, E., Oddi, S., Terrinoni, A., Paradisi, A., Ranalli, M., Finazzi-Agro, A. and Melino, G.** (2001). Transglutaminase 5 cross-links loricrin, involucrin, and small proline-rich proteins in vitro. *J. Biol. Chem.* 276, 35014-35023.
- Candi, E., Oddi, S., Paradisi, A., Terrinoni, A., Ranalli, M., Teofoli, P., Citro, G., Scarpato, S., Puddu, P. and Melino, G.** (2002). Expression of transglutaminase 5 in normal and pathologic human epidermis. *J. Invest Dermatol.* 119, 670-677.
- Candi, E., Paradisi, A., Terrinoni, A., Pietroni, V., Oddi, S., Cadot, B., Jogini, V., Meiyappan, M., Clardy, J., Finazzi-Agro, A. et al.** (2004). Transglutaminase 5 is regulated by guanine-adenine nucleotides. *Biochem. J.* 381, 313-319.
- Capila, I. and Linhardt, R. J.** (2002). Heparin-protein interactions. *Angew. Chem. Int. Ed Engl.* 41, 391-412.
- Cardin, A. D. and Weintraub, H. J.** (1989). Molecular modeling of protein-glycosaminoglycan interactions. *Arteriosclerosis* 9, 21-32.
- Carey, D. J., Conner, K., Asundi, V. K., O'Mahony, D. J., Stahl, R. C., Showalter, L., Cizmeci-Smith, G., Hartman, J. and Rothblum, L. I.** (1997). cDNA cloning, genomic organization, and in vivo expression of rat N-syndecan. *J. Biol. Chem.* 272, 2873-2879.
- Carey, D. J.** (1997). Syndecans: multifunctional cell-surface co-receptors. *Biochem. J.* 327 ( Pt 1), 1-16.
- Cassidy, A. J., van Steensel, M. A., Steijlen, P. M., van, G. M., van, d., V, Morley, S. M., Terrinoni, A., Melino, G., Candi, E. and McLean, W. H.** (2005). A homozygous missense mutation in TGM5 abolishes epidermal transglutaminase 5 activity and causes acral peeling skin syndrome. *Am. J. Hum. Genet.* 77, 909-917.

- Cecil, D. L. and Terkeltaub, R.** (2008). Transamidation by transglutaminase 2 transforms S100A11 calgranulin into a procatabolic cytokine for chondrocytes. *J. Immunol.* 180, 8378-8385.
- Cevikbas, F., Schaefer, L., Uhlig, P., Robenek, H., Theilmeier, G., Echtermeyer, F. and Bruckner, P.** (2008). Unilateral nephrectomy leads to up-regulation of syndecan-2- and TGF-beta-mediated glomerulosclerosis in syndecan-4 deficient male mice. *Matrix Biol.* 27, 42-52.
- Chau, D. Y., Collighan, R. J., Verderio, E. A., Addy, V. L. and Griffin, M.** (2005). The cellular response to transglutaminase-cross-linked collagen. *Biomaterials* 26, 6518-6529.
- Chen, R. and Doolittle, R. F.** (1971). - cross-linking sites in human and bovine fibrin. *Biochemistry* 10, 4487-4491.
- Chen, Y., Shi-wen, X., van, B. J., Kennedy, L., McLeod, M., Renzoni, E. A., Bou-Gharios, G., Wilcox-Adelman, S., Goetinck, P. F., Eastwood, M. et al.** (2005). Matrix contraction by dermal fibroblasts requires transforming growth factor-beta/activin-linked kinase 5, heparan sulfate-containing proteoglycans, and MEK/ERK: insights into pathological scarring in chronic fibrotic disease. *Am. J. Pathol.* 167, 1699-1711.
- Cheng, T., Hitomi, K., van Vlijmen-Willems, I. M., de Jongh, G. J., Yamamoto, K., Nishi, K., Watts, C., Reinheckel, T., Schalkwijk, J. and Zeeuwen, P. L.** (2006). Cystatin M/E is a high affinity inhibitor of cathepsin V and cathepsin L by a reactive site that is distinct from the legumain-binding site. A novel clue for the role of cystatin M/E in epidermal cornification. *J. Biol. Chem.* 281, 15893-15899.
- Chevalier, R. L., Forbes, M. S. and Thornhill, B. A.** (2009). Ureteral obstruction as a model of renal interstitial fibrosis and obstructive nephropathy. *Kidney Int.* 75, 1145-1152.
- Chin, B. Y., Mohsenin, A., Li, S. X., Choi, A. M. and Choi, M. E.** (2001). Stimulation of pro-alpha(1)(I) collagen by TGF-beta(1) in mesangial cells: role of the p38 MAPK pathway. *Am. J. Physiol Renal Physiol* 280, F495-F504.
- Citron, B. A., Suo, Z., SantaCruz, K., Davies, P. J., Qin, F. and Festoff, B. W.** (2002). Protein crosslinking, tissue transglutaminase, alternative splicing and neurodegeneration. *Neurochem. Int.* 40, 69-78.
- Clayton, A., Thomas, J., Thomas, G. J., Davies, M. and Steadman, R.** (2001). Cell surface heparan sulfate proteoglycans control the response of renal interstitial fibroblasts to fibroblast growth factor-2. *Kidney Int.* 59, 2084-2094.
- Corbett, S. A. and Schwarzbauer, J. E.** (1997). Modulation of protein tyrosine phosphorylation by the extracellular matrix. *J. Surg. Res.* 69, 220-225.
- Couchman, J. R. and Woods, A.** (1999). Syndecan-4 and integrins: combinatorial signaling in cell adhesion. *J. Cell Sci.* 112 ( Pt 20), 3415-3420.
- Couchman, J. R., Chen, L. and Woods, A.** (2001). Syndecans and cell adhesion. *Int. Rev. Cytol.* 207, 113-150.
- Couchman, J. R., Vogt, S., Lim, S. T., Lim, Y., Oh, E. S., Prestwich, G. D., Theibert, A., Lee, W. and Woods, A.** (2002). Regulation of inositol phospholipid binding and signaling through syndecan-4. *J. Biol. Chem.* 277, 49296-49303.
- Couchman, J. R.** (2003). Syndecans: proteoglycan regulators of cell-surface microdomains? *Nat. Rev. Mol. Cell Biol.* 4, 926-937.

- Curtis, C. G., Brown, K. L., Credo, R. B., Domanik, R. A., Gray, A., Stenberg, P. and Lorand, L.** (1974). Calcium-dependent unmasking of active center cysteine during activation of fibrin stabilizing factor. *Biochemistry* 13, 3774-3780.
- Datta, S., Antonyak, M. A. and Cerione, R. A.** (2007). GTP-binding-defective forms of tissue transglutaminase trigger cell death. *Biochemistry* 46, 14819-14829.
- David, G., Van der, S. B., Marynen, P., Cassiman, J. J. and Van den, B. H.** (1992). Molecular cloning of amphiglycan, a novel integral membrane heparan sulfate proteoglycan expressed by epithelial and fibroblastic cells. *J. Cell Biol.* 118, 961-969.
- David, G.** (1993). Integral membrane heparan sulfate proteoglycans. *FASEB J.* 7, 1023-1030.
- Davis, G. E., Bayless, K. J., Davis, M. J. and Meininger, G. A.** (2000). Regulation of tissue injury responses by the exposure of matricryptic sites within extracellular matrix molecules. *Am. J. Pathol.* 156, 1489-1498.
- De Laurenzi, V. and Melino, G.** (2001). Gene disruption of tissue transglutaminase. *Mol. Cell Biol.* 21, 148-155.
- DeCristofaro, T., Affaitati, A., Cariello, L., Avvedimento, E. V. and Varrone, S.** (1999). The length of polyglutamine tract, its level of expression, the rate of degradation, and the transglutaminase activity influence the formation of intracellular aggregates. *Biochem. Biophys. Res. Commun.* 260, 150-158.
- Defilippi, P., Venturino, M., Gulino, D., Duperray, A., Boquet, P., Fiorentini, C., Volpe, G., Palmieri, M., Silengo, L. and Tarone, G.** (1997). Dissection of pathways implicated in integrin-mediated actin cytoskeleton assembly. Involvement of protein kinase C, Rho GTPase, and tyrosine phosphorylation. *J. Biol. Chem.* 272, 21726-21734.
- Del Duca, S., Beninati, S. and Serafini-Fracassini, D.** (1995). Polyamines in chloroplasts: identification of their glutamyl and acetyl derivatives. *Biochem. J.* 305 ( Pt 1), 233-237.
- Dieterich, W., Ehnis, T., Bauer, M., Donner, P., Volta, U., Riecken, E. O. and Schuppan, D.** (1997). Identification of tissue transglutaminase as the autoantigen of celiac disease. *Nat. Med.* 3, 797-801.
- Dolynchuk, K. N., dor-Samuel, R. and Bowness, J. M.** (1994). Effect of putrescine on tissue transglutaminase activity in wounds: decreased breaking strength and increased matrix fucoprotein solubility. *Plast. Reconstr. Surg.* 93, 567-573.
- Doolittle, R. F.** (1995). The multiplicity of domains in proteins. *Annu. Rev. Biochem.* 64, 287-314.
- Driscoll, H. K., Adkins, C. D., Chertow, T. E., Cordle, M. B., Matthews, K. A. and Chertow, B. S.** (1997). Vitamin A stimulation of insulin secretion: effects on transglutaminase mRNA and activity using rat islets and insulin-secreting cells. *Pancreas* 15, 69-77.
- Dubbink, H. J., de, W. L., van, H. R., Verkaik, N. S., Trapman, J. and Romijn, J. C.** (1998). The human prostate-specific transglutaminase gene (TGM4): genomic organization, tissue-specific expression, and promoter characterization. *Genomics* 51, 434-444.
- Echtermeyer, F., Baci, P. C., Saoncella, S., Ge, Y. and Goetinck, P. F.** (1999). Syndecan-4 core protein is sufficient for the assembly of focal adhesions and actin stress fibers. *J. Cell Sci.* 112 ( Pt 20), 3433-3441.

- Echtermeyer, F., Streit, M., Wilcox-Adelman, S., Saoncella, S., Denhez, F., Detmar, M. and Goetinck, P.** (2001). Delayed wound repair and impaired angiogenesis in mice lacking syndecan-4. *J. Clin. Invest* 107, R9-R14.
- Egberts, F., Heinrich, M., Jensen, J. M., Winoto-Morbach, S., Pfeiffer, S., Wickel, M., Schunck, M., Steude, J., Saftig, P., Proksch, E. et al.** (2004). Cathepsin D is involved in the regulation of transglutaminase 1 and epidermal differentiation. *J. Cell Sci.* 117, 2295-2307.
- Eitan, S. and Schwartz, M.** (1993). A transglutaminase that converts interleukin-2 into a factor cytotoxic to oligodendrocytes. *Science* 261, 106-108.
- El Nahas, A. M., Muchaneta-Kubara, E. C., Essawy, M. and Soylemezoglu, O.** (1997). Renal fibrosis: insights into pathogenesis and treatment. *Int. J. Biochem. Cell Biol.* 29, 55-62.
- El Nahas, A. M., bo-Zenah, H., Skill, N. J., Bex, S., Wild, G., Griffin, M. and Johnson, T. S.** (2004). Elevated epsilon-(gamma-glutamyl)lysine in human diabetic nephropathy results from increased expression and cellular release of tissue transglutaminase. *Nephron Clin. Pract.* 97, c108-c117.
- Elenius, K., Vainio, S., Laato, M., Salmivirta, M., Thesleff, I. and Jalkanen, M.** (1991). Induced expression of syndecan in healing wounds. *J. Cell Biol.* 114, 585-595.
- Esposito, C. and Caputo, I.** (2005). Mammalian transglutaminases. Identification of substrates as a key to physiological function and physiopathological relevance. *FEBS J.* 272, 615-631.
- Essner, J. J., Chen, E. and Ekker, S. C.** (2006). Syndecan-2. *Int. J. Biochem. Cell Biol.* 38, 152-156.
- Facchiano, A. and Facchiano, F.** (2009). Transglutaminases and their substrates in biology and human diseases: 50 years of growing. *Amino. Acids* 36, 599-614.
- Faham, S., Hileman, R. E., Fromm, J. R., Linhardt, R. J. and Rees, D. C.** (1996). Heparin structure and interactions with basic fibroblast growth factor. *Science* 271, 1116-1120.
- Fan, Q., Shike, T., Shigihara, T., Tanimoto, M., Gohda, T., Makita, Y., Wang, L. N., Horikoshi, S. and Tomino, Y.** (2003). Gene expression profile in diabetic KK/Ta mice. *Kidney Int.* 64, 1978-1985.
- Faye, C., Moreau, C., Chautard, E., Jetne, R., Fukai, N., Ruggiero, F., Humphries, M. J., Olsen, B. R. and Ricard-Blum, S.** (2009). Molecular interplay between endostatin, integrins, and heparan sulfate. *J. Biol. Chem.* 284, 22029-22040.
- Feng, J. F., Rhee, S. G. and Im, M. J.** (1996). Evidence that phospholipase delta1 is the effector in the Gh (transglutaminase II)-mediated signaling. *J. Biol. Chem.* 271, 16451-16454.
- Fesus, L., Metsis, M. L., Muszbek, L. and Koteliansky, V. E.** (1986). Transglutaminase-sensitive glutamine residues of human plasma fibronectin revealed by studying its proteolytic fragments. *Eur. J. Biochem.* 154, 371-374.
- Fesus, L., Thomazy, V. and Falus, A.** (1987). Induction and activation of tissue transglutaminase during programmed cell death. *FEBS Lett.* 224, 104-108.
- Fesus, L. and Piacentini, M.** (2002). Transglutaminase 2: an enigmatic enzyme with diverse functions. *Trends Biochem. Sci.* 27, 534-539.
- Fesus, L. and Szondy, Z.** (2005). Transglutaminase 2 in the balance of cell death and survival. *FEBS Lett.* 579, 3297-3302.

- Fisher, M., Jones, R., Huang, L., Haylor, J. L., El Nahas, A. M., Griffin, M. and Johnson, T. S.** (2008).
- Fisher, M., Jones, R. A., Huang, L., Haylor, J. L., El, N. M., Griffin, M. and Johnson, T. S.** (2009). Modulation of tissue transglutaminase in tubular epithelial cells alters extracellular matrix levels: a potential mechanism of tissue scarring. *Matrix Biol.* 28, 20-31.
- Fok, J. Y., Ekmekcioglu, S. and Mehta, K.** (2006). Implications of tissue transglutaminase expression in malignant melanoma. *Mol. Cancer Ther.* 5, 1493-1503.
- Folk, J. E. and Finlayson, J. S.** (1977). The epsilon-(gamma-glutamyl)lysine crosslink and the catalytic role of transglutaminases. *Adv. Protein Chem.* 31, 1-133.
- Folk, J. E.** (1980). Transglutaminases. *Annu. Rev. Biochem.* 49, 517-531.
- Fransson, L. A., Edgren, G., Havsmark, B. and Schmidtchen, A.** (1995). Recycling of a glycosylphosphatidylinositol-anchored heparan sulphate proteoglycan (glypican) in skin fibroblasts. *Glycobiology* 5, 407-415.
- Fraser, P. E., Nguyen, J. T., Surewicz, W. K. and Kirschner, D. A.** (1991). pH-dependent structural transitions of Alzheimer amyloid peptides. *Biophys. J.* 60, 1190-1201.
- Freund, K. F., Doshi, K. P., Gaul, S. L., Claremon, D. A., Remy, D. C., Baldwin, J. J., Pitzenberger, S. M. and Stern, A. M.** (1994). Transglutaminase inhibition by 2-[(2-oxopropyl)thio]imidazolium derivatives: mechanism of factor XIIIa inactivation. *Biochemistry* 33, 10109-10119.
- Fromm, J. R., Hileman, R. E., Caldwell, E. E., Weiler, J. M. and Linhardt, R. J.** (1997). Pattern and spacing of basic amino acids in heparin binding sites. *Arch. Biochem. Biophys.* 343, 92-100.
- Fuki, I. V., Kuhn, K. M., Lomazov, I. R., Rothman, V. L., Tuszyński, G. P., Iozzo, R. V., Swenson, T. L., Fisher, E. A. and Williams, K. J.** (1997). The syndecan family of proteoglycans. Novel receptors mediating internalization of atherogenic lipoproteins in vitro. *J. Clin. Invest* 100, 1611-1622.
- Gagliardini, E. and Benigni, A.** (2006). Role of anti-TGF-beta antibodies in the treatment of renal injury. *Cytokine Growth Factor Rev.* 17, 89-96.
- Gallo, R., Kim, C., Kokenyesi, R., Adzick, N. S. and Bernfield, M.** (1996). Syndecans-1 and -4 are induced during wound repair of neonatal but not fetal skin. *J. Invest Dermatol.* 107, 676-683.
- Gambetti, S., Dondi, A., Cervellati, C., Squerzanti, M., Pansini, F. S. and Bergamini, C. M.** (2005). Interaction with heparin protects tissue transglutaminase against inactivation by heating and by proteolysis. *Biochimie* 87, 551-555.
- Gandhi, N. S. and Mancera, R. L.** (2008). The structure of glycosaminoglycans and their interactions with proteins. *Chem. Biol. Drug Des* 72, 455-482.
- Gaudry, C. A., Verderio, E., Aeschlimann, D., Cox, A., Smith, C. and Griffin, M.** (1999). Cell surface localization of tissue transglutaminase is dependent on a fibronectin-binding site in its N-terminal beta-sandwich domain. *J. Biol. Chem.* 274, 30707-30714.
- Gentile, V., Saydak, M., Chiocca, E. A., Akande, O., Birckbichler, P. J., Lee, K. N., Stein, J. P. and Davies, P. J.** (1991). Isolation and characterization of cDNA clones to mouse macrophage and human endothelial cell tissue transglutaminases. *J. Biol. Chem.* 266, 478-483.

- Gentile, V., Thomazy, V., Piacentini, M., Fesus, L. and Davies, P. J.** (1992). Expression of tissue transglutaminase in Balb-C 3T3 fibroblasts: effects on cellular morphology and adhesion. *J. Cell Biol.* 119, 463-474.
- Gentile, V., Davies, P. J. and Baldini, A.** (1994). The human tissue transglutaminase gene maps on chromosome 20q12 by in situ fluorescence hybridization. *Genomics* 20, 295-297.
- Germack, R. and Dickenson, J. M.** (2006). Induction of beta3-adrenergic receptor functional expression following chronic stimulation with noradrenaline in neonatal rat cardiomyocytes. *J. Pharmacol. Exp. Ther.* 316, 392-402.
- Granes, F., Urena, J. M., Rocamora, N. and Vilaro, S.** (2000). Ezrin links syndecan-2 to the cytoskeleton. *J. Cell Sci.* 113 ( Pt 7), 1267-1276.
- Greenberg, C. S., Birckbichler, P. J. and Rice, R. H.** (1991). Transglutaminases: multifunctional cross-linking enzymes that stabilize tissues. *FASEB J.* 5, 3071-3077.
- Greene, D. K., Tumova, S., Couchman, J. R. and Woods, A.** (2003). Syndecan-4 associates with alpha-actinin. *J. Biol. Chem.* 278, 7617-7623.
- Grenard, P., Bresson-Hadni, S., El, A. S., Chevallier, M., Vuitton, D. A. and Ricard-Blum, S.** (2001). Transglutaminase-mediated cross-linking is involved in the stabilization of extracellular matrix in human liver fibrosis. *J. Hepatol.* 35, 367-375.
- Grenard, P., Bates, M. K. and Aeschlimann, D.** (2001). Evolution of transglutaminase genes: identification of a transglutaminase gene cluster on human chromosome 15q15. Structure of the gene encoding transglutaminase X and a novel gene family member, transglutaminase Z. *J. Biol. Chem.* 276, 33066-33078.
- Griffin, M., Smith, L. L. and Wynne, J.** (1979). Changes in transglutaminase activity in an experimental model of pulmonary fibrosis induced by paraquat. *Br. J. Exp. Pathol.* 60, 653-661.
- Griffin, M., Casadio, R. and Bergamini, C. M.** (2002). Transglutaminases: nature's biological glues. *Biochem. J.* 368, 377-396.
- Gronthos, S., Stewart, K., Graves, S. E., Hay, S. and Simmons, P. J.** (1997). Integrin expression and function on human osteoblast-like cells. *J. Bone Miner. Res.* 12, 1189-1197.
- Gulyas, M. and Hjerpe, A.** (2003). Proteoglycans and WT1 as markers for distinguishing adenocarcinoma, epithelioid mesothelioma, and benign mesothelium. *J. Pathol.* 199, 479-487.
- Gundemir, S. and Johnson, G. V.** (2009). Intracellular localization and conformational state of transglutaminase 2: implications for cell death. *PLoS. One.* 4, e6123.
- Hacker, U., Nybakken, K. and Perrimon, N.** (2005). Heparan sulphate proteoglycans: the sweet side of development. *Nat. Rev. Mol. Cell Biol.* 6, 530-541.
- Hang, J., Zemskov, E. A., Lorand, L. and Belkin, A. M.** (2005). Identification of a novel recognition sequence for fibronectin within the NH2-terminal beta-sandwich domain of tissue transglutaminase. *J. Biol. Chem.* 280, 23675-23683.
- Haroon, Z. A., Hettasch, J. M., Lai, T. S., Dewhirst, M. W. and Greenberg, C. S.** (1999). Tissue transglutaminase is expressed, active, and directly involved in rat dermal wound healing and angiogenesis. *FASEB J.* 13, 1787-1795.

- Hasegawa, G., Suwa, M., Ichikawa, Y., Ohtsuka, T., Kumagai, S., Kikuchi, M., Sato, Y. and Saito, Y.** (2003). A novel function of tissue-type transglutaminase: protein disulphide isomerase. *Biochem. J.* 373, 793-803.
- Hayashi, N., Sugimura, Y., Kawamura, J., Donjacour, A. A. and Cunha, G. R.** (1991). Morphological and functional heterogeneity in the rat prostatic gland. *Biol. Reprod.* 45, 308-321.
- Heath, D. J., Downes, S., Verderio, E. and Griffin, M.** (2001). Characterization of tissue transglutaminase in human osteoblast-like cells. *J. Bone Miner. Res.* 16, 1477-1485.
- Herman, M. L., Farasat, S., Steinbach, P. J., Wei, M. H., Toure, O., Fleckman, P., Blake, P., Bale, S. J. and Toro, J. R.** (2009). Transglutaminase-1 gene mutations in autosomal recessive congenital ichthyosis: summary of mutations (including 23 novel) and modeling of TGase-1. *Hum. Mutat.* 30, 537-547.
- Hileman, R. E., Fromm, J. R., Weiler, J. M. and Linhardt, R. J.** (1998). Glycosaminoglycan-protein interactions: definition of consensus sites in glycosaminoglycan binding proteins. *Bioessays* 20, 156-167.
- Hitomi, K.** (2005). Transglutaminases in skin epidermis. *Eur. J. Dermatol.* 15, 313-319.
- Ho, K. C., Quarmby, V. E., French, F. S. and Wilson, E. M.** (1992). Molecular cloning of rat prostate transglutaminase complementary DNA. The major androgen-regulated protein DP1 of rat dorsal prostate and coagulating gland. *J. Biol. Chem.* 267, 12660-12667.
- Hoffner, G. and Djian, P.** (2005). Transglutaminase and diseases of the central nervous system. *Front Biosci.* 10, 3078-3092.
- Horowitz, A. and Simons, M.** (1998). Phosphorylation of the cytoplasmic tail of syndecan-4 regulates activation of protein kinase Calpha. *J. Biol. Chem.* 273, 25548-25551.
- Horowitz, A. and Simons, M.** (1998). Regulation of syndecan-4 phosphorylation in vivo. *J. Biol. Chem.* 273, 10914-10918.
- Hu, H., Wang, G., Batteux, F. and Nicco, C.** (2009). Gender differences in the susceptibility to renal ischemia-reperfusion injury in BALB/c mice. *Tohoku J. Exp. Med.* 218, 325-329.
- Huang, L., Haylor, J. L., Hau, Z., Jones, R. A., Vickers, M. E., Wagner, B., Griffin, M., Saint, R. E., Coutts, I. G., El Nahas, A. M. et al.** (2009). Transglutaminase inhibition ameliorates experimental diabetic nephropathy. *Kidney Int.* 76, 383-394.
- Huang, Y., Zhang, R., Culler, S. D. and Kutner, N. G.** (2008). Costs and effectiveness of cardiac rehabilitation for dialysis patients following coronary bypass. *Kidney Int.* 74, 1079-1084.
- Hwang, J. Y., Mangala, L. S., Fok, J. Y., Lin, Y. G., Merritt, W. M., Spannuth, W. A., Nick, A. M., Fiterman, D. J., Vivas-Mejia, P. E., Deavers, M. T. et al.** (2008). Clinical and biological significance of tissue transglutaminase in ovarian carcinoma. *Cancer Res.* 68, 5849-5858.
- Hwang, K. C., Gray, C. D., Sivasubramanian, N. and Im, M. J.** (1995). Interaction site of GTP binding Gh (transglutaminase II) with phospholipase C. *J. Biol. Chem.* 270, 27058-27062.
- Ichinose, A., Tamaki, T. and Aoki, N.** (1983). Factor XIII-mediated cross-linking of NH<sub>2</sub>-terminal peptide of alpha 2-plasmin inhibitor to fibrin. *FEBS Lett.* 153, 369-371.
- Ichinose, A., Hendrickson, L. E., Fujikawa, K. and Davie, E. W.** (1986). Amino acid sequence of the a subunit of human factor XIII. *Biochemistry* 25, 6900-6906.

- Ichinose, A., McMullen, B. A., Fujikawa, K. and Davie, E. W.** (1986). Amino acid sequence of the b subunit of human factor XIII, a protein composed of ten repetitive segments. *Biochemistry* 25, 4633-4638.
- Ichinose, A., Bottenus, R. E. and Davie, E. W.** (1990). Structure of transglutaminases. *J. Biol. Chem.* 265, 13411-13414.
- Ichinose, A.** (2005). Extracellular transglutaminase: factor XIII. *Prog. Exp. Tumor Res.* 38, 192-208.
- Ideguchi, H., Nishimura, J., Nawata, H. and Hamasaki, N.** (1990). A genetic defect of erythrocyte band 4.2 protein associated with hereditary spherocytosis. *Br. J. Haematol.* 74, 347-353.
- Iismaa, S. E., Wu, M. J., Nanda, N., Church, W. B. and Graham, R. M.** (2000). GTP binding and signaling by Gh/transglutaminase II involves distinct residues in a unique GTP-binding pocket. *J. Biol. Chem.* 275, 18259-18265.
- Iismaa, S. E., Mearns, B. M., Lorand, L. and Graham, R. M.** (2009). Transglutaminases and disease: lessons from genetically engineered mouse models and inherited disorders. *Physiol Rev.* 89, 991-1023.
- Iizuka, R., Chiba, K. and Imajoh-Ohmi, S.** (2003). A novel approach for the detection of proteolytically activated transglutaminase 1 in epidermis using cleavage site-directed antibodies. *J. Invest Dermatol.* 121, 457-464.
- Ikura, K., Yokota, H., Sasaki, R. and Chiba, H.** (1989). Determination of amino- and carboxyl-terminal sequences of guinea pig liver transglutaminase: evidence for amino-terminal processing. *Biochemistry* 28, 2344-2348.
- Ikura, K., Shinagawa, R., Suto, N. and Sasaki, R.** (1994). Increase caused by interleukin-6 in promoter activity of guinea pig liver transglutaminase gene. *Biosci. Biotechnol. Biochem.* 58, 1540-1541.
- Imberty, A., Lortat-Jacob, H. and Perez, S.** (2007). Structural view of glycosaminoglycan-protein interactions. *Carbohydr. Res.* 342, 430-439.
- Iozzo, R. V.** (2005). Basement membrane proteoglycans: from cellar to ceiling. *Nat. Rev. Mol. Cell Biol.* 6, 646-656.
- Ishiguro, K., Kadomatsu, K., Kojima, T., Muramatsu, H., Tsuzuki, S., Nakamura, E., Kusugami, K., Saito, H. and Muramatsu, T.** (2000). Syndecan-4 deficiency impairs focal adhesion formation only under restricted conditions. *J. Biol. Chem.* 275, 5249-5252.
- Ishiguro, K., Kadomatsu, K., Kojima, T., Muramatsu, H., Matsuo, S., Kusugami, K., Saito, H. and Muramatsu, T.** (2001). Syndecan-4 deficiency increases susceptibility to kappa-carrageenan-induced renal damage. *Lab Invest* 81, 509-516.
- Jackson, R. L., Busch, S. J. and Cardin, A. D.** (1991). Glycosaminoglycans: molecular properties, protein interactions, and role in physiological processes. *Physiol Rev.* 71, 481-539.
- Janus, T. J., Lewis, S. D., Lorand, L. and Shafer, J. A.** (1983). Promotion of thrombin-catalyzed activation of factor XIII by fibrinogen. *Biochemistry* 22, 6269-6272.
- Jeong, J., Han, I., Lim, Y., Kim, J., Park, I., Woods, A., Couchman, J. R. and Oh, E. S.** (2001). Rat embryo fibroblasts require both the cell-binding and the heparin-binding domains of fibronectin for survival. *Biochem. J.* 356, 531-537.

- Jeong, J. M., Murthy, S. N., Radek, J. T. and Lorand, L.** (1995). The fibronectin-binding domain of transglutaminase. *J. Biol. Chem.* 270, 5654-5658.
- Johnson, T., Fisher, M., Haylor, J. L., Hau Z, Skill, N. J., Jones, R. A., Coutts, I. G., Saint, R. E., Vickers M., Nahas M.E. et al.** (2007). Transglutaminase inhibition reduces fibrosis and preserves function in experimental chronic kidney disease. pp. 3078-3088.
- Johnson, T. S., Griffin, M., Thomas, G. L., Skill, J., Cox, A., Yang, B., Nicholas, B., Bireckbichler, P. J., Muchaneta-Kubara, C. and Meguid El, N. A.** (1997). The role of transglutaminase in the rat subtotal nephrectomy model of renal fibrosis. *J. Clin. Invest* 99, 2950-2960.
- Johnson, T. S., Skill, N. J., El Nahas, A. M., Oldroyd, S. D., Thomas, G. L., Douthwaite, J. A., Haylor, J. L. and Griffin, M.** (1999). Transglutaminase transcription and antigen translocation in experimental renal scarring. *J. Am. Soc Nephrol.* 10, 2146-2157.
- Johnson, T. S., Haylor, J. L., Thomas, G. L., Fisher, M. and El Nahas, A. M.** (2002). Matrix metalloproteinases and their inhibitions in experimental renal scarring. *Exp. Nephrol.* 10, 182-195.
- Johnson, T. S., El-Koraie, A. F., Skill, N. J., Baddour, N. M., El Nahas, A. M., Njloma, M., Adam, A. G. and Griffin, M.** (2003). Tissue transglutaminase and the progression of human renal scarring. *J. Am. Soc. Nephrol.* 14, 2052-2062.
- Johnson, T. S., bo-Zenah, H., Skill, J. N., Bex, S., Wild, G., Brown, C. B., Griffin, M. and El Nahas, A. M.** (2004). Tissue transglutaminase: a mediator and predictor of chronic allograft nephropathy? *Transplantation* 77, 1667-1675.
- Jones, R. A., Nicholas, B., Mian, S., Davies, P. J. and Griffin, M.** (1997). Reduced expression of tissue transglutaminase in a human endothelial cell line leads to changes in cell spreading, cell adhesion and reduced polymerisation of fibronectin. *J. Cell Sci.* 110 ( Pt 19), 2461-2472.
- Jones, R. A., Kotsakis, P., Johnson, T. S., Chau, D. Y., Ali, S., Melino, G. and Griffin, M.** (2006). Matrix changes induced by transglutaminase 2 lead to inhibition of angiogenesis and tumor growth. *Cell Death. Differ.* 13, 1442-1453.
- Junn, E., Ronchetti, R. D., Quezado, M. M., Kim, S. Y. and Mouradian, M. M.** (2003). Tissue transglutaminase-induced aggregation of alpha-synuclein: Implications for Lewy body formation in Parkinson's disease and dementia with Lewy bodies. *Proc. Natl. Acad. Sci. U. S. A* 100, 2047-2052.
- Kanaji, T., Ozaki, H., Takao, T., Kawajiri, H., Ide, H., Motoki, M. and Shimonishi, Y.** (1993). Primary structure of microbial transglutaminase from *Streptovorticillium* sp. strain s-8112. *J. Biol. Chem.* 268, 11565-11572.
- Kato, M., Wang, H., Bernfield, M., Gallagher, J. T. and Turnbull, J. E.** (1994). Cell surface syndecan-1 on distinct cell types differs in fine structure and ligand binding of its heparan sulfate chains. *J. Biol. Chem.* 269, 18881-18890.
- Kato, M., Wang, H., Kainulainen, V., Fitzgerald, M. L., Ledbetter, S., Ornitz, D. M. and Bernfield, M.** (1998). Physiological degradation converts the soluble syndecan-1 ectodomain from an inhibitor to a potent activator of FGF-2. *Nat. Med.* 4, 691-697.
- Kim, H. C., Lewis, M. S., Gorman, J. J., Park, S. C., Girard, J. E., Folk, J. E. and Chung, S. I.** (1990). Protransglutaminase E from guinea pig skin. Isolation and partial characterization. *J. Biol. Chem.* 265, 21971-21978.

- Kim, H. C., Nemes, Z., Idler, W. W., Hyde, C. C., Steinert, P. M. and Ahvazi, B.** (2001). Crystallization and preliminary X-ray analysis of human transglutaminase 3 from zymogen to active form. *J. Struct. Biol.* 135, 73-77.
- Kim, S. Y., Chung, S. I. and Steinert, P. M.** (1995). Highly active soluble processed forms of the transglutaminase 1 enzyme in epidermal keratinocytes. *J. Biol. Chem.* 270, 18026-18035.
- Kim, S. Y. and Bae, C. D.** (1998). Calpain inhibitors reduce the cornified cell envelope formation by inhibiting proteolytic processing of transglutaminase 1. *Exp. Mol. Med.* 30, 257-262.
- Kleman, J. P., Aeschlimann, D., Paulsson, M. and van der, R. M.** (1995). Transglutaminase-catalyzed cross-linking of fibrils of collagen V/XI in A204 rhabdomyosarcoma cells. *Biochemistry* 34, 13768-13775.
- Kojima, S., Nara, K. and Rifkin, D. B.** (1993). Requirement for transglutaminase in the activation of latent transforming growth factor-beta in bovine endothelial cells. *J. Cell Biol.* 121, 439-448.
- Kojima, S., Inui, T., Muramatsu, H., Suzuki, Y., Kadomatsu, K., Yoshizawa, M., Hirose, S., Kimura, T., Sakakibara, S. and Muramatsu, T.** (1997). Dimerization of midkine by tissue transglutaminase and its functional implication. *J. Biol. Chem.* 272, 9410-9416.
- Kojima, T., Takagi, A., Maeda, M., Segawa, T., Shimizu, A., Yamamoto, K., Matsushita, T. and Saito, H.** (2001). Plasma levels of syndecan-4 (ryudocan) are elevated in patients with acute myocardial infarction. *Thromb. Haemost.* 85, 793-799.
- Kokenyesi, R. and Bernfield, M.** (1994). Core protein structure and sequence determine the site and presence of heparan sulfate and chondroitin sulfate on syndecan-1. *J. Biol. Chem.* 269, 12304-12309.
- Kolset, S. O. and Gallagher, J. T.** (1990). Proteoglycans in haemopoietic cells. *Biochim. Biophys. Acta* 1032, 191-211.
- Kolset, S. O., Prydz, K. and Pejler, G.** (2004). Intracellular proteoglycans. *Biochem. J.* 379, 217-227.
- Korponay-Szabo, I. R., Halttunen, T., Szalai, Z., Laurila, K., Kiraly, R., Kovacs, J. B., Fesus, L. and Maki, M.** (2004). In vivo targeting of intestinal and extraintestinal transglutaminase 2 by coeliac autoantibodies. *Gut* 53, 641-648.
- Korsgren, C. and Cohen, C. M.** (1986). Purification and properties of human erythrocyte band 4.2. Association with the cytoplasmic domain of band 3. *J. Biol. Chem.* 261, 5536-5543.
- Korsgren, C. and Cohen, C. M.** (1988). Associations of human erythrocyte band 4.2. Binding to ankyrin and to the cytoplasmic domain of band 3. *J. Biol. Chem.* 263, 10212-10218.
- Korsgren, C., Lawler, J., Lambert, S., Speicher, D. and Cohen, C. M.** (1990). Complete amino acid sequence and homologies of human erythrocyte membrane protein band 4.2. *Proc. Natl. Acad. Sci. U. S. A* 87, 613-617.
- Kotsakis, P.** (2005). Physiological and therapeutic roles of tissue transglutaminase in tumour growth and angiogenesis.
- Kotsakis, P. and Griffin, M.** (2007). Tissue transglutaminase in tumour progression: friend or foe? *Amino Acids* 33, 373-384.
- Kramer, K. L., Barnette, J. E. and Yost, H. J.** (2002). PKCgamma regulates syndecan-2 inside-out signaling during xenopus left-right development. *Cell* 111, 981-990.

- Krasnikov, B. F., Kim, S. Y., McConoughey, S. J., Ryu, H., Xu, H., Stavrovskaya, I., Iismaa, S. E., Mearns, B. M., Ratan, R. R., Blass, J. P. et al.** (2005). Transglutaminase activity is present in highly purified nonsynaptosomal mouse brain and liver mitochondria. *Biochemistry* 44, 7830-7843.
- Kuncio, G. S., Tsyganskaya, M., Zhu, J., Liu, S. L., Nagy, L., Thomazy, V., Davies, P. J. and Zern, M. A.** (1998). TNF-alpha modulates expression of the tissue transglutaminase gene in liver cells. *Am. J. Physiol* 274, G240-G245.
- Kuschert, G. S., Coulin, F., Power, C. A., Proudfoot, A. E., Hubbard, R. E., Hoogewerf, A. J. and Wells, T. N.** (1999). Glycosaminoglycans interact selectively with chemokines and modulate receptor binding and cellular responses. *Biochemistry* 38, 12959-12968.
- Laemmli, U. K.** (1970). Cleavage of structural proteins during the assembly of the head of bacteriophage T4. *Nature* 227, 680-685.
- Lai, T. S., Tucker, T., Burke, J. R., Strittmatter, W. J. and Greenberg, C. S.** (2004). Effect of tissue transglutaminase on the solubility of proteins containing expanded polyglutamine repeats. *J. Neurochem.* 88, 1253-1260.
- Lansdown, A. B.** (2002). Calcium: a potential central regulator in wound healing in the skin. *Wound. Repair Regen.* 10, 271-285.
- Lee, J., Kim, Y. S., Choi, D. H., Bang, M. S., Han, T. R., Joh, T. H. and Kim, S. Y.** (2004). Transglutaminase 2 induces nuclear factor-kappaB activation via a novel pathway in BV-2 microglia. *J. Biol. Chem.* 279, 53725-53735.
- Lee, J. H., Jang, S. I., Yang, J. M., Markova, N. G. and Steinert, P. M.** (1996). The proximal promoter of the human transglutaminase 3 gene. Stratified squamous epithelial-specific expression in cultured cells is mediated by binding of Sp1 and ets transcription factors to a proximal promoter element. *J. Biol. Chem.* 271, 4561-4568.
- LeMosy, E. K., Erickson, H. P., Beyer, W. F., Jr., Radek, J. T., Jeong, J. M., Murthy, S. N. and Lorand, L.** (1992). Visualization of purified fibronectin-transglutaminase complexes. *J. Biol. Chem.* 267, 7880-7885.
- Leppa, S., Vlemineckx, K., Van, R. F. and Jalkanen, M.** (1996). Syndecan-1 expression in mammary epithelial tumor cells is E-cadherin-dependent. *J. Cell Sci.* 109 ( Pt 6), 1393-1403.
- Lewis, S. D., Janus, T. J., Lorand, L. and Shafer, J. A.** (1985). Regulation of formation of factor XIIIa by its fibrin substrates. *Biochemistry* 24, 6772-6777.
- Li, X., Verderio, E. and Griffin, M.** (2002). Effects of tissue transglutaminase expression on cell stress induced by 3-nitropropionic acid (3NP). p. 209.
- Liu, J., Shriver, Z., Pope, R. M., Thorp, S. C., Duncan, M. B., Copeland, R. J., Raska, C. S., Yoshida, K., Eisenberg, R. J., Cohen, G. et al.** (2002). Characterization of a heparan sulfate octasaccharide that binds to herpes simplex virus type 1 glycoprotein D. *J. Biol. Chem.* 277, 33456-33467.
- Liu, S., Cerione, R. A. and Clardy, J.** (2002). Structural basis for the guanine nucleotide-binding activity of tissue transglutaminase and its regulation of transamidation activity. *Proc. Natl. Acad. Sci. U. S. A* 99, 2743-2747.
- Livak, K. J. and Schmittgen, T. D.** (2001). Analysis of relative gene expression data using real-time quantitative PCR and the 2(-Delta Delta C(T)) Method. *Methods* 25, 402-408.

- Lohnes, D., Mark, M., Mendelsohn, C., Dolle, P., Decimo, D., LeMeur, M., Dierich, A., Gorry, P. and Chambon, P.** (1995). Developmental roles of the retinoic acid receptors. *J. Steroid Biochem. Mol. Biol.* 53, 475-486.
- Longley, R. L., Woods, A., Fleetwood, A., Cowling, G. J., Gallagher, J. T. and Couchman, J. R.** (1999). Control of morphology, cytoskeleton and migration by syndecan-4. *J. Cell Sci.* 112 ( Pt 20), 3421-3431.
- Lorand, L. and Konishi, K.** (1964). Activation of the fibrin stabilising factor of plasma by thrombin. *Arch. Biochem. Biophys.* 105, 58-67.
- Lorand, L., Gray, A. J., Brown, K., Credo, R. B., Curtis, C. G., Domanik, R. A. and Stenberg, P.** (1974). Dissociation of the subunit structure of fibrin stabilizing factor during activation of the zymogen. *Biochem. Biophys. Res. Commun.* 56, 914-922.
- Lorand, L., Losowsky, M. S. and Miloszewski, K. J.** (1980). Human factor XIII: fibrin-stabilizing factor. *Prog. Hemost. Thromb.* 5, 245-290.
- Lorand, L., Credo, R. B. and Janus, T. J.** (1981). Factor XIII (fibrin-stabilizing factor). *Methods Enzymol.* 80 Pt C, 333-341.
- Lorand, L. and Conrad, S. M.** (1984). Transglutaminases. *Mol. Cell Biochem.* 58, 9-35.
- Lorand, L.** (2001). Factor XIII: structure, activation, and interactions with fibrinogen and fibrin. *Ann. N. Y. Acad. Sci.* 936, 291-311.
- Lorand, L. and Graham, R. M.** (2003). Transglutaminases: crosslinking enzymes with pleiotropic functions. *Nat. Rev. Mol. Cell Biol.* 4, 140-156.
- Lu, S., Saydak, M., Gentile, V., Stein, J. P. and Davies, P. J.** (1995). Isolation and characterization of the human tissue transglutaminase gene promoter. *J. Biol. Chem.* 270, 9748-9756.
- Lu, S. and Davies, P. J.** (1997). Regulation of the expression of the tissue transglutaminase gene by DNA methylation. *Proc. Natl. Acad. Sci. U. S. A* 94, 4692-4697.
- Lundqvist, K. and Schmidtchen, A.** (2001). Immunohistochemical studies on proteoglycan expression in normal skin and chronic ulcers. *Br. J. Dermatol.* 144, 254-259.
- MacArthur, J. M., Bishop, J. R., Stanford, K. I., Wang, L., Bensadoun, A., Witztum, J. L. and Esko, J. D.** (2007). Liver heparan sulfate proteoglycans mediate clearance of triglyceride-rich lipoproteins independently of LDL receptor family members. *J. Clin. Invest* 117, 153-164.
- Maccarana, M., Sakura, Y., Tawada, A., Yoshida, K. and Lindahl, U.** (1996). Domain structure of heparan sulfates from bovine organs. *J. Biol. Chem.* 271, 17804-17810.
- MacDonald, M. E., Ambrose, C. M., Dujao, M. P. and et al.** (1993). A novel gene containing a trinucleotide repeat that is expanded and unstable on Huntington's disease chromosomes. *Cell* 72, 971-983.
- Maglio, M., Florian, F., Vecchiet, M., Auricchio, R., Paparo, F., Spadaro, R., Zanzi, D., Rapacciuolo, L., Franzese, A., Sblattero, D. et al.** (2009). Majority of children with type 1 diabetes produce and deposit anti-tissue transglutaminase antibodies in the small intestine. *Diabetes* 58, 1578-1584.
- Mahley, R. W. and Ji, Z. S.** (1999). Remnant lipoprotein metabolism: key pathways involving cell-surface heparan sulfate proteoglycans and apolipoprotein E. *J. Lipid Res.* 40, 1-16.

- Mahoney, D. J., Whittle, J. D., Milner, C. M., Clark, S. J., Mulloy, B., Buttle, D. J., Jones, G. C., Day, A. J. and Short, R. D.** (2004). A method for the non-covalent immobilization of heparin to surfaces. *Anal. Biochem.* 330, 123-129.
- Makalowski, W., Mitchell, G. A. and Labuda, D.** (1994). Alu sequences in the coding regions of mRNA: a source of protein variability. *Trends Genet.* 10, 188-193.
- Mallone, R. and Van Endert P.** (2008). T cells in the pathogenesis of type 1 diabetes. *Curr. Diab. Rep.* 8, 101-106.
- Mangala, L. S. and Mehta, K.** (2005). Tissue transglutaminase (TG2) in cancer biology. *Prog. Exp. Tumor Res.* 38, 125-138.
- Mann, A. P., Verma, A., Sethi, G., Manavathi, B., Wang, H., Fok, J. Y., Kunnumakkara, A. B., Kumar, R., Aggarwal, B. B. and Mehta, K.** (2006). Overexpression of tissue transglutaminase leads to constitutive activation of nuclear factor-kappaB in cancer cells: delineation of a novel pathway. *Cancer Res.* 66, 8788-8795.
- Martinez, J., Chalupowicz, D. G., Roush, R. K., Sheth, A. and Barsigian, C.** (1994). Transglutaminase-mediated processing of fibronectin by endothelial cell monolayers. *Biochemistry* 33, 2538-2545.
- Mastroberardino, P. G., Iannicola, C., Nardacci, R., Bernassola, F., De, L., V, Melino, G., Moreno, S., Pavone, F., Oliverio, S., Fesus, L. et al.** (2002). 'Tissue' transglutaminase ablation reduces neuronal death and prolongs survival in a mouse model of Huntington's disease. *Cell Death. Differ.* 9, 873-880.
- Matsuki, M., Yamashita, F., Ishida-Yamamoto, A., Yamada, K., Kinoshita, C., Fushiki, S., Ueda, E., Morishima, Y., Tabata, K., Yasuno, H. et al.** (1998). Defective stratum corneum and early neonatal death in mice lacking the gene for transglutaminase 1 (keratinocyte transglutaminase). *Proc. Natl. Acad. Sci. U. S. A* 95, 1044-1049.
- McKee, P. A., Mattock, P. and Hill, R. L.** (1970). Subunit structure of human fibrinogen, soluble fibrin, and cross-linked insoluble fibrin. *Proc. Natl. Acad. Sci. U. S. A* 66, 738-744.
- Mearns B., Nanda M., Michalick J., Iismaa S. and Graham, R. M.** (2002). Impaired wound healing and altered fibroblast cytoskeletal dynamics in Gh knockout mice.
- Mehta, K., Rao, U. R., Vickery, A. C. and Fesus, L.** (1992). Identification of a novel transglutaminase from the filarial parasite *Brugia malayi* and its role in growth and development. *Mol. Biochem. Parasitol.* 53, 1-15.
- Mehta, K., Fok, J., Miller, F. R., Koul, D. and Sahin, A. A.** (2004). Prognostic significance of tissue transglutaminase in drug resistant and metastatic breast cancer. *Clin. Cancer Res.* 10, 8068-8076.
- Mehta, K.** (2005). Mammalian transglutaminases: a family portrait. *Prog. Exp. Tumor Res.* 38, 1-18.
- Mishra, S. and Murphy, L. J.** (2004). Tissue transglutaminase has intrinsic kinase activity: identification of transglutaminase 2 as an insulin-like growth factor-binding protein-3 kinase. *J. Biol. Chem.* 279, 23863-23868.
- Mishra, S., Melino, G. and Murphy, L. J.** (2007). Transglutaminase 2 kinase activity facilitates protein kinase A-induced phosphorylation of retinoblastoma protein. *J. Biol. Chem.* 282, 18108-18115.

- Mitra, S. K., Hanson, D. A. and Schlaepfer, D. D.** (2005). Focal adhesion kinase: in command and control of cell motility. *Nat. Rev. Mol. Cell Biol.* 6, 56-68.
- Mohammed, N., Haylor, J. L., au Z, I Nahas, A. M., riffin, M. and ohnson, T. S.** (2006).
- Molberg, O., McAdam, S. N. and Sollid, L. M.** (2000). Role of tissue transglutaminase in celiac disease. *J. Pediatr. Gastroenterol. Nutr.* 30, 232-240.
- Monsonogo, A., Friedmann, I., Shani, Y., Eisenstein, M. and Schwartz, M.** (1998). GTP-dependent conformational changes associated with the functional switch between Galpha and cross-linking activities in brain-derived tissue transglutaminase. *J. Mol. Biol.* 282, 713-720.
- Morgan, M. R., Humphries, M. J. and Bass, M. D.** (2007). Synergistic control of cell adhesion by integrins and syndecans. *Nat. Rev. Mol. Cell Biol.* 8, 957-969.
- Morita, H., David, G., Mizutani, A., Shinzato, T., Habuchi, H., Maeda, K. and Kimata, K.** (1994). Heparan sulfate proteoglycans in the human sclerosing and scarring kidney. Changes in heparan sulfate moiety. *Contrib. Nephrol.* 107, 174-179.
- Morris, G. M., Goodsell, D. S., Huey, R. and Olson, A. J.** (1996). Distributed automated docking of flexible ligands to proteins: parallel applications of AutoDock 2.4. *J. Comput. Aided Mol. Des* 10, 293-304.
- Muesch, A., Hartmann, E., Rohde, K., Rubartelli, A., Sitia, R. and Rapoport, T. A.** (1990). A novel pathway for secretory proteins? *Trends Biochem. Sci.* 15, 86-88.
- Murthy, S. N., Iismaa, S., Begg, G., Freymann, D. M., Graham, R. M. and Lorand, L.** (2002). Conserved tryptophan in the core domain of transglutaminase is essential for catalytic activity. *Proc. Natl. Acad. Sci. U. S. A* 99, 2738-2742.
- Muszbek, L., Bagoly, Z., Bereczky, Z. and Katona, E.** (2008). The involvement of blood coagulation factor XIII in fibrinolysis and thrombosis. *Cardiovasc. Hematol. Agents Med. Chem.* 6, 190-205.
- Nakaoka, H., Perez, D. M., Baek, K. J., Das, T., Husain, A., Misono, K., Im, M. J. and Graham, R. M.** (1994). Gh: a GTP-binding protein with transglutaminase activity and receptor signaling function. *Science* 264, 1593-1596.
- Nanda, N., Iismaa, S. E., Copeland, N. G., Gilbert, D. J., Jenkins, N., Graham, R. M. and Sutrave, P.** (1999). Organization and chromosomal mapping of mouse Gh/tissue transglutaminase gene (Tgm2). *Arch. Biochem. Biophys.* 366, 151-156.
- Nardacci, R., Lo, I. O., Ciccocanti, F., Falasca, L., Adesso, M., Amendola, A., Antonucci, G., Craxi, A., Fimia, G. M., Iadevaia, V. et al.** (2003). Transglutaminase type II plays a protective role in hepatic injury. *Am. J. Pathol.* 162, 1293-1303.
- Nemes, Z., Marekov, L. N., Fesus, L. and Steinert, P. M.** (1999). A novel function for transglutaminase 1: attachment of long-chain omega-hydroxyceramides to involucrin by ester bond formation. *Proc. Natl. Acad. Sci. U. S. A* 96, 8402-8407.
- Nicholas, B., Smethurst, P., Verderio, E., Jones, R. and Griffin, M.** (2003). Cross-linking of cellular proteins by tissue transglutaminase during necrotic cell death: a mechanism for maintaining tissue integrity. *Biochem. J.* 371, 413-422.
- Nickel, W.** (2007). Unconventional secretion: an extracellular trap for export of fibroblast growth factor 2. *J. Cell Sci.* 120, 2295-2299.

- Noguchi, K., Ishikawa, K., Yokoyama, K., Ohtsuka, T., Nio, N. and Suzuki, E.** (2001). Crystal structure of red sea bream transglutaminase. *J. Biol. Chem.* 276, 12055-12059.
- Nunes, I., Gleizes, P. E., Metz, C. N. and Rifkin, D. B.** (1997). Latent transforming growth factor-beta binding protein domains involved in activation and transglutaminase-dependent cross-linking of latent transforming growth factor-beta. *J. Cell Biol.* 136, 1151-1163.
- Oh, E. S., Woods, A. and Couchman, J. R.** (1997a). Multimerization of the cytoplasmic domain of syndecan-4 is required for its ability to activate protein kinase C. *J. Biol. Chem.* 272, 11805-11811.
- Oh, E. S., Woods, A. and Couchman, J. R.** (1997b). Syndecan-4 proteoglycan regulates the distribution and activity of protein kinase C. *J. Biol. Chem.* 272, 8133-8136.
- Oh, E. S., Woods, A., Lim, S. T., Theibert, A. W. and Couchman, J. R.** (1998). Syndecan-4 proteoglycan cytoplasmic domain and phosphatidylinositol 4,5-bisphosphate coordinately regulate protein kinase C activity. *J. Biol. Chem.* 273, 10624-10629.
- Ophascharoensuk, V., Pippin, J. W., Gordon, K. L., Shankland, S. J., Couser, W. G. and Johnson, R. J.** (1998). Role of intrinsic renal cells versus infiltrating cells in glomerular crescent formation. *Kidney Int.* 54, 416-425.
- Oppen-Berntsen, D. O., Helvik, J. V. and Walther, B. T.** (1990). The major structural proteins of cod (*Gadus morhua*) eggshells and protein crosslinking during teleost egg hardening. *Dev. Biol.* 137, 258-265.
- Owen, J. D., Ruest, P. J., Fry, D. W. and Hanks, S. K.** (1999). Induced focal adhesion kinase (FAK) expression in FAK-null cells enhances cell spreading and migration requiring both auto- and activation loop phosphorylation sites and inhibits adhesion-dependent tyrosine phosphorylation of Pyk2. *Mol. Cell Biol.* 19, 4806-4818.
- Owen, R. A., Bungay, P. J., Hussain, M. and Griffin, M.** (1988). Transglutaminase-catalysed cross-linking of proteins phosphorylated in the intact glucose-stimulated pancreatic beta-cell. *Biochim. Biophys. Acta* 968, 220-230.
- Park, H., Kim, Y., Lim, Y., Han, I. and Oh, E. S.** (2002). Syndecan-2 mediates adhesion and proliferation of colon carcinoma cells. *J. Biol. Chem.* 277, 29730-29736.
- Pedersen, L. C., Yee, V. C., Bishop, P. D., Le, T., I, Teller, D. C. and Stenkamp, R. E.** (1994). Transglutaminase factor XIII uses proteinase-like catalytic triad to crosslink macromolecules. *Protein Sci.* 3, 1131-1135.
- Pellegrini, L., Burke, D. F., von, D. F., Mulloy, B. and Blundell, T. L.** (2000). Crystal structure of fibroblast growth factor receptor ectodomain bound to ligand and heparin. *Nature* 407, 1029-1034.
- Peng, X., Zhang, Y., Zhang, H., Graner, S., Williams, J. F., Levitt, M. L. and Lokshin, A.** (1999). Interaction of tissue transglutaminase with nuclear transport protein importin-alpha3. *FEBS Lett.* 446, 35-39.
- Pierce, A., Lyon, M., Hampson, I. N., Cowling, G. J. and Gallagher, J. T.** (1992). Molecular cloning of the major cell surface heparan sulfate proteoglycan from rat liver. *J. Biol. Chem.* 267, 3894-3900.
- Pietroni, V., Di, G. S., Paradisi, A., Ahvazi, B., Candi, E. and Melino, G.** (2008). Inactive and highly active, proteolytically processed transglutaminase-5 in epithelial cells. *J. Invest Dermatol.* 128, 2760-2766.

- Pinkas, D. M., Strop, P., Brunger, A. T. and Khosla, C.** (2007). Transglutaminase 2 undergoes a large conformational change upon activation. *PLoS. Biol.* 5, e327.
- Piper, J. L., Gray, G. M. and Khosla, C.** (2004). Effect of prolyl endopeptidase on digestive-resistant gliadin peptides in vivo. *J. Pharmacol. Exp. Ther.* 311, 213-219.
- Porta, R., Esposito, C., De, S. A., Fusco, A., Iannone, M. and Metafora, S.** (1986). Sperm maturation in human semen: role of transglutaminase-mediated reactions. *Biol. Reprod.* 35, 965-970.
- Porzio, O., Massa, O., Cunsolo, V., Colombo, C., Malaponti, M., Bertuzzi, F., Hansen, T., Johansen, A., Pedersen, O., Meschi, F. et al.** (2007). Missense mutations in the TGM2 gene encoding transglutaminase 2 are found in patients with early-onset type 2 diabetes. Mutation in brief no. 982. Online. *Hum. Mutat.* 28, 1150.
- Prince, C. W., Dickie, D. and Krumdieck, C. L.** (1991). Osteopontin, a substrate for transglutaminase and factor XIII activity. *Biochem. Biophys. Res. Commun.* 177, 1205-1210.
- Puszkin, E. G. and Raghuraman, V.** (1985). Catalytic properties of a calmodulin-regulated transglutaminase from human platelet and chicken gizzard. *J. Biol. Chem.* 260, 16012-16020.
- Qiu, J. F., Zhang, Z. Q., Chen, W. and Wu, Z. Y.** (2007). Cystamine ameliorates liver fibrosis induced by carbon tetrachloride via inhibition of tissue transglutaminase. *World J. Gastroenterol.* 13, 4328-4332.
- Quarsten, H., Molberg, O., Fugger, L., McAdam, S. N. and Sollid, L. M.** (1999). HLA binding and T cell recognition of a tissue transglutaminase-modified gliadin epitope. *Eur. J. Immunol.* 29, 2506-2514.
- Radek, J. T., Jeong, J. M., Murthy, S. N., Ingham, K. C. and Lorand, L.** (1993). Affinity of human erythrocyte transglutaminase for a 42-kDa gelatin-binding fragment of human plasma fibronectin. *Proc. Natl. Acad. Sci. U. S. A* 90, 3152-3156.
- Raghunath, M., Hopfner, B., Aeschlimann, D., Luthi, U., Meuli, M., Altermatt, S., Gobet, R., Bruckner-Tuderman, L. and Steinmann, B.** (1996). Cross-linking of the dermo-epidermal junction of skin regenerating from keratinocyte autografts. Anchoring fibrils are a target for tissue transglutaminase. *J. Clin. Invest* 98, 1174-1184.
- Raulo, E., Chernousov, M. A., Carey, D. J., Nolo, R. and Rauvala, H.** (1994). Isolation of a neuronal cell surface receptor of heparin binding growth-associated molecule (HB-GAM). Identification as N-syndecan (syndecan-3). *J. Biol. Chem.* 269, 12999-13004.
- Ren, X. D., Kiosses, W. B. and Schwartz, M. A.** (1999). Regulation of the small GTP-binding protein Rho by cell adhesion and the cytoskeleton. *EMBO J.* 18, 578-585.
- Ren, X. D., Kiosses, W. B., Sieg, D. J., Otey, C. A., Schlaepfer, D. D. and Schwartz, M. A.** (2000). Focal adhesion kinase suppresses Rho activity to promote focal adhesion turnover. *J. Cell Sci.* 113 ( Pt 20), 3673-3678.
- Richards, R. J., Masek, L. C. and Brown, R. F.** (1991). Biochemical and cellular mechanisms of pulmonary fibrosis. *Toxicol. Pathol.* 19, 526-539.
- Rintala, M., Inki, P., Klemi, P., Jalkanen, M. and Grenman, S.** (1999). Association of syndecan-1 with tumor grade and histology in primary invasive cervical carcinoma. *Gynecol. Oncol.* 75, 372-378.

- Ritter, S. J. and Davies, P. J.** (1998). Identification of a transforming growth factor-beta1/bone morphogenetic protein 4 (TGF-beta1/BMP4) response element within the mouse tissue transglutaminase gene promoter. *J. Biol. Chem.* 273, 12798-12806.
- Robinson, N. J., Baker, P. N., Jones, C. J. and Aplin, J. D.** (2007). A role for tissue transglutaminase in stabilization of membrane-cytoskeletal particles shed from the human placenta. *Biol. Reprod.* 77, 648-657.
- Rock, M. J., Cain, S. A., Freeman, L. J., Morgan, A., Melody, K., Marson, A., Shuttleworth, C. A., Weiss, A. S. and Kielty, C. M.** (2004). Molecular basis of elastic fiber formation. Critical interactions and a tropoelastin-fibrillin-1 cross-link. *J. Biol. Chem.* 279, 23748-23758.
- Rosenberg, R. D., Shworak, N. W., Liu, J., Schwartz, J. J. and Zhang, L.** (1997). Heparan sulfate proteoglycans of the cardiovascular system. Specific structures emerge but how is synthesis regulated? *J. Clin. Invest* 100, S67-S75.
- Roughley, P. J.** (2006). The structure and function of cartilage proteoglycans. *Eur. Cell Mater.* 12, 92-101.
- Ruan, Q. and Johnson, G. V.** (2007). Transglutaminase 2 in neurodegenerative disorders. *Front Biosci.* 12, 891-904.
- Rudd, T. R., Guimond, S. E., Skidmore, M. A., Duchesne, L., Guerrini, M., Torri, G., Cosentino, C., Brown, A., Clarke, D. T., Turnbull, J. E. et al.** (2007). Influence of substitution pattern and cation binding on conformation and activity in heparin derivatives. *Glycobiology* 17, 983-993.
- Rybicki, A. C., Heath, R., Wolf, J. L., Lubin, B. and Schwartz, R. S.** (1988). Deficiency of protein 4.2 in erythrocytes from a patient with a Coombs negative hemolytic anemia. Evidence for a role of protein 4.2 in stabilizing ankyrin on the membrane. *J. Clin. Invest* 81, 893-901.
- Sakata, Y. and Aoki, N.** (1982). Significance of cross-linking of alpha 2-plasmin inhibitor to fibrin in inhibition of fibrinolysis and in hemostasis. *J. Clin. Invest* 69, 536-542.
- Salamat-Miller, N., Fang, J., Seidel, C. W., Assenov, Y., Albrecht, M. and Middaugh, C. R.** (2007). A network-based analysis of polyanion-binding proteins utilizing human protein arrays. *J. Biol. Chem.* 282, 10153-10163.
- Sambrook, J., Fritsch, E. and Maniatis, T.** (1989). *Molecular cloning*.
- Sane, D. C., Moser, T. L., Pippen, A. M., Parker, C. J., Achyuthan, K. E. and Greenberg, C. S.** (1988). Vitronectin is a substrate for transglutaminases. *Biochem. Biophys. Res. Commun.* 157, 115-120.
- Sane, D. C., Moser, T. L., Parker, C. J., Seiffert, D., Loskutoff, D. J. and Greenberg, C. S.** (1990). Highly sulfated glycosaminoglycans augment the cross-linking of vitronectin by guinea pig liver transglutaminase. Functional studies of the cross-linked vitronectin multimers. *J. Biol. Chem.* 265, 3543-3548.
- Sane, D. C., Kontos, J. L. and Greenberg, C. S.** (2007). Roles of transglutaminases in cardiac and vascular diseases. *Front Biosci.* 12, 2530-2545.
- Saoncella, S., Echtermeyer, F., Denhez, F., Nowlen, J. K., Mosher, D. F., Robinson, S. D., Hynes, R. O. and Goetinck, P. F.** (1999). Syndecan-4 signals cooperatively with integrins in a Rho-dependent manner in the assembly of focal adhesions and actin stress fibers. *Proc. Natl. Acad. Sci. U. S. A* 96, 2805-2810.

- Sarang, Z., Molnar, P., Nemeth, T., Gomba, S., Kardon, T., Melino, G., Cotecchia, S., Fesus, L. and Szondy, Z.** (2005). Tissue transglutaminase (TG2) acting as G protein protects hepatocytes against Fas-mediated cell death in mice. *Hepatology* 42, 578-587.
- Sardy, M., Odenthal, U., Karpati, S., Paulsson, M. and Smyth, N.** (1999). Recombinant human tissue transglutaminase ELISA for the diagnosis of gluten-sensitive enteropathy. *Clin. Chem.* 45, 2142-2149.
- Sarkar, N., Clarke, D. and Waelsch, H.** (1957). An enzymically catalysed incorporation of amines into proteins.
- Sasisekharan, R. and Venkataraman, G.** (2000). Heparin and heparan sulfate: biosynthesis, structure and function. *Curr. Opin. Chem. Biol.* 4, 626-631.
- Scarpellini, A., Germack, R., Johnson, T. S., Muramatsu, T., Griffin, M. and Verderio, E. A.** (2008). In *Biochem Soc Trans* 36(2) P022: Biochem Soc Trans.
- Scarpellini, A., Germack, R., Lortat-Jacob, H., Muramatsu, T., Billett, E., Johnson, T. and Verderio, E. A.** (2009). Heparan Sulfate Proteoglycans Are Receptors for the Cell-surface Trafficking and Biological Activity of Transglutaminase-2. *J. Biol. Chem.* 284, 18411-18423.
- Schainuck, L. I., Striker, G. E., Cutler, R. E. and Benditt, E. P.** (1970). Structural-functional correlations in renal disease. II. The correlations. *Hum. Pathol.* 1, 631-641.
- Schuksz, M., Fuster, M. M., Brown, J. R., Crawford, B. E., Ditto, D. P., Lawrence, R., Glass, C. A., Wang, L., Tor, Y. and Esko, J. D.** (2008). Surfen, a small molecule antagonist of heparan sulfate. *Proc. Natl. Acad. Sci. U. S. A* 105, 13075-13080.
- Schwartz, M. L., Pizzo, S. V., Hill, R. L. and McKee, P. A.** (1973). Human Factor XIII from plasma and platelets. Molecular weights, subunit structures, proteolytic activation, and cross-linking of fibrinogen and fibrin. *J. Biol. Chem.* 248, 1395-1407.
- Scotchford, C. A., Cascone, M. G., Downes, S. and Giusti, P.** (1998). Osteoblast responses to collagen-PVA bioartificial polymers in vitro: the effects of cross-linking method and collagen content. *Biomaterials* 19, 1-11.
- Seelenmeyer, C., Wegehingel, S., Tews, I., Kunzler, M., Aebi, M. and Nickel, W.** (2005). Cell surface counter receptors are essential components of the unconventional export machinery of galectin-1. *J. Cell Biol.* 171, 373-381.
- Seikaly, M. G., Ho, P. L., Emmett, L., Fine, R. N. and Tejani, A.** (2003). Chronic renal insufficiency in children: the 2001 Annual Report of the NAPRTCS. *Pediatr. Nephrol.* 18, 796-804.
- Seitz, R., Wolf, M., Egbring, R. and Havemann, K.** (1989). The disturbance of hemostasis in septic shock: role of neutrophil elastase and thrombin, effects of antithrombin III and plasma substitution. *Eur. J. Haematol.* 43, 22-28.
- Shan, L., Molberg, O., Parrot, I., Hausch, F., Filiz, F., Gray, G. M., Sollid, L. M. and Khosla, C.** (2002). Structural basis for gluten intolerance in celiac sprue. *Science* 297, 2275-2279.
- Sharma, A., Askari, J. A., Humphries, M. J., Jones, E. Y. and Stuart, D. I.** (1999). Crystal structure of a heparin- and integrin-binding segment of human fibronectin. *EMBO J.* 18, 1468-1479.
- Shin, J., Lee, W., Lee, D., Koo, B. K., Han, I., Lim, Y., Woods, A., Couchman, J. R. and Oh, E. S.** (2001). Solution structure of the dimeric cytoplasmic domain of syndecan-4. *Biochemistry* 40, 8471-8478.

- Shweke, N., Boulos, N., Jouanneau, C., Vandermeersch, S., Melino, G., Dussaule, J. C., Chatziantoniou, C., Ronco, P. and Boffa, J. J.** (2008). Tissue transglutaminase contributes to interstitial renal fibrosis by favoring accumulation of fibrillar collagen through TGF-beta activation and cell infiltration. *Am. J. Pathol.* 173, 631-642.
- Sibille, N., Sillen, A., Leroy, A., Wieruszkeski, J. M., Mulloy, B., Landrieu, I. and Lippens, G.** (2006). Structural impact of heparin binding to full-length Tau as studied by NMR spectroscopy. *Biochemistry* 45, 12560-12572.
- Siefring, G. E., Jr., Apostol, A. B., Velasco, P. T. and Lorand, L.** (1978). Enzymatic basis for the Ca<sup>2+</sup>-induced cross-linking of membrane proteins in intact human erythrocytes. *Biochemistry* 17, 2598-2604.
- Siegel, M. and Khosla, C.** (2007). Transglutaminase 2 inhibitors and their therapeutic role in disease states. *Pharmacol. Ther.* 115, 232-245.
- Siegel, M., Strnad, P., Watts, R. E., Choi, K., Jabri, B., Omary, M. B. and Khosla, C.** (2008). Extracellular transglutaminase 2 is catalytically inactive, but is transiently activated upon tissue injury. *PLoS. One.* 3, e1861.
- Signorini, M., Bortolotti, F., Poltronieri, L. and Bergamini, C. M.** (1988). Human erythrocyte transglutaminase: purification and preliminary characterisation. *Biol. Chem. Hoppe Seyler* 369, 275-281.
- Simons, M. and Horowitz, A.** (2001). Syndecan-4-mediated signalling. *Cell Signal.* 13, 855-862.
- Singer, A. J. and Clark, R. A.** (1999). Cutaneous wound healing. *N. Engl. J. Med.* 341, 738-746.
- Singh, R. N. and Mehta, K.** (1994). Purification and characterization of a novel transglutaminase from filarial nematode *Brugia malayi*. *Eur. J. Biochem.* 225, 625-634.
- Skill, N. J., Griffin, M., El Nahas, A. M., Sanai, T., Haylor, J. L., Fisher, M., Jamie, M. F., Mould, N. N. and Johnson, T. S.** (2001). Increases in renal epsilon-(gamma-glutamyl)-lysine crosslinks result from compartment-specific changes in tissue transglutaminase in early experimental diabetic nephropathy: pathologic implications. *Lab Invest* 81, 705-716.
- Skill, N. J., Johnson, T. S., Coutts, I. G., Saint, R. E., Fisher, M., Huang, L., El Nahas, A. M., Collighan, R. J. and Griffin, M.** (2004). Inhibition of transglutaminase activity reduces extracellular matrix accumulation induced by high glucose levels in proximal tubular epithelial cells. *J. Biol. Chem.* 279, 47754-47762.
- Slater, S. J., Seiz, J. L., Stagliano, B. A. and Stubbs, C. D.** (2001). Interaction of protein kinase C isozymes with Rho GTPases. *Biochemistry* 40, 4437-4445.
- Small, K., Feng, J. F., Lorenz, J., Donnelly, E. T., Yu, A., Im, M. J., Dorn, G. W. and Liggett, S. B.** (1999). Cardiac specific overexpression of transglutaminase II (G(h)) results in a unique hypertrophy phenotype independent of phospholipase C activation. *J. Biol. Chem.* 274, 21291-21296.
- Smethurst, P. A. and Griffin, M.** (1996). Measurement of tissue transglutaminase activity in a permeabilized cell system: its regulation by Ca<sup>2+</sup> and nucleotides. *Biochem. J.* 313 ( Pt 3), 803-808.
- Sobel, M., Soler, D. F., Kermode, J. C. and Harris, R. B.** (1992). Localization and characterization of a heparin binding domain peptide of human von Willebrand factor. *J. Biol. Chem.* 267, 8857-8862.
- Sollid, L. M.** (2000). Molecular basis of celiac disease. *Annu. Rev. Immunol.* 18, 53-81.

- Stanley, M. J., Liebersbach, B. F., Liu, W., Anhalt, D. J. and Sanderson, R. D.** (1995). Heparan sulfate-mediated cell aggregation. Syndecans-1 and -4 mediate intercellular adhesion following their transfection into human B lymphoid cells. *J. Biol. Chem.* 270, 5077-5083.
- Steinert, P. M., Candi, E., Tarcsa, E., Marekov, L. N., Sette, M., Paci, M., Ciani, B., Guerrieri, P. and Melino, G.** (1999). Transglutaminase crosslinking and structural studies of the human small proline rich 3 protein. *Cell Death. Differ.* 6, 916-930.
- Stephens, P., Grenard, P., Aeschlimann, P., Langley, M., Blain, E., Errington, R., Kipling, D., Thomas, D. and Aeschlimann, D.** (2004). Crosslinking and G-protein functions of transglutaminase 2 contribute differentially to fibroblast wound healing responses. *J. Cell Sci.* 117, 3389-3403.
- Stringer, K. D., Komers, R., Osman, S. A., Oyama, T. T., Lindsley, J. N. and Anderson, S.** (2005). Gender hormones and the progression of experimental polycystic kidney disease. *Kidney Int.* 68, 1729-1739.
- Subramanian, S. V., Fitzgerald, M. L. and Bernfield, M.** (1997). Regulated shedding of syndecan-1 and -4 ectodomains by thrombin and growth factor receptor activation. *J. Biol. Chem.* 272, 14713-14720.
- Takagi, T. and Doolittle, R. F.** (1975). Amino acid sequence studies on the alpha chain of human fibrinogen. Location of four plasmin attack points and a covalent cross-linking site. *Biochemistry* 14, 5149-5156.
- Takahashi, H., Isobe, T., Horibe, S., Takagi, J., Yokosaki, Y., Sheppard, D. and Saito, Y.** (2000). Tissue transglutaminase, coagulation factor XIII, and the pro-polypeptide of von Willebrand factor are all ligands for the integrins alpha 9beta 1 and alpha 4beta 1. *J. Biol. Chem.* 275, 23589-23595.
- Takahashi, N., Takahashi, Y. and Putnam, F. W.** (1986). Primary structure of blood coagulation factor XIIIa (fibrinolygase, transglutaminase) from human placenta. *Proc. Natl. Acad. Sci. U. S. A* 83, 8019-8023.
- Telci, D., Wang, Z., Li, X., Verderio, E. A., Humphries, M. J., Baccarini, M., Basaga, H. and Griffin, M.** (2008). Fibronectin-tissue transglutaminase matrix rescues RGD-impaired cell adhesion through syndecan-4 and beta1 integrin co-signaling. *J. Biol. Chem.* 283, 20937-20947.
- Telci, D., Collighan, R. J., Basaga, H. and Griffin, M.** (2009). Increased TG2 expression can result in induction of TGF{beta}1 causing increased synthesis and deposition of matrix proteins which can be regulated by nitric oxide. *J. Biol. Chem.*
- Thacher, S. M. and Rice, R. H.** (1985). Keratinocyte-specific transglutaminase of cultured human epidermal cells: relation to cross-linked envelope formation and terminal differentiation. *Cell* 40, 685-695.
- Thiebach, L., John, S., Paulsson, M. and Smyth, N.** (2007). The role of TG3 and TG6 in hair morphogenesis and in the establishment of the skin barrier function. In *9th international conference on transglutaminases and protein cross-linking, Morocco, Sept 1-4, 2007.*
- Thomazy, V. and Fesus, L.** (1989). Differential expression of tissue transglutaminase in human cells. An immunohistochemical study. *Cell Tissue Res.* 255, 215-224.
- Tkachenko, E., Rhodes, J. M. and Simons, M.** (2005). Syndecans: new kids on the signaling block. *Circ. Res.* 96, 488-500.
- Tomiyoshi, Y., Sakemi, T., Aoki, S. and Miyazono, M.** (2002). Different effects of castration and estrogen administration on glomerular injury in spontaneously hyperglycemic Otsuka Long-Evans Tokushima Fatty (OLETF) rats. *Nephron* 92, 860-867.

- Tucholski, J. and Johnson, G. V.** (2002). Tissue transglutaminase differentially modulates apoptosis in a stimuli-dependent manner. *J. Neurochem.* 81, 780-791.
- Turner, P. M. and Lorand, L.** (1989). Complexation of fibronectin with tissue transglutaminase. *Biochemistry* 28, 628-635.
- Upchurch, H. F., Conway, E., Patterson, M. K., Jr. and Maxwell, M. D.** (1991). Localization of cellular transglutaminase on the extracellular matrix after wounding: characteristics of the matrix bound enzyme. *J. Cell Physiol* 149, 375-382.
- Varki, A., Cummings, R., Esko, J., Freeze, H., Hart, G. and Marth, J.** (2009). Essentials of glycobiology. **Cold Spring Harbor Laboratory Press.**
- Velasco, P. T., Murthy, P., Goll, D. E. and Lorand, L.** (1990). Cross-linking and proteolysis in Ca<sup>2+</sup>(+)-treated lens homogenates. *Biochim. Biophys. Acta* 1040, 187-191.
- Verderio, E., Nicholas, B., Gross, S. and Griffin, M.** (1998). Regulated expression of tissue transglutaminase in Swiss 3T3 fibroblasts: effects on the processing of fibronectin, cell attachment, and cell death. *Exp. Cell Res.* 239, 119-138.
- Verderio, E., Gaudry, C., Gross, S., Smith, C., Downes, S. and Griffin, M.** (1999). Regulation of cell surface tissue transglutaminase: effects on matrix storage of latent transforming growth factor-beta binding protein-1. *J. Histochem. Cytochem.* 47, 1417-1432.
- Verderio, E., Coombes, A., Jones, R. A., Li, X., Heath, D., Downes, S. and Griffin, M.** (2001). Role of the cross-linking enzyme tissue transglutaminase in the biological recognition of synthetic biodegradable polymers. *J. Biomed. Mater. Res.* 54, 294-304.
- Verderio, E. A., Telci, D., Okoye, A., Melino, G. and Griffin, M.** (2003). A novel RGD-independent cell adhesion pathway mediated by fibronectin-bound tissue transglutaminase rescues cells from anoikis. *J. Biol. Chem.* 278, 42604-42614.
- Verderio, E. A., Johnson, T. and Griffin, M.** (2004). Tissue transglutaminase in normal and abnormal wound healing: review article. *Amino. Acids* 26, 387-404.
- Verderio, E. A., Johnson, T. S. and Griffin, M.** (2005). Transglutaminases in wound healing and inflammation. *Prog. Exp. Tumor Res.* 38, 89-114.
- Verderio, E. A., Scarpellini, A. and Johnson, T. S.** (2008). Novel interactions of TG2 with heparan sulfate proteoglycans: reflection on physiological implications. *Amino. Acids*.36:671-677.
- Verma, A., Wang, H., Manavathi, B., Fok, J. Y., Mann, A. P., Kumar, R. and Mehta, K.** (2006). Increased expression of tissue transglutaminase in pancreatic ductal adenocarcinoma and its implications in drug resistance and metastasis. *Cancer Res.* 66, 10525-10533.
- Verma, A. K., Shoemaker, A., Simsiman, R., Denning, M. and Zachman, R. D.** (1992). Expression of retinoic acid nuclear receptors and tissue transglutaminase is altered in various tissues of rats fed a vitamin A-deficient diet. *J. Nutr.* 122, 2144-2152.
- Watanabe, N., Kato, T., Fujita, A., Ishizaki, T. and Narumiya, S.** (1999). Cooperation between mDia1 and ROCK in Rho-induced actin reorganization. *Nat. Cell Biol.* 1, 136-143.
- Wilcox-Adelman, S. A., Denhez, F. and Goetinck, P. F.** (2002). Syndecan-4 modulates focal adhesion kinase phosphorylation. *J. Biol. Chem.* 277, 32970-32977.

- Williams-Ashman, H. G.** (1984). Transglutaminases and the clotting of mammalian seminal fluids. *Mol. Cell Biochem.* 58, 51-61.
- Wilson, E. M. and French, F. S.** (1980). Biochemical homology between rat dorsal prostate and coagulating gland. Purification of a major androgen-induced protein. *J. Biol. Chem.* 255, 10946-10953.
- Woods, A. and Couchman, J. R.** (1994). Syndecan 4 heparan sulfate proteoglycan is a selectively enriched and widespread focal adhesion component. *Mol. Biol. Cell* 5, 183-192.
- Woods, A. and Couchman, J. R.** (2000). Integrin modulation by lateral association. *J. Biol. Chem.* 275, 24233-24236.
- Woods, A., Longley, R. L., Tumova, S. and Couchman, J. R.** (2000). Syndecan-4 binding to the high affinity heparin-binding domain of fibronectin drives focal adhesion formation in fibroblasts. *Arch. Biochem. Biophys.* 374, 66-72.
- Woods, A. and Couchman, J. R.** (2001). Syndecan-4 and focal adhesion function. *Curr. Opin. Cell Biol.* 13, 578-583.
- Xia, J., Siegel, M., Bergseng, E., Sollid, L. M. and Khosla, C.** (2006). Inhibition of HLA-DQ2-mediated antigen presentation by analogues of a high affinity 33-residue peptide from alpha2-gliadin. *J. Am. Chem. Soc.* 128, 1859-1867.
- Xu, L., Begum, S., Hearn, J. D. and Hynes, R. O.** (2006). GPR56, an atypical G protein-coupled receptor, binds tissue transglutaminase, TG2, and inhibits melanoma tumor growth and metastasis. *Proc. Natl. Acad. Sci. U. S. A* 103, 9023-9028.
- Yamaguchi, H. and Wang, H. G.** (2006). Tissue transglutaminase serves as an inhibitor of apoptosis by cross-linking caspase 3 in thapsigargin-treated cells. *Mol. Cell Biol.* 26, 569-579.
- Yasueda, H., Kumazawa, Y. and Motoki, M.** (1994). Purification and characterization of a tissue-type transglutaminase from red sea bream (*Pagrus major*). *Biosci. Biotechnol. Biochem.* 58, 2041-2045.
- Yee, V. C., Pedersen, L. C., Le, T., I, Bishop, P. D., Stenkamp, R. E. and Teller, D. C.** (1994). Three-dimensional structure of a transglutaminase: human blood coagulation factor XIII. *Proc. Natl. Acad. Sci. U. S. A* 91, 7296-7300.
- Yuan, L., Siegel, M., Choi, K., Khosla, C., Miller, C. R., Jackson, E. N., Piwnica-Worms, D. and Rich, K. M.** (2007). Transglutaminase 2 inhibitor, KCC009, disrupts fibronectin assembly in the extracellular matrix and sensitizes orthotopic glioblastomas to chemotherapy. *Oncogene* 26, 2563-2573.
- Yung, S., Woods, A., Chan, T. M., Davies, M., Williams, J. D. and Couchman, J. R.** (2001). Syndecan-4 up-regulation in proliferative renal disease is related to microfilament organization. *FASEB J.* 15, 1631-1633.
- Zamir, E. and Geiger, B.** (2001). Components of cell-matrix adhesions. *J. Cell Sci.* 114, 3577-3579.
- Zehe, C., Engling, A., Wegehingel, S., Schafer, T. and Nickel, W.** (2006). Cell-surface heparan sulfate proteoglycans are essential components of the unconventional export machinery of FGF-2. *Proc. Natl. Acad. Sci. U. S. A* 103, 15479-15484.
- Zemskov, E. A., Mikhailenko, I., Strickland, D. K. and Belkin, A. M.** (2007). Cell-surface transglutaminase undergoes internalization and lysosomal degradation: an essential role for LRP1. *J. Cell Sci.* 120, 3188-3199.

**Zhang, J. and Masui, Y.** (1997). Role of amphibian egg transglutaminase in the development of secondary cytotstatic factor in vitro. *Mol. Reprod. Dev.* 47, 302-311.

**Zhang, J., Lesort, M., Guttman, R. P. and Johnson, G. V.** (1998). Modulation of the in situ activity of tissue transglutaminase by calcium and GTP. *J. Biol. Chem.* 273, 2288-2295.

**Zhang, Z., Xing, J., Ma, L., Gong, R., Chin, Y. E. and Zhuang, S.** (2009). Transglutaminase-1 regulates renal epithelial cell proliferation through activation of Stat-3. *J. Biol. Chem.* 284, 3345-3353.

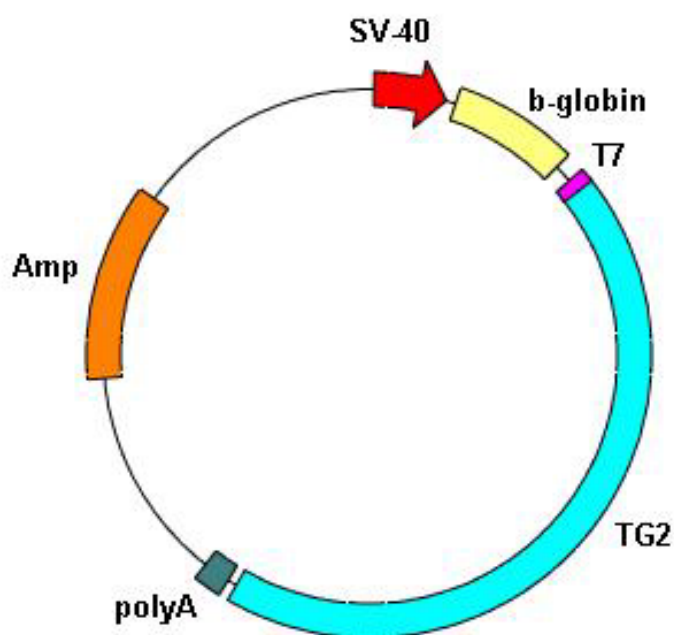
Substrates	Isoenzyme	Localization
<b>Proteins acting as amine donor</b>		
Actin	TG2	Intracellular
Aldehyde dehydrogenase	TG activity of the nematode <i>C. elegans</i>	
Amines (monoamines, diamines, polyamines): cadaverine and monodansilcadaverine, histamine, putrescine, serotonin, spermidine, spermine	Different isoenzymes	
Beta amyloid peptide	TG2	
Aspartyl protease	TG2 and Factor XIII	Viral protein (HIV-1)
Bacteriorhodopsin	Bacterial TG	
Calgizzarin—S100C protein—MLN 70—S100A11	TG1 and TG2	Keratinocyte cornified envelope (CE)
Cell adhesion molecule C-CAM	TG2	
Alpha B-crystallin	TG2	Intracellular
Cystatin	TG2 and possibly others	
Beta-endorphin	TG2	Endogenous opiates
Fibrinogen A alpha	TG2 and factor XIII	Extracellular
Glutamate dehydrogenase	TG activity of the nematode <i>Caenorhabditis elegans</i>	
Glutathione S-transferase	TG2	Intracellular
Glyceraldehyde 3 phosphate dehydrogenase	TG2	Intracellular
gp41	TG2	Transmembrane
Keratin, type II cytoskeletal 1	TG2 and TG3	
Keratin, type II cytoskeletal 2 epidermal	TG2 and TG3	
Keratin, type II cytoskeletal 5	TG2 and TG3	
Keratin, type II cytoskeletal 6	TG2 and TG3	
Alpha ketoglutarate dehydrogenase	TG2	Intracellular (Mitochondrial)
Alpha-lactalbumin	TG2 and <i>Streptovorticillium</i> TG (MTG)	Secretory protein
Beta lactoglobulin	TG2 (?)	Secretory protein
Laminin	FXIII	
Loricrin		Cell envelopes
Microtubule-associated protein tau—isoform Tau-F (Tau-4)	TG2	Intracellular
Monellin (analog of)	Microbial TG	
Root and leaf pea proteins		
Protein disulfide isomerase	TG activity of the nematode <i>Caenorhabditis elegans</i>	
Seminal vesicle secretory protein IV	TG2	Extracellular
S-peptide	Microbial TG (MTG) from <i>Streptomyces mobaraensis</i>	
Thymosin beta 4		Intracellular (cytoplasmatic)
Vasoactive intestinal peptide (VIP)	TG2	
Vimentin	TG2	
<b>Proteins acting as amine acceptor (i.e. glutamine donor)</b>		
Acetylcholine esterase	TG2	Intracellular
Actin	TG2	Intracellular (cytoplasmatic)

Substrates	Isoenzyme	Localization
Beta amyloid peptide	TG2	
Annexin I (lipocortin I)	TG2	Intracellular
Alpha(2)-antiplasmin	FXIII better than TG2	Extracellular
Aspartyl protease	TG2 and Factor XIII	Viral protein (HIV-1)
ATP synthase alpha subunit	TG of the nematode <i>C. elegans</i>	
Bacteriorhodopsin	Bacterial TG	
Calgizzarin—S100C protein—MLN 70—S100A11	TG1 and TG2	Keratinocyte cornified envelope (CE)
Calpactin I light chain (S100A10)	TG2	
Caraxin-1 (horseshoe crab)		
Beta casein	Factor XIII	Secreted protein
Chloroplast proteins	Plant TG(s)	
Collagen alpha 1(III)	TG2	Extracellular
Beta A3 crystallin	TG2	Intracellular
Beta B3 crystallin		Intracellular
Beta Bp (betaB2) crystallin		Intracellular
Cytocrome c	TG2	Intracellular
Beta-endorphin	TG2	Endogenous opiates
Enolase	Transglutaminase of the nematode <i>Caenorhabditis elegans</i>	Intracellular (Cytoplasmic)
Erythrocyte anion transporter—band 3 anion transport protein	Intrinsic TG of human red blood cell	Intracellular
Fibrinogen A alpha	TG2 and factor XIII	Extracellular
Fibrinogen gamma	Factor XIII	Extracellular
FibN (peptide derived from the N-terminal sequence of fibronectin)		Extracellular
Glucagon	TG2	
Glutathione S-transferase	TG2	Intracellular
gp41	TG2	Transmembrane
gp120	TG2	Viral envelope
H3 histone	TG2	Intracellular
H4 histone	TG2	Intracellular
H2A histone	TG2	Intracellular
H2B histone	TG2	Intracellular
Hemoglobin (denatured)		
Hepatitis C virus core protein	TG2	Viral protein
Insulin A chain	TG2	
Insulin B chain	TG2	
Insulin-like growth factor-binding protein-1	TG2	
Interleukin 2	Microbial transglutaminase (M-TG)	
Involucrin	TG1	Membrane
Alpha-lactalbumin	TG2 and <i>Streptovorticillium</i> TG (MTG)	Secretory protein
Beta lactoglobulin	TG2 (?)	Secretory protein
Laminin	FXIII	
Loricrin		Cell envelopes

Substrates	Isoenzyme	Localization
Alpha-2-macroglobulin receptor-associated protein		Extracellular
Mellittin	TG2	
Microtubule-associated protein tau—isoform Tau-F (Tau-4)	TG2	Intracellular
Midkine	TG2	
Monellin (analog of)	Microbial TG	
Nidogen (entactin)	TG2	Extracellular
Osteonectin	TG2	Extracellular
Osteopontin (extracellular matrix cell adhesion protein)	TG2	Extracellular
Root and leaf pea proteins		
Phosphoglycerate kinase		Intracellular ?
Phospholipase A2	TG2	Extracellular
Alpha2 plasmin inhibitor	FXIII	Extracellular?
Plasminogen-activator inhibitor type-2	TG2 and FXIII	
Polyglutamine repeats	TG2	
Procarboxypeptidase U (EC 3.4.17.20) plasma procarboxypeptidase B	TG2 and factor XIII	
S100 calcium-binding protein A7—Psoriasin (S100A7 or PSOR1)	TG2	
Seminal vesicle secretory protein IV	TG2	Extracellular
S-peptide	Microbial TG (MTG) from <i>Streptomyces mobaraensis</i>	
Substance P	TG2	Extracellular
Synapsin I	TG2	Intracellular
Tetanus toxin	TG2	
Vasoactive intestinal peptide—VIP	TG2	
Vimentin	TG2	
Vitronectin	Factor XIII	Extracellular
Von Willebrand factor	Factor XIII	
<b>Unknown acceptor/donor function, non-protein substrates, other molecules and activities</b>		
Aldolase		Intracellular
Androgen receptor	TG2	Intracellular (nuclear receptor)
CD38	TG2	Intracellular
Clara Cell p10 Kda		
eIF5A (initiation factor 5A)	TG2 and Factor XIII	Intracellular
Drugs (antibiotics)	TG homologue	
Fibronectin	Factor XIII	Extracellular
Filaggrin linker segment peptide (FLSP)	TG3	
Galectin 3	TG2	
Glutathione S-transferase	TG2	Intracellular
Gluten proteins (alpha/beta-, gamma-gliadin, and low molecular weight glutenin)	TG2	Extracellular
Growth hormone	TG2	
Small GTPases		Intracellular
Histidine-rich glycoprotein	FXIII	Expressed by the liver and secreted in plasma
Alpha2 HS-glycoprotein (AHSG)	TG2	

Substrates	Isoenzyme	Localization
Huntingtin	TG2	
Importin alpha3	TG2	Nuclear transport protein
Insulin-like growth factor binding protein-3 (IGFBP-3)	TG2	
Latent TGF-beta binding protein-1 (LTBP-1)	TG2	Extracellular
Lipoprotein a	TG2 and FXIII	
Alpha2 macroglobulin		
Myoglobin	TG2	
Myosin		Intracellular
Nucleotide(s) binding/hydrolyzing	TG2 TG3 TG5	Intracellular
Osteocalcin		Extracellular
Periplakin	TG2	
Phosphorylase kinase		Intracellular
Proapoptotic kinase DLK	TG2	
Protein disulfide isomerase	TG activity of the nematode <i>Caenorhabditis elegans</i>	
Retinoblastoma protein		
Rho A		Intracellular
Ribonuclease A	TG2	
Semenogelin I	Factor XIII	
Semenogelin II	Factor XIII	
Bone sialoprotein (BSP)	TG2	Bone matrix
Soybean proteins		Extracellular
Alpha-synuclein	TG2	Intracellular
Thrombospondin	factor XIII	Extracellular
Troponin T		Intracellular
Tubulin		Intracellular
Uteroglobin	TG2 FXIII?	Extracellular
Vinculin	Factor XIII	
Whey proteins	Microbial TG	Extracellular

**Appendix 1 Substrates of transglutaminases (Facchiano and Facchiano, 2009).**



**Appendix 2 Schematic representation of the human TG2 expression vector pSG5-TGase (Gentile et al., 1992).** Human TG2 cDNA was *EcoRI* inserted into pSG5 vector. SV-40 early gene enhancer and promoter, intron II of the rabbit beta-globin gene (*b-globin*), T7 bacteriophage promoter, and SV-40 polyadenylation sequence (*polyA*) are shown; *Amp*, ampicillin resistance gene.